

DOCTORAL THESIS

Xavier Bernat Camí

Treatment of biorefractory wastewater through membrane-assisted oxidation processes

February 2010



UNIVERSITAT ROVIRA I VIRGILI

TREATMENT OF BIOREFRACTORY WASTEWATER THROUGH MEMBRANE-ASSISTED OXIDATION PROCESSES

Xavier Bernat Camí

ISBN:978-84-693-1529-3/DL:T-652-2010

UNIVERSITAT ROVIRA I VIRGILI

TREATMENT OF BIOREFRACTORY WASTEWATER THROUGH MEMBRANE-ASSISTED OXIDATION PROCESSES

Xavier Bernat Camí

ISBN:978-84-693-1529-3/DL:T-652-2010

UNIVERSITAT ROVIRA I VIRGILI

TREATMENT OF BIOREFRACTORY WASTEWATER THROUGH MEMBRANE-ASSISTED OXIDATION PROCESSES

Xavier Bernat Camí

ISBN:978-84-693-1529-3/DL:T-652-2010

Xavier Bernat Camí

TREATMENT OF BIOREFRACTORY WASTEWATER
THROUGH MEMBRANE-ASSISTED
OXIDATION PROCESSES

DOCTORAL THESIS

supervised by Dr. José Font Capafons

Departament d'Enginyeria Química



UNIVERSITAT ROVIRA I VIRGILI

Tarragona

2010

UNIVERSITAT ROVIRA I VIRGILI

TREATMENT OF BIOREFRACTORY WASTEWATER THROUGH MEMBRANE-ASSISTED OXIDATION PROCESSES

Xavier Bernat Camí

ISBN:978-84-693-1529-3/DL:T-652-2010



**UNIVERSITAT
ROVIRA I VIRGILI**

Escola Tècnica Superior d'Enginyeria Química
Departament d'Enginyeria Química

Avinguda dels Països Catalans, 26
43007 Tarragona (Spain)
Tel. 977559603
Fax: 977559621

I, Dr. José Font Capafons, associate professor in the Department of Chemical Engineering of the Rovira i Virgili University,

CERTIFY:

That the present study, entitled "Treatment of biorefractory wastewater through membrane-assisted oxidation processes", presented by Xavier Bernat Camí for the award of the degree of Doctor, has been carried out under my supervision at the Department of Chemical Engineering of this university, and that it fulfils all the requirements to be eligible for the European Doctorate Label.

Tarragona, 21st December 2009

UNIVERSITAT ROVIRA I VIRGILI

TREATMENT OF BIOREFRACTORY WASTEWATER THROUGH MEMBRANE-ASSISTED OXIDATION PROCESSES

Xavier Bernat Camí

ISBN:978-84-693-1529-3/DL:T-652-2010

*Als meus pares, als meus padrins
i a tots els qui m'heu ajudat
a arribar fins aquí*

UNIVERSITAT ROVIRA I VIRGILI

TREATMENT OF BIOREFRACTORY WASTEWATER THROUGH MEMBRANE-ASSISTED OXIDATION PROCESSES

Xavier Bernat Camí

ISBN:978-84-693-1529-3/DL:T-652-2010

Acknowledgements

Research needs planning, executing and discussing. In my opinion, planning and discussing play a major role in research because, from them, the research plan is adapted step by step and preset goals accordingly fulfilled. The research cycle is usually fed by several opinions, types of contributions and support in order to maximise the quality of the results obtained. For this reason, a thesis is not a personal achievement but the result of a four-year experience involving more than one person. During these last years, I have been supported by many people, to whom I am very grateful.

First of all, I want to express my sincere gratitude to Dr. Font. Josep, thank you for giving me the opportunity to work with you and for all you have done for me and for our work during the last years. Apart from improving my knowledge on oxidation and membrane technologies, you have succeeded in showing me how to plan research and, particularly, how to discuss results. Thank you for guiding me and transferring me your research methodology.

I am really indebted to you, CREPI members, seniors and juniors, for your constant support during the time we spent together. Josep, Agustí, Christophe, Frank and Azael, thank you for sharing your time with junior members and for allowing me to do research in an autonomous way. MariE, despite the fact that we had little time to work together, you invested a lot of effort in teaching me and helping me to orientate my research career. Thank you. Alícia, I must acknowledge you for your lessons, organisation and advice but, what I appreciate the most is the help you always offered me and our friendship. Esther, thank you for the arguments, for the COD's, for your stubbornness...for being my main lab supplier, for your daily support, for your patience and specially, for being a friend. Isa and Ana: the perfect tandem. I am sure that, even though we were geographically separated, our paths would always find common points to share moments and experiences. Thank you for being always there. Mare, Irama and Rita, thank you for the special moments: vials, songs, laughs, filters, parties, arepas, pipettes, rumba and many other pleasant moments. Ivonne, I am sure that you will be an excellent *membranator*. Good luck and, in case you need help, I will be there. I would also like to thank Nigus, Debora, Gergo, Dongmei, Cathy and Tom for the time we spent in the lab discussing about our research and life projects.

My best wishes to Sergio, Marlene, Sibel, Bartek and Albert, with whom I shared unforgettable moments in the offices and corridors. Albert, thank you for being a valued friend. Meeting each other again in the university has been an excellent opportunity to share both achievements and troubles. Without you, I could have forgotten that life was more than performing experiments and writing abstracts. Pilar Obón is gratefully acknowledged for encouraging and advising me when I needed it. Last but not least, I would like to thank Joana, Marta, Oriol and Benoît, who have suffered the last hard months of this thesis. Thank you for understanding the situation.

I want to express my gratitude to Prof. Marianne Nyström for accepting me as visiting PhD student in the Lappeenranta University of Technology (Lappeenranta, Finland) and to Prof. Enrico Drioli for allowing me to carry out a research stage in the *Istituto per la Tecnologia delle Membrane* (Rende, Italy). In addition, I want to acknowledge Dr. Arto Pihlajamäki and Dr. Lidietta Giorno for their support during the stages in Finland and Italy, respectively. Claudia, Vasileios and Mehrdad, thank you for the special moments we shared in Finland. In Italy, I would have not enjoyed my stage and life as much as I did without Rosalinda, Fabio, Simona, Marco, Angelo, GB and, more

specially, without Emma. Emma, *sei bravissima!* Thank you for supporting me there and being a friend.

I would like to gratefully acknowledge Dr. Ortiz, Dr. Stüber, Dr. Giorno, Dr. Pihlajamäki and Dr. Suárez Ojeda for their acceptance to participate in the evaluation committee of this thesis. Furthermore, Dr. Fortuny and Dr. Güell are acknowledged for being substitutes in the abovementioned committee and Dr. Roux-de Balmann and Dr. Figoli for being external reviewers of this thesis.

An experimental PhD thesis cannot be carried out without financial support. For this reason, I am indebted to the Universitat Rovira i Virgili for the PhD grant. The *Ministerio de Educación y Ciencia* and the *Ministerio de Ciencia e Innovación* are acknowledged for their financial support through the projects CTM2005-01873/TECNO and CTM2008-03338/TECNO, respectively. Furthermore, the *DIUE - Generalitat de Catalunya* and the European Commission are also acknowledged for their economic support through the projects 2007ITT-00008 and FP7-018525, respectively.

L'agraïment més important va a dirigit als meus pares. Els vostres ànims i suport incondicional han estat el motor que ha fet que orientés el meu camí cap a on desitjava i que no l'abandonés en els moments més difícils. Gràcies per recolzar-me sempre en aquesta cursa i per haver comprès la importància que tenia per mi poder arribar fins aquí. Sense vosaltres, no hauria estat possible.

Resum

La manca d'aigua és un problema global que pot frenar el desenvolupament humà. Aproximadament la meitat de l'aigua captada a Europa es destina a la indústria. La indústria química produeix un elevat volum d'aigües residuals que, junt amb les municipals, representen el focus més elevat de contaminació de l'aigua. Algunes aigües residuals són massa biorecalcitrants per a ser tractades en estacions depuradores d'aigües residuals (EDARs) convencionals. Per tant, aquestes aigües necessiten ser pretractades abans de ser enviades a una EDAR convencional. Els Processos d'Oxidació Avançada (POAs) han demostrat ser efectius en la descontaminació d'aquesta tipologia d'aigües abans de la seva depuració biològica. En concret, el procés Fenton es presenta com un dels POAs més simples per pretractar aigües biorecalcitrants. El procés Fenton es basa en l'oxidació de compostos orgànics mitjançant el seu atac per radicals oxidants generats a partir de la reacció del peròxid d'hidrogen amb ions de ferro. Malgrat la seva coneguda eficiència, el procés presenta dues limitacions principals: la pèrdua contínua dels ions de ferro a l'efluent del reactor i la de peròxid d'hidrogen degut a la seva autodescomposició i/o al seu efecte eliminador de radicals oxidants. Ambdues desavantatges influencien negativament l'eficiència ambiental i econòmica del procés global de tractament. Com a conseqüència, es fa necessari el disseny, l'assaig experimental i l'aplicació de solucions que permetin reduir o fins i tot eliminar les limitacions identificades.

En aquesta tesi, s'ha avaluat el potencial dels processos de membrana per millorar el tractament d'aigües fenòliques mitjançant el procés d'oxidació Fenton. Les alternatives proposades es van dissenyar per recuperar (o confinar) les espècies de ferro utilitzades com a catalitzador o bé per a incrementar l'ús del peròxid d'hidrogen per degradar matèria orgànica. Es van fer assaigs amb ultrafiltració (UF) i nanofiltraació (NF) a fi de recuperar espècies de ferro a partir de solucions aquoses sintètiques. Malgrat el fet inesperat que la UF permetia obtenir retencions de ferro(III) de fins al 91.6% a pH 2.00 amb una membrana ceràmica comercial de 5 kDa, la retenció de ferro(II) fou nul·la. Com a conseqüència, es va estudiar la NF amb la mateixa finalitat i es van obtenir retencions de ferro(II) i de ferro(III) de fins al 99.7% a pH 2.00 utilitzant membranes comercials. En aquest moment, es va realitzar l'estudi de l'acoblament de l'oxidació amb la NF. En concret, es va investigar l'efecte de les variables d'operació sobre la qualitat dels efluentes de l'oxidació i, seguidament, sobre la dels permeats de la NF. La combinació del procés Fenton i la NF va demostrar ser una configuració prometedora tant en termes de rebuig de ferro com per a ajustar la qualitat dels efluentes del procés Fenton per a què poguessin ser depurats biològicament. Mitjançant aquesta configuració, seleccionant adequadament les condicions d'operació, la retenció global de ferro pot arribar fins al 98.8%.

La influència de la presència de surfactants als efluentes fenòlics va ser també estudiada amb l'esquema combinat de tractament. La mescla va ser considerada per estudiar la capacitat de confinament de ferro en les micel·les de surfactant que serien, després de ser utilitzades com a catalitzador, recuperades fàcilment mitjançant membranes de microfiltració (MF) o bé UF i reutilitzades a l'etapa de reacció. Els surfactants es van degradar considerablement durant l'oxidació, cosa que limita l'aplicabilitat de la proposta. Malgrat això, es va continuar amb l'estudi de la combinació de l'oxidació amb la NF per tractar els efluentes mixtes de fenol i surfactant com a exemple d'efluent industrial. El procés acoblat va permetre recuperar completament, dels efluentes de l'oxidació, el ferro, el fenol i el surfactant no degradats així com els compostos de tipus quinona. Per tant, el procés combinat va demostrar millorar la qualitat dels efluentes de l'oxidació Fenton, la qual cosa pot assegurar l'operació segura de la subsegüent EDAR.

L'oxidació de fenol mitjançant el procés Fenton es va estudiar també utilitzant emulsions d'oli-en-aigua, formulades mitjançant processos d'emulsificació amb membranes, que contenen ferro a la interfície de les gotes. Aquestes emulsions van ser utilitzades com a catalitzador Fenton heterogeni amb la finalitat de que poguessin ser fàcilment recuperades mitjançant MF. Malgrat això, les emulsions es desestabilitzaven en ser sotmeses a condicions d'oxidació, probablement a causa de la degradació del surfactant utilitzat com a emulsionant, fent-les així no utilitzables per a aquesta aplicació.

Finalment, l'ús de peròxid d'hidrogen per a l'oxidació de matèria orgànica va ser millorat utilitzant un reactor de membrana inert. L'alimentació d'oxidant es va efectuar a través de la paret d'una membrana tubular que permetia així mantenir la seva concentració a un nivell baix al llarg del reactor, la qual cosa reduïa la seva autodescomposició i/o el seu comportament eliminador de radicals. Mitjançant aquesta configuració de reactor es van obtenir conversions de fenol i mineralitzacions un 20% superiors a les aconseguïdes en un reactor tubular convencional.

Es pot concloure que l'acoblament del procés Fenton i la NF permet recuperar eficientment els ions de ferro i augmentar l'adequació de l'efluent de l'oxidació a ser tractat en una EDAR convencional. Això soluciona el principal problema relacionat amb el procés d'oxidació Fenton, és a dir, el lligat amb la necessitat d'una addició contínua de ferro al reactor. Paral·lelament, un reactor de membrana inert, en el qual el peròxid d'hidrogen és uniformement distribuït a través de la paret del mateix, millora la degradació del fenol i la mineralització de l'efluent en comparació amb un reactor convencional operant a les mateixes condicions. Aquesta segona proposta de procés redueix la problemàtica associada amb la pèrdua de peròxid d'hidrogen deguda a la seva autodescomposició i/o efecte eliminador de radicals. Per tant, es pot afirmar que les tecnologies de membrana, si es seleccionen i operen adequadament, poder ser una eina potent per pal·liar o fins i tot eliminar les limitacions del procés Fenton millorant així l'eficiència del tractament d'aigües residuals biorecalcitrants.

Resumen

La escasez de agua es un problema global que puede desacelerar el desarrollo humano. Aproximadamente el cincuenta por ciento del total de agua captada en Europa se utiliza para fines industriales. La industria química produce un elevado volumen de aguas residuales que, junto con las municipales, son el foco más importante de polución del agua. Algunas aguas residuales son demasiado biorecalcitrantes para ser tratadas en estaciones depuradoras de aguas residuales (EDARs) convencionales. Por tanto, dichas aguas necesitan ser pretratadas antes de ser enviadas a una EDAR convencional. Los Procesos de Oxidación Avanzada (POAs) han demostrado ser efectivos para la descontaminación de esta tipología de aguas antes de su depuración biológica. En concreto, el proceso Fenton se presenta como uno de los POAs más simples para pretratar aguas biorecalcitrantes. El proceso Fenton se basa en la oxidación de compuestos orgánicos mediante su ataque por radicales oxidantes generados a partir de la reacción del peróxido de hidrógeno con iones de hierro. A pesar de la demostrada eficiencia de la oxidación, el proceso presenta dos limitaciones principales: la pérdida continua de los iones de hierro en el efluente del reactor y el desperdicio de peróxido debido a su autodescomposición y/o a su efecto eliminador de radicales oxidantes. Ambas desventajas influyen negativamente la eficiencia ambiental y económica del proceso global de tratamiento. Consecuentemente, se hace necesario el diseño, el ensayo experimental y la implementación de soluciones novedosas que permitan reducir o incluso eliminar las limitaciones identificadas.

En esta tesis, se ha evaluado el potencial de los procesos de membrana para mejorar las prestaciones del tratamiento de aguas fenólicas mediante la oxidación Fenton. Las alternativas propuestas fueron diseñadas para recuperar (o confinar) las especies de hierro usadas como catalizador o bien para incrementar el uso del peróxido de hidrógeno para degradar materia orgánica. La ultrafiltración (UF) y la nanofiltración (NF) fueron ensayadas preliminarmente para recuperar especies de hierro a partir de soluciones acuosas sintéticas. A pesar de que la UF permitió obtener inesperadamente retenciones de hierro(III) de hasta el 91.6% a pH 2.00 con una membrana cerámica comercial de 5 kDa, la retención de hierro(II) fue nula. En consecuencia, la NF fue seguidamente probada con la misma finalidad y se obtuvieron retenciones de hierro(II) y hierro(III) de hasta el 99.7% utilizando membranas comerciales. En este punto, se realizó el estudio del acoplamiento de la oxidación con la NF. Concretamente, se investigó el efecto de las variables de operación sobre la calidad de los efluentes de la oxidación y, a continuación, sobre la de los permeados de la NF. La combinación del proceso Fenton y la NF demostró ser una configuración prometedora tanto en términos de rechazo de hierro como para ajustar la calidad de los efluentes del proceso Fenton para que pudieran ser depurados biológicamente. Mediante esta configuración, seleccionando adecuadamente las condiciones de operación, la retención global de hierro puede llegar hasta el 98.8%.

La influencia de la presencia de surfactantes en los efluentes fenólicos fue también estudiada en el esquema combinado de tratamiento. Esta mezcla fue considerada para estudiar la capacidad de confinamiento de hierro en las micelas de surfactante que serían, después de ser utilizadas como catalizador, fácilmente retenibles mediante microfiltración (MF) o UF y reutilizables en la etapa de reacción. Los surfactantes se degradaron notablemente durante la oxidación y, por tanto, su aplicabilidad como soporte de hierro se vio mermada. A pesar de esto, se estudió la combinación de la oxidación con la NF para tratar efluentes mixtos de fenol y surfactante como ejemplo de efluente industrial. El proceso acoplado permitió recuperar completamente, de los efluentes de la oxidación, el hierro, el fenol y el surfactante no degradados así como

los compuestos de tipo quinona. Por lo tanto, el proceso combinado demostró mejorar la calidad de los efluentes de la oxidación Fenton, lo que puede asegurar la operación segura de la subsiguiente EDAR.

La oxidación del fenol mediante el proceso Fenton se estudió también empleando emulsiones de aceite-en-agua, formuladas mediante procesos de emulsificación con membranas, que contenían hierro en la interfase de las gotas. Dichas emulsiones fueron probadas como catalizador Fenton heterogéneo con la finalidad de que fueran fácilmente recuperadas mediante MF. Sin embargo, las emulsiones se desestabilizaron durante la oxidación probablemente debido a la degradación del surfactante utilizado como emulsionante, haciéndolas así inutilizables para dicha aplicación.

Finalmente, el uso del peróxido de hidrógeno para la oxidación de materia orgánica fue mejorado empleando un reactor de membrana inerte. La alimentación del oxidante se realizó a través de la pared de una membrana tubular que permitía así mantener su concentración a un nivel bajo a lo largo del reactor, lo cual redujo su autodescomposición y/o su capacidad para eliminar radicales. Mediante esta configuración de reactor se obtuvieron conversiones de fenol y mineralizaciones un 20% superiores a las conseguidas en un reactor tubular convencional.

Se puede concluir que el acoplamiento del proceso Fenton y la NF permite recuperar eficientemente los iones de hierro y aumentar la adecuación del efluente de la oxidación a ser tratado en una EDAR convencional. Esto soluciona el principal problema relacionado con el proceso de oxidación Fenton, es decir, la necesidad de una adición continua de hierro al reactor. Paralelamente, un reactor de membrana inerte, en el cual el peróxido de hidrógeno es uniformemente distribuido a través de la pared del mismo, mejora la degradación de fenol y la mineralización del efluente en comparación con un reactor tubular convencional operando a las mismas condiciones. Esta segunda propuesta reduce la problemática asociada con la pérdida de peróxido de hidrógeno debida a su autodescomposición y/o efecto eliminador de radicales. Por lo tanto, se puede afirmar que las tecnologías de membrana, si se seleccionan y operan adecuadamente, pueden ser una herramienta potente para paliar o incluso eliminar las limitaciones del proceso Fenton mejorando así la eficiencia del tratamiento de aguas residuales biorecalcitrantes.

Summary

Water scarcity is a problem of major concern that can slow down mankind development. Over fifty percent of water withdrawal in Europe is used in industrial applications. Chemical industry produces huge amounts of contaminated wastewaters that, together with municipal wastewaters, are the most important water pollution source. Some wastewaters are too refractory to be treated in a conventional biological wastewater treatment plant (BWWTP). Thus, biorefractory wastewater needs to be pre-treated before entering the BWWTP. Advanced Oxidation Processes (AOP's) have been found to be effective for the decontamination of these wastewaters prior to the biological degradation. In particular, the Fenton process is recognised to be one of the simplest AOP's to amend them. The process is based on the oxidation of organics through their attack by oxidant radicals generated from the reaction of hydrogen peroxide and iron ions. Despite the efficiency of the oxidation, two main drawbacks have been identified: the continuous loss of iron ions from the reactor and the waste of bulk oxidant due to its self-decomposition and/or radical scavenging effect. Both disadvantages influence the environmental suitability and the economy of the overall treatment. Hence, solutions allowing the reduction or even elimination of these identified drawbacks need to be designed, experimentally tested and implemented.

In this thesis, the efficiency of membrane processes to enhance the treatment of phenolic aqueous streams by Fenton oxidation was evaluated. The proposed alternatives were designed to either recover (or confine) the iron species or increase the use of hydrogen peroxide to destroy organic matter. Ultrafiltration (UF) and nanofiltration (NF) were preliminarily tested to recover iron from synthetic aqueous solutions. Although UF unexpectedly gave up to 91.6% iron(III) retention at pH 2.00 with a 5-kDa commercial ceramic membrane, it exhibited nil iron(II) retention. Thus, due to this limitation, NF was tested for the same purpose. NF showed to be an efficient technology to be coupled with Fenton oxidation because it allowed achieving up to 99.7% iron(II) and iron(III) retentions at pH 2.00 using commercial membranes. Research focused on testing the feasibility of coupling the oxidation and the subsequent NF was then carried out. The influence of the oxidation conditions over the quality of the Fenton effluents and later over those from NF was examined. The sequential combination of Fenton and NF showed to be a promising configuration not only in terms of iron rejection but also to amend the toxicity of the Fenton effluents prior feeding to a BWWTP. By properly tailoring the operation conditions, global iron retention could be up to 98.8%.

The influence of the presence of surfactants in phenolic effluents was also studied in the combined process scheme. The goal of studying this mixture was to test whether or not surfactants could confine iron ions in their micelles which would be easily retained by microfiltration (MF) or UF, after the oxidation reactor, and then re-used. However, surfactants were appreciably degraded by the Fenton reaction. Thus, a continuous addition of surfactants would be needed, which renders the process unviable. Despite the unfeasibility, the combination of Fenton and NF to treat mixed phenol and surfactant effluents was studied as relevant model of many industrial effluents. The coupled process was able to completely retain iron, non-reacted phenol and surfactant as well as quinone-like compounds from Fenton effluents. Thus, the combined process improved the quality of the pre-oxidised effluents, which could assure the proper operation of the subsequent BWWTP.

The Fenton oxidation of phenol was also carried out using oil-in-water emulsions formulated by membrane emulsification, containing iron at the droplets' interface. The emulsions intended to be used as heterogeneous Fenton catalysts, which could

subsequently be easily removed by MF. Nevertheless, the emulsions were destabilised by Fenton oxidation probably due to the degradation of the surfactant used as emulsifier, making them unfeasible to be used in practice.

Finally, the use of hydrogen peroxide for organic matter degradation was enhanced using an inert ceramic membrane reactor. Feeding the oxidant through the wall of the tubular membrane allowed keeping its concentration at a low level throughout the continuous reactor, which reduced its self-decomposition and/or radical scavenging behaviour. An increase on phenol degradation and mineralisation of around 20% was achieved when the membrane reactor performance was compared to that of a conventional tubular reactor.

It can be concluded that coupling Fenton process and NF allows recovering iron ions and increasing oxidised effluent adequacy to be treated in a BWWTP. This solves the major Fenton drawback, i.e. the needed for continuous iron addition to the reactor. Besides, an inert membrane reactor, where hydrogen peroxide is uniformly fed through its wall, increases phenol abatement and mineralisation when compared to a conventional tubular reactor. This second approach overcomes in part the Fenton drawback associated to the waste of oxidant through its self-decomposition and/or its radical scavenging effect. To sum up, it can be confirmed that membrane technologies, if appropriately selected and operated, can be an efficient tool for decreasing or even avoiding Fenton process inconveniences and thus enhancing the efficiency of the treatment of biorefractory wastewater.

Contents

1. Introduction	1
1.1. Water scarcity and alternative water resources	1
1.2. Water and wastewater in industry	6
1.2.1. Industrial wastewater model pollutants	7
1.3. Industrial wastewater treatment	10
1.3.1. Oxidation in industrial wastewater treatment	10
1.3.1.1. Fenton process	13
1.3.2. Membrane technologies in industrial wastewater treatment	17
1.3.3. Coupled processes in industrial wastewater treatment	21
1.3.3.1. Coupling Fenton process and biological degradation	21
1.3.3.2. Coupling Fenton process and biological degradation assisted by membrane technology	23
2. Hypotheses and objectives	27
2.1. Hypotheses	27
2.2. Objectives	29
3. Methodology	31
3.1. Fenton oxidation	31
3.1.1. Model pollutants, oxidant and catalyst	31
3.1.2. Fenton oxidation set-up	32
3.1.3. Homogeneous Fenton oxidation protocol	33
3.2. Membrane separation processes	34
3.2.1. Reagents and membrane cleaning agents	34
3.2.2. Membranes and membrane processes	35
3.2.2.1. Ceramic UF membranes	35
3.2.2.2. Polymeric UF membranes	36
3.2.2.3. Polymeric NF membranes	36
3.2.3. Membrane filtration set-up	37
3.2.3.1. Crossflow filtration set-up	37
3.2.3.2. Dead-end filtration set-up	38
3.2.4. Filtration of synthetic solutions of heavy metals	39
3.2.4.1. Crossflow filtration protocol	39
3.2.4.2. Dead-end filtration protocol	40
3.2.5. Filtration of Fenton effluents	40

3.2.6. Membrane filtration efficiency assessment	41
3.2.6.1. Permeate flux decline, fouling and cleaning efficiency	41
3.2.6.2. Retention efficiency	42
3.3. Phenol oxidation with ferrous O/W emulsions prepared by membrane emulsification	42
3.3.1. Reagents.....	42
3.3.2. Membrane emulsification experiments	43
3.3.2.1. Stirred membrane emulsification	43
3.3.2.2. Crossflow membrane emulsification	44
3.3.2.3. Formulation of Fe(II)-containing emulsions.....	45
3.3.3. Characterisation of emulsions	46
3.3.4. Fenton oxidation experiments using emulsions as catalyst.....	47
3.4. Inert ceramic membrane reactor.....	48
3.4.1. Reagents.....	48
3.4.2. Membrane reactor set-up and operation.....	48
3.5. Characterisation of aqueous samples.....	49
3.5.1. Phenol and phenol oxidation intermediates	49
3.5.2. Surfactants	51
3.5.3. Metals	52
3.5.4. Hydrogen peroxide	52
3.5.5. TOC	52
3.5.6. COD.....	53
3.5.7. Colour	53
3.5.8. Biodegradability, toxicity and inhibition	53
3.6. Characterisation of membranes.....	57
3.6.1. Streaming potential measurements	57
3.6.2. Microscopic characterisation	58
4. Recovery of iron from aqueous solutions by ultrafiltration	59
4.1. Introduction	59
4.2. Role of the solution chemistry on the iron(III) recovery with ceramic UF membranes	60
4.2.1. Influence of the feed pH	60
4.2.2. Influence of the feed concentration.....	65
4.2.3. Influence of the iron valence.....	67
4.2.4. Influence of the iron chelation.....	70
4.2.5. Influence of the background electrolyte	73

4.3. Cu(II) and Cr(III) filtration with ceramic membranes.....	75
4.4. Membrane MWCO and composition effect on the iron(III) recovery with ceramic membranes.....	80
4.4.1. Streaming potential characterisation	80
4.4.2. Iron(III) filtration with T membranes	82
4.4.3. Iron(III) filtration with F and M5 membranes	85
4.5. Iron(III) recovery with polymeric UF membranes	87
4.6. Conclusions.....	88
5. Recovery of iron from aqueous solutions by nanofiltration	91
5.1. Introduction	91
5.2. Iron(III) and iron(II) recovery	92
5.2.1. Influence of the stirring rate	92
5.2.2. Influence of the transmembrane pressure	94
5.2.3. Influence of the background electrolyte	94
5.2.4. Influence of the iron valence and membrane.....	96
5.3. Iron(III)-EDTA recovery	99
5.4. Conclusions.....	103
6. Treatment of phenol effluents coupling Fenton process and nanofiltration	105
6.1. Introduction	105
6.2. Phenol oxidation pathway by the Fenton process.....	106
6.3. Influence of the hydrogen peroxide dose on the Fenton process and NF efficiency	109
6.3.1. Effect of the hydrogen peroxide dose on the Fenton process efficiency	109
6.3.2. Effect of the membrane on the NF efficiency	113
6.3.3. Effect of the hydrogen peroxide dose on the NF efficiency	117
6.4. Influence of the iron(II) concentration on the Fenton process and NF efficiency	120
6.4.1. Effect of the iron(II) concentration on the Fenton process efficiency...	121
6.4.2. Effect of the iron(II) concentration on the NF efficiency	122
6.5. Membrane cleaning and reusability assessment	125
6.6. Conclusions.....	129
7. Treatment of phenol effluents by surfactant-assisted Fenton process and nanofiltration	131

7.1. Introduction	131
7.2. Fenton oxidation of effluents polluted by phenol and SDS or phenol and CPC.....	132
7.2.1. Influence of the hydrogen peroxide dose on the Fenton process efficiency	133
7.2.2. Influence of the iron(II) concentration on the Fenton process efficiency	138
7.2.3. Influence of the surfactant:cmc ratio on the Fenton process efficiency	142
7.3. Coupling of Fenton process and NF: treatment of effluents containing phenol and SDS	144
7.3.1. Influence of the membrane on the NF efficiency.....	145
7.3.2. Influence of the hydrogen peroxide dose on the NF efficiency.....	148
7.3.3. Influence of the iron(II) concentration on the NF efficiency	150
7.3.4. Influence of the surfactant:cmc ratio on the NF efficiency.....	153
7.4. Conclusions.....	156
8. Treatment of phenol effluents with ferrous emulsions formulated by membrane emulsification	157
8.1. Introduction	157
8.2. Formulation of O/W emulsions	158
8.2.1. Effect of the stirring rate and membrane pore size on the emulsion properties	158
8.2.2. Effect of the SDS concentration on the emulsion properties.....	159
8.2.3. Effect of the %O/W on the emulsion properties	160
8.3. Formulation of ferrous O/W emulsions	161
8.3.1. Formulation of emulsions with iron-containing W_o	161
8.3.2. Addition of iron to previously-prepared emulsions	164
8.4. Oxidation of phenol effluents with ferrous emulsions	168
8.5. Conclusions.....	171
9. Fenton treatment of phenol effluents in an inert membrane reactor	173
9.1. Introduction	173
9.2. Influence of the hydrogen peroxide dose on the membrane reactor performance	174
9.3. Influence of the iron(II) concentration on the membrane reactor performance	176

9.4. Influence of the Reynolds number on the membrane reactor performance...	177
9.5. Oxidation efficiency of tubular versus membrane reactor	179
9.6. Degradation of phenol oxidation intermediates in an inert membrane reactor.....	180
9.7. Conclusions.....	182
10. Conclusions and future work	185
10.1. Conclusions.....	185
10.2. Future work	188
References	189

UNIVERSITAT ROVIRA I VIRGILI

TREATMENT OF BIOREFRACTORY WASTEWATER THROUGH MEMBRANE-ASSISTED OXIDATION PROCESSES

Xavier Bernat Camí

ISBN:978-84-693-1529-3/DL:T-652-2010

List of Figures

Figure 1.1	Annual water withdrawals per capita by country, 2000.....	2
Figure 1.2	Water stress in Europe 2000 versus 2030	3
Figure 1.3	Annual production of surfactants in West Europe 2000-2007.....	9
Figure 1.4	Membrane filtration operation modes.....	19
Figure 1.5	Concentration polarisation phenomenon.....	20
Figure 3.1	Fenton oxidation set-up	32
Figure 3.2	Crossflow filtration set-up.....	38
Figure 3.3	Dead-end filtration set-up.....	39
Figure 3.4	Stirred cell emulsification set-up	43
Figure 3.5	Crossflow membrane emulsification set-up.....	45
Figure 3.6	Inert membrane reactor set-up.....	49
Figure 3.7	Respirometry set-up.....	54
Figure 3.8	DO and OUR profiles of 10 mg/L N-NH ₄ ⁺ obtained in a LFS respirometer	55
Figure 4.1	Filtration of 0.90 mM Fe(III) solution. Effect of the pH on the permeate flux evolution of T5 at several TMP	60
Figure 4.2	Filtration of 0.90 mM Fe(III) solution. Effect of the pH on T5 fouling at several TMP	62
Figure 4.3	Filtration of 0.90 mM Fe(III) solution. Effect of the pH on T5 iron retention at several TMP	63
Figure 4.4	Chemical speciation diagram of a 0.90 mM Fe(III) solution	63
Figure 4.5	Chemical speciation diagram of a Fe(III) solution at pH 2.00 and variable Fe(III) concentration	65
Figure 4.6	Filtration of Fe(III) solutions at pH 2.00. Effect of the Fe(III) concentration on the permeate flux evolution of T5 at several TMP	66
Figure 4.7	Filtration of Fe(III) solutions at pH 2.00. Effect of the Fe(III) concentration on T5 iron retention at several TMP.....	67
Figure 4.8	Chemical speciation diagram of a 0.90 mM Fe(II) solution.....	68
Figure 4.9	T5 permeate flux evolution when filtering binary iron solutions at pH 2.00 and at several TMP	68
Figure 4.10	Fouling percentages obtained when filtering binary iron solutions with T5 at pH 2.00 and at several TMP	69
Figure 4.11	T5 global iron retention when filtering binary iron solutions at pH 2.00 and at several TMP	70

Figure 4.12	Chemical speciation diagram of a 0.90 mM Fe(III) solution at pH 2.00 and variable EDTA concentration	71
Figure 4.13	T5 permeate flux evolution when filtering Fe(III)-EDTA solutions at pH 2.00 and at several TMP	71
Figure 4.14	Fouling percentage obtained when filtering Fe(III)-EDTA solutions with T5 at pH 2.00 and at several TMP	72
Figure 4.15	T5 iron retention when filtering Fe(III)-EDTA solutions at pH 2.00 and at several TMP	73
Figure 4.16	Effect of the NaCl concentration on the permeate flux evolution of T5 at pH 2.00 and at several TMP	74
Figure 4.17	NaCl concentration effect on T5 iron retention at pH 2.00 and at several TMP	74
Figure 4.18	Chemical speciation diagram of a 0.90 mM Cu(II) solution.....	75
Figure 4.19	Chemical speciation diagram of a 0.90 mM Cr(III) solution	76
Figure 4.20	Filtration of 0.90 mM Cr(III) solution. Effect of the pH on the permeate flux evolution of T5 at several TMP	76
Figure 4.21	Filtration of 0.90 mM Cr(III) solution. Effect of the pH on T5 fouling at several TMP	77
Figure 4.22	Filtration of 0.90 mM Cr(III) solution. Effect of the pH on T5 chromium retention at several TMP	77
Figure 4.23	Filtration of Cr(III) solutions at pH 3.80. Effect of the Cr(III) concentration on the permeate flux evolution of T5 at several TMP	78
Figure 4.24	Chemical speciation diagram of a Cr(III) solution at pH 3.80 and variable Cr(III) concentration.....	78
Figure 4.25	Filtration of Cr(III) solutions at pH 3.80. Effect of the Cr(III) concentration on T5 fouling at several TMP	79
Figure 4.26	Filtration of Cr(III) solutions at pH 3.80. Effect of the Cr(III) concentration on T5 chromium retention at several TMP	79
Figure 4.27	Apparent zeta potential of T1, T15 and T50 membranes at several pH	81
Figure 4.28	Apparent zeta potential of F5 and F10 membranes at several pH.....	81
Figure 4.29	Apparent zeta potential of M5 membrane at several pH.....	82
Figure 4.30	Filtration of 0.90 mM Fe(III) solution at pH 2.00. Permeate flux evolution of T membranes at several TMP	83
Figure 4.31	Filtration of 0.90 mM Fe(III) solution at pH 2.00. Iron retention of T membranes at several TMP	84

Figure 4.32	Filtration of 0.90 mM Fe(III) solution at pH 2.00. Fouling of T membranes at several TMP	84
Figure 4.33	Filtration of 0.90 mM Fe(III) solution at pH 2.00. Permeate flux evolution of F and M5 membranes at several TMP	86
Figure 4.34	Filtration of 0.90 mM Fe(III) solution at pH 2.00. Iron retention of F and M5 membranes at several TMP	87
Figure 4.35	Filtration of 0.90 mM Fe(III) solution at pH 2.00. Fouling of F and M5 membranes at several TMP	87
Figure 5.1	Filtration of 0.90 mM Fe(III) solution at pH 2.00 and 6 bar by NF-D. Effect of the stirring rate on the %J _P /J _W and iron retention evolution.....	93
Figure 5.2	Filtration of 0.90 mM Fe(III) solution at pH 2.00 and 300 rpm by NF-D. Effect of the TMP on the %J _P /J _W and iron retention evolution	94
Figure 5.3	Filtration of 0.90 mM Fe(III) solution at pH 2.00, 6 bar and 300 rpm by NF-D. Effect of the NaCl concentration on the %J _P /J _W and iron retention evolution	95
Figure 5.4	Filtration of 0.90 mM Fe solution at pH 2.00, 6 bar and 300 rpm by NF-D. Effect of the iron valence on the %J _P /J _W and iron retention evolution	96
Figure 5.5	Filtration of 0.90 mM Fe solution at pH 2.00, 6 bar and 300 rpm by NF90. Effect of the iron valence on the %J _P /J _W and iron retention evolution	97
Figure 5.6	Filtration of 0.90 mM Fe solution at pH 2.00, 6 bar and 300 rpm by NF270. Effect of the iron valence on the %J _P /J _W and iron retention evolution	98
Figure 5.7	Chemical speciation diagram of a 0.90 mM Fe(III)+0.90 mM EDTA solution.....	100
Figure 5.8	Filtration of 0.90 mM Fe(III)+0.90 mM EDTA solution at 6 bar and 300 rpm by NF-D. Effect of the pH on the %J _P /J _W and iron retention evolution	100
Figure 5.9	Filtration of 0.90 mM Fe(III)+0.90 mM EDTA solution at 6 bar and 300 rpm by NF90. Effect of the pH on the %J _P /J _W and iron retention evolution	101
Figure 5.10	Filtration of 0.90 mM Fe(III)+0.90 mM EDTA solution at 6 bar and 300 rpm by NF270. Effect of the pH on the %J _P /J _W and iron retention evolution	102
Figure 6.1	Fenton oxidation pathway of phenol.....	107

Figure 6.2	Possible condensation products formed in the Fenton oxidation of phenol.....	108
Figure 6.3	Absorbance spectrum of an oxidised phenol effluent after 90 min.....	110
Figure 6.4	Effect of the H ₂ O ₂ dose on the concentration of intermediates after 90 min oxidation.....	112
Figure 6.5	Effect of the membrane on the %J _P /J _W evolution when pre-oxidised effluents are filtered at 6 bar and 30°C	113
Figure 6.6	Effect of the membrane on the normalised fluxes when pre-oxidised effluents are filtered at 6 bar and 30°C.....	114
Figure 6.7	Effect of the membrane on the retention of organics when pre-oxidised effluents are filtered at 6 bar and 30°C.....	114
Figure 6.8	Effect of the membrane on the retention of general parameters when pre-oxidised effluents are filtered at 6 bar and 30°C	116
Figure 6.9	Effect of the H ₂ O ₂ dose on the %J _P /J _W evolution when pre-oxidised effluents are filtered with NF90 at 6 bar and 30°C.....	118
Figure 6.10	Effect of the H ₂ O ₂ dose on the normalised fluxes when pre-oxidised effluents are filtered with NF90 at 6 bar and 30°C.....	118
Figure 6.11	Effect of the H ₂ O ₂ dose on the retention of general parameters when pre-oxidised effluents are filtered with NF90 at 6 bar and 30°C.....	119
Figure 6.12	Effect of the Fe(II) concentration on the concentration of intermediates after 90 min oxidation	121
Figure 6.13	Effect of the Fe(II) concentration on the %J _P /J _W evolution when pre-oxidised effluents are filtered with NF90 at 6 bar and 30°C.....	123
Figure 6.14	Effect of the Fe(II) concentration on the normalised fluxes when pre-oxidised effluents are filtered with NF90 at 6 bar and 30°C.....	123
Figure 6.15	Effect of the Fe(II) concentration on the retention of general parameters when pre-oxidised effluents are filtered with NF90 at 6 bar and 30°C.....	124
Figure 6.16	Micrographies of virgin and used NF90 membrane.....	126
Figure 6.17	Effect of the membrane reusability on the %J _P /J _W evolution when pre-oxidised effluents are filtered with NF90 at 6 bar and 30°C.....	127
Figure 6.18	Effect of the membrane reusability on the normalised fluxes when pre-oxidised effluents are filtered with NF90 at 6 bar and 30°C.....	128
Figure 6.19	Effect of the membrane reusability on the retention of general parameters when pre-oxidised effluents are filtered with NF90 at 6 bar and 30°C.....	128

Figure 7.1	Effect of the H ₂ O ₂ dose and surfactant presence on phenol conversion.....	134
Figure 7.2	Effect of the H ₂ O ₂ dose on the organic compounds' concentration after 90 min oxidation.....	137
Figure 7.3	Effect of the Fe(II) concentration and surfactant presence on phenol conversion.....	138
Figure 7.4	Effect of the Fe(II) concentration on the organic compounds' concentration after 90 min oxidation	141
Figure 7.5	Effect of the [surf]:cmc on the organic compounds' concentration after 90 min oxidation.....	144
Figure 7.6	Effect of the membrane on the %J _p /J _w evolution when pre-oxidised effluents are filtered at 6 bar and 30°C.....	145
Figure 7.7	Effect of the membrane on the normalised fluxes when pre-oxidised effluents are filtered at 6 bar and 30°C.....	146
Figure 7.8	Effect of the membrane on the retention of general parameters when pre-oxidised effluents are filtered at 6 bar and 30°C	147
Figure 7.9	Effect of the H ₂ O ₂ dose on the %J _p /J _w evolution when pre-oxidised effluents are filtered with NF90 at 6 bar and 30°C.....	148
Figure 7.10	Effect of the H ₂ O ₂ dose on the normalised fluxes when pre-oxidised effluents are filtered with NF90 at 6 bar and 30°C.....	149
Figure 7.11	Effect of the H ₂ O ₂ dose on the retention of general parameters when pre-oxidised effluents are filtered with NF90 at 6 bar and 30°C.....	150
Figure 7.12	Effect of the Fe(II) concentration on the %J _p /J _w evolution when pre-oxidised effluents are filtered with NF90 at 6 bar and 30°C.....	151
Figure 7.13	Effect of the Fe(II) concentration on the normalised fluxes when pre-oxidised effluents are filtered with NF90 at 6 bar and 30°C.....	152
Figure 7.14	Effect of the Fe(II) concentration on the retention of general parameters when pre-oxidised effluents are filtered with NF90 at 6 bar and 30°C.....	152
Figure 7.15	Effect of the [surf]:cmc on the %J _p /J _w evolution when pre-oxidised effluents are filtered with NF90 at 6 bar and 30°C.....	154
Figure 7.16	Effect of the [surf]:cmc on the normalised fluxes when pre-oxidised effluents are filtered with NF90 at 6 bar and 30°C.....	154
Figure 7.17	Effect of the [surf]:cmc on the retention of general parameters when pre-oxidised effluents are filtered with NF90 at 6 bar and 30°C ..	155
Figure 8.1	Effect of the stirring rate and membrane pore size on the D[3,2], D[4,3] and Span.....	158

Figure 8.2	Effect of the %SDS in W_o on the D[3,2], D[4,3] and Span	159
Figure 8.3	Effect of the %O/W on the D[3,2], D[4,3] and Span.....	160
Figure 8.4	Effect of the [Fe(II)] in W_o on the D[3,2], D[4,3] and Span evolution	162
Figure 8.5	Effect of the %O/W on the D[3,2], D[4,3] and Span of emulsions prepared with Fe(II) in W_o	163
Figure 8.6	Effect of the [Fe(II)] in W_n on the D[3,2], D[4,3] and Span evolution	165
Figure 8.7	Effect of the [Fe(II)] in W_n on the %O/W evolution.....	166
Figure 8.8	Effect of the [Fe(II)] in W_n on the D[3,2], D[4,3] and Span evolution	167
Figure 8.9	Effect of the [Fe(II)] in W_n on the %O/W evolution.....	167
Figure 8.10	Optical micrographies at 20x of a virgin emulsion (A) and after replacing its continuous phase by a 15 mg/L Fe(II) solution (B)	168
Figure 8.11	Effect of the [Fe(II)] in W_o on the average phenol removal	169
Figure 9.1	Effect of the H_2O_2 dose on phenol and TOC conversion	175
Figure 9.2	Effect of the H_2O_2 dose on the distribution of intermediates	175
Figure 9.3	Effect of the Fe(II) concentration on phenol and TOC conversion	176
Figure 9.4	Effect of the Fe(II) concentration on the distribution of intermediates ...	177
Figure 9.5	Effect of the Re_{out} on phenol and TOC conversion	178
Figure 9.6	Effect of the Re_{out} on the distribution of intermediates	178
Figure 9.7	Effect of the reactor configuration on the distribution of intermediates .	180
Figure 9.8	Oxidation of phenol intermediates in an inert membrane reactor	181

List of Tables

Table 1.1	Water resources and annual withdrawals, 2000.....	2
Table 1.2	Impacts of alternative water resources on various vectors	5
Table 1.3	European emissions of phenolic compounds to water in 2004	8
Table 1.4	Operation conditions and limitations of direct oxidation processes.....	11
Table 1.5	Standard reduction potential of common oxidants.....	11
Table 1.6	Classification of conventional AOP's.....	13
Table 1.7	Membrane processes classification as function of the driving force	17
Table 1.8	Short review of studies coupling oxidation and aerobic biological treatment for the detoxification of phenolic wastewaters	22
Table 3.1	Properties of model pollutants.....	32
Table 3.2	Sources of heavy metals and cleaning agents	34
Table 3.3	Ceramic UF membranes' properties.....	35
Table 3.4	Polymeric UF membranes' properties	36
Table 3.5	Polymeric NF membranes' properties	37
Table 3.6	Phenol and its Fenton oxidation intermediates analysed by HPLC	50
Table 4.1	Filtration of 0.90 mM Fe(III) solution. Effect of the pH and TMP on T5 additional resistance	61
Table 4.2	Filtration of Fe(III) solutions at pH 2.00. Effect of the Fe(III) concentration and TMP on T5 additional resistance.....	66
Table 4.3	T5 additional resistance when filtering binary iron solutions at pH 2.00 and at several TMP	69
Table 4.4	Filtration of 0.90 mM Fe(III) solution at pH 2.00 with T membranes. Effect of the membrane on the additional resistance	83
Table 4.5	Filtration of 0.90 mM Fe(III) solution at pH 2.00 with F and M5 membranes. Effect of the membrane on the additional resistance	86
Table 5.1	0.90 mM Fe(III) solution speciation at pH 2.00.....	94
Table 5.2	% J_P/J_w and iron retention by NF-D, NF90 and NF270. Filtration of 0.90 mM Fe(III) or Fe(II) solution at pH 2.00, 6 bar and 300 rpm	99
Table 5.3	% J_P/J_w and iron retention by NF-D, NF90 and NF270. Filtration of 0.90 mM Fe(III)+0.90 mM EDTA solution at 6 bar and 300 rpm	102
Table 6.1	Properties of the organic compounds identified.....	109
Table 6.2	Effect of the H ₂ O ₂ dose on the conversion and colour formation after 90 min oxidation.....	110
Table 6.3	%ID and biodegradability parameters of the effluents after Fenton and after NF.....	117

Table 6.4	Effect of the H ₂ O ₂ dose on the %ID and biodegradability parameters of the effluents after Fenton and after NF.....	120
Table 6.5	Effect of the Fe(II) concentration on the conversion and colour formation after 90 min oxidation.....	122
Table 6.6	Effect of the Fe(II) concentration on the %ID and biodegradability parameters of the effluents after Fenton and after NF.....	125
Table 6.7	Elemental composition of virgin and used NF90 membrane.....	127
Table 7.1	Effect of the H ₂ O ₂ dose and surfactant presence on phenol, surfactants' and TOC conversion after 90 min oxidation	135
Table 7.2	Effect of the Fe(II) concentration and surfactant presence on phenol, surfactants' and TOC conversion after 90 min oxidation	139
Table 7.3	Effect of the [surf]:cmc on phenol, surfactants' and TOC conversion after 90 min oxidation	143
Table 7.4	%ID of the effluents after Fenton and after NF.....	147
Table 7.5	Effect of the H ₂ O ₂ dose on the %ID of the effluents after Fenton and after NF.....	150
Table 7.6	Effect of the Fe(II) concentration on the %ID of the effluents after Fenton and after NF.....	153
Table 7.7	Effect of the [surf]:cmc on the %ID of the effluents after Fenton and after NF.....	155
Table 8.1	Effect of the stirring rate and membrane pore size on ESI	159
Table 8.2	Effect of the %SDS in W _o on ESI	160
Table 8.3	Effect of the %O/W on ESI.....	161
Table 8.4	Effect of the [Fe(II)] in W _o on ESI, remaining %O/W and final [Fe(II)] in W.....	162
Table 8.5	Effect of the %O/W on ESI, remaining %O/W and final [Fe(II)] in W of emulsions prepared with Fe(II) in W _o	164
Table 8.6	Effect of the [Fe(II)] in W _o on ESI of emulsions tested for phenol oxidation.....	170
Table 9.1	Effect of the reactor configuration on phenol, TOC and H ₂ O ₂ conversion	179
Table 9.2	Distribution of by-products of the oxidation of phenol intermediates in an inert membrane reactor	182

Nomenclature and abbreviations

AAS	Atomic absorption spectrometry
Abs	Absorbance
Ads	Mass of solute adsorbed onto the membrane (mol or g)
%Ads	Percentage of solute adsorption onto the membrane
A_f	Membrane filtration area (cm^2)
AOP	Advanced oxidation process
BOD	Biological oxygen demand (mg/L or mmol/L)
C_f	Feed concentration (mg/L or mmol/L)
$C_{f,\text{initial}}$	Initial feed concentration (mg/L or mmol/L)
cmc	Critical micellar concentration (mg/L or mmol/L)
COD	Chemical oxygen demand (mg/L or mmol/L)
$\text{COD}_{\text{added}}$	Added COD (mg/L)
$\%\text{COD}_{\text{rb}}$	Percentage of readily-biodegradable COD
C_p	Permeate concentration (mg/L or mmol/L)
CPC	Cetylpyridinium chloride
$C_{p,\text{final}}$	Final permeate concentration (mg/L or mmol/L)
$C_{R,\text{final}}$	Final retentate concentration (mg/L or mmol/L)
CWAO	Catalytic wet air oxidation
$D[0.1]$	Droplet diameter below which 10% of sample lies (μm)
$D[0.5]$	Droplet diameter at which 50% of sample is smaller/larger (μm)
$D[0.9]$	Droplet diameter below which 90% of sample lies (μm)
$D[3,2]$	Surface weighted mean diameter or Sauter diameter (μm)
$D[4,3]$	Volume weighted mean diameter or De Broukere diameter (μm)
D_i	Droplet diameter in class i (μm)
DO	Dissolved oxygen
EDDA	Ethylenediaminedisuccinate
EDS	Energy dispersive spectroscopy
EDTA	Ethylenediaminetetraacetic acid
ESEM	Environmental scanning electron microscopy
ESEM-EDS	ESEM coupled to EDS
ESI	Emulsion stability index
HPLC	High-performance liquid chromatography
i	Van't Hoff factor
%ID	Sample identification percentage
IEP	Isoelectric point

IS	Ionic strength (mg/L or mmol/L)
J_a	Permeate flux after filtration ($L/h \cdot m^2$)
J_{ac}	Permeate flux after chemical cleaning ($L/h \cdot m^2$)
J_p	Permeate flux during filtration ($L/h \cdot m^2$)
J_w	Clean membrane permeate flux ($L/h \cdot m^2$)
$k_L \cdot a$	Oxygen mass transfer coefficient (min^{-1})
LFS	Liquid-flow static
M	Molar concentration (mol/L)
MBAS	Methylene blue active substances
MBR	Membrane bioreactor
MEUF	Micellar-enhanced ultrafiltration
MF	Microfiltration
MW	Molecular weight (g/mol)
MWCO	Molecular weight cut-off (Da or kDa)
n_c	Number of channels in membrane element
NDIR	Non-diffractive infrared
NF	Nanofiltration
NHE	Normal hydrogen electrode
NHP 2001	National Hydrological Plan 2001
n_i	Number of droplets in class i (μm)
NPOC	Non-purgeable organic carbon
OC	Oxygen consumption (mg/L)
OUR	Oxygen uptake rate (mg DO/L \cdot min)
OUR_{end}	Endogenous oxygen uptake rate (mg DO/L \cdot min)
OUR_{ex}	Exogenous oxygen uptake rate (mg DO/L \cdot min)
OUR_{MAX}	Maximum oxygen uptake rate (mg DO/L \cdot min)
O/W	Oil-in-water
%O/W	Percentage of oil-in-water
PA	Polyamide
PA_p	Semi-aromatic piperazine-based polyamide
PES	Polyethersulfone
PEUF	Polymer-enhanced ultrafiltration
PS	Polysulfone
PWP	Pure water permeability ($L/h \cdot m^2 \cdot bar$)
R	Gas constant (0.083 bar \cdot L/K \cdot mol)
R(%)	Retention percentage
R_a	Additional resistance (m^{-1})

Re_{out}	Reynolds number calculated in the reactor outlet stream
R_m	Membrane resistance (m^{-1})
RO	Reverse osmosis
R_t	Total resistance (m^{-1})
SDS	Sodium dodecylsulphate
%SDS	Percentage of SDS in the continuous phase
S_o	Dissolved oxygen concentration (mg/L)
S_{oe}	Equilibrium oxygen concentration (mg/L)
S_{oMIN}	Minimum dissolved oxygen concentration (mg/L)
[surf]	Surfactant concentration (mg/L or mmol/L)
SWAO	Supercritical wet air oxidation
T	Temperature ($^{\circ}C$ or K)
TFC	Thin-film composite
TMP	Transmembrane pressure (bar)
TOC	Total organic carbon (mg/L or mmol/L)
TSS	Total suspended solids (mg/L)
UF	Ultrafiltration
V_f	Feed solution volume (mL)
V_P	Total permeate volume (mL)
V_R	Final retentate volume (mL)
VRF	Volume reduction factor
VSS	Volatile suspended solids (mg/L)
WAO	Wet air oxidation
WEI	Water exploitation index
W_n	New continuous phase
W_o	Original continuous phase
WWTP	Wastewater treatment plant
X(%)	Conversion percentage
Y_H	Heterotrophic yield coefficient
α	Dissociation constant
ϕ	Membrane internal diameter (mm)
λ	Wavelength (nm)
μ	Dynamic viscosity (Pa·s)
π	Osmotic pressure (bar)
ω	Stirring rate (rpm)
ζ	Zeta potential (mV)

UNIVERSITAT ROVIRA I VIRGILI

TREATMENT OF BIOREFRACTORY WASTEWATER THROUGH MEMBRANE-ASSISTED OXIDATION PROCESSES

Xavier Bernat Camí

ISBN:978-84-693-1529-3/DL:T-652-2010

CHAPTER 1

Introduction

1.1. Water scarcity and alternative water resources

Water is an invaluable natural resource essential to ensure the adequate development of human life. The fast economic development and the human population raise have increased freshwater withdrawals (The United Nations World Water Development Report 3, 2009). Around 300 km³ of water are annually abstracted in Europe (European Environment Outlook, 2005), representing an average of 500 m³ per capita/year. An average of 600 m³ of water per capita/year is abstracted in the world. (Water resources across Europe – confronting water scarcity and drought, 2009)

Water abstraction strongly depends on the geographical region, as shown in Figure 1.1. Generally, where irrigation is most required for agriculture (arid and semi-arid regions), water withdrawal is obviously higher. For this reason, those regions abstract higher water volumes than tropical countries do (The United Nations World Water Development Report 3, 2009).

As Table 1.1 illustrates, in Europe, around 32% of abstracted water is used for agricultural purposes whilst industrial and domestic applications employ 53% and 15% of total abstracted water, respectively. However, as it can be seen in Table 1.1, agriculture is in many regions the main water user. From the previous data, it can be summarised that water use is strongly affected by geographic factors, which is in turn linked to water culture and social development and not only to final use of water. After its use, a fraction of the used water is treated and returned to the water body. However, the other fraction is consumed or evaporated (Water resources across Europe –

confronting water scarcity and drought, 2009). In consequence, water is an unbalanced resource due to its losses.

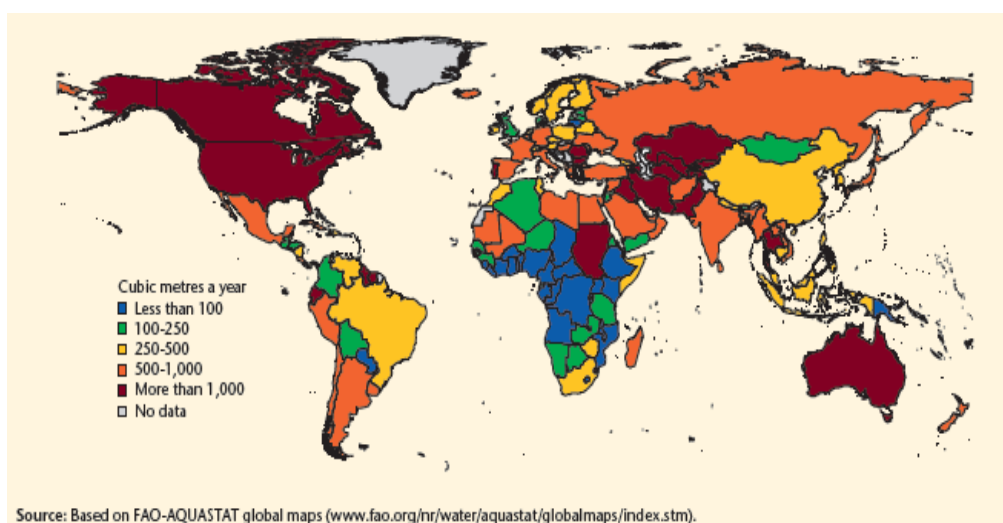


*Figure 1.1. Annual water withdrawals per capita by country, 2000
 (The United Nations World Water Development Report 3, 2009)*

*Table 1.1. Water resources and annual withdrawals, 2000
 (The United Nations World Water Development Report 3, 2009)*

Region	Renewable water resources (km ³)	Total water Withdrawals (km ³)	Water withdrawals						Withdrawals as percentage of renewable resources
			Agriculture		Industry		Domestic (urban)		
			Amount (km ³)	%	Amount (km ³)	%	Amount (km ³)	%	
Africa	3936	217	186	86	9	4	22	10	5.5
Asia	11594	2378	1936	81	270	11	172	7	20.5
Latin America	13477	252	178	71	26	10	47	19	1.9
Caribbean	93	13	9	69	1	8	3	23	14.0
North America	6253	525	203	39	252	48	70	13	8.4
Oceania	1703	26	18	73	3	12	5	19	1.5
Europe	6603	418	132	32	223	53	63	15	6.3
World	43659	3829	2663	70	784	20	382	10	8.8

Source: Based on Comprehensive Assessment of Water Management in Agriculture 2007

Globally, freshwater can be obtained from natural sources such as groundwater and surface water among other alternative sources, which can include rainwater harvesting, groundwater recharge, desalination and reuse of regenerated water. The main source of freshwater in Europe is surface water followed by groundwater. In Spain and Cyprus, desalted water also accounts a small fraction of water supply (EU Water Saving Potential - Part 1, 2007).

The population in the world is increasing at a rate of 80 million people/year. An increase of around 64 billion cubic meters of freshwater a year is consequently required to satisfy their needs. Around 90% of the 3 milliard people expected to be added to the population by 2050 will live in developing countries. In those countries, sustainable access to safe drinking water and adequate sanitation is not guaranteed (The United Nations World Water Development Report 3, 2009). In addition, by 2080, climate change could contribute to the increase on the number of people facing water scarcity problems (Human Development Report 2007/2008, 2007). Thus, an important part of humans will suffer from a variety of water and sanitation problems. The Water Exploitation Index (WEI) is an indicator of stress on freshwater and is calculated as the ratio of total freshwater withdrawal to the total renewable source. A WEI higher than 20% indicates that the water resource is under stress whilst a WEI higher than 40% implies a situation of severe water stress and clearly indicates that an unsustainable and inadequate use of water resources is occurring (Raskin et al. 1997). As Figure 1.2 shows, water stress in European countries will be aggravated in a near future due to the increase of the WEI in some regions.

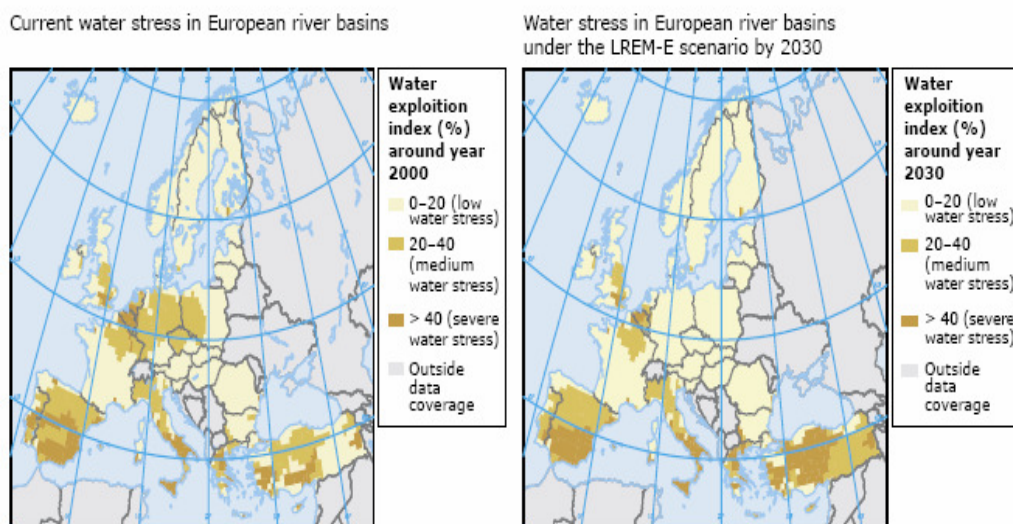


Figure 1.2. Water stress in Europe 2000 versus 2030
(European Environment Outlook, 2005)

Although WEI calculation from national estimates is a useful water stress indicator, special attention has to be focused on particular situations. For example, although the average national WEI of Spain is around 34%, the southern river basins of Andalucia and Segura have extremely high WEI values of 164% and 127%, respectively (Water resources across Europe – confronting water scarcity and drought, 2009). A survey completed in 2007 demonstrated that Spanish and Portuguese river basins led the classification of the most-stressed river basins among the 35 total surveyed European river basins (Water resources across Europe – confronting water scarcity and drought, 2009). Thus, water-related problems are evident in those regions and need to be softened and, if possible, eliminated in the upcoming years.

As aforementioned, the population will grow and the predicted water stress increase in the following years. Thus, efficient water management measures have to be adopted to ensure water availability to future generations. This passes through the use of alternative water resources or through the implementation of technologies helping to increase the preservation of the natural sources or to use it more efficiently.

Alternative water supply options play a crucial role in water conservation. Alternative technologies are those representing a non-conventional way of abstracting and/or producing water. Due to their essential importance for the sustainable development, they must be adequately developed and installed. Main alternative water supply technologies include desalination, rainwater harvesting, groundwater recharge and wastewater reuse (Assessment of alternative water supply options, 2008). Table 1.2 reviews the benefits and risks of the abovementioned alternative technologies. As noted in the table, the four alternative water supply technologies have advantages and inconveniences. Thus, a suitable study of every particular situation has to be carried out to correctly decide which alternative water supply option has to be installed so that society benefits are maximised and both environmental impact and economic costs reduced. Despite the alternative technologies' risks, the implementation of an alternative water supply option will always help to increase water availability and even water quality. Hence, evaluation of associated risks to the implementation of an alternative water supply technology must be evaluated keeping in mind the importance of the intrinsic benefit to water availability and quality.

In Spain, vast efforts are being invested in desalted water production and wastewater reuse alternatives, especially for irrigation purposes. Regenerated water uses in function of produced water quality are currently regulated by the Spanish Water Act 1620/2007. In Spain, the AGUA programme is decisive for the implementation of urgent tools to satisfy water demand. In 2004, the AGUA programme (*Actuaciones para la Gestión y la Utilización del Agua – Water Management and Use Action Programme*) was born as an alternative to the National Hydrological Plan of 2001 (NHP 2001 – *Plan Hidrológico Nacional*). The NHP 2001 pretended to transfer about 1 Mm³ from the Ebro river basin to the Catalanian, Jucar, Segura and South basins. The aim of the NHP 2001 was to satisfy water necessities to regions presenting a water deficit by transporting water from high-capacity rivers. The NHP 2001 was rapidly discussed and, after a long debate, the Spanish Water Act 11/2005 amended the NHP 2001 and refused the rules about the Ebro water transfer. The AGUA programme approved a number of urgent priority actions to increase water availability in Mediterranean basins. This goal is being achieved through the implementation of actions to improve management in wastewater reuse and saving as well as through the installation of desalination plants (Assessment of alternative water supply options, 2008). As result, Spain has nowadays the forth-largest desalination capacity in the world after Saudi Arabia, USA, and Kuwait. Despite the importance of desalination in Spain, it has not to be considered an ideal and unique alternative option and has to consequently coexist with other technologies such as wastewater reuse and new policies to improve water demand management (Conditions for the sustainable development of alternative water supply options, 2008).

Wastewater reuse in Spain has been promoted by, apart from the AGUA programme, the National Irrigation Plan, which incentives regenerated water use for irrigation (Assessment of the risks and impacts of four alternative water supply options, 2008). Despite those efforts, in 2005, Spain only reused 496 hm³ of treated wastewater over a total of 5.015 hm³. 80% of this amount is used for agricultural applications (Water Supply and wastewater treatment in Spain, 2006). Thus, there is still an imperative work to be developed in terms of extending wastewater reuse practices.

Table 1.2. Impacts of alternative water resources on various vectors (adapted from Assessment of alternative water supply options, 2008 and Potential impacts of desalination development on energy consumption, 2008)

Desalination		
Impact to	Benefits	Risks
Environment	- Reduces demand on main water sources	- Increase on greenhouse gas emissions (if fuel is used) - Aquifer/marine environment damage
Economy	- Encouragement of general development - Supports new economic activities	- High capital and operation costs because of plants location and energy needs
Society	- It is a reliable water source in arid regions	- Value of land can be affected by plants location
Rainwater harvesting		
Impact to	Benefits	Risks
Environment	- Reduces demand on main water sources - Reduces amount of urban storm runoff	- Not identified
Economy	- Decreases water costs paid by households or industry	- Required financing of large storage tanks in regions with poor rainfall
Society	- Not identified	- Assumption of poor water quality - Difficulty for poorer families to have access because of high investments needed - Tenants do not have opportunity to reap the benefits of lower costs
Groundwater recharge		
Impact to	Benefits	Risks
Environment	- Reduces over-exploitation of aquifers - Decreases seawater intrusion in costs/aquifers	- Environmental pollution and human health effects in case of non-strict quality controls
Economy	- Small and cost-effective storage structures are needed	- Extensive and expensive wastewater treatments required
Society	- Employable for many uses - Allowed in many EU regions	- People can refuse consumption of products linked to groundwater recharge (the “yuk” factor)
Wastewater reuse		
Impact to	Benefits	Risks
Environment	- Reduces freshwater demand - Pollution reduction in rivers and groundwater by nutrients	- Strict quality controls for avoiding human health effects and environmental contamination
Economy	- Low / medium capital costs - Capital costs are recoverable in short times	- Economically unfeasible because additional distribution network is needed
Society	- Employable for many uses - Allowed in many EU regions	- People can refuse consumption of products associated to wastewater reuse (the “yuk” factor)

The Spanish Water Act 1620/2007 determines chemical, physical and microbiological limit quality parameters required for several regenerated water uses. Despite the continuous increase on the number of wastewater treatment plants (WWTP's) and more especially of urban WWTP's, an immense work has to be carried out in terms of WWTP's installation and development. As a clear example, in 2005, about 55% of households were connected to municipal sewage plants (Environmental Performance reviews: Spain, Paris, 2004). At the municipal sewage plants, 40% of wastewater received secondary treatment and only 3% received tertiary treatment (Effectiveness of urban wastewater treatment policies in selected countries: an EEA pilot study, 2005). Tertiary treatment is required for satisfying the qualities needed for treated wastewater reuse applications. The Spanish authorities indicated in 2003 that 46 of 114 cities had not yet installed the advanced treatment required by 1998. Thus, this undoubtedly confirms that significant efforts have to be made in wastewater treatment development and implementation in Spain in the near future to ensure sustainable development and more especially water availability and quality.

1.2. Water and wastewater in industry

In Europe, more than fifty percent of withdrawn water is used in industrial applications. In 2000, worldwide water withdrawal for industrial purposes was 784 km³/year (The United Nations World Water Development Report 3, 2009). According to UNESCO predictions, the annual water volume used by industry will rise to 1170 km³ in 2025. Water consumption can be linked to product quality and, in consequence, better final product qualities may be associated to higher water requirements for its manufacture. This has been particularly shown by chemical, paper and textile industries (EU Water Saving Potential - Part 1, 2007). Thus, water consumption can be raised in a certain country by an increase on industrial activity, inherent to human evolution.

Huge amounts of water are used in industrial sectors such as pulp & paper, textile, leather (tanning), chemical, oil and gas, pharmaceutical, food, energy and metal. In addition, water is the most-used solvent in industry. It is concretely used for cooling, heating, cleaning and washing, transport and as part of final products and/or as raw material. Thus, water is used in a high variety of industrial processes and for many purposes.

The total amount of different chemicals produced is vast and continuously increasing. About 100000 different chemicals can be found in the market (Charpentier 2003). Despite their different properties and uses, their production processes are very similar. The need and use of water in chemical and pharmaceutical processes is defined by the required unit operations, raw materials and process equipment. The majority of water is typically used in unit operations and wastewater is generated in them. Wastewater can appear from raw materials production and/or conditioning but it can also be generated during reaction processes and/or to control process conditions. In consequence, regardless of its origin, wastewater is produced in industrial processes and its quality and volume depends on the chemicals manufactured and the unit processes chosen. As a rule of thumb, 20% of total wastewater flow from chemical and pharmaceutical industries contains 80% of the pollutant load (EU Water Saving Potential - Part 1, 2007).

Toxic and complex effluents are produced in industrial processes. As abovementioned, pollutants nature and composition varies in function of the industrial sector. However, effluents polluted with toxic, persistent or difficult-to-degrade compounds are typically produced in industrial processes. Industrial wastewaters, together with those municipal

are the most important source of water pollution. In consequence, if they are directly disposed of to the nature, environmental hazards will arise from. Thus, efficient remediation technologies have to be implemented to avoid environmental pollution. Municipal wastewaters are treated in conventional municipal WWTP's. Non-conventional wastewater treatments are generally required to abate and/or degrade pollutants contained in industrial effluents due to their complex nature. The variable composition and flowrates of industrial effluents also make necessary the use of alternative treatments. Thus, designing efficient and cost-effective industrial wastewater treatment processes is indispensable for ensuring a sustainable technological development.

In addition to the design of efficient industrial wastewater treatment schemes, additional water saving measures should be studied and implemented in industry. Water saving measures include changes in production processes, reduction in wastage and leakage, water recycling and reuse, changes in cooling technology, on-site rainwater harvesting and implementation of classical water devices considered for the household sector (EU Water Saving Potential - Part 1, 2007). Water saving measures, apart from the evident water pollution lessening, can also contribute to decrease the production costs due to the direct water consumption reduction. Auditing of water quality and quantity is needed to choose the appropriate water saving technology for each particular situation.

1.2.1. Industrial wastewater model pollutants

Phenols, surfactants, pesticides, herbicides, aromatic hydrocarbons, among many others are typically found in industrial effluents (Dojilido and Best 1993). Those substances are examples of toxic and therefore non-biodegradable organic pollutants. Their persistence to the environment has been demonstrated and, many times, the symptoms of contamination may not manifest themselves until several generations after initial contact with the chemical of concern (Stirling 2001). Thus, wastewaters containing such non-biodegradable pollutants need to be treated and pollutants removed so that to avoid associated environmental pollution.

Phenol is a white crystalline solid at room temperature. It is both the simplest hydroxybenzene and the most commercially important. Nowadays, all produced phenol is obtained through cumene peroxidation. In 2008, bisphenol-A accounted for 44% of total phenol production in 2007, followed by phenol-formaldehyde resins at 27% (Chemical Industries Newsletter – July 2008). In 2004, global production of phenol was nearly 8 million tones. A phenol production of around 14 million tones of phenol is estimated for 2011 (Chemical Economics Handbook – November 2007).

Phenolic effluents are discharged to the environment in large amounts every year. As Table 1.3 summarises, in 2004, around 500 tones of phenol were directly discharged to water in Europe and around 2000 tones were indirectly discharged. Direct discharges include emissions from facilities directly to water whilst indirect ones are emissions transferred from facilities to off-site wastewater treatment plants. Around 44% of direct emissions of phenolic compounds were released in Spain, positioning it as the largest emissary country in 2004. Concerning the indirect emissions, Spain was the tenth indirect emissary country. The previous percentages clearly indicate that inefficient and/or insufficient wastewater treatments are applied in Spain in terms of phenolic effluents decontamination. This evidence is highlighted by the fact that phenol, the simplest phenolic compound, is a priority substance (EC 1179/94, OJ L131, 26.5.94, p.3) under the Regulation 793/93. Thus, significant efforts have to be invested in Spain

in developing efficient, green and cost-effective treatments of phenol effluents. Due to the significance of phenolic emissions in Spain, phenol has been selected as main model pollutant in this research.

Table 1.3. European emissions of phenolic compounds to water in 2004 (EPER)

Country	Direct emissions		Indirect emissions	
	Total (t/year)	% of European emissions	Total (t/year)	% of European emissions
Latvia	-	-	0.208	0.01
Slovenia	-	-	0.125	0.01
Portugal	0.1138	0.02	3.15	0.14
Finland	0.156	0.03	3.56	0.16
Austria	0.47	0.09	340.13	15.63
Denmark	0.4645	0.09	1.20	0.06
Ireland	0.692	0.13	0.049	0.00
Belgium	0.7162	0.14	2.28	0.10
Czech Republic	0.9623	0.18	611.60	28.10
Hungary	1.34	0.26	-	-
Greece	1.85	0.36	-	-
Netherlands	3.07	0.59	22.20	1.02
Slovakia	3.13	0.60	108.00	4.96
Sweden	7.82	1.50	-	-
Germany	13.45	2.58	841.97	38.68
Italy	21.75	4.17	149.82	6.88
France	35.54	6.82	10.13	0.47
Poland	38.13	7.32	18.99	0.87
United Kingdom	162.38	31.16	55.47	2.55
Spain	229.06	43.96	7.82	0.36
Total	521.10	100.00	2176.70	100.00

On the other hand, surfactants are chemicals designed to show cleaning and solubilisation properties. Their molecules have a polar head group (charged or uncharged) and a non-polar hydrocarbon tail. Surfactants are commonly classified according to their ionic properties and thus grouped as anionic (negatively-charged), cationic (positively-charged), non-ionic (uncharged) and amphoteric (either positively- or negatively-charged depending on the pH). Thanks to their configuration, surfactants are used in cleaning and personal care formulations, textiles, household and industrial detergents, paints, polymers, pesticide formulations, pharmaceutical, mining, oil recovery and pulp & paper industry (Ying 2006). The production of surfactants has increased over the last years. In 2000, 2.5 Mt/year of surfactants were produced in

Western Europe countries. In 2007, surfactants' production had already shifted to 3.00 Mt/year, according to CESIO (*Comité Européen des Agents de Surface et leurs Intermédiaire Organiques*) statistics for surfactants' production in 2007 (CESIO Statistics 2006/2007, 2008). The statistics surveyed Western European companies, representing more than 90% of the European surfactants' market (CESIO News – June 2008). As it can be seen in Figure 1.3, non-ionic surfactants are the most produced type of surfactant followed by anionic ones. Cationic and amphoteric surfactants production is quite lower than those non-ionic and anionic. Due to the significant production and its associated use in surfactant-based formulations, wastewaters containing surfactants are generally encountered.

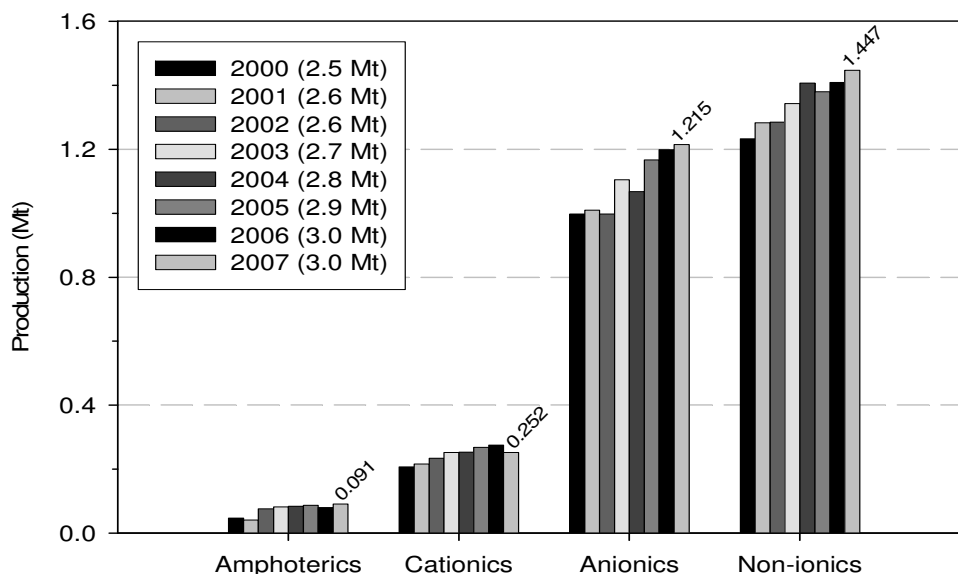


Figure 1.3. Annual production of surfactants in West Europe 2000-2007 (CESIO Statistics 2006/2007, 2008)

Surfactant-containing wastewaters directly discharged to rivers cause foam formation and may origin anomalies to algae growth and toxicity to aquatic organisms. In addition, due to the uncontrolled use of surfactants and detergents in the past, both in the chemical industry and domestically, drinking water polluted by surfactants was identified (Tabor and Barber 1996). For those reasons, surfactant-containing wastewaters have to be treated prior to be disposed of to the final receptor. Aerobic biological treatment processes have been found to be effective for the degradation of some surfactants. On the contrary, anaerobic degradation has not shown to be efficient for the same purpose (CESIO Recommendation for the classification of and labelling of surfactants as “dangerous for the environment”, 2007). Even though biological treatment has been applied for the decontamination of surfactant-containing wastewaters, the process still suffers from foaming problems, retarded biodegradation of co-contaminants and decreased activity of the activated sludge. Consequently, alternative wastewater treatment schemes have to be designed and tested to avoid operation problems found in conventional biological treatments by the presence of surfactants (Masuyama et al. 2000). For those reasons, surfactants have also been considered as model industrial water pollutants in this study. Sodium dodecylsulphate (SDS) and cetylpyridinium chloride (CPC) have been selected as anionic and cationic model surfactants, respectively. In addition, the degradation of mixed phenol and surfactant effluents has been considered to simulate complex wastewaters.

1.3. Industrial wastewater treatment

Wastewater treatment technologies have to guarantee the required quality of the treated effluents for its final use. Thus, depending on whether the treated effluent will be reused in the process or rejected, treatment requirements will vary. There exist a high number of wastewater treatment processes (and their combinations) that could fulfil regulation requirements in treated waters. Thus, an intensive labour in R&D is needed for designing, testing and installing efficient and inexpensive wastewater treatments depending on polluted effluents and their projected final quality. This work is focused on the study of the treatment of polluted effluents containing organic compounds. Other sources of contamination will not be accordingly discussed.

Biological treatment is the most used technology to degrade organic compounds present in municipal wastewater treatment plants. Aerobic processes are most employed than anaerobic ones owing to their simple operation and high efficiency (Ruiz et al. 1992). Industrial wastewaters are complex, variable and often contain biorefractory or troubling compounds. Biorefractory substances cannot be directly treated in those systems because of their resistance, inhibitory character or toxicity. Accordingly, industrial wastewaters often have to be treated by non-conventional technologies able to render them adequate for their final use. Phenols and surfactants are an example of these compounds. Phenolic effluents cannot be directly treated in a biological system because of its inherent toxicity (González 1993). In turn, surfactants cannot be driven to the biological treatment because of the foam formation, retarded co-contaminant degradation and activated sludge deactivation (Masuyama et al. 2000).

1.3.1. Oxidation in industrial wastewater treatment

Oxidation processes have been widely studied as efficient treatments to degrade biorefractory substances. Incineration, Wet Air Oxidation (WAO), Catalytic Wet Air Oxidation (CWAO), Supercritical Wet Air Oxidation (SWAO) are direct oxidation technologies able to degrade organic compounds present in water. As shown in Table 1.4, high degradation efficiencies can be obtained with direct oxidation processes. Pollutant load, process limitations and operation conditions will determine the selection of the most appropriate oxidation process for a particular compound degradation. Despite the demonstrated efficiency of direct oxidation processes, they need demanding operation conditions (temperature and pressure) to degrade the target compounds and this punish the economy of the process.

Advanced Oxidation Processes (AOP's) are alternative wastewater treatment processes able to degrade biorefractory organic compounds. AOP's typically operate with less energy requirements than direct oxidation. Glaze et al. defined AOP's as "near ambient temperature and pressure water treatment processes which involve the generation of hydroxyl radicals in sufficient quantity to affect water purification" (Glaze et al. 1987). AOP's group a large list of technologies using the oxidant power of oxidative radicals, mainly hydroxyl one ($\cdot\text{OH}$). As Table 1.5 shows, hydroxyl radical standard reduction potential compared to normal hydrogen electrode (NHE) is 2.80 V (Weast 1977).

Table 1.4. Operation conditions and limitations of direct oxidation processes (Rodríguez et al. 2006)

Process	Typical conditions	Maximum efficiency (%)	Process Limitations
Incineration	> 800°C	> 99%	- Need of an external fuel source if heat content < 3000 kJ/kg
SWAO	400 – 650°C > 250 bar	> 99.9%	- COD _{feed} > 50000 mg/L - Corrosive reaction environment - Scaling problems - N-containing organics difficult to oxidise
WAO	150 – 350°C 20 – 200 bar	75 – 90%	- 500 < COD _{feed} < 15000 mg/L - High energy consumption - Total mineralisation difficult
CWAO	120 – 250°C 5 – 25 bar	75 – 99%	- COD _{feed} > 10000 mg/L - Catalyst-dependant process - Catalyst instability problems

Table 1.5. Standard reduction potential of common oxidants (Weast 1977)

Oxidant	Standard reduction potential (V) versus NHE
Fluorine (F ₂)	3.03
Hydroxyl radical (·OH)	2.80
Atomic oxygen (O)	2.42
Ozone (O ₃)	2.07
Hydrogen peroxide (H ₂ O ₂)	1.77
Hydroperoxyl radical (·O ₂ H)	1.70 ^(a)
Potassium permanganate (KMnO ₄)	1.67
Hypobromous acid (HBrO)	1.59
Chlorine dioxide (ClO ₂)	1.50
Hypochlorous acid (HClO)	1.49
Chlorine (Cl ₂)	1.36
Bromine (Br ₂)	1.09

^(a) Legrini et al. 1993

As Table 1.5 shows, hydroxyl radical is the second strongest oxidant, preceded by fluorine, and it reacts 10^6 - 10^{12} times faster than ozone depending on the substrate to be degraded (Munter 2001). It should thus virtually attack almost all organic compounds. However, some small carboxylic acids or chloride derivatives have shown to be non-attackable by hydroxyl radicals. Acetic or oxalic acids as well as acetone, chloroform or tetrachloroethane are an example of substances not attacked by hydroxyl radicals (Bigda 1995). The degradation kinetics seems to be first order with respect to hydroxyl radical concentration and to model pollutant (Glaze and Kang 1989). Kinetic constants are in the range from 10^8 to 10^{11} $\text{L}\cdot\text{mol}^{-1}\cdot\text{s}^{-1}$ depending on the degraded organic (Munter 2001) whereas radical concentration in the steady state in AOP's is between 10^{-10} and 10^{-12} $\text{mol}\cdot\text{L}^{-1}$. Therefore, the pseudo-first order constant is in the range of 1 - 10^{-4} s^{-1} (Chamarro et al. 1996). For phenols' degradation, the reaction rate constant is in the range of 10^9 to 10^{10} $\text{L}\cdot\text{mol}^{-1}\cdot\text{s}^{-1}$ when using hydroxyl radicals as oxidant. When ozone is directly used as oxidant, the reaction rate constant falls down to 10^3 $\text{L}\cdot\text{mol}^{-1}\cdot\text{s}^{-1}$ (Munter 2001). Therefore, the degradation efficiency is dependant on both compound and AOP. Accordingly, the selection of the most-appropriate AOP and optimisation of the oxidation conditions for a particular compound have to be preliminarily tested at laboratory scale.

The hydroxyl radical may initiate the attack of an organic compound by three different mechanisms (Buxton et al. 1988; Legrini et al. 1993; Pignatello et al. 2006):

- Abstraction of a hydrogen atom from the C-H, N-H or O-H bonds of organic molecules as it often happens with alkanes or alcohols:



- Electron transfer to hydroxyl radicals:



- Addition to one atom of a multiple atom compound as it often happens with aromatic structures or olefins:



After the initiation by the attack to the organic compound, a degradation mechanism is followed and, after all the existing degradation steps (identified by different degradation intermediates), mineralisation is achieved. Mineralisation is considered as the production of carbon dioxide, water and inorganic ions. The degradation mechanism of organic contaminants is still unclear and depends on the properties of the studied molecules. For instance, chlorinated molecules are first degraded to intermediates such as aldehydes and carboxylic acids and, at the end, to carbon dioxide and water.

There exist many types of AOP's that can be selected to degrade organic compounds. Their classification is often difficult and could be done following distinct aspects such as the mechanism followed for the production of radicals, the number of phases, their cost or their efficiency among many others. Ozone, hydrogen peroxide, UV light and solid catalysts are typically used to generate hydroxyl radicals in most of conventional AOP's (Pera-Titus et al. 2004). For this reason, Table 1.6 lists conventional AOP's by the source used for the generation of hydroxyl radicals. The table does not aim to be an exhaustive summary of existent AOP's but only a general map of the most-used conventional AOP's. Processes involving more than one hydroxyl radical production way (e.g. $\text{O}_3 + \text{UV}$) are obviously grouped only in one category. Non-conventional AOP's, not shown in Table 1.6, may include ultrasounds, electrochemical oxidation,

ionising radiation, microwaves, pulsed plasma or ferrate radiation (Klavarioti et al. 2009). In addition, solar-irradiated processes have been studied in order to decrease costs associated to the use of light from non-natural sources (Anderson et al. 1991; Malato et al. 2009). In this later case, process applicability will be restricted to countries receiving solar radiation with enough energy and during enough hours a day. However, solar photocatalysis is an example of how poor economically viable processes could be improved by using green technologies and renewable energy sources.

Table 1.6. Classification of conventional AOP's

	Photolysis-based processes
	UV
	H₂O₂ – based processes
	H ₂ O ₂ + UV
	Fenton: H ₂ O ₂ + Fe ²⁺
	Fenton-like: H ₂ O ₂ + Fe ³⁺ / M ⁿ⁺
	Photo-Fenton (-like): H ₂ O ₂ + Fe ²⁺ / Fe ³⁺ / M ⁿ⁺ + UV
	O₃-based processes
	O ₃
	O ₃ + UV
	O ₃ + H ₂ O ₂
	O ₃ + UV + H ₂ O ₂
Homogeneous	
	H ₂ O ₂ + Fe ²⁺ / Fe ³⁺ / M ⁿ⁺ -solid
Heterogeneous (photo-) catalysis	TiO ₂ / ZnO / CdS + UV

1.3.1.1. Fenton process

The Fenton reaction was discovered by H.J.H. Fenton in 1894 (Fenton 1894). Fenton process reagents are only hydrogen peroxide and iron (II) ions, whose source is commonly iron sulphate. The oxidation mechanism was not discovered until forty years after when Haber and Weiss (Haber and Weiss 1934) recognised hydroxyl radicals as the oxidant generated during the Fenton reaction. Later, Barb and collaborators (Barb et al. 1949; Barb et al. 1951a; Barb et al. 1951b) modified the reaction mechanism proposed by Haber and Weiss. The mechanism obtained is still nowadays the most-accepted version for explaining Fenton reaction chemistry although posterior works proposed that ferryl ion might also be formed and contribute to the oxidation of organic molecules (Sychev and Isaak 1995; Bossmann et al. 1998). It was not until the 1960s that the Fenton process started being used for wastewater applications (Brown et al. 1964). Nowadays, the Fenton reaction is known to be a very efficient wastewater treatment process in the removal of many hazardous organics from water (Neyens and Baeyens 2003) and has been used in industrial wastewater applications (Bautista et al. 2008).

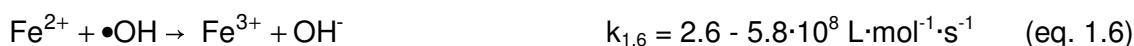
The traditional accepted Fenton mechanism is represented by equations 1.4 – 1.12, whose reaction rates have been reported by Sychev and Isaak (Sychev and Isaak 1995). Equation 1.4 is recognised as the Fenton reaction and implies the oxidation of ferrous to ferric ions to decompose hydrogen peroxide into hydroxyl radicals. Its reaction rate constant has been found to be between 40 - 80 L·mol⁻¹·s⁻¹ (Rigg et al. 1954; Sychev and Isaak 1995) and, although it is usually considered the core of the Fenton chemistry, the other reactions must be considered to understand the whole process.



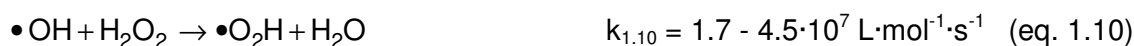
After the oxidation of ferrous to ferric ion, the latter may be reduced again to the former through the equation 1.5 with excess hydrogen peroxide. This reaction is called Fenton-like reaction (or process) and is slower than the Fenton one, as revealed by their reaction rates. In the Fenton-like reaction, apart from ferrous ion regeneration, hydroperoxyl radicals ($\bullet\text{O}_2\text{H}$) are produced. Hydroperoxyl radicals may also attack organic contaminants but, as Table 1.5 demonstrates, they are less powerful than hydroxyl ones. Thus, by inspecting only equations 1.4 and 1.5, it can be seen that the Fenton process follows a cyclic mechanism in terms of iron species where continuous consumption of hydrogen peroxide occurs during the process. Thus, iron can be considered a catalyst in the Fenton reaction whilst hydrogen peroxide is a reagent.



The following reactions complete the mechanistic cycle of reactions involved in the Fenton chemistry.



Equations 1.5 and 1.8 represent the rate-limiting step in the Fenton chemistry, as they are responsible for the regeneration of ferrous ions from the previously produced ferric ones. Equations 1.9-1.12 also take place during the Fenton process and are radical-radical reactions or hydrogen peroxide-radical reactions.



In absence of any other molecule to be oxidised, the decomposition of hydrogen peroxide to molecular oxygen and water occurs according to equation 1.13. However, even when an organic contaminant is present in solution, equation 1.13 takes place at some extent, meaning a waste of bulk oxidant (Pignatello et al. 2006) and thus an unnecessary increase on the treatment costs.

Fe³⁺). In this study, the same notation has been used to clearly distinguish the iron species present in solution.

The Fenton process is strongly dependent on the solution pH mainly due to iron and hydrogen peroxide speciation factors. The optimum pH for the Fenton reaction has been found to be around 3, regardless of the target substrate (Eisenhauer 1964; Ma et al. 2000; Rivas et al. 2001). At higher pH values, lower activity is detected due to the presence of relatively inactive iron oxohydroxides or even iron (III) hydroxide precipitates (Parsons 2004). In this situation, less free iron ions are reachable by hydrogen peroxide and less hydroxyl radicals are accordingly generated. Besides, the oxidation potential of hydroxyl radicals decreases with increasing pH. Oxidation potential for the redox couple $\cdot\text{OH}/\text{H}_2\text{O}$ has been reported to be 2.59 V at pH 0 and 1.64 V at pH 14 (Bossmann et al. 1998). In addition, hydrogen peroxide autodecomposition is accelerated (see equation 1.13) at high pH (Szpyrkowicz et al. 2001). At pH below 3, decreased degradation efficiency is also observed (Kavitha and Palanivelu 2005a). At very low pH values and depending on the iron concentration, iron (III) exists mainly as the hexaquo ion. Hexaquo ion has been found to react more slowly with hydrogen peroxide than other iron species. Thus, at very low pH, Fenton reaction efficiency is decreased again due to iron speciation. Moreover, solvation of hydrogen peroxide occurs at these conditions and stable oxonium ions, $(\text{H}_3\text{O}_2)^+$, are thus formed. Oxonium ion makes hydrogen peroxide more stable and presumably reduces its reactivity with ferrous ions (Kwon et al. 1999). Therefore, the efficiency of the Fenton process to degrade organic compounds is reduced both at high and low pH. Thus, an adequate control of pH would increase process efficiency. However, reaction buffering will always represent an increase on the operating costs. Therefore, final decision of whether or not using buffers will vary depending on each situation.

The Fenton process presents many operation advantages such as its operation at room temperature and atmospheric pressure. In addition, required reagents are readily available, easy to store and handle, safe and they do not cause environmental damages (Pignatello et al. 2006). However, two main Fenton process drawbacks can be identified. The first is related to the waste of oxidant due to the radical scavenger effect of hydrogen peroxide (see equation 1.10) and its self-decomposition (equation 1.13). The second refers to the continuous loss of iron ions dissolved in the treated effluent ending, once required effluent neutralisation is performed, in form of solid sludge. Several environmental problems have been reported to occur with Fenton sludge (Feng et al. 2004; Benatti et al. 2009). In addition, the current regional legislation regulating the aqueous effluents' rejections to a WWTP (Catalan Water Act 130/2003) states that iron concentrations beyond 10 mg/L are difficult to be degraded in WWTP's and have significant impact to the receptor media quality objectives and to the potential uses of the treated water. In consequence, previously identified drawbacks cause an economic and environmental impact. Thus, technologies allowing an efficient use of hydrogen peroxide have to be studied. Furthermore, recovery of iron ions and their subsequent recycle and reuse has to be performed.

With this goal, the hydrogen peroxide radical scavenger effect of hydroxyl radicals has been decreased by keeping its concentration at a low level. This has been carried out by periodically adding hydrogen peroxide to the Fenton reactor (Bremmer et al. 2006; Monteagudo et al. 2009; Zazo et al. 2009), decreasing the oxidant waste during the treatment.

Iron reusability has been typically carried out by precipitation-filtration-acidification-reduction process or by supporting iron ions onto heterogeneous supports that would allow them to be confined in the Fenton reactor. Despite the high efficiency shown by the step to step recovery process, four units are needed to have iron species in its

active form (Kavitha and Palanivelu 2004). Thus, proposed recovery and reuse system needs high site area availability. Supporting metal ions onto a solid matrix has been used to confine them in Fenton and Fenton-like reactors (Al-Hayek and Doré 1990; Liou et al. 2005; Dantas et al. 2006; Makhotkina et al. 2006; Castro et al. 2009; Liotta et al. 2009). However, supported metals have shown to decrease their catalytic activity when compared to their homogeneous state (Cuzzola et al. 2002). In addition, metal leaching from solid supports during the oxidation is typically observed (Parra et al. 2004; Pariente et al. 2008). Hence, alternative technologies have to be implemented to assure iron reusability with the minimum number of process steps.

1.3.2. Membrane technologies in industrial wastewater treatment

Membranes are permselective barriers that separate two different phases. Membranes leave certain solutes to selectively permeate, allowing therefore their separation from one side to another (Mulder 1997). In practical terms, a membrane process is a separation process where a feed stream (polluted effluent) is separated in a clean water stream (permeate or filtrate) and a concentrated one (retentate or concentrate). In water and wastewater treatment, membranes can be used for the separation of contaminants from polluted sources thus purifying original waters. Membrane processes work thanks to a gradient of pressure, chemical potential, electrical potential or temperature across the membrane. Table 1.7 summarises the most-used membrane processes in function of the driving force that they use for the separation.

Table 1.7. Membrane processes classification as function of the driving force (Mulder 1997)

Driving force			
ΔP	ΔC	ΔT	ΔE
Microfiltration	Gas separation		
Ultrafiltration	Dialysis	Thermo-osmosis	Electrodialysis
Nanofiltration	Pervaporation	Membrane distillation	Electro-osmosis
Reverse Osmosis	Liquid membranes		

In wastewater treatment, pressure-driven membrane processes are preferred for purification and decontamination processes. When pressure is applied in the feed side of a membrane, thanks to the pressure gradient (transmembrane pressure, TMP) between both sides of the membrane (feed and permeate), part of the feed stream goes across the membrane, being the permeate. Depending on solute, solution and membrane properties, some of the products present in the feed stream are (partially or totally) retained by the membrane whilst others permeate. Four different pressure-driven membrane processes can be classically distinguished depending on the solutes that they can retain: microfiltration (MF), ultrafiltration (UF), nanofiltration (NF) and reverse osmosis (RO). This classification is done according to the range of solutes or particles that are typically rejected by the membranes.

MF is considered a solid-liquid separation process. This is, only eye-seen particles can be practically retained by MF membranes. MF membrane pore size ranges from 0.1 to

10 μm . MF consequently allows the separation of suspended solids although certain bacteria and some colloids can also be partially retained. MF separation occurs by sieving effects and due to the low resistance exhibited by MF membranes, low TMP's are needed to efficiently operate (0.1-2 bar). MF has been successfully employed in water and wastewater treatment applications (Belfort et al. 1994; Parameshwaran et al. 2001; Wang et al. 2008). In addition, together with UF membranes, MF membranes are being chosen more and more in membrane bioreactor (MBR) technology (Marrot et al. 2004; Judd 2006; Le-Clech et al. 2006). MBR's consists in the performance of both secondary and tertiary treatment of wastewater in one single process unit, a clear example of process intensification.

UF is a separation process that allows the retention of macromolecules, soluble polymers, particles and biological species such as bacteria and viruses from waters and wastewaters. Membrane pore sizes range from around 1 to 100 nm and TMP is typically between 1 and 5 bar. UF membranes are generally classified according to its Molecular Weight Cut-Off (MWCO). The MWCO is defined as the molar mass of a solute that is retained 90% by the membrane. Generally, the MWCO of UF membranes is found to be between 1000 and 100000 g/mol. The unit of MWCO's is Dalton (Da), which is equivalent to one gram per mol. UF is mainly used for the concentration of macromolecular solutions and for the elimination of macropollutants and biological matter present in domestic or industrial wastewaters (Aoustin et al. 2001; Qin et al. 2006; Arkhangelsky and Gitis 2008; Benítez et al. 2008b). UF separation mechanism is mainly based on sieving effects as for MF. Therefore, compounds with a molecular weight (MW) higher than the membrane MWCO are retained whilst those having MW below the MWCO are scarcely retained by the membrane. Thanks to this characteristic, UF can be used together with the addition of soluble polymers or surfactants to allow (or enhance) the retention of ions and organics from aqueous streams (Molinari et al. 2004a; Beolchini et al. 2006; Majewska-Nowak et al. 2008). The complexation-UF hybrid processes are generally identified as Polymer-Enhanced UF (PEUF) and Micellar-Enhanced UF (MEUF) when soluble polymers and surfactants are used as macromolecular additives, respectively. However, there is a process limitation concerning the reuse of such additives. The process has to be installed together with a subsequent recovery unit for ensuring the additives' reuse (Kim et al. 2006).

RO, although it separates smaller compounds than NF, will be explained before due to the fact that NF was developed as result of the application of RO. RO is able to retain small organic compounds and ions from polluted waters (Chai et al. 1997; Into et al. 2004). However, the RO major application is as both brackish and seawater desalination technology (Fritzmann et al. 2007; Alghoul et al. 2009). RO membranes are dense and have "non-measurable" pores. This nature is translated into a high resistance, which implies the need of significant TMP's for water permeation. The transport mechanism is based on the sorption-diffusion concept. This is, non-retainable solutes are adsorbed onto the membrane material and transported by diffusion from the feed to the concentrate side, where they meet the permeate stream. Typical TMP's range from 10 to 100 bar.

NF is a pressure-driven membrane process in the filtration range between UF and RO. NF membranes were born from the modification of RO ones. Its name refers to the fact that its "virtual pore size" is expected to be around 1 nm, or more generally, in the nanometre range. Its MWCO is typically found to be between 200 and 1000 Da. NF membranes require lower TMP's (i.e. lower energy demand) to operate than RO. Applied TMP ranges between 3 and 15 bar. Thanks to their MWCO and solute MW, NF membranes are able to efficiently retain organic micropollutants and multivalent ions from water and wastewater (Ahn et al. 1999; Kimura et al. 2003; Van der Bruggen and

Vandecasteele 2003; Garcia et al. 2006; Choi et al. 2008). Apart from the sieving effects involved on the retention of organics, electrostatic interactions and solute-membrane interactions may also contribute to it (Bowen et al. 1996; Van der Bruggen et al. 1999; Bellona et al. 2004; Verliefde et al. 2008). Solution-diffusion is the mechanism that generally explains transport through NF membranes (Schäfer et al. 2005).

Each effluent to be filtered has to be particularly studied because of the great influence of the water medium on membrane filtration efficiency. Hence, the efficiency of a certain membrane process for a specific separation can be globally predicted from the previous characteristics. However, experimental studies are required in order to evaluate the real membrane efficiency as well as the separation mechanisms taking place. Membrane process efficiency can be generally expressed in terms of solute retention percentage and permeate flux. The retention percentage gives the ratio of solute retained by the membrane to the solute fed. Thus, it gives an idea of the selectivity of the membrane to reject a certain compound. Permeate flux is used for the quantification of the purified water flow permeated per unit of membrane area and also to know losses of permeate flux occurring in the filtration process.

In membrane processes, two main operation modes exist: dead-end and crossflow, as illustrated in Figure 1.4. In dead-end mode, all feed water permeates through the membrane, leaving the retained species in the feed compartment. Retained compounds thus accumulate at the membrane surface. In crossflow mode, feed solution tangentially circulates along the membrane surface. Thanks to the TMP, part of the feed stream permeates and retained species remain in the concentrate stream. In this filtration mode, limited accumulation of retained compounds occurs over the membrane surface due to the continuous flow circulation in the feed section.

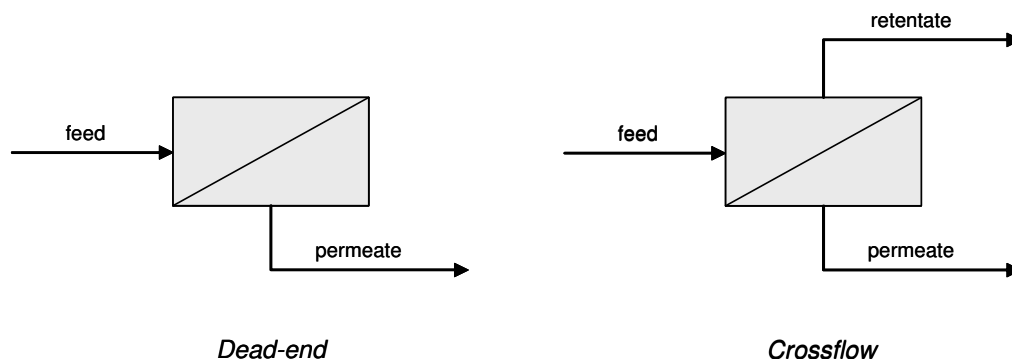


Figure 1.4. Membrane filtration operation modes

Despite the decrease on the accumulation of solutes over the membrane surface in crossflow mode operation, membrane fouling cannot be completely eliminated in membrane processes and usually represents the process bottleneck. Progressive accumulation of solutes in the neighbourhoods of the membrane surface inevitably occurs and creates solute concentration gradients in those regions. This phenomenon is known as concentration polarisation (Mulder 1997). As Figure 1.5 shows, solute concentration is increased in the concentration polarisation zone until it reaches its maximal value in the membrane surface. As it can be observed in Figure 1.5, there is a convective solute flux towards the membrane and a back-diffusion flux of solute due to the concentration gradient between bulk and interfacial (or membrane surface) solute concentration. These fluxes are finally balanced so a steady concentration polarisation layer exists under stable operation.

Concentration polarisation is a reversible phenomenon that causes a decrease on the membrane permeate flux and can also cause a variation on the solute retention. The decrease on the permeate flux may be due to the increase on the osmotic pressure (π), that decreases the net pressure gradient and consequently the permeate flux. In addition, the decrease on the permeate flux may be also favoured by the increase on the resistance to the water passage due to the accumulation of compounds in the membrane surface. Concentration polarisation can have either positive or negative effects on the solute retention. For instance, the accumulation of charged solutes on membrane surface may favour the repulsion of opposite charge solutes and increase their retention. On the other hand, the accumulation of solutes over the membrane surface increases the effective concentration, favouring their transport through the membrane by solution-diffusion phenomena. Membrane process efficiency has to be experimentally determined due to the high number of possible effects of process variables and solution chemistry on it.

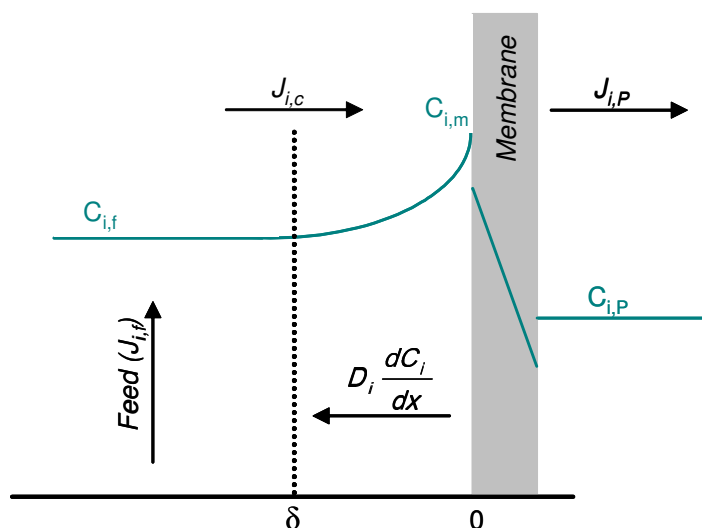


Figure 1.5. Concentration polarisation phenomenon (adapted from Mulder 1997; Rodríguez et al. 2006; Stratmann et al. 2006)

The decrease on the permeate flux due to concentration polarisation phenomena is stabilised along the time and reaches a pseudo-stable value. However, when fouling occurs, permeate flux continuously decreases along the time (Mulder 1997). As concentration polarisation is defined as reversible process causing a permeate flux decline, it cannot be considered fouling. The difference is in the reversibility concept. The fraction of the flux decline that is still present when pure water is applied as feed solution after the end of filtration process is considered to be fouling. On the contrary, the fraction of the flux decline that is not present anymore at end of the filtration process is considered to own to concentration polarisation (Mulder 1997; Stratmann et al. 2006).

Fouling irreversibility has to be considered in terms of spontaneous recovery of water permeability without any external help. Membrane fouling has to be periodically removed to maintain membrane efficiency and enlarge as much as possible membrane lifetime. Membrane cleaning procedures can be performed hydraulically, chemically, mechanically or even electrically. In this study, chemical cleaning has been used to remove severe foulants. Accordingly, the other procedures will not be considered. Chemical cleaning success depends on the cleaning conditions and especially on the affinity of the foulants for the cleaning agent. Chemical cleaning can be a successful strategy for removing inorganic, colloidal, organic and biological fouling. Depending on

the nature of the foulants, acid, basic, enzymatic cleaners or their combinations may be required for efficiently removing fouling from membranes. Thus, apart from the study of the effect of the filtration variables on the membrane process efficiency, fouling quantification and design of cleaning strategies has to be done in parallel in order to determine both process feasibility and requirements. High fouling degree may occur in a membrane showing high selectivity for the rejection of a particular compound. However, if efficient cleaning is not performed, membrane efficiency will decrease and its lifetime will shorten. Thus, although permeate flux and solute retention are crucial process efficiency indicators, fouling identification and cleaning strategies have to be also taken into account.

1.3.3. Coupled processes in industrial wastewater treatment

1.3.3.1. Coupling Fenton process and biological degradation

Degradation efficiency versus oxidant and catalyst dose needs to be studied in the Fenton process so that the degradation process can be optimised in technical, economic and environmental impact terms. Other variables affecting degradation efficiency have also to be considered in experimental studies concerning Fenton reagent. In general, hydroxyl radical generation is a relatively expensive process. Thus, process optimisation and, when possible, process integration with less expensive technologies needs to be considered. In this sense, several efforts have been invested in studying the integration of AOP's with biological treatment (Bautista et al. 2008). In this process scheme, AOP's act as pre-treatment to enhance biodegradability and reduce toxicity. Then, pre-treated effluents can be safely sent to the biological treatment that will reduce contamination levels down to the legislation limits (Comninellis et al. 2008). The success of the combined process is probably due to the following aspects (Klavarioti et al. 2009):

- Biological treatment is less costly and more environmentally friendly than other degradation treatments.
- Complete mineralisation by AOP's results in excessive costs since the highly oxidised end products (i.e. carboxylic acids such as acetic, oxalic, etc.) formed tend to be refractory to further oxidation by chemical means.
- Oxidation end-products are typically easily degraded by biological means.

Thus, AOP's have to be performed as efficient pre-treatment to biological treatment so that non-biodegradable compounds are not driven to the latter, which would cause both economic and technical problems. Process optimisation arises in those conditions in which non-biodegradable substances are eliminated with a minimum cost (Akata and Gurol 1992), this is, with minimum use of oxidant, catalyst, buffers, among many other process variables. Therefore, complete mineralisation of organic matter cannot be the goal of the AOP's when they are combined to a biological degradation because the treatment costs would be accordingly increased.

Biodegradability assessment is required in order to know whether the effluents can be safely sent to the aerobic biological treatment or not. The success of the coupled oxidation-biological treatment will depend on the potential impact to the biomass of the oxidation intermediates formed and/or of the unreacted pollutants. Chemical analysis (e.g. chromatographic methods) may help in the identification of the pre-treated effluent chemical character. However, incomplete analysis may result in an unrealistic

prediction of the effluent biodegradability or toxicity. Biodegradability determinations are the other option, more realistic, for the biodegradability assessment. The most used biodegradability measurement methods are the Biochemical methane potential, the Biological Oxygen Demand (BOD) and comparisons based on BOD/COD ratio, Nitrification/denitrification inhibition, Respirometry, Enzyme inhibition, the Microtox® bioassay and Molecular based sensors (Dalzell et al. 2002; Ren 2004). Microtox® and respirometry tests are probably the most used for the evaluation of biodegradability of partially-treated effluents (Santos et al 2004a; Santos et al. 2004b; Boshcke et al. 2007; Suárez-Ojeda et al. 2007a). However, this method can give an overestimation of the toxicity since the bacteria used corresponds to a single marine microbial specie (*Vibrio fischeri*) whose habitat is mostly different from that of WWTP biomass. Respirometric tests seem to be more representative of the real WWTP behaviour than Microtox® because they can directly use the biomass from a WWTP (Gutiérrez et al. 2002; Ricco et al. 2004). In addition, respirometry has been recently applied to evaluate the biodegradation, toxicity and inhibition effects of oxidised and non-oxidised phenol (Ourpold et al. 2001; Rubalcaba et al. 2007a; Rubalcaba et al. 2007b; Suárez-Ojeda et al. 2007a) and surfactant effluents (Suárez-Ojeda et al. 2007b), which makes it even more attractive for the application considered in this thesis.

Diverse pollutants and oxidation technologies can be considered to couple oxidation and biological treatment due to the high number of possible pairs compound-technology. Table 1.8 reviews some published studies about the treatment of phenolic compounds through coupled oxidation processes to aerobic biological treatment.

Table 1.8. Short review of studies coupling oxidation and aerobic biological treatment for the detoxification of phenolic wastewaters

Pollutant	Initial concentration	Oxidation process	Reference
2,4-dichlorophenol	100 mg/L	O ₃	Contreras et al. 2003
2,4-dichlorophenol	100 mg/L	photo-Fenton	Al Momani et al. 2004 Al Momani et al. 2006
chlorophenols	50 mg/L	UV/TiO ₂ UV/H ₂ O ₂ UV/TiO ₂ /H ₂ O ₂	Essam et al. 2007
o-cresol	COD=9500 mg/L	CWAO	Suárez-Ojeda et al. 2007a

Despite the fact that Table 1.8 is obviously a non-complete literature review on this topic, it can be seen that coupled oxidation and aerobic biological processes can be applied for several phenolic pollutants, concentrations and with diverse oxidation processes. Effluents polluted with surfactants have also been efficiently degraded by

coupling oxidation and biological treatment (Mantzavinos et al. 1999). Thus, coupled processes seem to be potential instruments for the efficient decontamination of polluted waters with a relatively low cost.

Coupling AOP's to a biological treatment has to be carried out by considering several additional aspects. Chemical oxidants cannot be mixed with biomass because of its inhibitor or toxic character to it (Larisch and Duff 1996; Chang et al. 2005). Thus, residual oxidants have to be eliminated before the biological degradation is performed. In the Fenton process, hydrogen peroxide will need to be eliminated prior to the biological treatment. Several methods exist to eliminate hydrogen peroxide from aqueous solutions. In fact, they are typically used for quenching Fenton reaction during sample withdrawal and storage in experimental studies.

Catalase enzyme addition can be used as hydrogen peroxide decomposition method (Liu et al. 2003). Catalase enzyme efficiently decomposes hydrogen peroxide into molecular oxygen and water. However, the appropriate enzyme form has to be selected so that typical acidic effluent pH obtained in the Fenton reaction does not affect its activity.

Thiosulphate addition adjusting the pH to 7-8 (Kitis et al. 1999; Rivas et al. 2001; Liu et al. 2003) can also be used as hydrogen peroxide destructor. The decomposition mechanism is based on the oxidation of thiosulphate ions to tetrathionate ions. Despite its proven efficiency, around 9 g/L of thiosulphate are required to destroy 1 g/L of residual hydrogen peroxide. Therefore, thiosulphate method would increase the costs associated with the coupled process.

Finally, basification up to around pH 10-12 has also been found to be effective for decomposing hydrogen peroxide (Goi and Trapido 2002; Kavitha and Palanivelu 2005b; Bautista et al. 2007; Deng 2007; Du et al. 2007). The mechanism is based on the accelerated self-decomposition of hydrogen peroxide into molecular oxygen and water occurring at high pH values. Basification typically uses NaOH, a non-expensive and common reagent. The main limitation of this method is that iron hydroxides precipitate due to the increased pH, generating residual sludge. Fenton residual sludge has been classified as hazardous because of the presence of toxic metals, which are co-precipitated and entrapped in iron hydroxides and oxides (Benatti et al. 2009). Thus, if basification is to be selected, a middle treatment unit between Fenton oxidation and biological treatment has to be installed in order to avoid damages in the subsequent biological treatment and/or to the environment. On the other hand, the pH of the effluents to be sent to the biological treatment has to be around the pH of the biological culture (typically around pH 7) so that its performance is not altered. Thus, the pH of pre-treated effluents has to be adjusted in order to avoid operation problems.

1.3.3.2. Coupling Fenton and biological degradation assisted by membrane technology

Fenton process and biological degradation coupled processes are able to efficiently deal with organically-polluted effluents. Nonetheless, several problems, which arise from the application of the Fenton process, have been identified and are summarised below.

- Iron ions (Fenton homogeneous catalyst) continuously leave the oxidation reactor ending in form of environmentally hazardous sludge, posing serious

environmental problems. Continuous injection of catalyst (due to its loss in the reactor effluent) is thus needed, which increases treatment costs.

- A waste of bulk oxidant occurs in the Fenton process as consequence of the hydrogen peroxide radical scavenging effect and of its autodecomposition.
- Residual oxidant in the effluent from the Fenton process can damage microorganisms selected for performing the succeeding biological degradation.
- The pH of the Fenton-treated effluent needs to be adjusted to a value close to that of the biomass used in the subsequent biological treatment.

The last two drawbacks can be straightforwardly solved if efficient oxidant decomposition methods and pH adjustment are applied. On the contrary and as abovementioned in the previous sections, alternative and innovative methods for the recovery of iron used as catalyst have to be developed. In addition, intelligent methods allowing an increase on hydrogen peroxide usage must also be studied. The solution to the previous drawbacks would undoubtedly improve the global efficiency of the coupled process. Thus, research and development has to be carried out in this sense.

Membrane processes by themselves are unable to decompose organics as they only transport them from one phase to another. However, they are useful in those applications where subsequent solute separation is required. Thus, if efficiently designed, membrane processes could be employed as iron recovery step after the Fenton reaction was carried out. Below, a short explanation of previous works dealing with oxidation processes and membrane technologies can be found. The following literature citations do not wish to be an intensive review but only a short summary of some relevant published works about coupling of oxidation and membrane processes.

Membranes have been successfully employed in coupled processes where they are combined with oxidation technologies. Examples of these combinations are H₂O₂/UV+NF (Song et al. 2004), O₃+MF/UF (Karnik et al. 2005; Benítez et al. 2008a), MF/UF/NF/RO+O₃ (László and Hodúr 2007; Mänttari et al. 2008) among many other hybrid processes. Catalytic membrane reactors and membrane contactors have also been developed as example of process integration and intensification in the degradation of organic compounds (Miachon et al. 2003; Raeder et al. 2003; Jansen et al. 2005; Iojoiu et al. 2006; Vospornik et al. 2006; Drioli et al. 2008). Membrane processes coupled to direct oxidation processes or to AOP's have also been studied. Particularly, there is one application that has been deeply studied over the last years: the retention or confining of photocatalysts, used in the abatement of organic contaminants by AOP's, in the reaction region (Xi and Geissen 2001; Mozia et al. 2005; Azrague et al. 2007; Huang et al. 2007; Erdei et al. 2008). It is worth mentioning that the group of Dr. Molinari and collaborators has been specially focused on coupling photocatalysis with membrane processes for the abatement of organic contaminants. Several references (Molinari et al. 2000; Molinari et al. 2001; Molinari et al. 2002a; Molinari et al. 2002b; Molinari et al. 2004b; Molinari et al. 2006) are a good example of their important contribution in this subject.

The coupling of Fenton with biological treatment needs an intermediate treatment step to recover iron ions used as catalyst. Membrane separation processes could efficiently fulfil this requisite because of their capacity to recover ionic species if the appropriate membrane and conditions are selected, as previously discussed. The application of AOP's using homogeneous catalysis coupled to a recovery step based on membrane separation has been proposed by Kim and co-workers (Kim et al. 2008). Their publication was focused on the nanofiltration of iron(III)-tetrasulfophthalocyanine, which

was used as catalyst in the oxidation of bisphenol-A by the Fenton-like process. The process demonstrated to be highly efficient in terms of catalyst recovery because of the high molecular weight of the catalyst (978 g/mol) compared to the MWCO of the selected membrane (200 Da). Results demonstrated to be encouraging for the integration of Fenton oxidation and membrane technologies. However, the application of membrane separation when iron catalyst is employed in its ionic state, as in the classical Fenton process, has not been previously published to the best of my knowledge. Thus, there is still much room to carry out research in this subject in order to solve the environmental and economic limitations associated to the use of the Fenton process as pre-treatment of the biological degradation.

Membrane emulsification, which has been found to be useful for the formulation of stable catalytic emulsions (Giorno et al. 2007; Giorno et al. 2008), could also find a place in the preparation of Fenton-active catalytic emulsions. The emulsions should allow supporting iron ions in the interface of the droplets and confining them in the reactor. Emulsions have been prepared and employed as catalyst, reagent deliverer, product separator and in many other applications (Li et al. 2005; Shchukin and Sviridov 2006). Nonetheless, to the best of my knowledge, they have never been tested as potential Fenton catalysts for the degradation of biorefractory pollutants.

Increase on hydrogen peroxide usage is usually addressed by keeping it in a lower concentration in the reaction environment in order to decrease its radical scavenging effect and its autodecomposition. This goal could also be achieved by applying membrane principles. Membranes used in a distributor mode and not as separation tool could be designed for this application. Hydrogen peroxide could be driven from the shell to the lumen of a membrane, where it would reach polluted effluent together with catalyst and perform the desired degradation. This inert membrane reactor would allow continuously feeding oxidant to the reactor and maintaining its concentration at a low level, thus increasing its usage.

All the previous membrane technology strategies in combined Fenton-biological degradation processes could help to solve the identified Fenton process drawbacks. For this reason, the approaches described above have been developed and studied in this thesis.

UNIVERSITAT ROVIRA I VIRGILI

TREATMENT OF BIOREFRACTORY WASTEWATER THROUGH MEMBRANE-ASSISTED OXIDATION PROCESSES

Xavier Bernat Camí

ISBN:978-84-693-1529-3/DL:T-652-2010

CHAPTER 2

Hypotheses and objectives

2.1. Hypotheses

Polluted effluents are conventionally treated in biological WWTP's. However, industrial aqueous effluents are polluted by the presence of biorefractory chemicals and/or by compounds causing a detrimental effect on the operation of the biological treatment. Thus, biological treatment, known to be an effective and efficient technology in wastewater treatment applications, cannot be directly employed in those situations. When this source of contamination exists, alternative pre-treatments are needed so that the effluent achieves enough biodegradability to be subsequently degraded by the conventional biological system. AOP's and, more concretely, the Fenton process can be satisfactorily used to deal with these situations.

The high efficiency of the Fenton process in abating organic biorefractory pollutants coexists with the formation of organic intermediates, which can be even more biorefractory than the initial contaminant. Thus, the final quality of the Fenton-treated effluent has to be established and modulated so that the presence of toxic intermediates is avoided and the efficiency of the subsequent biological treatment efficiency accordingly guaranteed.

The Fenton process uses iron ions as homogeneous catalyst that continuously exit the reaction zone dissolved in the partially-treated effluent. This causes an increase on the associated treatment costs due to the imperative need of a continuous iron source. When a high iron dose is needed, the subsequent biological treatment can also undergo damages from it. In fact, current legislation indicates that an iron concentration

beyond 10 mg/L is difficult to be assimilated by conventional biomass. Iron ions are classically removed from the pre-treated effluents through its neutralisation and precipitation, which has found to result in the formation of toxic iron sludge. Hence, for environmental, technical and economic reasons, efficient methods need to be implemented to confine or recover (and reuse) iron ions employed in the Fenton oxidation of biorefractory organics before the biological treatment step.

The use of hydrogen peroxide as source of hydroxyl radicals in the Fenton chemistry implies an increase on the treatment costs because of its proven radical scavenging character. In addition, hydrogen peroxide can also be self-decomposed at high concentrations. As result, the economic impact of the waste of bulk oxidant is evident. Hence, designed methods allowing the decrease of the oxidant waste would reduce treatment costs. Hydrogen peroxide may also detrimentally affect the operation of the coupled biological treatment because of its toxic or inhibitory effect on biomass. Thus, there is a necessity of decreasing the concentration of hydrogen peroxide used in the Fenton oxidation to reduce its wastage and its disadvantageous effect on the biomass used in the successive biological treatment.

Membrane processes could help decreasing all the abovementioned drawbacks when coupling chemical pre-treatments such as the Fenton process to an aerobic biological degradation. The proposed alternatives of using membrane technologies are explained below and have all been studied in this thesis.

Pressure-driven membrane processes could decrease the concentration of refractory organic intermediates to a biodegradability level enough for allowing the efficient degradation of the pre-treated effluent by a conventional biological treatment. In the right separation range, only highly biodegradable organic acids would exit the system. Therefore, the installation of the membrane process as intermediate step between Fenton and biological degradation would guarantee the correct operation of all the process units.

Pressure-driven membrane processes could also perform as iron recovery step after the Fenton oxidation and thus before the pre-treated effluent is fed to the biological treatment. The coupling of Fenton-NF-biological treatment would decrease (or avoid) the need of a continuous iron feed. UF or NF could be used for this purpose because of their expected capability of separating target compounds from wastewaters.

Membrane emulsification could be employed for preparing Fenton catalytic emulsions. The formulated emulsions would allow confining iron species in their interfaces, be used as catalyst in the Fenton process and then be easily retained by a subsequent low-pressure membrane process such as MF. This treatment strategy would decrease, in principle, the expected treatment costs as MF is a membrane technology working at lower TMP's than UF or NF.

An inert membrane reactor acting as a hydrogen peroxide dispenser would palliate its waste due to its self-decomposition and its radical scavenging effect when working at high oxidant concentrations. The peroxide membrane diffuser would maintain the oxidant concentration at a low level because of its continuous addition throughout the membrane and thus increase its efficient usage during the oxidation step. In addition, this approach would allow using continuous tubular reactors instead of stirred tanks working in continuous or discontinuous mode.

2.2. Objectives

The main objective of this thesis was to test the improvement of coupled Fenton-biological treatment of organic contaminants by means of membrane technologies. This main objective can be split in the following concrete goals.

- To establish the feasibility of the Fenton process to partially treat polluted synthetic effluents by
 - Assessing the effect of the H_2O_2 dose and Fe(II) concentration on the Fenton process efficiency.
 - Evaluating the Fenton process efficiency to partially degrade phenol as well as the tandems phenol/SDS and phenol/CPC.
- To determine the feasibility of membrane processes as efficient technologies to enhance the degradation of organic contaminants by the Fenton process by
 - Testing the UF and NF efficiency for recovering iron ions from aqueous solutions.
 - Examining the feasibility of coupling UF or NF to Fenton process in terms of retention of organic intermediates, non-oxidised pollutants and iron from partially-treated effluents.
 - Exploring the membrane emulsification usefulness for formulating emulsion droplets able to confine iron ions and testing their efficiency as Fenton heterogeneous catalysts.
 - Designing and testing a new inert ceramic membrane reactor for decreasing the hydrogen peroxide waste during the Fenton oxidation of phenol effluents.
- To examine the biodegradability amelioration when coupling Fenton and membrane processes by
 - Characterising the biodegradability enhancement of the Fenton effluents and of the filtered Fenton effluents.

UNIVERSITAT ROVIRA I VIRGILI

TREATMENT OF BIOREFRACTORY WASTEWATER THROUGH MEMBRANE-ASSISTED OXIDATION PROCESSES

Xavier Bernat Camí

ISBN:978-84-693-1529-3/DL:T-652-2010

CHAPTER 3

Methodology

3.1. Fenton oxidation

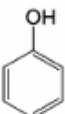
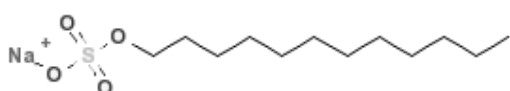
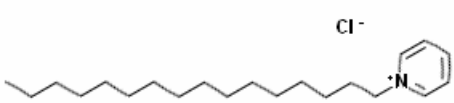
3.1.1. Model pollutants, oxidant and catalyst

Model effluents were prepared by dissolving known quantities of model contaminants in deionised water. Model pollutants were phenol and two surfactants: sodium dodecylsulphate (SDS) and cetylpyridinium chloride (CPC). Commercial reagents were employed as source of target compounds. Representative properties of the three model compounds considered in this thesis are summarised in Table 3.1. It is worth mentioning that, as SDS and CPC are surfactants, their MW's are significantly higher than phenol one.

Hydrogen peroxide (H_2O_2) and iron (II) sulphate heptahydrate ($FeSO_4 \cdot 7H_2O$) were used as Fenton oxidant and catalyst sources, respectively. Hydrogen peroxide was received and employed as 30% w/v solution and ferrous sulphate heptahydrate as 99.0% purity solid. Both reagents were manufactured by Panreac.

All the reagents were used as received and stored at room temperature in the dark with the exception of phenol and hydrogen peroxide that were stored at 4°C in the fridge. This was done for avoiding phenol melting and hydrogen peroxide decomposition at room conditions.

Table 3.1. Properties of model pollutants

Pollutant	Formula	MW (g/mol)	Supplier	Purity (%)
Phenol		94.11	Panreac	99.0
SDS		288.38	Fluka	96.0
CPC		340.01	Sigma	99.9

3.1.2. Fenton oxidation set-up

The experimental set-up used in the Fenton oxidation experiments is schematised in Figure 3.1. The system was composed of a jacketed glass reactor of 1200 mL capacity. The reaction temperature was set by circulating deionised water from a thermostatic bath (Haake, model T3). As the thermostatic unit did not allow cooling, a stainless steel coil was immersed into the reactor to decrease the temperature by flowing water when necessary. The reactor was stirred by a magnetic bar and a magnetic stirrer (Selecta, model Agimatic REV-S). The pH and temperature were monitored by means of a pH probe (Metler Toledo, model InoLab® 412) and a temperature sensor (Metler Toledo, model Cyberscan 510), respectively.

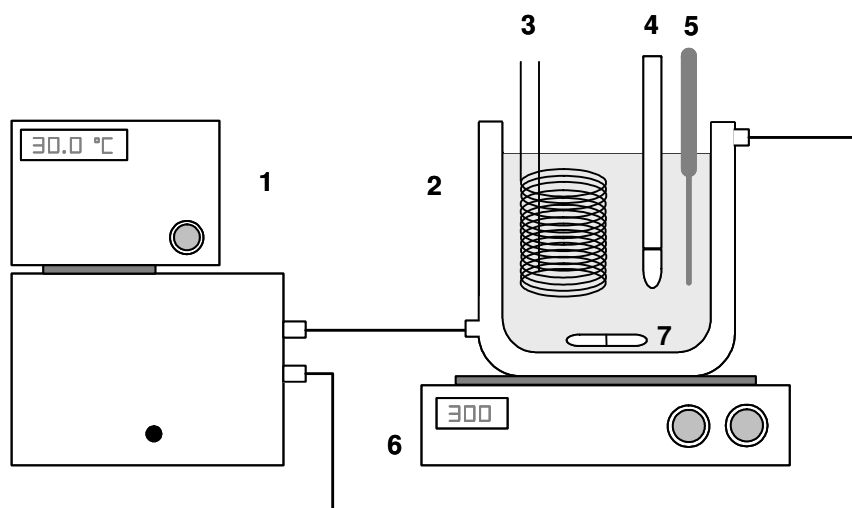


Figure 3.1. Fenton oxidation set-up
 (1) Thermostatic bath ; (2) Reactor ; (3) Cooling coil ; (4) pH probe ;
 (5) Temperature sensor ; (6) Magnetic stirrer ; (7) Magnet

3.1.3. Homogeneous Fenton oxidation protocol

In this section, the experimental protocol designed and employed for the study of the degradation of model compounds by the Fenton process is exposed. The Fenton process efficiency was tested in single solutions of phenol and also in mixtures of phenol+SDS and phenol+CPC.

The Fenton oxidation experiments started by preparing the synthetic model solutions. Apart from the model compound/s, the initial solution also contained Fe(II). The solution was prepared by dissolving known masses of model compound/s and iron sulphate heptahydrate in deionised water. The concentration of reagents in the solutions was calculated taking into account that hydrogen peroxide would be added later, diluting the initial solutions. Special attention was paid when surfactant was present in the initial synthetic effluent in order to avoid foaming during its preparation. Iron hydrolysis was found to affect Fenton process efficiency (Pignatello et al. 2006). In order to avoid it, the mixtures were immediately used after their preparation.

990 mL of synthetic effluent was introduced into the batch reactor and stirring was switched on. After the solution had achieved the desired temperature, a known volume of hydrogen peroxide 30% w/v commercial solution was added. The reaction started at this moment as blank experiments performed without hydrogen peroxide showed no model compound degradation. All the Fenton experiments were carried out at $30.0 \pm 0.5^\circ\text{C}$ and at a stirring rate of 300 rpm.

The Fenton reaction was performed during 90 min. During this time, 5 mL samples were periodically withdrawn from the reactor for analysis. Analyses included target compound concentration, TOC, COD, total iron and UV-VIS spectra. The analytical procedures are explained later in this chapter. The concentration of phenol oxidation intermediates was also determined in the last sample withdrawn (after 90 min).

The Fenton reaction, due to the homogeneous nature of the catalyst, can continue in sample vials. Basification at pH 11-12 can be used to rapidly decompose hydrogen peroxide and precipitate iron, instantaneously stopping the reaction after the withdrawal of samples. 200 μL NaOH 6N solution per 3 mL sample were added into sample vials prior to introduce the sample. Hydrogen peroxide was instantaneously decomposed and iron precipitated. However, it was found that, when basification was not performed, analysed parameters remained practically unchanged. In fact, they only varied $\pm 3\%$ in the worst case during the two consecutive days after sampling when they were stored unstirred in the fridge at $4 \pm 1^\circ\text{C}$. Thus, residual hydrogen peroxide concentration was not enough to significantly change effluent matrix at least for two-day observation. Apart from this, when the effluents were prepared with the goal of testing the efficiency of the subsequent membrane treatment, basification could not be used because iron would precipitate and the nature of the effluent change, affecting the filtration efficiency and thus the reliability of the filtration results. Therefore, vials containing the samples and the remaining effluent after 90 min oxidation were kept in the fridge until analyses or filtration experiments were performed. Nevertheless, residual hydrogen peroxide was indeed found to affect COD determinations (Talinli and Anderson 1992; Kang et al. 1999) and present toxic or inhibitor character to biomass (Larisch and Duff 1996; Chang et al. 2005). In addition, when adapting the respirometry protocol to characterise Fenton effluents, it was found that residual hydrogen peroxide made the procedure ineffective because of the increase on the dissolved oxygen level when an effluent pulse was added to the biomass. Consequently, basification at the abovementioned ratio was conducted only in samples for COD and respirometric analyses.

3.2. Membrane separation processes

3.2.1. Reagents and membrane cleaning agents

Two main types of experiments were performed to test the membrane efficiency for the application studied. On the one hand, experiments designed to test the feasibility of UF and NF membranes to recover iron and other metals (copper and chromium) from aqueous synthetic solutions were carried out. On the other hand, experiments planned to know the membrane filtration efficiency when dealing with real Fenton effluents were performed. It is clear that, the latter application did not require any effluent preparation as they consisted of real pre-oxidised effluents. On the contrary, the former needed the preparation of solutions to be filtered and thus, the use of reagents that served as source of dissolved metal ions. Table 3.2 lists the reagents used as source of heavy metals for this case. Apart from those reagents, HCl (37% fuming, Fluka) and NaOH (98%, Sigma) were used for adjusting the pH of the prepared solutions to the desired level.

Table 3.2. Sources of heavy metals and cleaning agents

Reagent	Formula	MW (g/mol)	Supplier	State	Purity (%)
Iron (II) sulphate heptahydrate	FeSO ₄ ·7H ₂ O	278.0	Panreac	Solid	99.0
Iron (III) nitrate nonahydrate	Fe(NO ₃) ₃ ·9H ₂ O	404.0	Riedel-de Hæn	Solid	98.0
Copper (II) sulphate pentahydrate	CuSO ₄ ·5H ₂ O	249.7	Fluka	Solid	99.0
Chromium (III) chloride hexahydrate	CrCl ₃ ·6H ₂ O	266.5	Fluka	Solid	98.0
Cleaning agent	Formula	MW (g/mol)	Supplier	State	Purity (%)
Hydrochloric acid	HCl	36.5	Fluka	Fuming	37
Phosphoric acid	H ₃ PO ₄	98.0	Baker	Solution	85
Oxalic acid	(HOOC) ₂	90.0	Aldrich	Solid	99.0
EDTA ^(a)	C ₁₀ H ₁₄ O ₈ N ₂ Na ₂ ·2H ₂ O	372.2	Fluka	Solid	97.0

^a *Ethylenediaminetetraacetic acid disodium salt dihydrate*

Several cleaning solutions were tested to recover initial membrane characteristics in certain experiments. The cleaning solutions were prepared by dissolving or diluting cleaning agents in deionised water. Table 3.2 collects the cleaning agents employed

for preparing all the cleaning solutions tested in this thesis together with some of their properties. In addition, during the preparation of the cleaning solutions, pH adjustment could be needed. When required, this was done by adding small amounts of either NaOH or HCl solutions during the cleaning solutions' formulation.

3.2.2. Membranes and membrane processes

The membranes used in this thesis were all commercially available in order to know the immediate application of the developed technologies using market-available membranes. Both ceramic and polymeric membranes were used and their characteristics are explained in detail in the following three subsections.

3.2.2.1. Ceramic UF membranes

Seven different tubular ceramic membranes of 10 mm diameter and 250 mm length were selected in this part of the research. Table 3.3 summarises some properties of the selected ceramic membranes such as the MWCO, number of channels (n_c) of each membrane element, available filtration area (A_f), internal diameter (ϕ) and the inorganic material of fabrication. In addition, the Pure Water Permeability (PWP) of the membranes, which was experimentally measured in the laboratory, has also been included in Table 3.3. In Section 3.2.4, the PWP determination procedure is explained.

Table 3.3. Ceramic UF membranes' properties

Membrane ^(a)	MWCO (kDa)	n_c	A_f (cm ²)	ϕ (mm)	Support	Active layer	PWP ^(b) (L/(h·m ² ·bar))
T1	1						19.6
T5	5	3	94	3.6 ^(c)	Al ₂ O ₃ - - ZrO ₂ - - TiO ₂	ZrO ₂ - TiO ₂	23.8
T15	15						58.2
T50	50						71.5
F5	5	1	47	6	TiO ₂	TiO ₂	52.3
F10	10						76.4
M5	5	1	55	7	α -Al ₂ O ₃	TiO ₂	61.4

^a T membranes (model InsideCéram) and F membranes (model Filtanium) are manufactured by Tami Industries. M5 membrane (model Membralox) is manufactured by Pall Exekia.

^b PWP was experimentally measured.

^c ϕ corresponds to the hydraulic diameter of each channel.

The names employed to designate membrane elements contain a letter and a number. The letter identifies the membrane manufacturer and the model whilst the number corresponds to the MWCO of the membranes expressed in kDa. T and F membranes were manufactured by Tami Industries (Nyons, France) and correspond to InsideCéram and Filtanium models, respectively. M5 membrane was manufactured by Pall Exekia (Tarbes, France). As Table 3.3 shows, T membranes have three-channel configuration whereas F and M membranes are monochannel elements. Apart from the

internal configuration, T, F and M5 membranes are made by different materials and MWCO's and thus they are particularly interesting for testing them in the same application. The membranes were used to test their filtration ability in recovering iron synthetic solutions. In addition, other heavy metals were also tested at several operation conditions to state the mechanisms of selectivity in those applications. Those tests were of particular importance because they represented the first step in the selection of the appropriate membrane range for its application in the filtration of Fenton effluents.

3.2.2.2. Polymeric UF membranes

Three commercially-available polymeric UF membranes were selected in this part of the study. The membranes were of flat-sheet configuration and were all manufactured by GE-Osmonics (USA). The membranes are designated as GH, PT and ER membranes and their properties are detailed in Table 3.4. The selected membranes were made of different materials and their MWCO's ranged from 1 to 30 kDa. Even though the MWCO of GH was lower than that of PT, their PWP was found to be slightly higher. This can be attributed to the differences in membrane material, which could affect water permeability. The selected UF membranes were used in this thesis to check their efficiency to retain iron species from aqueous media.

Table 3.4. Polymeric UF membranes' properties

Membrane	MWCO (kDa)	Support	Active layer	PWP ^(a) (L/(h·m ² ·bar))
GH	1	TFC ^(b)	TFC ^(b)	20.1
PT	5	PES ^(c)	PES ^(d)	16.0
ER	30	PS ^(c)	PS ^(d)	39.2

^a PWP was experimentally measured

^b Thin Film Composite (proprietary confidential)

^c Polyethersulfone

^d Polysulfone

3.2.2.3. Polymeric NF membranes

Three commercial flat-sheet NF membranes were selected for testing their ability to recover iron ions from aqueous streams and also as separation step after the Fenton oxidation of polluted effluents. The membranes were manufactured by DOW-Filmtec (Minneapolis, USA) and were gently provided free of charge. Table 3.5 gives the most important characteristics of the selected membranes. The membranes are designated as NF-D, NF90 and NF270. These names correspond to the commercial designations with the exception of NF-D. NF-D is commercially designated as NF but, for avoiding confusions with the universally accepted acronym for nanofiltration, NF, this membrane is named NF-D throughout the text. As Table 3.5 summarises, the membranes are made of diverse materials and exhibit different isoelectric points (IEP's). The PWP of NF-D and NF90 are quite close whilst that of NF270 is around twice. In fact, whilst NF270 can be considered a loose NF membrane, NF90 has shown properties of tight NF membranes (Nghiem et al. 2004). Therefore, thanks to the varied membranes'

characteristics, these elements have been extensively used as purification technologies in textile industry (Alcaina-Miranda et al. 2009), pulp and paper (Mänttari et al. 2004; Mänttari et al. 2008), as tertiary treatment (Bellona and Drewes 2007), for the removal of organic acids (Choi et al. 2008), heavy metals (Tanninen et al. 2006), pharmaceuticals (Nghiem et al. 2005; Radjenović et al. 2008), disinfection by-products precursors (Ates et al. 2009), herbicides (Plakas et al. 2006), pesticides (Plakas and Karavelas 2009) and in many other applications in water and wastewater treatment areas. Here, these membranes were selected to check their ability to both retain iron from model solutions and also perform as membrane separation step after the Fenton oxidation of phenol and phenol+SDS solutions.

Table 3.5. Polymeric NF membranes' properties

Membrane	MWCO (kDa)	Support	Active layer	Isoelectric point pH	PWP ^(a) (L/(h·m ² ·bar))
NF-D	-	PS ^(b)	PA _p - TFC ^(c)	5.1 ⁽¹⁾	5.9
NF90	-	PS ^(b)	PA - TFC ^(d)	4.0 ⁽²⁾	5.6
NF270	-	PS ^(b)	PA _p - TFC ^(c)	3.3 ⁽¹⁾	9.3

^a PWP was experimentally measured

^b Polysulfone

^c Semi-aromatic piperazine-based polyamide – Thin Film Composite

^d Polyamide – Thin Film Composite

¹ Tanninen et al. 2006

² Nghiem et al. 2005

3.2.3. Membrane filtration set-up

3.2.3.1. Crossflow filtration set-up

Both ceramic and polymeric membranes were tested in crossflow operation mode. As explained in Chapter 1, in crossflow mode, fouling formation is expected to be lower than in dead-end mode thanks to the tangential flow of the feed stream. Figure 3.2 shows the experimental set-up designed and built-up for testing membranes' performance in crossflow mode. As shown by Figure 3.2, both permeate and retentate streams exiting the membrane were recycled back to the feed tank to maintain the feed solution concentration constant during the filtration experiment. Only a small fraction of permeate was not recycled to the feed tank because permeate samples were periodically withdrawn to characterise them. The permeate flux was measured with the help of a balance (A&D Instruments, model GF-1200).

A 5-L glass feed tank (filled with 3 L of solution to be filtered) was used for performing experiments with synthetic solutions of heavy metals, tested only with ceramic membranes. A 1.2-L jacketed glass reactor, used also for performing Fenton oxidation experiments (see Section 3.1.2), was employed for performing crossflow filtration experiments with the other solutions studied. In this case, the same thermostatic bath and cooling system than for Fenton experiments was installed. A pulsation pump (Prominent, model Vario) was selected for feeding the solutions to be filtered or the cleaning solutions to the membrane module. Tangential flow velocities of 27 and 8.3 cm/s were achieved when filtering with ceramic and polymeric membranes, respectively. A pulse dampener (Hydracar S.A., model U002A18V1-AI) was installed

before the membrane module in order to transform the periodic flow to continuous flow to reproduce a real membrane operation performance. The pulse dampener was actuated by means of a backpressure valve installed after it.

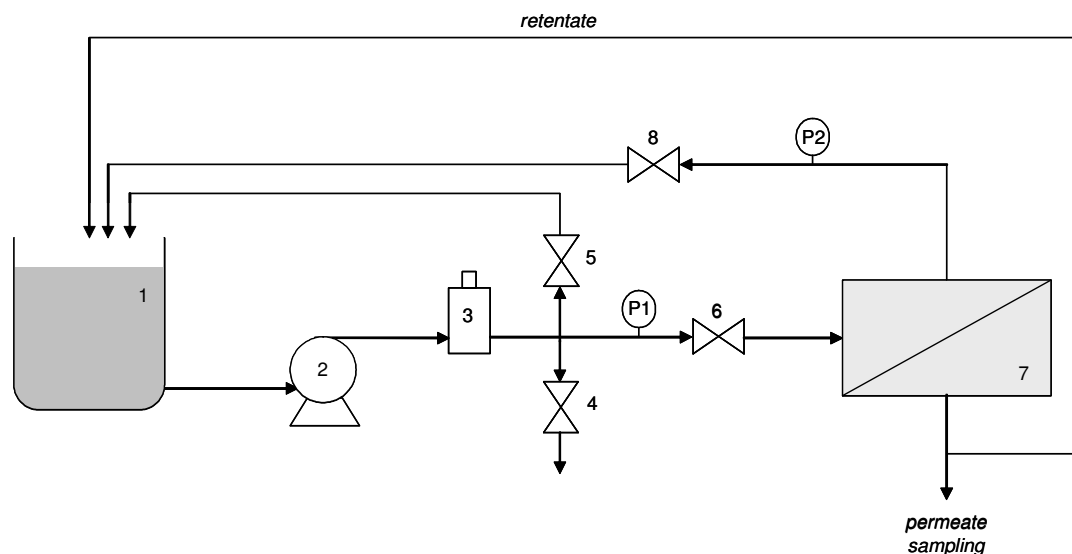


Figure 3.2. Crossflow filtration set-up

(1) Feed tank ; (2) Pump ; (3) Dampener ; (4) Relief valve ; (5) Bypass valve ; (6) and (8) Backpressure valves ; (7) Membrane module ; (P1) and (P2) pressure gauges

The crossflow filtration unit was designed for testing both tubular ceramic membranes and flat-sheet polymeric ones. Depending on whether ceramic or polymeric membranes were used, membrane modules had to be changed due to their different configuration. Ceramic membranes were hosted in a Membralox stainless steel module designed to test 250 mm length elements whilst flat-sheet polymeric membranes were hosted in a Sterlitech commercial cell (model CF042). The available filtration area of the ceramic membranes can be found in Table 3.3 and the Sterlitech module hosted membrane coupons of 42 cm² of filtration area. The backpressure valve installed in the concentrate stream close to the membrane module was used to fix and maintain the TMP during the membrane filtration experiments.

3.2.3.2. Dead-end filtration set-up

Dead-end filtration, despite the increase on membrane fouling due to the accumulation of retained solutes, is useful to perform membrane screening tests allowing the selection of the most-adequate membrane for a certain application. Moreover, dead-end experiments, as the concentration of solutes is always increasing in the fed solution as long as the filtration proceeds, are also useful to test the effect of the solute feed concentration on the membrane performance efficiency. However, as abovementioned, results are not representative or are not a scale-down of an actual membrane operation. In this thesis, dead-end mode was selected for testing the retention of heavy metals from synthetic solutions with polymeric flat-sheet membranes.

The dead-end filtration set-up is drawn in Figure 3.3 and its main unit was a commercial filtration dead-end cell (Sterlitech, model HP4750). The cell had a total capacity of 300 mL and could be stirred with a suspended magnet and an external

magnetic stirrer (Selecta, model Agimatic REV-S), which was placed below the cell. The system was pressurised by means of nitrogen gas, which served to fix the TMP during the experiments, read in the pressure gauge. As in the crossflow filtration set-up, a balance (Acculab, model VIC 303) was used for measuring the membrane permeate flux along the experiment.

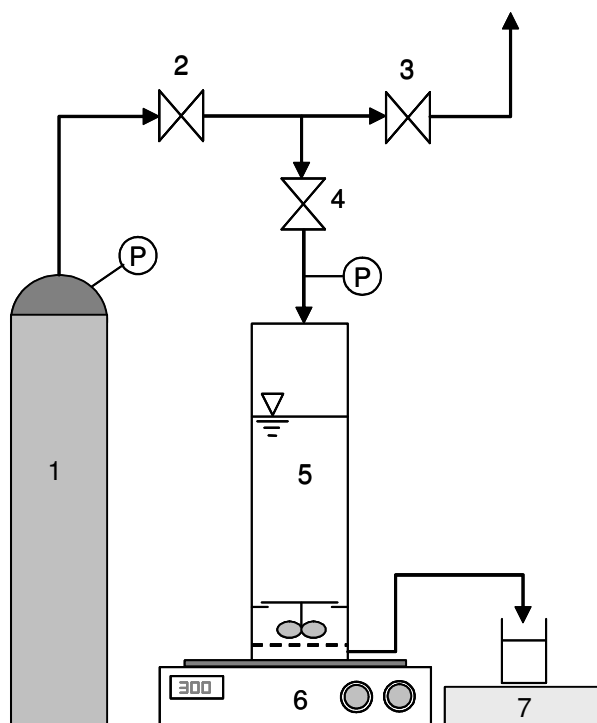


Figure 3.3. Dead-end filtration set-up
(1) N_2 cylinder ; (2) (3) (4) Valves ; (5) Filtration cell ;
(6) Magnetic stirrer ; (7) Balance ; (P) Pressure gauge

3.2.4. Filtration of synthetic solutions of heavy metals

Synthetic solutions of heavy metals were prepared by dissolving the appropriate amount of heavy metal salts (see Table 3.2) in deionised water and adjusting the pH at the desired value by acid/base addition. After this, the solutions were ready to be filtered. Depending on whether crossflow or dead-end experiments wanted to be performed, different experimental protocols, whose details are explained below, were designed.

3.2.4.1. Crossflow filtration protocol

Crossflow filtration of heavy metal solutions was performed with ceramic membranes. The tests were performed in total recycling mode. Thus, both retentate and permeate were recycled back to the feed tank in order to keep the heavy metals' concentration constant during the filtration experiments. Before every test, the pure water flux of the clean membrane (J_w) was measured at TMP's of 2, 4, 6 and 8 bar. At each TMP, the permeate flux was measured three times for five minutes. After that, the feed tank was filled with 3 L of heavy metal/s' solution. Then, the pump was switched on and the TMP was set to 2 bar. The tangential velocity through the ceramic membrane tubes was 27 cm/s in all the experiments. Permeate samples were periodically withdrawn and the

permeate flux (J_p) was obtained from the permeate weight measured for a certain time with the installed balance. Once the steady-state was achieved, the TMP was subsequently changed to a higher value. The previous procedure was repeated at 4, 6 and 8 bar. Once the test at 8 bar was finished, the membrane was rinsed with deionised water for 15 min. The permeate water flux (J_a) was then measured again at 2, 4, 6 and 8 bar as described for the determination of J_w . After J_a was determined, the efficiency of cleaning solutions in restoring the membrane properties to their initial status was tested by measuring again the membrane permeate flux with deionised water (J_{ac}). After the experimental work was finished, the ceramic membranes were stored in a humid environment to preserve their hydration state, as recommended by the manufacturer.

3.2.4.2. Dead-end filtration protocol

The filtration ability of both UF and NF polymeric flat-sheet membranes was tested in dead-end mode when dealing with synthetic solutions of heavy metals. The experiments started by compacting the membranes at 10 bar for one hour. Before this, the membranes were soaked in deionised water overnight. Then, J_w was determined following the same protocol than in crossflow mode. However, in this case, J_w was determined at only one TMP, which was fixed to the same value than that subsequently set for the filtration of the heavy-metal solution. After J_w determination, 250 mL of the prepared solution was fed into the filtration cell and 10 mL of sample was withdrawn. The stirring rate (ω) and the TMP were fixed at the desired level. Then, the filtration experiment started. During the filtration, J_p was periodically determined with the balance and permeate samples were withdrawn and stored for their analytical characterisation. The filtration was stopped at a Volume Reduction Factor (VRF) of 6. The VRF is defined as the ratio of the initial feed volume to the volume of concentrate. Thus, a VRF of 6 indicates that the filtration was carried out until the concentrate volume was 1/6 of the initial feed one. In fact, when operating in dead-end mode, the VRF is used to report the evolution of the filtration parameters or efficiency along the experiment instead of using the experimental time. After the last permeate sample had been taken, the filtration cell was dismantled and a concentrate sample was withdrawn for its analysis. The difference between the expected final concentrate concentration (calculated by mass balance assuming no adsorption on the membrane) and that analytically determined gives the percentage of solute adsorption onto the membrane material, as reported in previous studies (Plakas et al. 2006). After this, the determination of the J_a and J_{ac} could also be carried out in this system following the same protocol than in crossflow operation mode. However, as in the J_w measurement, only one TMP equal to that selected for testing the filtration ability was employed for measuring those permeate fluxes. A virgin membrane was used for every experiment unless otherwise noted.

3.2.5. Filtration of Fenton effluents

Fenton effluents were oxidised following the procedure described in Section 3.1.3. Those effluents were filtered by UF and NF polymeric membranes in crossflow mode and in total recycling mode to know the membranes' potentiality as middle separation unit between Fenton oxidation and aerobic biological treatment.

The first step was the measurement of the J_w using deionised water at 30°C and at a TMP of 6 bar using a new membrane with the exception of when membrane reusability wanted to be determined. Before the J_w measurement, the membranes were stored

soaked in deionised water overnight and compacted at 10 bar for one hour with deionised water.

900 mL of Fenton effluent was added to the feed tank and the magnetic stirrer, placed below it, was switched on at a stirring rate of 300 rpm. Then, the thermostatic bath was switched on and, once the temperature had reached 30°C, the filtration experiment started after withdrawing a feed sample and fixing the TMP at 6 bar. The tangential velocity during the experiments was always 8.3 cm/s and the experiments were carried out for 6 hours. When cooling was required, tap water was forced to circulate inside the cooling device to adjust the temperature of the solution being filtered. Measurement of J_P and permeate sampling were periodically carried out during the filtration experiment.

Once the filtration was finished, the remaining Fenton effluent was replaced by deionised water and, after rinsing the membranes for 10 min with deionised water and after filtering deionised water at 30°C during 5 min at a TMP of 6 bar, the membrane permeate flux (J_a) was measured again at 6 bar and 30°C with deionised water. After this and only when the cleaning efficiency of a certain agent wanted to be examined, the membranes were chemically cleaned. Later, the water permeate flux (J_{ac}) was determined with deionised water at 30°C at a TMP of 6 bar after ensuring the neutrality of both permeate and retentate streams by rinsing the system with deionised water.

3.2.6. Membrane filtration efficiency assessment

Membrane efficiency is not determined from one unique indicator but from a set of several efficiency indexes. Efficiency assessment includes not only filtration variables but also fouling quantification and ability of cleaning agents and protocols for eliminating it. The membrane efficiency parameters employed in this thesis are briefly described in this section.

3.2.6.1. Permeate flux decline, fouling and cleaning efficiency

As described in Sections 3.2.4 and 3.2.5, permeate flux is measured several times during a filtration experiment. In general, J_w , J_P , J_a and J_{ac} can be obtained from a filtration test. Combinations between those flux parameters is of high value for understanding phenomena associated to the permeate flux loss occurring during the filtration processes at constant TMP.

The ratio J_P/J_w can be used to assess the permeate flux evolution as long as the filtration proceeds when J_P is periodically monitored. This ratio is known as normalised permeate flux because at time zero, it is equal to one and then starts decreasing as result of concentration polarisation and fouling phenomena. Thus, the ratio is a direct measure of the **permeate flux decline**. The ratio can be given as a percentage and, in that case, it obviously can go from 100 to 0. A $\%J_P/J_w$ equal to 60% would indicate that 40% of permeate flux loss has occurred at the tested conditions due to concentration polarisation and/or fouling phenomena.

The ratio J_a/J_w is useful to determine the fouling phenomena remaining after softly rinsing the membranes with deionised water. Thus, the ratio is an indicator of the **severe fouling** percentage when it is expressed as percentage. A $\%J_a/J_w$ equal to 70% would mean that only 30% of severe fouling has occurred during filtration and, if the previous example is taken, partial flux recovery has taken place as result of the membrane rinsing.

The ratio J_{ac}/J_w , measured after a cleaning protocol is performed in a fouled membrane, is an indicator of the **cleaning protocol efficiency**. The ratio can be expressed as a percentage as with the previous ratios. A $\%J_{ac}/J_w$ of 90% would mean that 10% of permeate flux loss remains after cleaning the membrane at the tested conditions. Thus, either other cleaning protocol needs to be designed or membrane damage has occurred during the operation (or even during the cleaning). Apart from the ratio of fluxes, the membrane separation efficiency has to be determined after a cleaning protocol is performed. For this, the efficiency of a membrane in retaining a certain ion/molecule is tested with a virgin membrane and with a used-and-cleaned membrane. This test is especially helpful to determine whether the cleaning conditions are harmful or not for the membrane. The ion/molecule selected for testing cleaning effects on membrane performance can be replaced by the solution/effluent under study. The repetition of operation-cleaning cycles and comparing both the ratios of permeate fluxes and the retention to the results obtained in the first operation with a virgin membrane gives an idea of both the cleaning efficiency and the membrane lifetime. The determination of retention percentages is explained in the following subsection.

3.2.6.2. Retention efficiency

The separation of certain ions or compounds is often the main objective when considering a membrane technology in wastewater treatment applications. The retention percentage, $R(\%)$, can refer to an individual ion, molecule or to a global parameter. For instance, the retention of iron ions, phenol or TOC can be of interest for a certain membrane application. The concentration of the species/parameter of interest in the feed solution (C_f) and in the permeate (C_p) are needed to calculate the associated $R(\%)$ by employing equation 3.1. Thus, analyses determining the species/parameters of interest in aqueous samples are needed. The analyses employed for the characterisation of aqueous samples in this thesis are explained in detail in Section 3.5.

$$R(\%) = 100 \cdot \left(\frac{C_f - C_p}{C_f} \right) = 100 \cdot \left(1 - \frac{C_p}{C_f} \right) \quad (\text{eq. 3.1})$$

3.3. Phenol oxidation with ferrous O/W emulsions prepared by membrane emulsification

Membrane emulsification was used for the formulation of oil-in-water (O/W) emulsions containing Fe(II) at the droplets' interface. These emulsions were later tested as heterogeneous Fenton catalysts for phenol degradation.

3.3.1. Reagents

Emulsions are formed by two immiscible phases in which one (dispersed phase) is dispersed into the other (continuous phase). Emulsions are generally unstable and, therefore, they tend to separate. The addition of surfactants is frequently employed to avoid phase separation and to form the emulsion droplets because they possess amphiphilic nature. Here, SDS (Sigma, purity 99%) was employed as emulsifier because of its anionic nature, allowing the iron ions to be attracted towards the

droplets' interface, where it is present. Commercial corn oil was used as dispersed phase of the prepared emulsions and iron (II) sulphate heptahydrate (Sigma-Aldrich, purity 99%) was used as source of Fe(II) ions. The continuous phase was an aqueous solution made of ultrapure water (USF Elsa, model Purelab Classic PL5221) with a resistivity of 18.2 M Ω -cm, containing SDS, Fe(II) or both depending on the experiment.

3.3.2. Membrane emulsification experiments

Membrane emulsification experiments and emulsions' characterisation were carried out during a research stay at the *Istituto per la Tecnologia delle Membrane* from the *Consiglio Nazionale delle Ricerche* (ITM-CNR) in Rende (Italy) from the 7th February 2008 until the 11th May 2008.

3.3.2.1. Stirred membrane emulsification

The stirred emulsification cell was manufactured by Micropore Technologies Ltd. (Leicestershire, United Kingdom). The system consists of a PTFE base (named injection chamber) that hosts a flat membrane coupled with a dismountable threaded glass cylinder. Between the glass cylinder and the membrane, a PTFE joint is placed in order to prevent leaks during the emulsions' preparation. A stainless steel stirrer, with a blade at the bottom ending, a motor at the top and a PTFE vortex breaker fixed at the stirrer, is placed over the glass cylinder and regulated by a voltage regulator connected to the power. A photograph of the stirred cell emulsification set-up can be seen in Figure 3.4 and a detailed scheme has been elsewhere published (Stillwell et al. 2007). The feeding system of the cell was modified from the original version as, instead of a gravimeter cylinder, a peristaltic micropump (Ismatec, model C.P. 78016-30) was connected to the injection chamber to permeate the dispersed phase at finely controlled flow rate.



Figure 3.4. Stirred cell emulsification set-up

Typical emulsification experiments started preparing the continuous phase by dissolving the appropriate amount of surfactant into ultrapure water and, depending on

the experiment, also iron sulphate. A graduated glass cylinder was subsequently filled with the oil to be dispersed. Then, both pump impulsion and aspiration tubes, as well as the injection chamber, were filled with the oil to be dispersed. Then, the membrane was placed inside the injection chamber, below the joint, and the glass cylinder was threaded. At that moment, 90 mL of continuous phase were added to the cylinder and the stirrer was placed at its correct position. The voltage regulator was set at the desired position and the pump was subsequently switched on. The pump was always operated so that the oil permeate flow rate through the membrane was 0.15 mL/min. The decrease on the level in the graduated cylinder of the liquid to be dispersed was controlled throughout the experiment to guarantee constant permeate flux. When the desired volume of the liquid to be dispersed had permeated, the pump and the stirrer were switched off and the emulsion was poured out into a glass beaker. After this, the system was dismantled and subjected to cleaning with soap and water.

Two hydrophilic metallic membranes, both purchased at Micropore Technologies Ltd, were used in the stirred emulsification experiments. The pore sizes of the membranes were 10 and 20 μm . The membranes were cleaned with soap and water after being used and were maintained submerged in ultrapure water until further use.

3.3.2.2. Crossflow membrane emulsification

Emulsification experiments in crossflow mode were carried out in a homemade lab-scale emulsification unit, schematised in Figure 3.5. The phase to be dispersed was contained in a pressurised nitrogen vessel. The TMP was fixed by regulating two backpressure valves located between the gas cylinder and the stainless steel membrane module. This way, the permeate flux of oil was perfectly controlled and kept constant during the experiments. Two valves that allowed the depressurisation of the system were installed before the oil vessel and in the shell of the module. A peristaltic pump (Amicon, model 54113#1728, Beverly, USA) was used to work at the desired continuous phase tangential velocity by selecting the adequate flowrate in the pump regulator. A 100-mL glass beaker was used as continuous phase container during the experiments. Finally, several manometers were installed to control and monitor the pressure during the emulsification tests. The membrane tested with this system was a tubular hydrophilic ceramic membrane with a pore size of 0.5 μm (manufactured by Membrflow, Germany). The membrane active layer was made of zirconium oxide and its total length was 100 mm. The internal and external diameter of the membrane was 7 and 10 mm, respectively.

A crossflow membrane emulsification experiment started by filling with oil the dispersed phase vessel, the tubes connecting the vessel, the membrane module as well as the shell of the module. The vessel containing the continuous phase was filled with 90 mL of ultrapure water and the pump was switched on at the desired flow rate for performing the emulsification experiment. The continuous phase was always recycled inside the lumen of the membrane. Once all the air was purged out from the module, a nitrogen pressure of 5 bar was fixed and the dispersed phase was allowed to permeate for one hour. Later, the dispersed phase circuit was depressurised, the water that had been circulating was purged out and a solution containing the ingredients desired for the emulsification experiment was circulated for five minutes in order to remove any oil that could have remained in the continuous phase circuit. After removing this solution, 90 mL of fresh continuous phase, prepared as in the stirred cell experiments, was then placed in the continuous phase vessel and kept circulating at the same flowrate than when water was circulated. Then, the dispersed phase circuit was pressurised at 1 bar and, at that moment, the emulsification process started. Once the desired volume of oil

had permeated, the dispersed phase circuit was depressurised to stop the oil permeation and the obtained emulsion was collected from the circuit and the continuous phase vessel. The emulsion obtained was kept in a glass beaker for further characterisation and/or iron addition experiments.

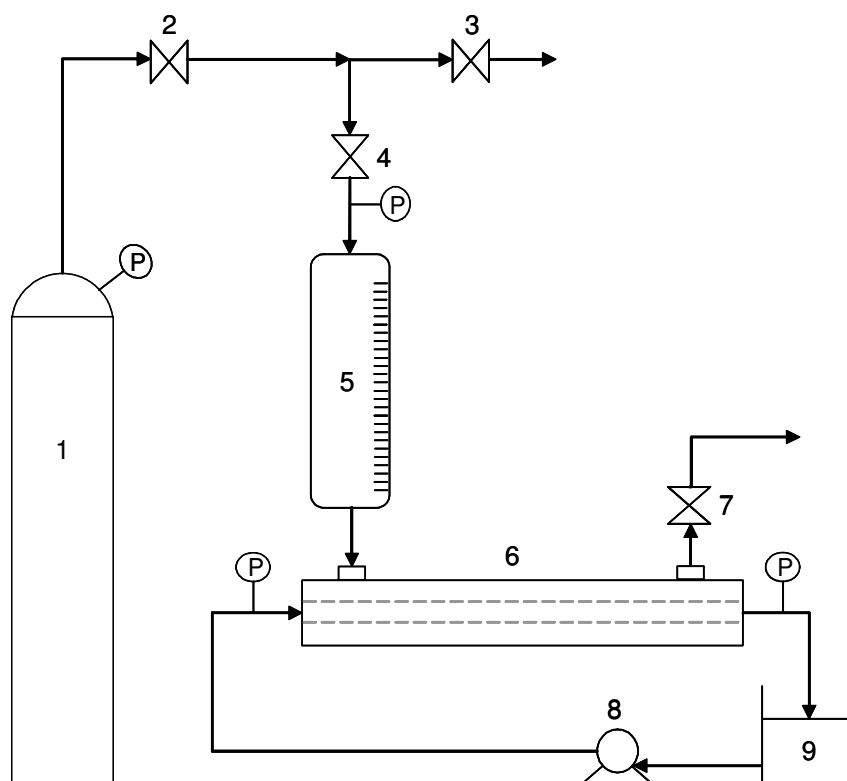


Figure 3.5. Crossflow membrane emulsification set-up
(1) N₂ cylinder ; (2) (4) Backpressure valves ; (3) (7) Purge valves ;
(5) Oil vessel ; (6) Membrane module ; (8) Peristaltic pump ;
(9) Continuous phase container ; (P) Pressure gauge

3.3.2.3. Formulation of Fe(II)-containing emulsions

Continuous phases containing Fe(II) and SDS dissolved in ultrapure water were prepared for formulating Fe(II)-containing emulsions. The emulsification experiments were conducted as when no Fe(II) was present.

When the effect of the Fe(II) presence and concentration on the emulsion properties of previously-prepared emulsions wanted to be explored, emulsions without Fe(II) in the initial continuous phase were obtained, following the protocols described in the preceding sections. Then, the obtained emulsions were left to settle overnight in separation funnels and the separated continuous phases were replaced by an Fe(II)-containing aqueous solution of known concentration. The new emulsions were mixed at 50 rpm at room temperature (20±1°C). At this point, the new emulsions were subjected to the same analyses than those performed in emulsions prepared with Fe(II)-containing continuous phase. Control experiments, in which the separated continuous phases were replaced by ultrapure water, were also carried out.

3.3.3. Characterisation of emulsions

Emulsions obtained in the stirred and crossflow membrane emulsification devices were characterised with the same techniques and following the same sampling and analysis protocol. After the emulsification experiments, emulsions were preserved unstirred in closed glass beakers at room temperature ($20 \pm 1^\circ\text{C}$). Given the size of the droplets, the emulsions suffered from creaming. To obtain a homogenous sample, the emulsions were stirred (50 rpm) before their characterisation and an emulsion sample was withdrawn from the centre of the beaker with a pipette. Any eventually separated oil was carefully eliminated from the sample and its mass and volume were measured. Five different samples were collected for each measure to evaluate the analysis reproducibility. After the sample withdrawal, the emulsions were left again without stirring.

The amount of oil present in the samples was measured by means of a moisture analyser (Ohaus, model MB45) composed by a precision balance and a dryer unit. The instrument operates on the thermo gravimetric principle: the oil percentage is determined from the weight of sample dried by heating the sample at 100°C . The percentage of oil-in-water (%O/W) can be determined from the initial and final (after evaporation) sample weight measurements. The analysis was carried out immediately after the emulsification. In certain emulsification experiments, the measurement was also repeated along one week to monitor the eventual changes on the %O/W as a function of time, caused by oil separation from the emulsion. As explained before, as separated oil was not collected during the sampling, the resulting %O/W only refers to the emulsified oil-in-water percentage. Therefore, a decrease of %O/W was an indicator of the emulsion breakage.

The emulsion droplet size distribution was obtained in a Malvern Mastersizer analyser (Malvern Instruments, model 2000), a laser light scattering analyser, equipped with a liquid sampling unit (Malvern Instruments, model Hydro 2000 MU). Reported data are averages of ten readings of three samples from at least two separate experiments. The analyser was used to obtain the droplet size distribution curve, the surface weighted mean diameter (or Sauter diameter), represented by $D[3,2]$, the volume weighted mean diameter (or De Brouckere diameter), represented by $D[4,3]$, and the value of the Span (indicator of the width of the distribution curve). $D[3,2]$, $D[4,3]$ and Span were determined, respectively, as follows:

$$D[3,2] = \frac{\sum D_i^3 n_i}{\sum D_i^2 n_i} \quad (\text{eq. 3.2})$$

$$D[4,3] = \frac{\sum D_i^4 n_i}{\sum D_i^3 n_i} \quad (\text{eq. 3.3})$$

$$\text{Span} = \frac{D[0.9] - D[0.1]}{D[0.5]} \quad (\text{eq. 3.4})$$

where D_i corresponds to the droplet diameter in class i and n_i corresponds to the number of droplets in class i . $D[0.5]$ is the diameter in microns at which 50% of sample is smaller and 50% is larger; $D[0.1]$ and $D[0.9]$ are the diameters below which 10% and 90% of the sample lies, respectively.

The droplet size distribution analysis was performed immediately after preparing the emulsions and followed during one week. Observed changes on the $D[3,2]$, $D[4,3]$ and Span are therefore an indicator of the changes on the properties of the prepared emulsions. $D[4,3]$ value is more sensitive to the presence of larger droplets than $D[3,2]$ value and therefore, it gives an indication of droplet coalescence. Emulsion stability index (ESI) was expressed as the ratio between the emulsion stored data (including $D[3,2]$, $D[4,3]$ and Span) and the initial emulsion data. Combining ESI value with %O/W for stored emulsions, it is possible to understand the occurred destabilisation process. In particular, $ESI=1$ and constant %O/W indicate that emulsion is stable. $ESI>1$ indicates emulsion droplets' coalescence. $ESI<1$ and decrease in the %O/W indicate emulsion breakage, i.e. larger emulsion droplets coalesce and then break causing oil separation.

Optical microscopy characterisation of the prepared emulsions was also carried out in some experiments to compare the visual observations of the droplet size distribution of the emulsions with those obtained using the light scattering analyser. The optical microscope (Zeiss, model Axiovert 25) was equipped with a camera (JVC, model TK-C1481BEG) to capture the images of the emulsions, which were then processed by the Scion Image software.

The Fe(II) content in the emulsion droplets was obtained in an atomic absorption spectrometer (Hitachi, model Z-8200). Emulsions were filtered through Nylon membrane disks of 0.2 μm pore size and 47 mm diameter (Whatman International) prior to Fe(II) analysis. A vacuum pump (Edwards, model D1) was used to filter the emulsion samples. The difference between the initial iron concentration in the continuous phase (original or exchanged) and the final iron concentration allowed the determination of the Fe(II) linked to the emulsion droplets.

3.3.4. Fenton oxidation experiments using emulsions as catalyst

The catalytic activity of the emulsions containing iron was tested in the degradation of phenol aqueous solutions using hydrogen peroxide as oxidant source. Thus, the effectiveness of the Fenton-like process using iron ions confined in emulsion droplets was studied. The experiments were performed in a batch glass reactor of 100 mL capacity. The reactor was magnetically stirred (Velp Scientifica, model Arex) at 50 rpm and the reaction experiments were performed at room temperature ($20\pm 1^\circ\text{C}$). The emulsions significantly destabilised after their preparation were not considered for phenol oxidation experiments.

The emulsion droplets of the emulsions to be catalytically tested were separated in glass separation funnels. Then, the continuous phase of the emulsions was discarded and 10 mL of concentrated emulsion was measured and added to the reactor together with 45 mL of phenolic solution. The Fenton reaction started after the addition of 5 mL of H_2O_2 solution to the reactor. The initial concentration of phenol and H_2O_2 in the reactor was 1000 mg/L and 5000 mg/L, respectively. Apart from the emulsions containing iron, a blank emulsion (without iron) was oxidised in order to distinct between the two possible phenomena occurring in the system: phenol partition between the bulk solution and the droplets and phenol degradation. Samples were periodically withdrawn from the reactor to analyse phenol content by HPLC. In order to avoid emulsion droplets and non-emulsified oil entering the chromatograph, the samples were first filtered through 0.45 μm mixed cellulose ester syringe filter (Millipore Corporation, cat. no. SLHA 025 NB) and later through 0.2 μm cellulose acetate syringe filter (Nalgene, 4-mm syringe filter, cat. no. 171-0020).

After 120 minutes oxidation, a sample from the reactor was characterised in terms of emulsion stability and droplet size distribution and the experiment was stopped. Iron analysis (to know the amount of leached iron from the emulsions) was done by Atomic Absorption Spectrometry (AAS). Samples for iron analysis were filtered through Nylon membrane disks of 0.2 μm pore size and 47 mm diameter (Whatman International, cat. No. 7402-004) prior to AAS analysis. A vacuum pump (Edwards, model D1, Crawley, Sussex, England) was used to perform samples' filtration. Both phenol and iron analyses' protocols are explained in detail in Section 3.5.

3.4. Inert ceramic membrane reactor

The main purpose of this part was, as explained in the Introduction chapter, to reduce hydrogen peroxide wasting during the Fenton oxidation of phenol synthetic solutions. This was tested by introducing hydrogen peroxide through the walls of a tubular reactor, which was a tubular ceramic membrane. Apart from the oxidation of phenol, the degradation of its Fenton oxidation intermediates was also studied in this reactor configuration.

3.4.1. Reagents

Phenol, hydrogen peroxide and ferrous sulphate were obtained from the same suppliers than those employed in phenol oxidation effluents' degradation. The intermediates used for preparing single model solutions to be oxidised were commercial and used as received. A solution of formic acid (95% wt.) was supplied by Baker. A 99.8% wt. solution of acetic acid was purchased at Aldrich. Oxalic acid dihydrate (purity of 99%), catechol (purity higher than 99%) and hydroquinone (purity of 99%) were purchased at Aldrich. Malonic acid (purity of 99%), maleic acid (purity higher than 99%), fumaric acid (purity higher than 99.5%), resorcinol (purity higher than 98%), p-benzoquinone (purity higher than 99.5%) and t,t-muconic acid (purity higher than 97 %) were supplied by Fluka.

3.4.2. Membrane reactor set-up and operation

One-channel tubular ultrafiltration ceramic Membralox® membrane, manufactured by Pall Exekia (Tarbes, France), was selected for this study. The molecular weight cut-off of the membrane was 5 kDa and its properties can be found in Table 3.3 as the membrane referred to as M5.

Figure 3.6 illustrates the experimental set-up used for performing the oxidation tests in the inert ceramic membrane reactor at room temperature. A nitrogen cylinder (1) gave the pressure needed to impulse the solutions contained in the two graduated glass vessels (6 and 7); the pressure was controlled and monitored by means of two backpressure valves (2 and 3) and two needle valves (4 and 5). The first vessel (6) contained the polluted solution (phenol or phenol intermediate) and the iron salt (iron sulphate). The second vessel (7) contained the oxidant solution. Both feed vessels had a capacity of 250 mL and were graduated so that the flowrate of each influent could be measured and controlled. A needle valve (8) was employed to fix the pollutant flowrate entering into the lumen of the membrane, hosted in a stainless steel membrane module (9). The hydrogen peroxide solution permeated through the membrane from shell-to-lumen, where it reached and reacted with iron ions, forming oxidative radicals. The

reactor effluent flowrate was measured by means of a balance (A&D Instruments, GF-1200) at periodic intervals of time.

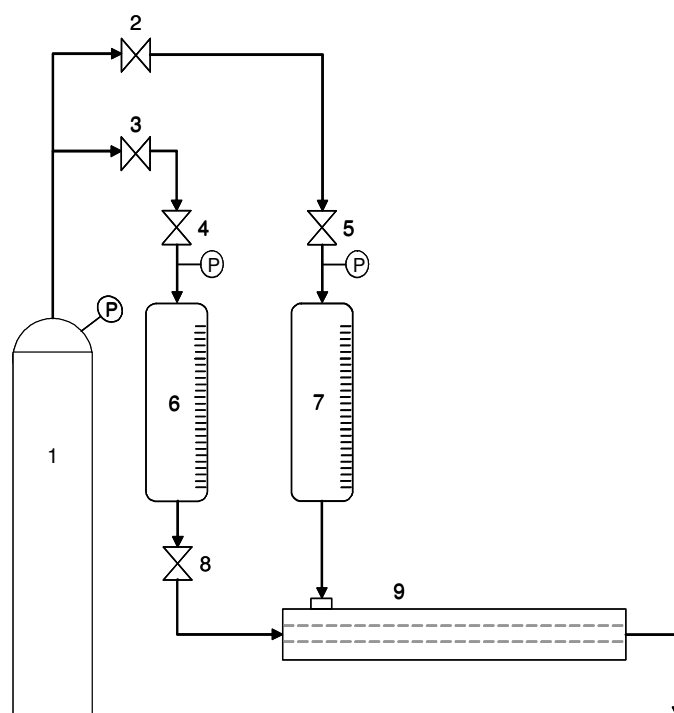


Figure 3.6. Inert membrane reactor set-up. (1) N_2 cylinder ; (2) (3) Backpressure valves ; (4) (5) Ball valves ; (6) Polluted solution vessel ; (7) Oxidant vessel ; (8) Needle valve ; (9) Membrane module ; (P) Pressure gauge

Reactor effluent samples were periodically withdrawn to analyse phenol, TOC, intermediates' concentration, iron concentration and hydrogen peroxide content. The samples were quenched with NaOH following the same procedures than those used for homogeneous Fenton experiments, explained in Section 3.1.3. The analyses were carried out according to the protocols explained in Section 3.5. The experiments had a total duration of four hours when phenol oxidation was under study. Instead, when single intermediates were oxidised, two-hour experiments were programmed. The steady-state was rapidly achieved because constant analyses' results of the samples were obtained since the very beginning of the experiments. However, the duration of the experiments was greatly lengthened so that the results were not influenced by possible fluctuations of the flowrates.

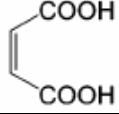
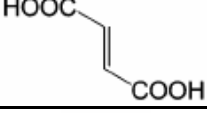
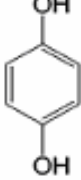
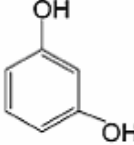
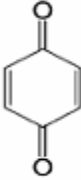
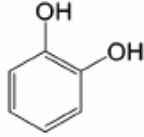
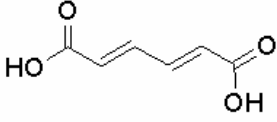
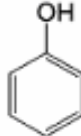
3.5. Characterisation of aqueous samples

3.5.1. Phenol and phenol oxidation intermediates

Phenol and its oxidation intermediates were analysed by High-performance liquid chromatography (HPLC) in an Agilent Technologies chromatograph (1100 Series). The chromatographic gradient method used was developed to analyse intermediates of the CWAO of phenol effluents and was published by Suárez-Ojeda et al. (2007c). Although the method was used in this thesis without any modification, the list of intermediates analysed was reduced to those appearing in the Fenton oxidation pathway of phenol (Zazo et al. 2005). The phenol Fenton oxidation intermediates determined by HPLC,

ordered by their retention time, can be seen in Table 3.6, where some of their properties and their retention times are summarised.

Table 3.6. Phenol and its Fenton oxidation intermediates analysed by HPLC

Compound	Formula	MW (g/mol)	Retention time (min)
Oxalic acid	HOOC—COOH	90.03	2.923
Formic acid	HCOOH	46.03	3.245
Malonic acid	HOOC—H ₂ C—COOH	104.06	4.157
Acetic acid	H ₃ C—COOH	60.05	4.433
Maleic acid		116.08	5.499
Fumaric acid		116.08	7.111
Hydroquinone		110.11	7.884
Resorcinol		110.11	10.547
p-benzoquinone		108.10	11.091
Catechol		110.11	11.640
t,t-muconic acid		142.11	13.809
Phenol		94.11	16.566

Commercial phenol and intermediates were used for calibrating the HPLC method. Their characteristics and suppliers have already been exposed in Sections 3.1.1 and 3.4.1. A C18 reverse-phase column (Agilent Technologies, model Hypersil ODS, 5 μm , 25 x 0.4 cm) was selected for performing the separation of the organic compounds at 30°C. A sample injection volume of 10 μL was required and the mobile phase was a mixture of methanol, especially produced and supplied for HPLC (99.9% purity, Sigma-Aldrich), and acidified ultrapure water (Millipore, model Direct-Q). The mobile phase flowrate was 0.75 mL/min and it passed from 100% acidified ultrapure water in time 0 to 50% acidified ultrapure water and 50% methanol in 25 minutes. Then, the mobile phase composition was returned to its initial value in 3 minutes. A diode array detector was used for detecting the organic compounds analysed at 254 nm or 210 nm, depending on the compound to be identified.

The previous method was employed when intermediates were present in the samples to be analysed. However, an isocratic method was employed when only phenol was present in the aqueous sample or it was the only organic compound whose concentration wanted to be determined. The selected method was developed and used in previous research studies (Fortuny et al. 1999; Suárez-Ojeda et al. 2005; Rubalcaba et al. 2007a; Sanchez et al. 2007). The analysis was performed in the same HPLC and with the same column. The only difference was that the sample injection volume was 20 μL and the composition of the mobile phase was 60% acidified ultrapure water and 40% methanol for the whole analysis. The mobile phase flowrate was constant to 1 mL/min during the total 7 minutes of the analysis and the temperature was controlled at 30°C. Phenol detection was carried out at 254 nm.

3.5.2. Surfactants

Surfactants studied in this thesis were not individually measured but analysed as total surfactant. Consequently, when testing surfactants' oxidation by the Fenton process, total surfactant concentration was considered. Thus, if a surfactant molecule was degraded into another surfactant, the latter was included in the surfactant concentration (or conversion).

The concentration of anionic surfactants was determined by using commercial kits manufactured by Hach Lange (reference LCK 332). The analytical principle is adapted from the methylene blue active substances (MBAS) method (Clesceri et al. 1989; Nollet 2007). Thus, it is based on the formation of ion-pair complexes between the dye and the anionic surfactant, which behaves as cationic specie, at buffered conditions. The ion-pair complex is extracted in an organic phase (chloroform) whilst unbound methylene blue remains in the aqueous phase. A sample volume of 4.0 mL was needed to carry out the extraction and analysis. The absorbance of the organic extract is measured at 650 nm, which was found to be the maximum absorbance wavelength. The absorbance was found to be linear against the concentration until 1.5 mg/L SDS. Thus, calibration was performed below this value and samples to be analysed were diluted so that the measured concentrations were also below 1.5 mg/L.

The concentration of cationic surfactants was determined by using commercial kits manufactured by Hach Lange (reference LCK 331). The method is based on the formation of ion-pair complexes between the cationic surfactants and bromophenol blue at buffered conditions, which is an adaptation of the two-phase titration with sodium tetraphenylborate (Nollet 2007). The ion-pair complexes are extracted in a dichloromethane phase, whose absorbance is measured at 420 nm. A sample volume of 4.5 mL was needed to perform the analyses. The absorbance was found to be in the

linearity range at CPC concentrations below 2.0 mg/L. Hence, calibration and analyses were performed so that measured concentrations were below this value.

3.5.3. Metals

The content of dissolved metals was measured by AAS. Iron and copper were quantified in a Perkin Elmer (model 3110) atomic absorption spectrometer. Chromium was analysed in a Hitachi Polarized Zeeman (model Z-8200) atomic absorption spectrometer. Each metal concentration was determined by absorbance reading at its characteristic wavelength and at specific analytical conditions. 1% wt./vol. HCl was used both for diluting samples prior to metal analyses in order to prevent hydrolysis inside the sample vials and for the preparation of the calibration solutions. Iron and copper were analysed in an oxidant acetylene-air flame and samples' absorbance was read at 248.8 nm and 324.8 nm, respectively. Chromium was analysed in a N₂O-C₂H₂ flame and the absorbance was measured at 359.3 nm.

3.5.4. Hydrogen peroxide

Hydrogen peroxide in aqueous samples was determined by iodometric titration with sodium thiosulphate, according to the Standard Method 4500-Cl B (Clesceri et al. 1989). In the titration process, potassium iodide is used as iodide ion source, ammonium molybdate as catalyst, starch as indicator and sulphuric acid as protons' source. The titration endpoint is marked by a colour change from blue to colourless.

3.5.5. TOC

TOC and COD are general parameters indicating somehow the contamination level of the analysed wastewaters. The TOC corresponds to the amount of carbon in the organic molecules present in the aqueous sample. As TOC is not able to discern organic compounds present in analysed samples, chromatographic methods have been used in parallel for this purpose. However, when dealing with samples composed of only one organic, TOC can be used to indirectly determine its concentration. Theoretical TOC concentration resulting from a certain concentration of an organic compound can be calculated from its concentration and the number of carbon atoms present in its molecule. Besides to the determination of TOC in aqueous samples, this general parameter has also been used to know the percentage of sample identification (%ID). Sample identification is defined as the ratio of theoretical TOC estimated from the concentration of organic compounds (analysed by HPLC and/or surfactant analysis) to the analysed TOC. In addition, percentage of TOC removal when oxidation experiments are performed indicates the percentage of mineralisation occurred at the tested conditions.

TOC concentration in aqueous samples was determined by the Non-Purgeable Organic Carbon (NPOC) method, which corresponds to the Standard Method 5310B (Clesceri et al. 1989). An Analytik Jena (model N/C 2100) TOC analyser was selected for this purpose. 4-mL samples were added into the analyser vials and 20 µL of HCL·2N (supplied by Fluka) were then automatically introduced in order to form carbon dioxide from inorganic carbon present in the sample. Carbon dioxide was purged from the vials by bubbling 160 mL/min of synthetic air for three minutes. After this, the sample was injected into a high-temperature furnace, filled with platinum catalyst, working at 800°C. At these conditions, organic carbon was combusted and formed

carbon dioxide was analysed by a non-diffractive infrared (NDIR) detector and thus TOC carbon determined. TOC calibration was regularly done with standard potassium phthalate solutions. The calibration curve ranged from 5 to 2000 mg/L TOC.

3.5.6. COD

COD, as TOC, is a general parameter determining the pollution level of a wastewater. COD corresponds to the amount of oxygen needed to chemically oxidise all the organic matter present in the wastewater characterised. As TOC, COD can be used as indirect estimator of the amount of an organic compound in an aqueous single synthetic solution. However, its main application is directly characterising the organic load and quality of waters and wastewaters. COD can be calculated from the concentration of the organic compounds and the stoichiometric amount of oxygen needed to completely oxidise them. COD can be used, as TOC does, to estimate the percentage of sample identification from the ratio of COD calculated from the organic compounds' content analysed by direct methods to the COD analysed. However, COD generally gives higher deviations than TOC does and the latter is thus preferred for this purpose.

Measurement of COD was carried out following the Closed Reflux Colorimetric Standard Method 5220D (Clesceri et al. 1989). The analytical procedure is based on the digestion of the organic matter present in the sample with potassium dichromate (oxidant) and silver sulphate (catalyst) for 120 min in acidic medium. Whilst organic compounds are oxidised during the digestion, dichromate anion is reduced to chromium (III) cation. The absorbance of the digested samples is then spectrophotometrically read. Potassium dichromate and silver sulphate were supplied by Sigma-Aldrich and used as received for the COD analyses. Two Velp ECO8 thermoreactors were used as sample digesters and an UV-VIS spectrophotometer from Dinko (model 8500) was chosen for absorbance reading. COD calibration was performed every time when COD wanted to be determined and COD standards were prepared from potassium phthalate solutions ranging between 5 and 500 mg/L COD.

3.5.7. Colour

Colour in oxidised and filtered Fenton effluents was measured by absorbance reading in the visible range using an UV-VIS spectrophotometer (Dinko, model 8500). A wavelength scan was carried out and the wavelength corresponding to the maximal absorbance was selected for assessing the colour of the samples.

3.5.8. Biodegradability, toxicity and inhibition

Respirometry was, as mentioned in Chapter 1, selected as biodegradability, toxicity and inhibition measurement method in oxidation samples and in samples of filtered oxidised effluents. The small biological aerobic reactor used as respirometer in this study was of the LFS (liquid-flow static) type, where dissolved oxygen concentration (S_o) was measured in the liquid phase, which was static and continuously aerated (Spanjers et al. 1998). The respirometer was already used in previous studies (Suárez-Ojeda et al. 2007a; Suárez-Ojeda et al. 2007b; Suárez-Ojeda et al. 2007c; Suárez-Ojeda et al. 2008; Rubalcaba et al. 2007a; Rubalcaba et al. 2007b). A diagram of the respirometer is shown in Figure 3.7. Compressed air, whose flowrate was controlled and measured by means of a gas rotameter equipped with a micro-regulation valve, was introduced into the respirometer through a metallic diffuser located in the bottom of

the reactor. A glass vessel of 1 L capacity was used as biological reactor. The vessel was stirred with a magnetic stirrer (Selecta, model Asincro) and a magnet during the respirometric measurements. This ensured continuous and complete sludge homogenisation. The temperature was controlled at 30°C by placing the glass vessel in a thermostatic bath (Selecta, model Termotronic). The S_{O_2} , pH and temperature were measured by a pH probe (WTW, model Sentix 81) and a dissolved oxygen probe (WTW, model Cellox 325) connected to a multiparametric module (WTW, model Inolab 3), which was linked to an external PC for data acquisition.

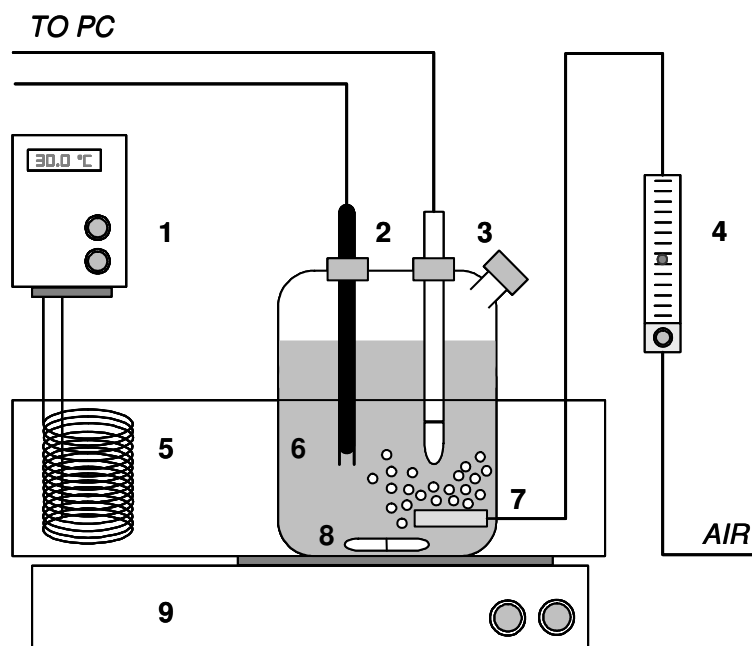


Figure 3.7. Respirometry set-up

(1) Thermostat ; (2) O_2/T probe ; (3) pH probe ; (4) Rotameter ; (5) Thermostatic bath ; (6) Aerobic reactor ; (7) Air diffuser ; (8) Magnet ; (9) Magnetic stirrer

The activated sludge used to perform respirometric measurements was taken from the WWTP in Reus (Spain). After its collection, the aerobic biomass was gently stirred and aerated overnight. This ensured that the biomass was under endogenous conditions when starting a respirometric measurement. A sludge sample was collected before feeding the biomass into the reactor. This sample was used to determine the total suspended solids (TSS) and volatile suspended solids (VSS), which was done following the Standard Methods 2540D and 2540E (Clesceri et al. 1989), respectively. The average value of the used biomass was 780 ± 60 mg VSS/L. 950 mL of aerobic biomass were introduced into the reactor and 2 mL of 20 mg/L allyl-2-thiourea solution were then added to avoid any interference from nitrifying microorganisms. At that point, the air was connected, the vessel stirred, the thermostatic bath switched on and the measurement probes introduced into the biological reactor. After the temperature had reached the set point and the S_{O_2} was stable, the measurement started.

Respirometric measurements were composed of four main steps in order to determine the percentage of readily-biodegradable COD ($\%COD_{rb}$), the inhibition and the toxic character of the tested effluent.

Step 1) A pulse of control substrate was added to the biological reactor

Step 2) After the control substrate consumption (i.e. the S_0 recovered the equilibrium level), a pulse of the sample to be tested was added

Step 3) After the S_0 equilibrium was recovered, a pulse of control substrate was added at the same concentration than in step 1

Step 4) New biomass was placed in the respirometer and control substrate (at the same COD concentration than in step 1) and sample (at the same COD concentration than in step 2) were fed together.

The control substrate (step 1) used was sodium acetate and it was added in order to ensure a concentration equal to 5 mg/L COD in the respirometer. This value was chosen in order to have a similar ratio COD_{added}/VSS to that selected in previous studies (Suárez-Ojeda et al. 2007b; Suárez-Ojeda et al. 2008), which was around 0.0059. In the present study, this ratio was 0.0064. The pulses of samples in steps 2, 3 and 4 were added at the same concentration than the control substrate pulse was.

The parameters determining the $\%COD_{rb}$ and the toxic and inhibitor character of the sample are obtained from the dissolved oxygen (DO) and the oxygen uptake rate (OUR) profiles. The former is directly obtained in a respirometric test whilst the latter is obtained by solving the oxygen mass balance in the respirometer liquid phase. In each of the four steps of the respirometry protocol, one DO profile and, consequently, one OUR profile are obtained. Before starting each step, the aeration is stopped in order to measure the value of endogenous OUR (OUR_{end}), which is equal to the slope value of the dissolved oxygen (DO) profile. Then, the vessel is aerated again and the DO level increases until it reaches a constant value called equilibrium oxygen concentration (S_{oe}) that balances the external oxygen transfer due to aeration with the OUR_{end} . The reaeration step allows the determination of the oxygen mass transfer coefficient ($k_L \cdot a$). Typical DO and OUR profiles obtained from a respirometry test can be observed in Figure 3.8, which was obtained by Guisasola et al. (2003) when the biodegradability of a 10 mg/L $N-NH_4^+$ was assessed in a LFS respirometer .

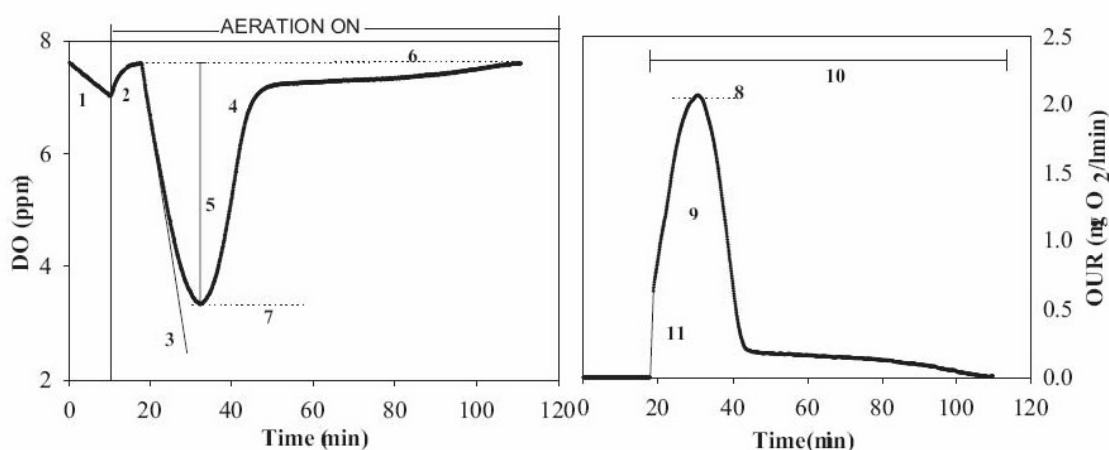


Figure 3.8. DO and OUR profiles of 10 mg/L $N-NH_4^+$ obtained in a LFS respirometer (1) OUR_{end} ; (2) reaeration profile; (3) initial peak slope; (4) peak area; (5) peak height; (6) S_{oe} ; (7) S_{oMIN} ; (8) OUR_{MAX} ; (9) oxygen consumption (OC); (10) consuming time; (11) OUR model (Guisasola et al. 2003)

As abovementioned, the OUR_{end} is obtained by stopping the aeration at the beginning of each step and it directly corresponds to the slope of the DO decay. Once the system

is reaerated again, it reaches the S_{oe} . The $k_L \cdot a$ value is estimated from DO profile through a non-linear least square regression according to equation 3.5.

$$\frac{dS_o}{dt} = k_L \cdot a \cdot (S_{oe} - S(t)) \quad (\text{eq. 3.5})$$

When a sample of substrate is added into the respirometer, the S_o starts decreasing as result of the exogenous OUR (OUR_{ex}) due to the addition. When the substrate is completely consumed, the DO level recovers again the S_{oe} value because, at this point, the OUR is equal to the OUR_{end} . The oxygen mass balance in the liquid phase of a continuously-aerated respirometer is given by equation 3.6. For the equation development, the respirometer volume has been considered constant and the OUR has been divided into OUR_{end} and OUR_{ex} . This equation is used to obtain the OUR profile by solving it in each point of the respirogram.

$$\frac{dS_o}{dt} = k_L \cdot a \cdot (S_{oe} - S_o(t)) - OUR_{end} - OUR_{ex} \quad (\text{eq. 3.6})$$

Two indirect parameters (OC and OUR_{MAX}), obtained from DO and OUR profiles, are enough for determining $\%COD_{rb}$, toxicity and inhibition character of the measured sample. Comparing the Oxygen Consumption (OC) obtained in steps 1 and 3, the sample toxicity can be determined using equation 3.7.

$$\% \text{toxicity} = \left(\frac{OC_{\text{step1}} - OC_{\text{step3}}}{OC_{\text{step1}}} \right) \cdot 100 \quad (\text{eq. 3.7})$$

The COD fraction with inhibitor character can be evaluated using the equation 3.8 from the OUR_{MAX} values obtained in steps 1, 2 and 4.

$$\% \text{inhibition} = \left[\frac{OUR_{MAX\text{step1}} - (OUR_{MAX\text{step4}} - OUR_{MAX\text{step2}})}{OUR_{MAX\text{step1}}} \right] \cdot 100 \quad (\text{eq. 3.8})$$

In the biological degradation process, part of the substrate is used for energy production and the rest for biomass growth. The heterotrophic coefficient yield (Y_H) represents the fraction of substrate used for growth (Brouwer et al. 1998) and needs to be calculated to estimate $\%COD_{rb}$. Y_H can be determined by respirometric procedures. For this, several respirometric tests are carried out with different known concentrations of biodegradable substrates (Ubay Çokgör et al. 1998; Strotmann et al. 1999). The values of OC obtained are directly related to the substrate concentration as shown by equation 3.9. The slope of the plot of the OC against added COD gives the value ($1 - Y_H$). The Y_H value determined in this study was 0.69 ± 0.06 .

$$OC = COD_{\text{added}} \cdot (1 - Y_H) \quad (\text{eq. 3.9})$$

From the Y_H and the OC value obtained in step 2, the $\%COD_{rb}$ can be assessed using equations 3.10 and 3.11.

$$COD_{rb} = \frac{OC_{\text{step2}}}{1 - Y_H} \quad (\text{eq. 3.10})$$

$$\% \text{COD}_{\text{rb}} = \left(\frac{\text{COD}_{\text{rb}}}{\text{COD}_{\text{added step2}}} \right) \cdot 100 \quad (\text{eq. 3.11})$$

As 10% reproducibility and match was attributed to the respirometry results obtained with the used set-up and procedure (Suárez-Ojeda et al. 2007a), %toxicity values lower or equal than 10% will not be considered in this study as toxic character but inert character.

3.6. Characterisation of membranes

Membranes were characterised in terms of permeability and retention percentage. However, in particular applications, a more intensive characterisation was performed. Advanced methods, such as streaming potential measurements and microscopic characterisations, were employed when necessary. In this section, the methods used are explained.

3.6.1. Streaming potential measurements

Streaming potential measurements were carried out during a research stay at the *Department of Chemical Technology at Lappeenranta University of Technology* in the research group of *Membrane Technology and Technical Polymer Chemistry* in Lappeenranta (Finland) from the 1st August 2007 until the 6th September 2007.

Charge density of a membrane and its isoelectric point (IEP) can be obtained by streaming potential measurements. The charge of the membranes (apparent zeta potential) can be measured through the membrane pores or along the membrane surface. Through the pores, the influence of the charge of all the layers composing the membrane is considered. Zeta potential (ζ) can be calculated by using the Helmholtz–Schmoluchowski equation without any corrections resulting in relative apparent zeta potentials (Nyström et al. 1989).

Characterisation of the surface charge of tubular ceramic membranes can be conducted without cutting or crashing the ceramic tubes (Condom et al. 2002; Condom et al. 2004; Fievet et al. 2004). However, it is also common to employ flat ceramic membranes (Moritz et al. 2001b; Sbaï et al. 2003) or cutting the membrane tubes for measuring it (Narong and James 2006). In this study, the streaming potential measurements were carried out without crashing the membrane elements so that, after characterisation, the membranes were used in the subsequent filtration experiments. Solutions containing 1 mmol/L KCl were chosen for the determination of the streaming potential through the pores at 25°C. Reversible Ag/AgCl electrodes were used to measure the pressure induced potential difference (0.2–1.0 bar) between the retentate and permeate sides of the ceramic membranes. The streaming potential equipment is described in detail elsewhere (Nyström et al. 1994). The membrane module was exclusively designed for this work in order to be able to host tubular ceramic elements of 10 mm diameter and 250 mm length. The membrane module was made of PVC and polycarbonate, and it was sealed with o-rings to prevent leaks during the tests. Before the streaming potential measurements, the membranes were kept in deionised water overnight in order to hydrate them.

3.6.2. Microscopic characterisation

Microscopic characterisation of membranes allows determining their morphological properties. A large list of membrane separation studies have used these tools to understand membrane properties as well as fouling and cleaning processes (Bowen et al. 1997; Al-Almoudi and Lovitt 2007; Chakrabarty et al. 2008; Kim et al. 2008).

Environmental Scanning Electron Microscopy (ESEM) allows membrane surface and transversal morphological characterisation by throwing electrons to the surface of the sample to be characterised. This causes interactions between the beam and the material, which give information on the membrane surface or transversal cut. When Energy Dispersive Spectroscopy (EDS) is coupled to ESEM (ESEM-EDS), semi-quantitative elemental composition of membrane surface can be obtained. ESEM-EDS was used in this study for characterising virgin polymeric NF membranes and after use. A FEI instrument (model Quanta 600) was used for this purpose.

CHAPTER 4

Recovery of iron from aqueous solutions by ultrafiltration

4.1. Introduction

Homogeneous iron recovery (and reuse) has been identified in Chapter 1 as one of the major drawbacks that the Fenton process presents. Iron separation from aqueous solutions by membrane technologies was tested with UF membranes of both ceramic and polymeric nature and the results are exposed and discussed in this chapter. This represents the first step into the selection of the best membrane separation option for using it as intermediate step between the Fenton oxidation and the biological treatment of industrially-polluted effluents.

The effect of the solution chemistry and membrane filtration variables on the UF efficiency was thoroughly studied. Fe(III) and Fe(II) single solutions were selected as model species for this purpose. Moreover, Cu(II) and Cr(III) solutions were also tested to validate the proposed filtration mechanism and extend the presented treatment option to other effluents' composition. In order to complete the study of the influence of the solution chemistry on the filtration performance, the recovery of iron from mixed Fe(III) and Fe(II) binary solutions was carried out. The effect of the pH, feed concentration, presence of chelating agents and solution ionic strength on the filtration feasibility was also investigated. The study of the filtration variables included the effect of the membrane MWCO, nature (ceramic or polymeric) and composition as well as the TMP on the filtration performance.

4.2. Role of the solution chemistry on the iron(III) recovery with ceramic UF membranes

In this section, the results of the study of the effect of the solution chemistry on the iron retention by ceramic UF using T5 membrane in all the experiments are presented. A Fe(III) solution was used as model feed solution, whose chemistry was altered in order to study the influence of the feed solution pH, iron concentration, iron speciation and presence of a chelating agent or background electrolyte on the filtration efficiency. The effect of the TMP was intrinsically studied in all the experiments because all the filtration tests were carried out at four TMP levels. A 0.90 mM Fe(III) aqueous solution at pH 2.00 was employed as reference solution. Thus, the filtration efficiency obtained with different filtration solutions was contrasted with that obtained with the previous solution.

4.2.1. Influence of the feed pH

The effect of the pH of the solution to filter was tested at three pH levels: 0.81, 2.00 and 2.89. At each pH, four TMP, ranging from 2 to 8 bar, were tested. The effect of the pH and TMP on the T5 membrane permeate flux decline, iron retention and fouling is presented in this section. The PWP of clean T5 membrane was 23.8 L/h·m²·bar.

The effect of the pH on the permeate flux evolution at the four TMP tested is shown in Figure 4.1. As it can be observed, J_p always decreased during filtration and almost all the permeate flux decline occurred during the first thirty minutes of operation, when a constant value was achieved. When increasing the TMP, after sixty minutes, the J_p temporarily increased. However, as long as the filtration proceeded, J_p decreased again as a new steady state was reached.

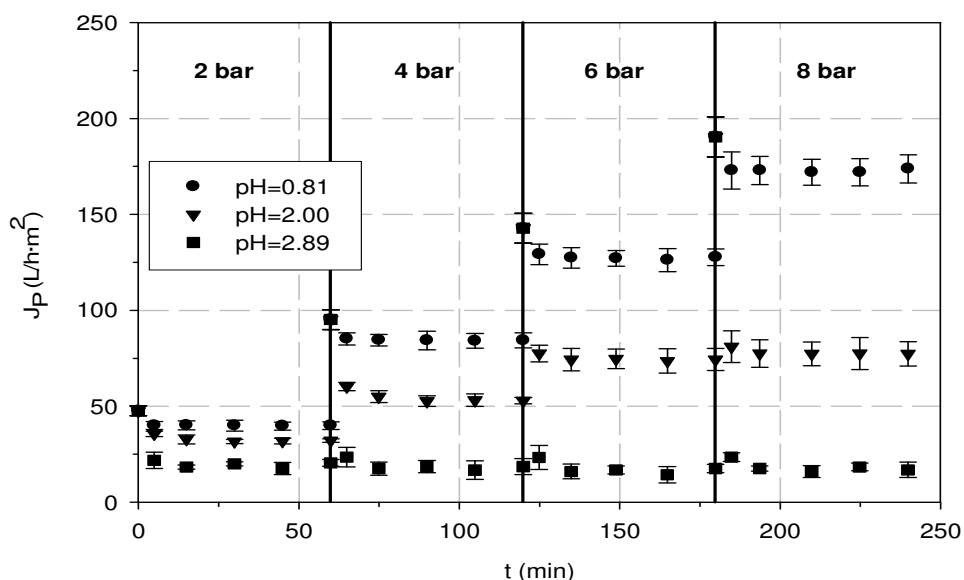


Figure 4.1. Filtration of 0.90 mM Fe(III) solution. Effect of the pH on the permeate flux evolution of T5 at several TMP

It can be observed in Figure 4.1 that, depending on the feed pH, there was a limiting flux beyond which an increase on the TMP did not cause a gain on the J_p . Then, flux

was limited by fouling and a TMP increase was only invested either in compacting the deposited fouling layer and/or increasing its thickness. For instance, at pH 2.00, an increase on TMP between 6 and 8 bar did not cause any increase on the J_p . At pH 2.89, the flux was already limited at 2 bar because measured J_p was found to be constant at any TMP tested. Limiting fluxes at pH 2.00 and 2.89 were around 75 and 17 L/h·m², respectively, as Figure 4.1 shows. Contrarily, at pH 0.81, no limiting flux was observed at the tested range of TMP. These differences may indicate that membrane-solute interactions strongly depend on the solution pH.

In order to deeply understand the filtration mechanisms, clean membrane resistance (R_m) and created additional resistance (R_a) during the filtration of the ferric solutions, responsible of the J_p decline, were calculated from the J_w and J_p values. The Darcy's law was adapted for this purpose as shown by equations 4.1 and 4.2. R_m is calculated from the water permeability experiments where J_w was measured. R_a is calculated as the difference between the total resistance (R_t) obtained during the filtration experiment and R_m . In order to infer the relevance of the formed layer, the ratio of R_a/R_m was also calculated.

$$J_w = \frac{\text{TMP}}{R_m \cdot \mu} \quad (\text{eq. 4.1})$$

$$J_p = \frac{\text{TMP}}{R_t \cdot \mu} = \frac{\text{TMP}}{(R_m + R_a) \cdot \mu} \quad (\text{eq. 4.2})$$

R_m for clean T5 membrane was found to be $1.72 \cdot 10^{16} \text{ m}^{-1}$. Table 4.1 shows the R_a values calculated at the three tested feed pH at several TMP. As it can be seen, once limiting flux was found (i.e. at pH 2.00 and 2.89), the increase on the TMP was invested in generating additional resistance values instead of increasing J_p . R_a at 2 bar and pH 2.00 was $8.16 \cdot 10^{15} \text{ m}^{-1}$ whilst this value increased up to $2.46 \cdot 10^{16}$ at 8 bar.

Table 4.1. Filtration of 0.90 mM Fe(III) solution. Effect of the pH and TMP on T5 additional resistance

TMP (bar)	$R_a \text{ (m}^{-1}\text{)}$			R_a/R_m		
	pH=0.81	pH=2.00	pH=2.89	pH=0.81	pH=2.00	pH=2.89
2	$3.09 \cdot 10^{15}$	$8.16 \cdot 10^{15}$	$2.47 \cdot 10^{16}$	0.18	0.47	1.44
4	$1.99 \cdot 10^{15}$	$1.34 \cdot 10^{16}$	$7.31 \cdot 10^{16}$	0.12	0.78	4.25
6	$1.89 \cdot 10^{15}$	$1.55 \cdot 10^{16}$	$1.32 \cdot 10^{17}$	0.11	0.90	7.67
8	$1.53 \cdot 10^{15}$	$2.46 \cdot 10^{16}$	$1.73 \cdot 10^{17}$	0.09	1.43	10.1

As shown in Table 4.1, the ratio R_a/R_m indicates that, when limiting flux was detected, the importance of the additional resistance increased with TMP. At pH 2.00 and 2 bar of TMP, the ratio R_a/R_m was 0.47. The same ratio at pH 2.00 but at 8 bar of TMP was 1.43, around three times the value obtained at 2 bar. The strong effect of the pH on the filtration resistance is clearer when R_a/R_m values of the three experiments at 8 bar of TMP are contrasted. At pH 2.00, R_a/R_m was around sixteen times higher than the ratio observed at pH 0.81 and R_a/R_m measured at pH 2.89 was about seven times higher than that measured at pH 2.00. The previous values, together with limiting flux trends, indicate that feed solution pH is a crucial variable affecting the filtration performance and the formation of a significant additional filtration resistance since the beginning of

the filtration. This additional resistance may include concentration polarisation and the formation of a solute layer on the membrane material, which would be promoted at high pH values. In order to correlate these observations with the physicochemical phenomena that could take place, iron retentions and fouling percentages need to be presented before.

As Figure 4.2 shows, fouling increased from around 2% at pH 0.81 to 56% and 91% at pH 2.00 and 2.89, respectively. Thus, the previous results corroborate that solute-membrane interactions, stronger at high pH, take place. It is worth mentioning that fouling percentages are practically equal to the values that would be estimated from J_p values measured at 8 bar and J_w . Thus, formed layers are stable and consolidated enough to be resistant to removal by a soft water rinsing.

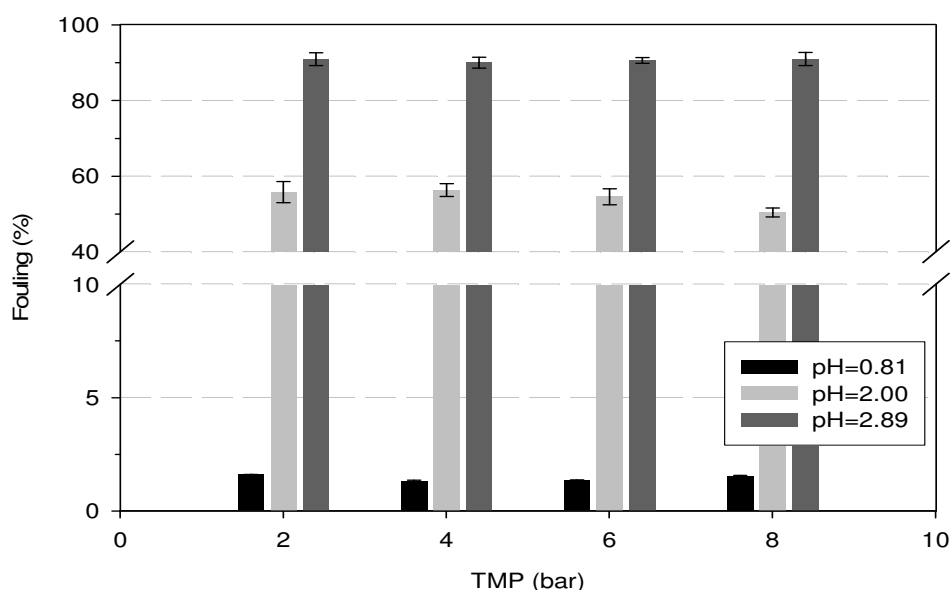


Figure 4.2. Filtration of 0.90 mM Fe(III) solution. Effect of the pH on T5 fouling at several TMP

UF retention mechanisms have been classically attributed to sieving effects because of the size of the compounds to be retained and membrane pore sizes, as explained in Chapter 1. Nevertheless, as shown in Figure 4.3, the retention of iron species (ions) is found to be between 20 and 30% at pH 0.81, between 80 and 90% at pH 2.00 and almost 100% at pH 2.89. Thus, sieving effects cannot be the (only) mechanism taking place in the tested system.

Iron species in solution could be retained by sieving effects, charge repulsions, iron-membrane interactions or a combination of them. In order to investigate the mechanisms, intensive knowledge on solution chemistry is essential. For this reason, the speciation diagram of the solution to filter, represented in Figure 4.4, was obtained with the Medusa software, a freely available tool to obtain chemical diagrams (Puigdomenech 2004). All the diagrams presented in the thesis, unless otherwise noted, have been obtained with this software. As shown by Figure 4.4, at pH 2.00, soluble charged hydroxides are the main iron species found in solution. Thus, repulsion between positively charged hydroxides and positively charged surface groups of the membranes could exist, but it is not expected to be mainly responsible of the ion rejection because of the large membrane MWCO in comparison with the low molecular

weight of the species to be retained. To distinguish the previous effects, Fe(III) hydrolysis and the molar masses of soluble hydroxides must be taken into account.

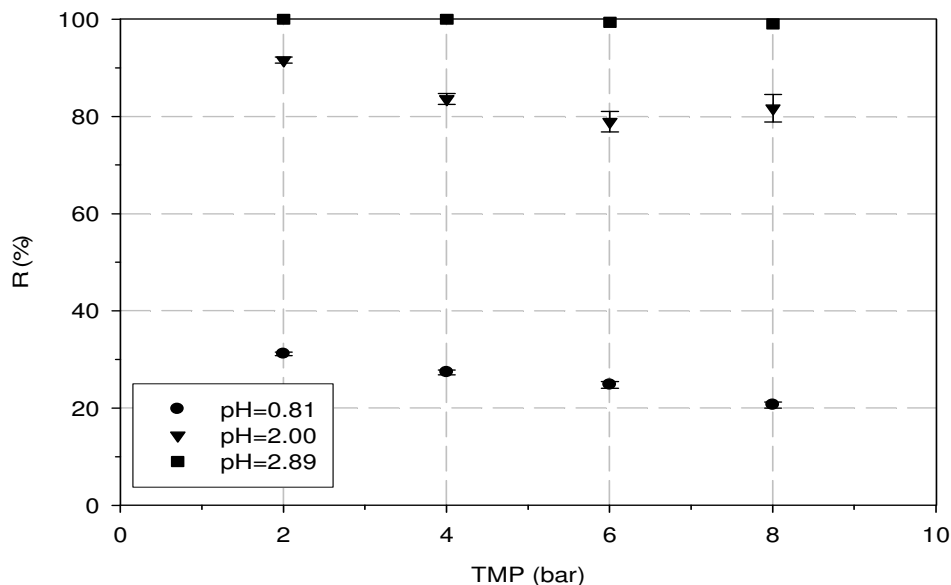


Figure 4.3. Filtration of 0.90 mM Fe(III) solution. Effect of the pH on T5 iron retention at several TMP

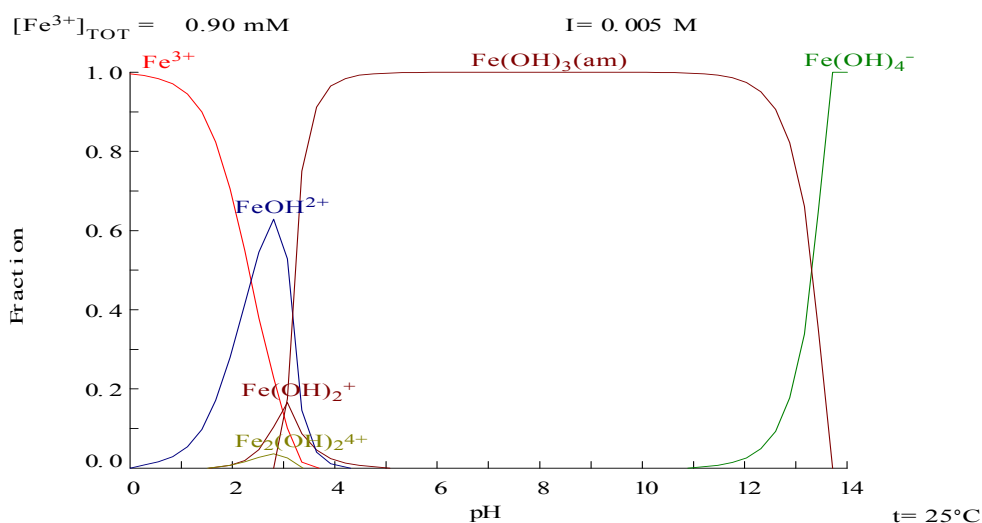
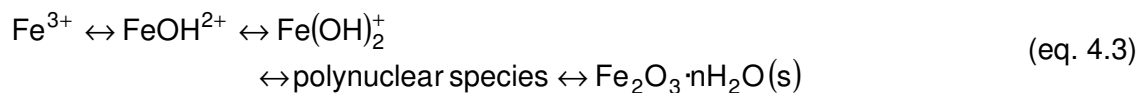


Figure 4.4. Chemical speciation diagram of a 0.90 mM Fe(III) solution

Soluble iron charged hydroxides present in solution occur as a result of Fe(III) hydrolysis. The hydrolysis process of ferric ion in aqueous media is classically explained by equation 4.3 (Pignatello et al. 2006).



However, equation 4.3 does not include water linked on iron species, as well as water and protons involved in the reactions according to the stoichiometry. In acidic solutions, taking into account water ligands, ferric ion exists as the hexaaquo ion, $\text{Fe}(\text{H}_2\text{O})_6^{3+}$ (MW=163.93 g/mol) (Blesa 1989). Accordingly, FeOH^{2+} and $\text{Fe}(\text{OH})_2^+$ are present as $\text{Fe}(\text{OH})(\text{H}_2\text{O})_5^{2+}$ (MW=162.93 g/mol) and $\text{Fe}(\text{OH})_2(\text{H}_2\text{O})_4^+$ (MW=161.92 g/mol), respectively. Thus, taking into account the molecular weights and the membrane MWCO, which is around thirty times greater, the iron retention cannot merely be assigned to a size-exclusion mechanism.

Apart from mononuclear iron species, polynuclear ones can coexist in solution. Iron hydrolysis has been considered as a polymerisation reaction because of the formation of polynuclear species of iron in aqueous solution, where $\text{Fe}(\text{H}_2\text{O})_6^{3+}$ can be taken as the monomer (Blesa 1989). Although different polymerisation processes may occur in aqueous media, the olation process seems to be the predominant, at least in the first stages of polymerisation. When olation occurs, hydroxide interactions are responsible for the formation of nearly all the polynuclear species of the M^{3+} cations. The polynuclear species formed from $\text{Fe}(\text{H}_2\text{O})_6^{3+}$ can be $\text{Fe}_2(\text{HO})_2^{4+}$ and $\text{Fe}_3(\text{HO})_4^{5+}$ (Baes and Mesmer 1976). Thus, mononuclear and polynuclear species appearing in solution could actually contribute to the retention in the filtration of Fe(III), because of the interaction (adsorption) with the membrane material thus forming a stable layer of these species on the membrane. Nevertheless, the speciation diagram of 0.90 mM Fe(III) solution at pH 2.00, shown in Figure 4.4, predicts the presence of mononuclear hydrolysed species in solution but not a significant fraction of polynuclear ones at this pH. It has been demonstrated that Fe(III) cations are adsorbed onto ceramic materials forming a monolayer and that their adsorption is closely related to the metal speciation (Anderson and Rubin 1981). A maximal iron adsorption capacity is observed when hydrolysed species are present in solution (James and Healy 1972a). Concretely, a range of pH between 1.5 and 2.6 has been found to be optimal for adsorbing Fe(III) species onto ceramic materials due to the appearance of Fe(III) hydrolysed species. In addition, adsorption studies of Fe(III) onto titania at pH 2 have shown that polymerisation of Fe(III) species favours the adsorption capacity of the material (Anderson and Rubin 1981; Piera et al. 2003). Thus, the initial mechanism allowing the retention of Fe(III) by ceramic membranes could be explained by the adsorption of the hydrolysed species of Fe(III) onto the ceramic material of the membrane, forming a deposit layer. The proposed mechanism is supported by the sharp decrease on the permeate flux, shown in Figure 4.1, as well as by the high resistances of the formed layers compared to those of the membranes before being used, demonstrated by R_a/R_m values presented in Table 4.1. After the Fe(III) species' adsorption, the retention may be enhanced by charge repulsions between the positively charged hydrolysed Fe(III) species adsorbed on the membrane and the positively charged species present in the bulk solution. Furthermore, the accumulation of metal soluble hydroxides, i.e. an increase of the local metal concentration, in the neighbourhood of the membrane, caused by concentration polarisation and deposit layer formation, can be expected. Thus, the chemical properties of the ferric solution would change, allowing the formation of polynuclear species, which can be more easily retained by size-exclusion phenomena although charge repulsions and adsorption phenomena may simultaneously occur. In fact, polynuclear hydrolysed species are more easily adsorbed onto ceramic material than mononuclear ones or even they can directly grow on it after the adsorption of their mononuclear predecessors (James et al. 1975).

The previous adsorption mechanism would explain why at pH 0.81, where practically all Fe(III) present is in its hexaaquo form and not in hydrolysed state, low retention and

fouling are observed. At pH 2.89, higher retention than at pH 2.00 is observed, fitting also with the proposed adsorption mechanism because at this pH, higher fraction of hydrolysed species occurs. Concretely, binuclear iron species, which are known to be more easily adsorbed onto ceramic materials than mononuclear ones (James et al. 1975), are present at this pH.

The proposed mechanism was validated by testing Fe(III) retention in other feed solution conditions and with membranes of different MWCO and materials. In addition, the filtration of other heavy metals was also carried out in order to know the applicability of the filtration process in different solution properties. The results are presented in the following sections.

4.2.2. Influence of the feed concentration

Two aqueous solutions, 4.52 mM Fe(III) and 9.42 mM Fe(III), were filtered with T5 membrane at pH 2.00. Their results, exposed in this section, have been compared to those obtained with the 0.90 mM Fe(III) solution in order to study the effect of the Fe(III) concentration on the filtration performance. The Fe(III) speciation diagram at variable metal concentration at pH 2.00 is presented in Figure 4.5. An increase on Fe(III) concentration increases the fraction of binuclear Fe(III) species. This speciation change is translated into a decrease on the J_p because, as shown in Figure 4.6, the higher the feed Fe(III) concentration, the lower the permeate flux.

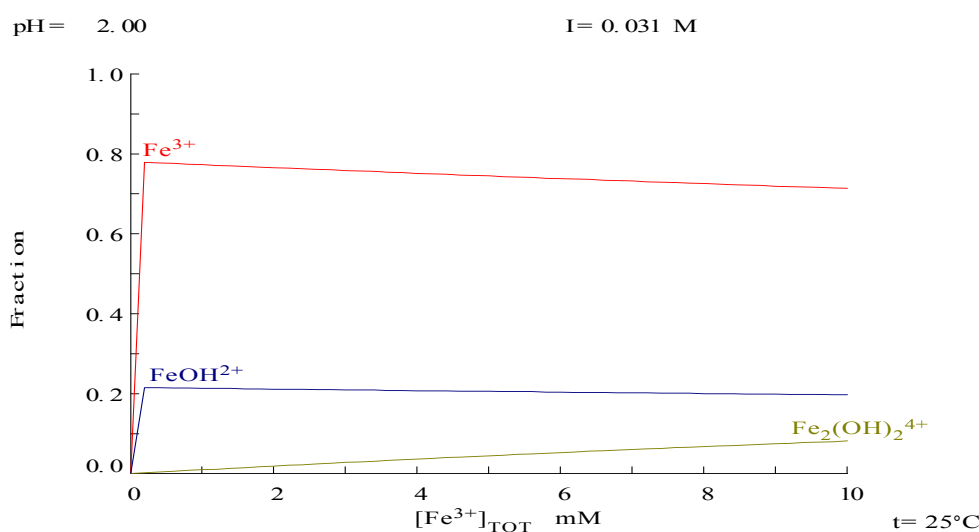


Figure 4.5. Chemical speciation diagram of a Fe(III) solution at pH 2.00 and variable Fe(III) concentration

In addition, as shown in Figure 4.6, despite the limiting flux observation in all the filtered solutions, its value was higher when the feed Fe(III) concentration was lower. These results could be explained by stronger and/or more interactions between the dissolved metal species and the membrane material occurring when the Fe(III) feed concentration was raised. In fact, not only the higher fraction of binuclear species occurring at high Fe(III) concentrations could explain the lower J_p but also the increased absolute feed concentration. A higher absolute iron concentration implies a higher content of Fe(III) hydrolysed species in solution, giving them more chance to interact with the ceramic material and form more stable and/or resistant layers.

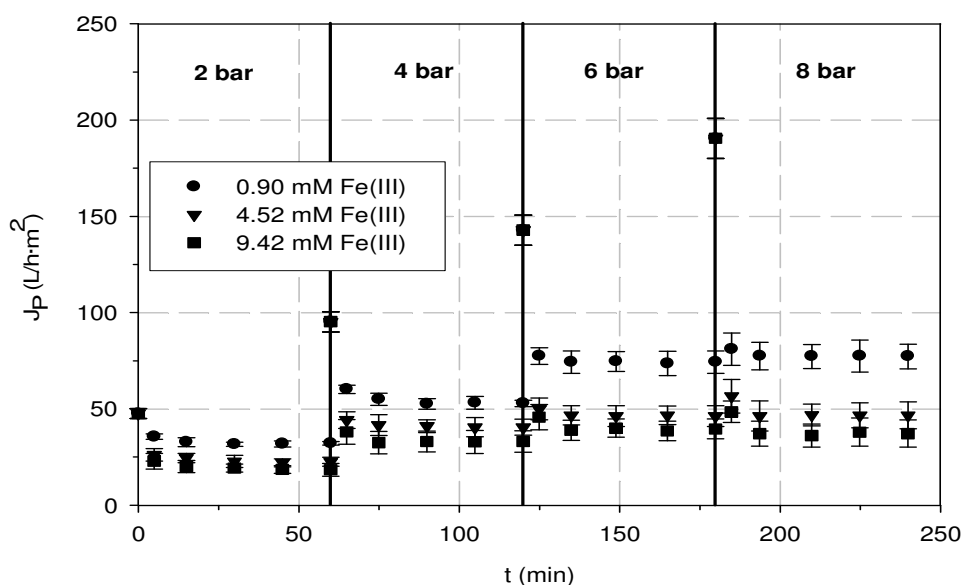


Figure 4.6. Filtration of Fe(III) solutions at pH 2.00. Effect of the Fe(III) concentration on the permeate flux evolution of T5 at several TMP

The calculated R_a , summarised in Table 4.2, support that when the initial Fe(III) concentration increased, formed layers of iron(III) species were more resistant to water passage. R_a passed from $2.46 \cdot 10^{16} \text{ m}^{-1}$ when 0.90 mM Fe(III) solution was filtered at 8 bar of TMP to $7.02 \cdot 10^{16} \text{ m}^{-1}$ when Fe(III) concentration was increased to 9.42 mM. The effect of the TMP, also included in Table 4.2, follows the same trend than when the pH effect was studied. This is, when TMP increased, regardless of the Fe(III) concentration, R_a also did.

Membrane fouling, measured as percentage of permeate flux loss, was practically constant regardless of the TMP. In addition, an increase on the feed Fe(III) concentration led to an increase of remaining fouling after rinsing the used membranes with deionised water. Fouling percentages were 56%, 72% and 78% when 0.90 mM, 4.52 mM and 9.42 mM Fe(III) solutions were tested, respectively.

Table 4.2. Filtration of Fe(III) solutions at pH 2.00. Effect of the Fe(III) concentration and TMP on T5 additional resistance

TMP (bar)	$R_a \text{ (m}^{-1}\text{)}$			R_a/R_m		
	0.90 mM	4.52 mM	9.42 mM	0.90 mM	4.52 mM	9.42 mM
2	$8.16 \cdot 10^{15}$	$1.88 \cdot 10^{16}$	$2.61 \cdot 10^{16}$	0.47	1.09	1.52
4	$1.34 \cdot 10^{16}$	$2.25 \cdot 10^{16}$	$3.19 \cdot 10^{16}$	0.78	1.31	1.85
6	$1.55 \cdot 10^{16}$	$3.50 \cdot 10^{16}$	$4.45 \cdot 10^{16}$	0.90	2.03	2.59
8	$2.46 \cdot 10^{16}$	$5.20 \cdot 10^{16}$	$7.02 \cdot 10^{16}$	1.43	3.02	4.08

Iron retention slightly decreased when iron feed concentration was raised, as shown in Figure 4.7. Retention changes were only observed at 2 and 4 bar of TMP. At 6 and 8 bar, no significant changes on iron retentions were detected. The different retention

could be related to the thickness and stability of the dynamic layer, which in turn depends on the TMP pressure, i.e. the permeate flux, and the iron concentration in the bulk solution. Thus, at high TMP and iron concentration, the formed layer is expected to be more stable and steady so the retention shows similar trends.

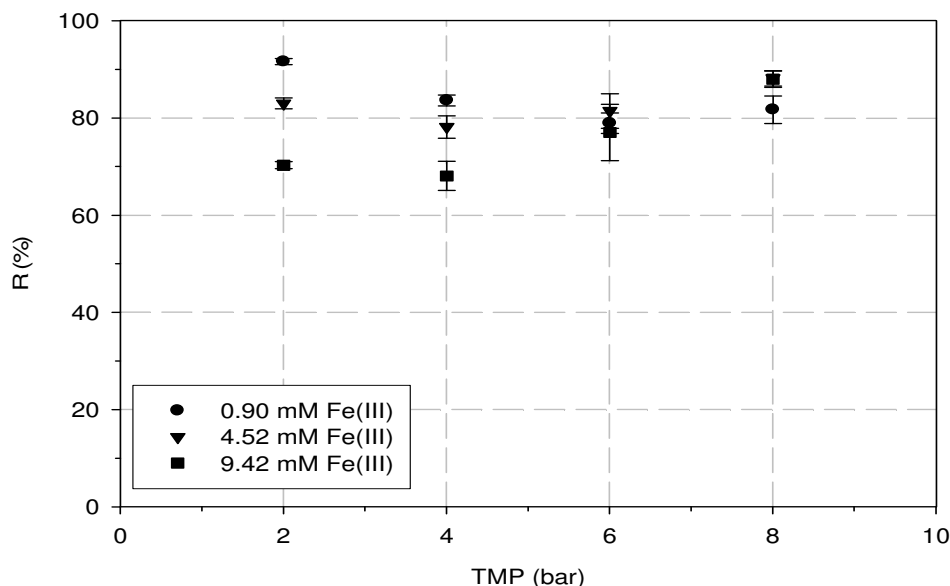


Figure 4.7. Filtration of Fe(III) solutions at pH 2.00. Effect of the Fe(III) concentration on T5 iron retention at several TMP

4.2.3. Influence of the iron valence

Fe(III) speciation was found to be crucial for ensuring its retention by T5 membrane as explained before. In this section, the effect of the iron valence (III or II) on T5 filtration performance is presented. For this, a 0.90 mM Fe(II) solution was filtered and its results are compared to those obtained with the 0.90 mM Fe(III) solution filtration. The pH of the model solutions was fixed at 2.00. The Fe(II) speciation diagram, represented in Figure 4.8, shows that no Fe(II) hydrolysis occurs at the tested conditions.

The Fe(II) filtration results indicated that no Fe(II) retention was achieved. Thus, the role of the hydrolysed species on the retention of iron from aqueous streams by ceramic UF membranes is validated.

The filtration of binary solutions containing both Fe(III) and Fe(II) has also been studied in order to assess the influence of the presence of a non-retainable specie on the retention of those retainable. One experiment was designed and carried out to test this effect. The experiment was based on the filtration of a combined aqueous solution containing 0.90 mM Fe(III) and 0.90 mM Fe(II) at pH 2.00. The results obtained were compared to those concerning the filtration of 0.90 mM Fe(III) solution and that of 0.90 mM Fe(II) solution, both at pH 2.00.

The J_p evolution of the three abovementioned solutions' filtration at four TMP's is shown in Figure 4.9. As it could be expected, no limiting flux appears when filtering the 0.90 mM Fe(II) solution due to the absence of soluble hydrolysed species that could be adsorbed onto the ceramic membranes. In contrast, permeate flux was limited at around 75 L/h·m² when the single 0.90 mM Fe(III) solution was filtered with T5 at pH

2.00. When ferric and ferrous species were together in the feed solution (both at 0.90 mM concentration) and filtered at the same conditions than when they were in separated solutions, the measured J_P values were lower than those measured when 0.90 mM Fe(III) solution was filtered. This indicates that the presence Fe(II) decreased the resultant J_P most probably because a J_P decline was also observed when filtering the 0.90 mM Fe(II) alone, which was added to the resultant flux decline.

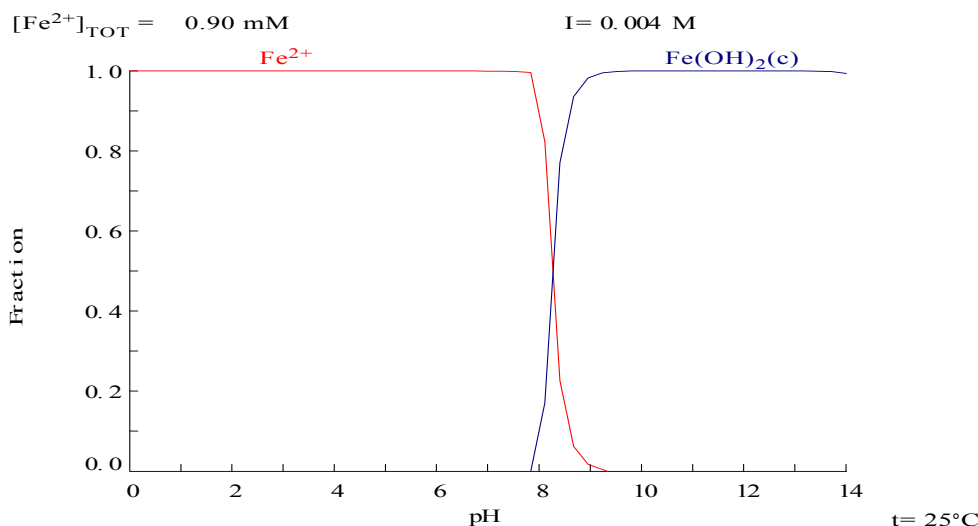


Figure 4.8. Chemical speciation diagram of a 0.90 mM Fe(II) solution

The additional resistances estimated from the sum of those individual, obtained when only Fe(III) or Fe(II) were filtered, are summarised in Table 4.3 together with those calculated directly from the experimental data. Significant differences can be observed between the R_a and R_a/R_m . Thus, there is not a simple and direct relationship between the individual resistances and the global one and some synergistic effects can exist when filtering binary solutions of Fe(III) and Fe(II).

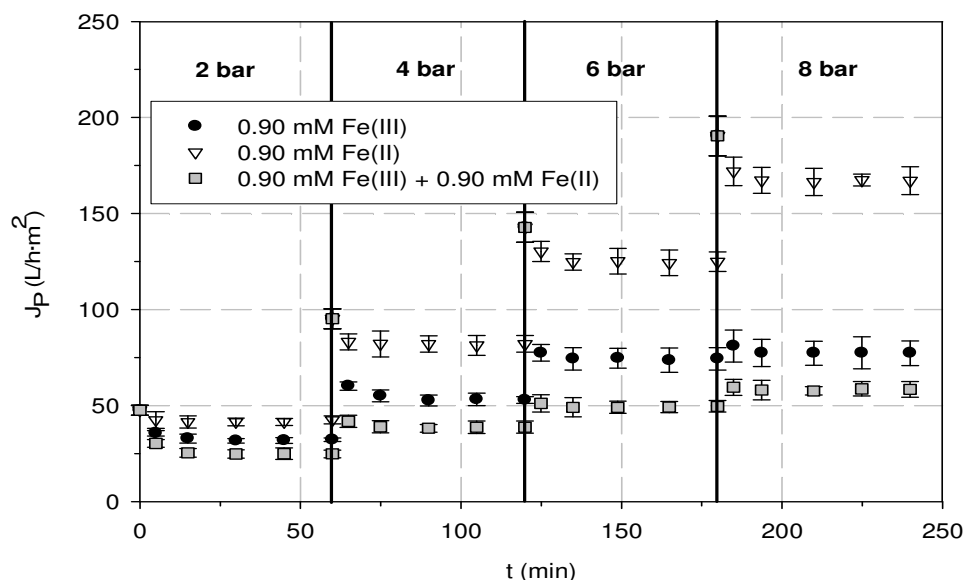


Figure 4.9. T5 permeate flux evolution when filtering binary iron solutions at pH 2.00 and at several TMP

Table 4.3. T5 additional resistance when filtering binary iron solutions at pH 2.00 and at several TMP

TMP (bar)	R_a (m^{-1})			
	Fe(III)	Fe(II)	Fe(III) + Fe(II) ^(measured)	Fe(III) + Fe(II) ^(predicted)
2	$8.16 \cdot 10^{15}$	$2.12 \cdot 10^{15}$	$1.53 \cdot 10^{16}$	$1.03 \cdot 10^{16}$
4	$1.34 \cdot 10^{16}$	$2.55 \cdot 10^{15}$	$2.47 \cdot 10^{16}$	$1.59 \cdot 10^{16}$
6	$1.55 \cdot 10^{16}$	$2.23 \cdot 10^{15}$	$3.20 \cdot 10^{16}$	$1.77 \cdot 10^{16}$
8	$2.46 \cdot 10^{16}$	$2.16 \cdot 10^{15}$	$3.83 \cdot 10^{16}$	$2.68 \cdot 10^{16}$

TMP (bar)	R_a/R_m			
	Fe(III)	Fe(II)	Fe(III) + Fe(II) ^(measured)	Fe(III) + Fe(II) ^(predicted)
2	0.47	0.12	0.89	0.59
4	0.78	0.15	1.44	0.93
6	0.90	0.13	1.86	1.03
8	1.43	0.13	2.23	1.56

^(measured) Calculated from measured experimental data
^(predicted) Calculated as the sum of Fe(III) and Fe(II)

Fouling percentages are summarised in Figure 4.10 and they were around 56% when the 0.90 mM Fe(III) was filtered and 2% when 0.90 mM Fe(II) was. It is worth mentioning that 13% of permeate flux loss occurred during the filtration of the Fe(II) solution and only 2% of permeate flux loss remained after rinsing the used membrane with water. This indicates that permeate flux recovery can be easily achieved. When filtering binary solutions, the fouling percentage was about 67%, which indicates again that binary solutions cause higher permeate flux losses than single ones.

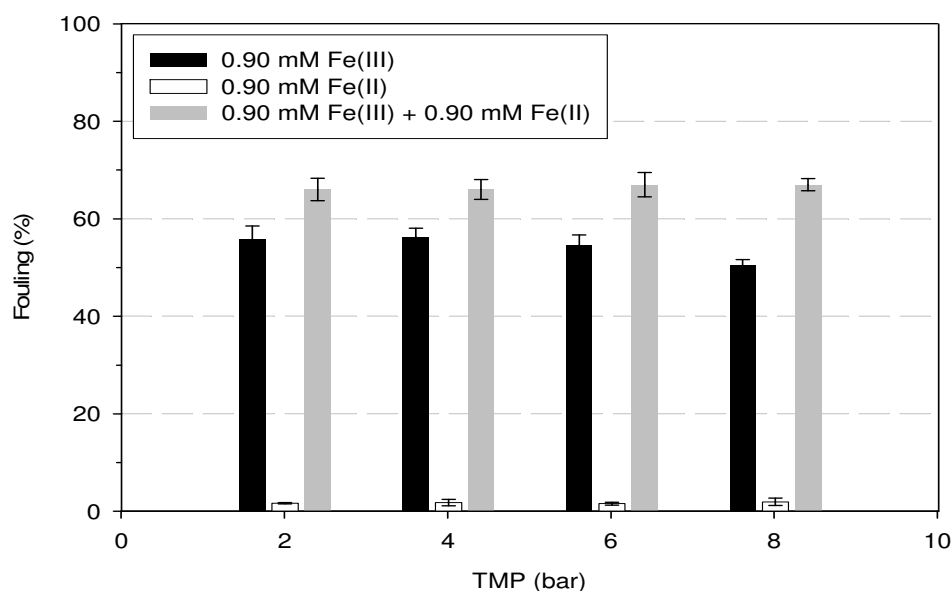


Figure 4.10. Fouling percentages obtained when filtering binary iron solutions with T5 at pH 2.00 and at several TMP

The speciation diagram of binary solutions (not shown) indicate that neither Fe(III) nor Fe(II) speciation is affected by the presence of the other co-ion at least at the tested pH and concentration. However, as shown in Figure 4.11, the resultant global iron retention when filtering binary solutions was around 45%, which is approximately 50% of the Fe(III) retention observed in a single solution. Thus, Fe(II) does not cause a decrease on the retention when it is present in Fe(III) solutions at least at the experimental conditions tested.

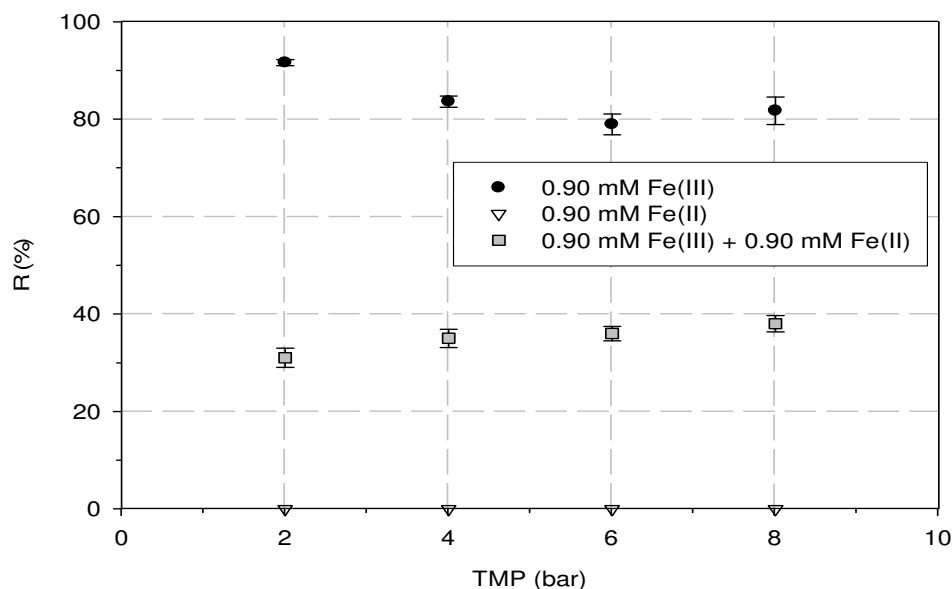


Figure 4.11. T5 global iron retention when filtering binary iron solutions at pH 2.00 and at several TMP

4.2.4. Influence of the iron chelation

Iron speciation is affected by the presence of chelating agents such as EDTA. Figure 4.12 shows the iron speciation diagram of a 0.90 mM Fe(III) solution at pH 2.00 at variable EDTA concentration. Fe(III) chelates vary depending on the EDTA concentration. Free Fe(III) ions and Fe(III) hydrolysed species decrease as long as the molar ratio Fe(III):EDTA approaches 1:1, the stoichiometric ratio (Skoog et al. 1996). Beyond the stoichiometric EDTA amount, Fe(HEDTA) and Fe(EDTA)⁻ are present in the solution and their fractions are unaffected by an EDTA concentration increase.

In order to study the effect of the Fe(III) chelation, five experiments were performed and their results are compared to those obtained when filtering a single Fe(III) solution. The five experiments consisted in testing the effect of the EDTA feed concentration on the filtration performance and efficiency. The feed concentration of Fe(III) and the solution pH were fixed in all the experiments at 0.90 mM and 2.00, respectively. The feed concentrations of EDTA were 0.45 mM, 0.90 mM, 1.35 mM and 1.80 mM. The filtration of a 0.90 mM EDTA single solution (without iron) was also carried out.

The J_P evolution measured in the five abovementioned experiments together with that observed when filtering a 0.90 mM EDTA single solution are grouped in Figure 4.13. Permeate flux was not limited at any of the tested TMP when filtering Fe(III)-EDTA solutions at/beyond the stoichiometric equimolar Fe(III):EDTA ratio. In addition, J_P evolution along the time at this conditions was equal to the one observed when filtering

a 0.90 mM EDTA single solution. When the ratio Fe(III):EDTA was lower than the stoichiometric value, a limiting flux could be observed but its value was higher than that detected when filtering a 0.90 mM Fe(III) single solution at the same pH and TMP conditions. Thus, chelated iron improved the filtration efficiency in terms of flux production.

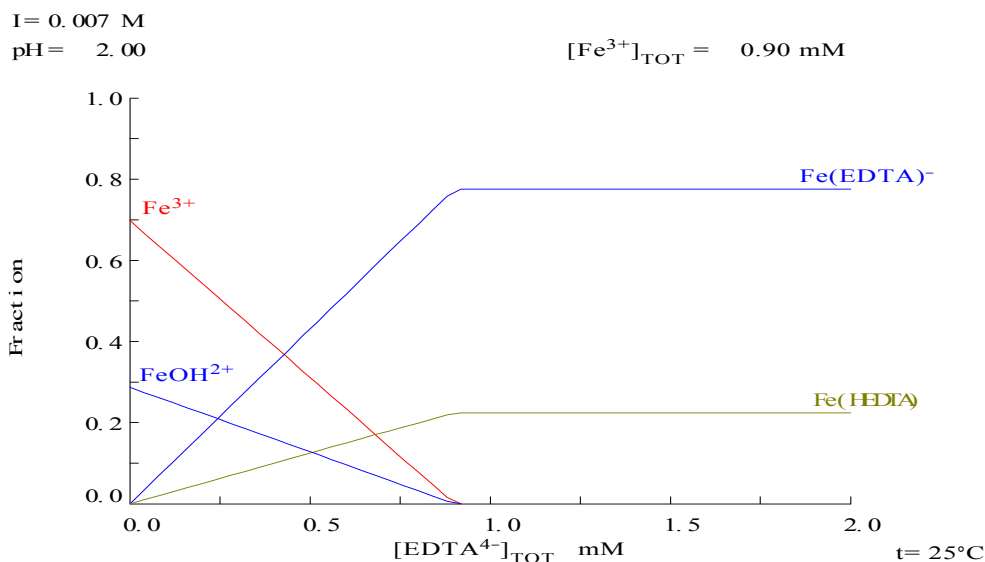


Figure 4.12. Chemical speciation diagram of a 0.90 mM Fe(III) solution at pH 2.00 and variable EDTA concentration

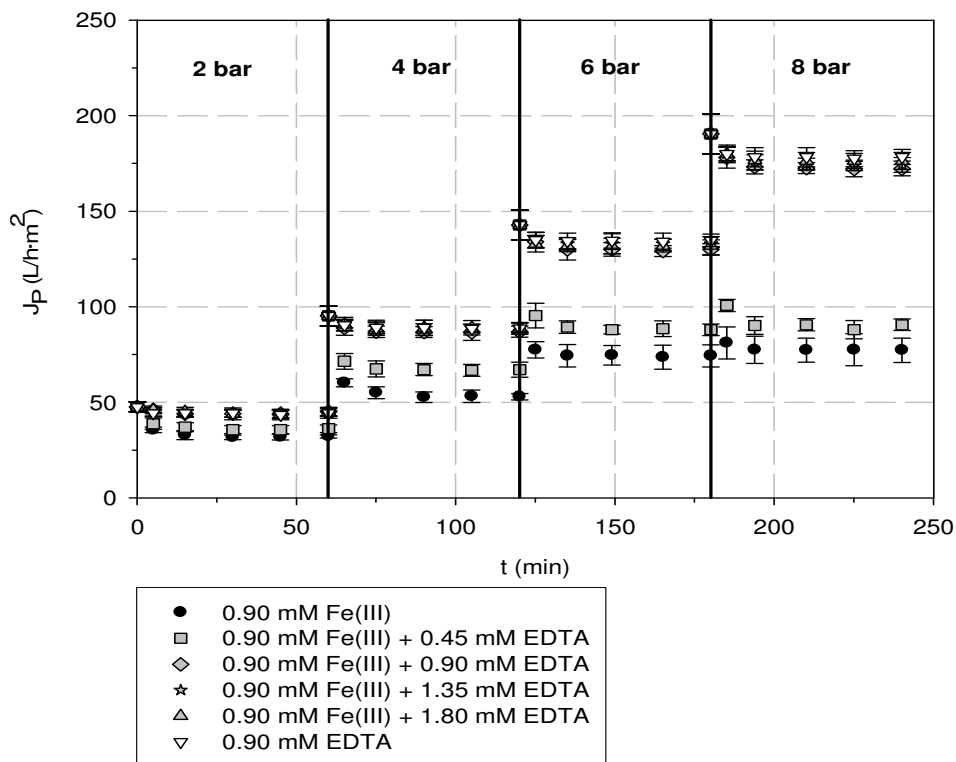


Figure 4.13. T5 permeate flux evolution when filtering Fe(III)-EDTA solutions at pH 2.00 and at several TMP

Fouling percentages are shown in Figure 4.14. As it can be observed, the permeate flux loss was strongly dependant on the ratio Fe(III):EDTA, which directly affects the type of species present in solution. Unbound Fe(III) species' filtration caused the highest fouling percentage (56%), measured when filtering a 0.90 mM Fe(III) single solution. This case was followed by the solution where partial Fe(III) chelation happened. This is, when filtering a 0.90 mM Fe(III) and 0.45 mM EDTA solution, whose average fouling percentages were around 20%. Low fouling percentages (around 7%) were observed when filtering solutions with all Fe(III) species chelated by EDTA molecules, regardless of the initial EDTA concentration. Finally, the lowest fouling percentage (about 3%) was observed when filtering the EDTA single solution. Thus, a direct correlation between iron chelation and T5 membrane fouling is evident. The higher the chelation degree, the lower the membrane fouling, which validates the hypothesis that Fe(III) hydrolysed species are those responsible of membrane-solute interactions taking place during the filtration of iron solutions.

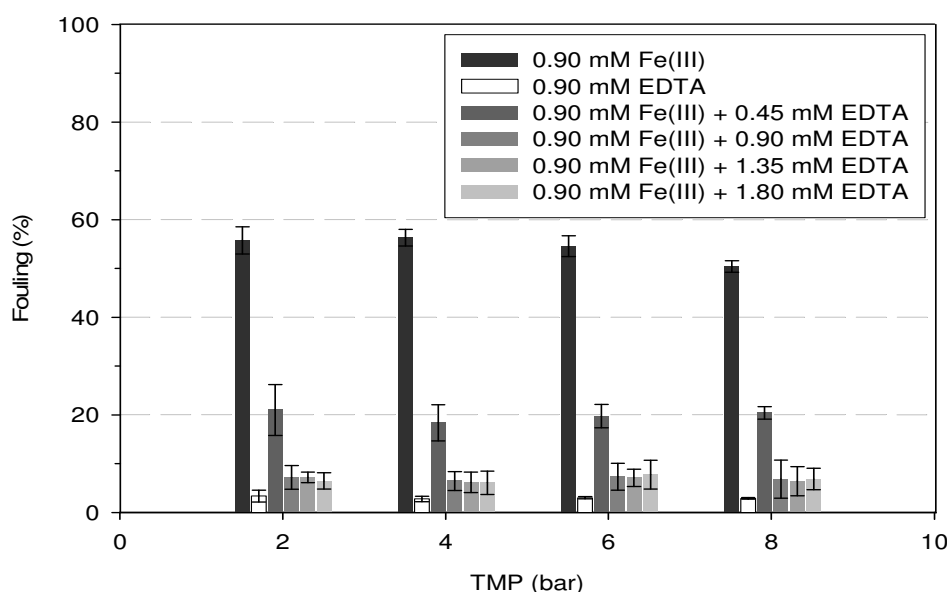


Figure 4.14. Fouling percentage obtained when filtering Fe(III)-EDTA solutions with T5 at pH 2.00 and at several TMP

The retention of iron is strongly influenced by the presence and concentration of EDTA. Figure 4.15 groups the iron retentions obtained in the filtration experiments where Fe(III) was present in the feed solution together with EDTA. Thus, the 0.90 mM EDTA solution does not obviously appear in Figure 4.15 because no Fe(III) retention could occur. The EDTA retention was also measured during the experiments and it was found to be always below 3% including the single EDTA solution filtration experiment. Thus, EDTA can be considered as non-retainable specie by T5 at least at the same conditions than Fe(III) species are. As Figure 4.15 demonstrates, iron retention strongly depended on the Fe(III) chelation. Iron retention decreased as long as the EDTA concentration increased and approached the Fe(III):EDTA stoichiometric ratio. At Fe(III):EDTA ratio equal or higher than this value, no significant iron retention decline was observed. This indicates that the responsible for the iron retention decrease is the chelation state and not the EDTA concentration. Thus, it can be concluded that T5 iron retention was negatively affected by Fe(III) chelation. When Fe(III) was completely chelated by EDTA, no hydrolysed species were present in the feed solution and iron retention was lowered. Thus, the previous findings reinforce the importance of the hydrolysed iron species in the retention of iron by the ceramic T5 membrane.

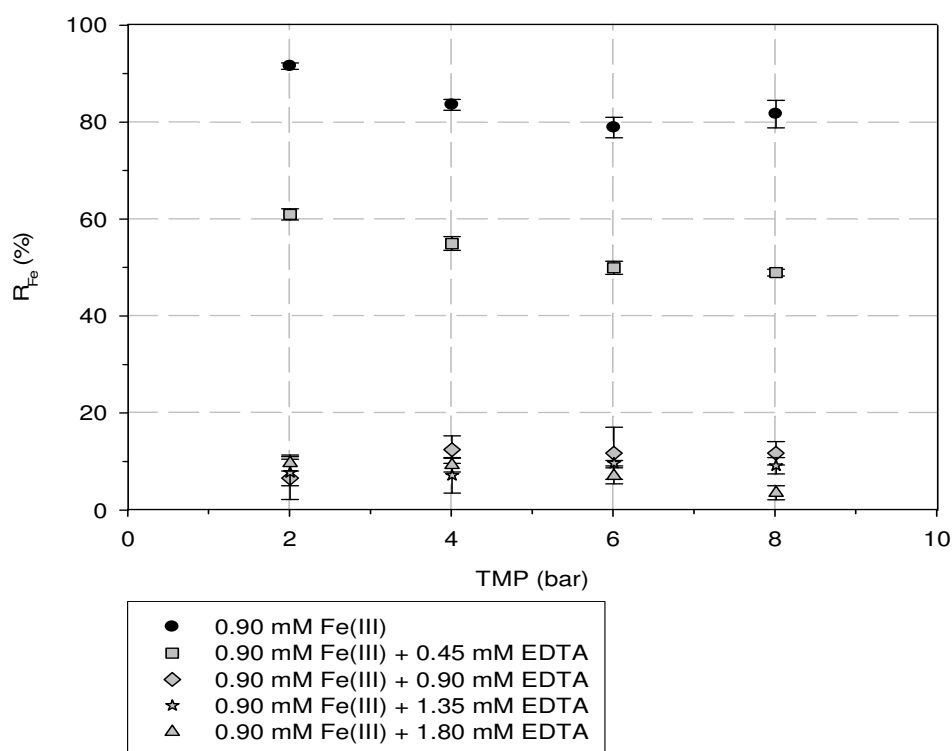


Figure 4.15. T5 iron retention when filtering Fe(III)-EDTA solutions at pH 2.00 and at several TMP

4.2.5. Influence of the background electrolyte

The effect of the presence of a background electrolyte (NaCl) was studied in order to evaluate the validity of the proposed filtration mechanism in high-salinity solutions. Two 0.90 mM Fe(III) solutions, one additionally containing 100 mM NaCl and the other 1000 mM NaCl were prepared and filtered through T5 at 2, 4, 6 and 8 bar of TMP. The pH was adjusted at 2.00 and the filtration performance is compared to the results obtained for the 0.90 mM Fe(III) solution without NaCl.

The J_p evolution along the time for the three filtration experiments is shown in Figure 4.16. A limiting flux was only achieved when filtering the solution without NaCl. The J_p decline measured when filtering the solutions with NaCl followed the same trend regardless of the TMP and feed NaCl concentration. The steady-state J_p values were found to be around 60% of the J_w , irrespective of the TMP and feed NaCl concentration. The average fouling percentage calculated after rinsing the used membrane with deionised water was only about 4%. Thus, the permeate flux decline observed during the filtration of Fe(III) solutions containing NaCl could be mainly attributed to concentration polarisation and/or reversible fouling phenomena.

Iron retentions measured when filtering the 0.90 mM Fe(III) solutions at variable NaCl concentration are shown in Figure 4.17. As it can be seen, the iron retention deeply dropped in presence of background electrolyte. Iron speciation diagram (not shown) demonstrates that the ionic strength does not significantly affect Fe(III) species' nature at pH 2.00 and only a very slight decrease on the $\text{Fe}(\text{OH})^{2+}$ fraction is observed, which is translated into a slight increase on the Fe^{3+} fraction. However, those insignificant

variations are not expected to be responsible for the iron retention decrease observed when NaCl is present.

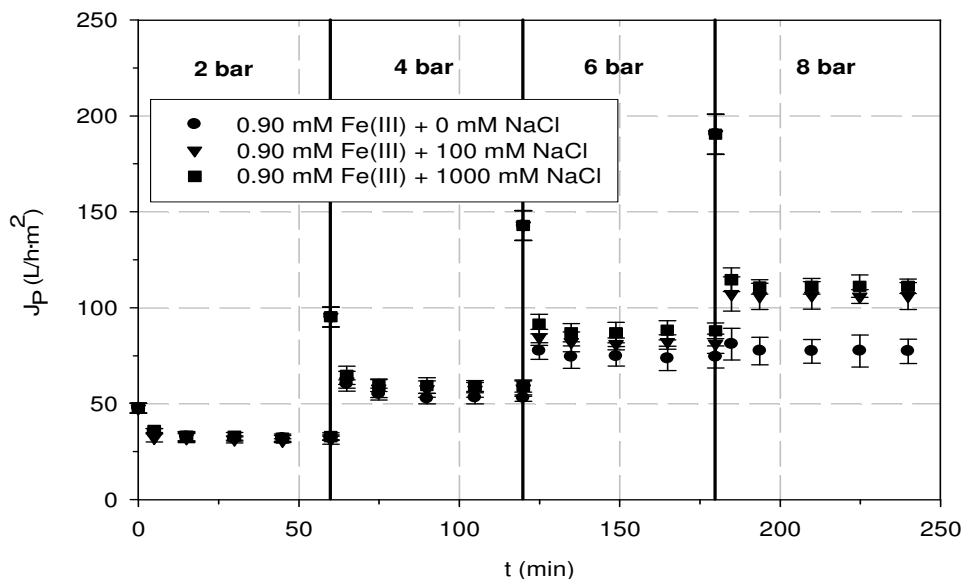


Figure 4.16. Effect of the NaCl concentration on the permeate flux evolution of T5 at pH 2.00 and at several TMP

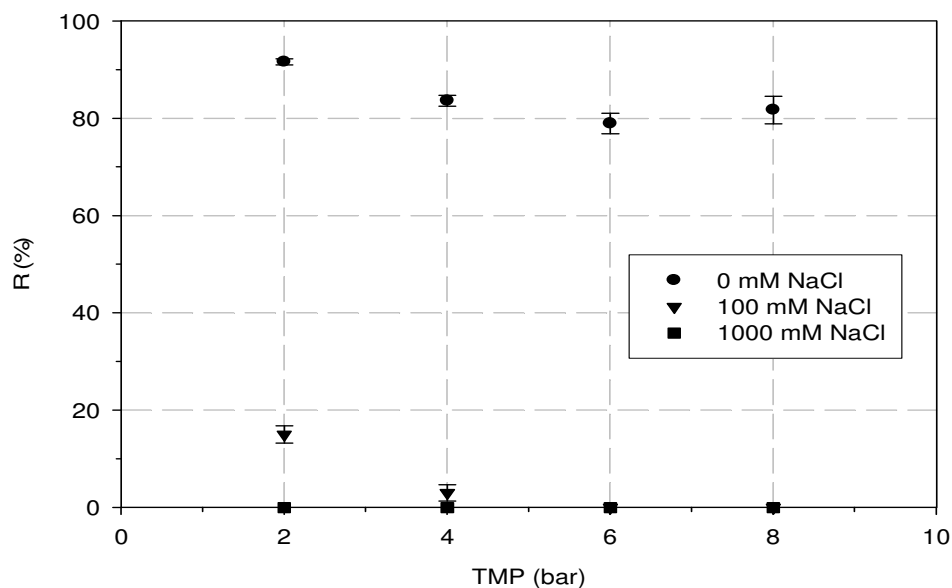


Figure 4.17. NaCl concentration effect on T5 iron retention at pH 2.00 and at several TMP

The retention mechanism postulated before is based on the adsorption of hydrolysed species on the ceramic material of the membrane. When NaCl is present in the feed solution, hydrolysed species are present in it at approximately the same concentration than when only Fe(III) was present at the same pH. However, as abovementioned, T5 retention was strongly diminished by the presence of NaCl. The difference on the system is probably not on the iron speciation but on the adsorption properties of the ceramic material. It has been demonstrated that an increase on the ionic strength,

achieved through a background electrolyte concentration raise, reduces the adsorption of a given ion onto a ceramic oxide (James and Healy 1972b). Thus, this could explain the decrease on the retentions observed when sodium chloride was present in the feed solution.

4.3. Cu(II) and Cr(III) filtration with ceramic membranes

Cu(II) and Cr(III) solutions were also filtered through T5 in order to know whether the process can be applied for the retention of other heavy metals from aqueous solution different than ferric species. For this, Cu(II) and Cr(III) were selected as model metals because Cu(II) is non-hydrolysed at the tested pH whilst Cr(III) is. Apart from investigating the applicability of the treatment process, it will be also possible to know whether the proposed filtration mechanism is only valid for iron solutions or has a more general applicability.

A 0.90 mM Cu(II) solution was filtered following the same protocol than in the previously-presented experiments. As Figure 4.18 shows, no copper hydrolysis occurs at the tested conditions. In addition, the filtration results showed that no copper retention (lower than 1%) was achieved, regardless of the TMP. In addition, the permeate flux decline (around 9%) was totally restored because only 1% of permeate flux loss remained after rinsing the membrane with deionised water.

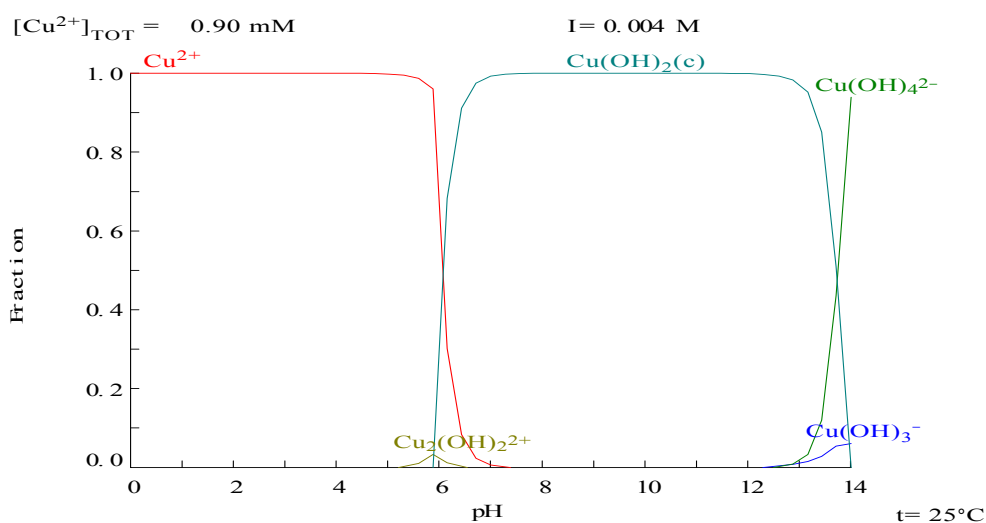


Figure 4.18. Chemical speciation diagram of a 0.90 mM Cu(II) solution

Concerning chromium filtration, four 0.90 mM Cr(III) solutions were prepared and adjusted at four different pH levels in order to test the effect of the feed pH and, consequently, of the chromium speciation on the T5 filtration performance at four TMP. The speciation of Cr(III) is quite similar to that of Fe(III) because, as shown in Figure 4.19, Cr(III) hydrolysis occurs and hydrolysis products vary in form and fraction along the whole pH range. The only advantage of Cr(III) is that, as its precipitation begins later than for Fe(III), a wider pH range can be studied. In addition, trinuclear species are formed at a pH range between around 3 and 7. The tested range of pH was between 1 and 5 because at higher pH, chromium hydroxide precipitation occurs.

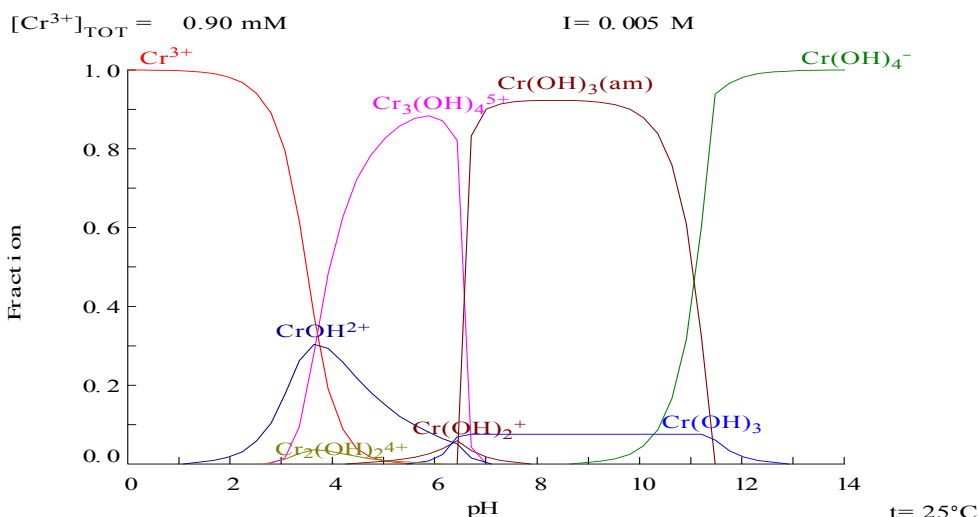


Figure 4.19. Chemical speciation diagram of a 0.90 mM Cr(III) solution

The J_p evolution data obtained at several TMP when filtering the chromium solutions is shown in Figure 4.20. As J_p evolution demonstrates, a similar behaviour was observed with Cr(III) solutions than with Fe(III). Thus, chromium retention mechanism is expected to be the same than for Fe(III), mainly based on the hydrolysed species' adsorption onto the ceramic membrane material.

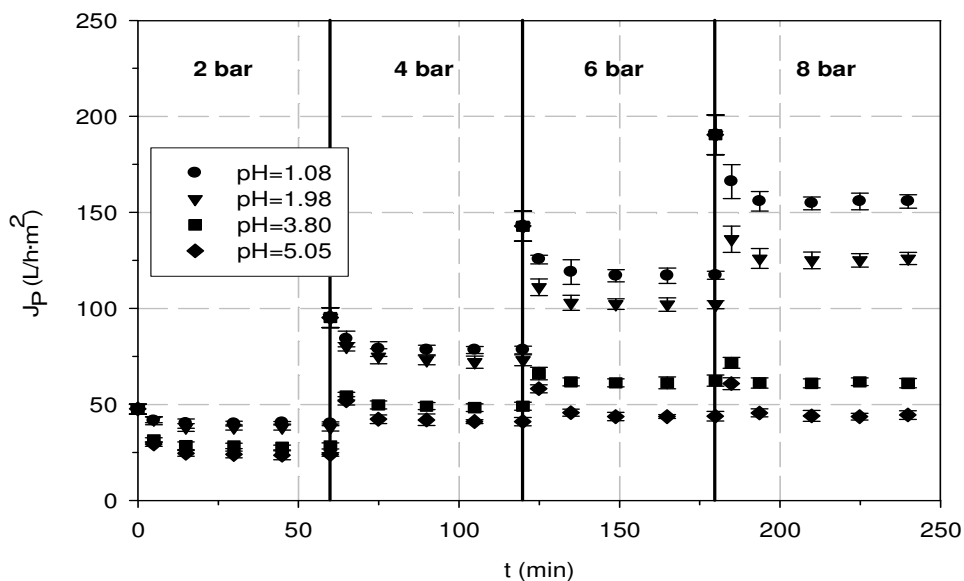


Figure 4.20. Filtration of 0.90 mM Cr(III) solution. Effect of the pH on the permeate flux evolution of T5 at several TMP

By inspecting Figure 4.19 and Figure 4.20 at once, it can be deduced that J_p decline increased as long as hydrolysis (pH) did. Furthermore, at pH where almost all Cr(III) was in its hydrolysed forms, a limiting flux could be observed. The limiting flux value decreased with an increase on the Cr(III) hydrolysis products' fraction. For instance, at pH 3.80, a limiting flux of 61 L/h·m² was found whilst, at pH 5.05, where a higher fraction of hydrolysed species was present, permeate flux was limited at around

45 L/h·m². Hence, stronger or denser adsorption takes place when high hydrolysis occurs, as observed with Fe(III) solutions. Fouling percentages for all the experiments are depicted in Figure 4.21. An increase on the solution pH resulted in a raise of the J_P loss due to the stronger and/or denser adsorption and layer formation expected to take place at high hydrolysis degree.

Figure 4.22 shows that the pH effect on retention of Cr(III) follows the same trend than for Fe(III). An increase on the feed pH enhanced the retention probably due to the presence of more-hydrolysed species, which are expected to be more easily adsorbed onto the membrane.

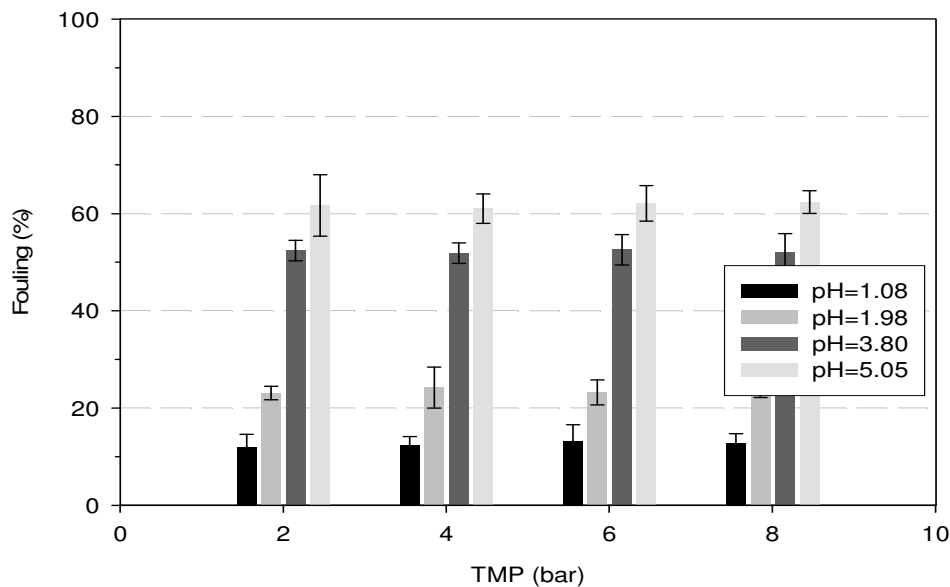


Figure 4.21. Filtration of 0.90 mM Cr(III) solution. Effect of the pH on T_5 fouling at several TMP

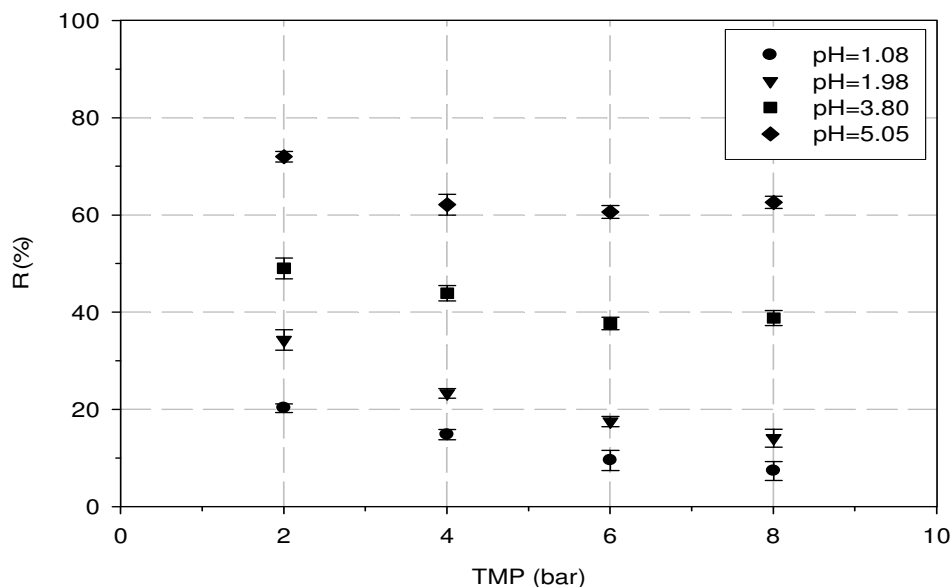


Figure 4.22. Filtration of 0.90 mM Cr(III) solution. Effect of the pH on T_5 chromium retention at several TMP

The effect of the Cr(III) concentration was also studied at pH 3.80. A 5.01 mM Cr(III) filtration experiment is compared to the results obtained when filtering a 0.90 mM Cr(III) solution. As Figure 4.23 shows, J_p values were lowered when increasing the Cr(III) concentration. Figure 4.24 illustrates that an increase on the Cr(III) concentration raises the fraction of trinuclear hydrolysed species, which are in principle more easily adsorbed onto ceramic oxides (James et al. 1975) or could be easily retained by size-exclusion phenomena once the additional layer was formed. This higher adsorption would turn into a higher J_p decline.

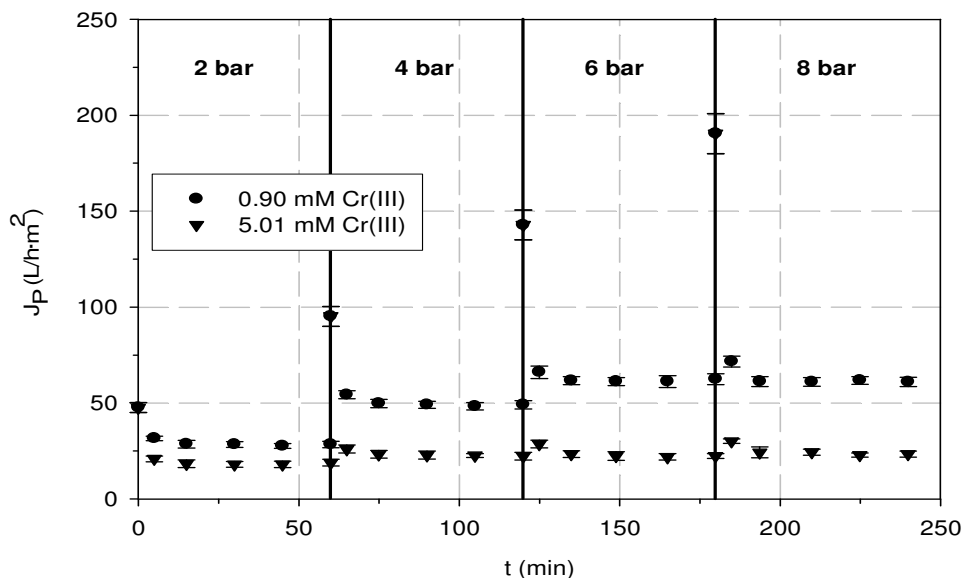


Figure 4.23. Filtration of Cr(III) solutions at pH 3.80. Effect of the Cr(III) concentration on the permeate flux evolution of T5 at several TMP

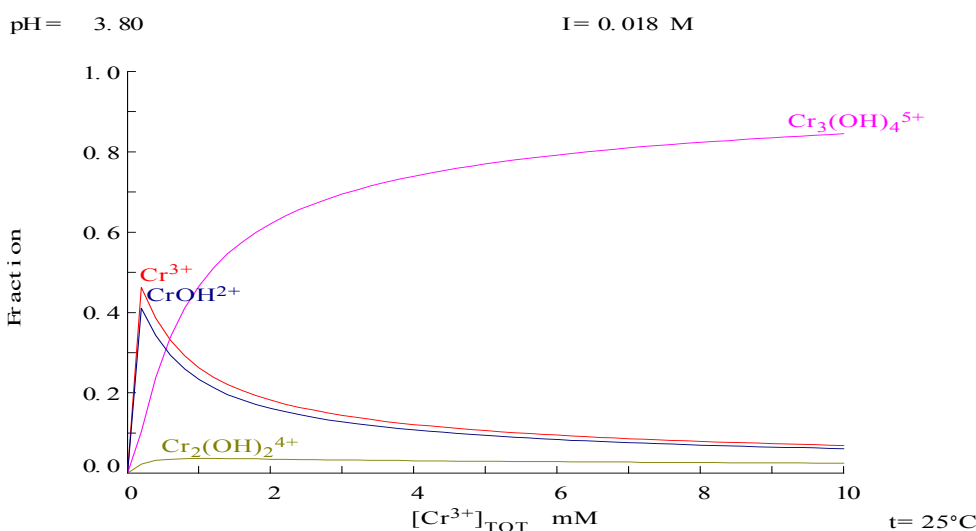


Figure 4.24. Chemical speciation diagram of a Cr(III) solution at pH 3.80 and variable Cr(III) concentration

The fouling percentage measured, whose values are represented in Figure 4.25, followed the tendencies that could have been predicted from Fe(III) results. An

increase on the Cr(III) concentration increased the remaining J_p loss after membrane rinsing. A rise on the Cr(III) concentration from 0.90 mM to 5.01 mM caused an increase on the average fouling percentage from 52% to 77%. Thus, strong Cr(III) adsorption is assumed to occur during the filtration process at high feed metal concentration, as encountered for Fe(III). The retention of Cr(III) was enhanced when the Cr(III) concentration increased, as shown in Figure 4.26. A concentration raise from 0.90 mM to 5.01 mM caused a retention improvement from around 42% to 64%. The Cr(III) concentration increase would lead to a higher occurrence of trinuclear hydrolysed chromium species, which can be more easily adsorbed on the ceramic oxides.

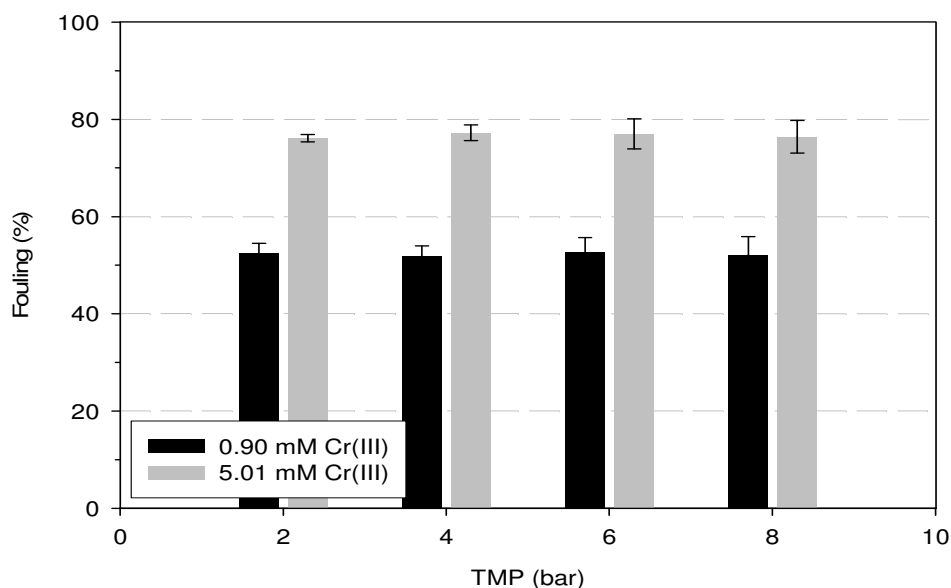


Figure 4.25. Filtration of Cr(III) solutions at pH 3.80. Effect of the Cr(III) concentration on T5 fouling at several TMP

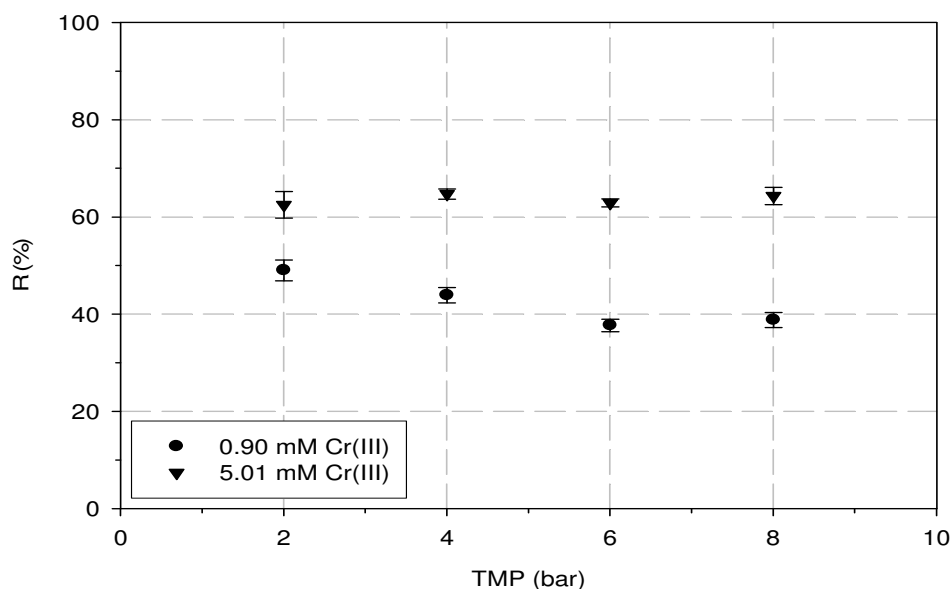


Figure 4.26. Filtration of Cr(III) solutions at pH 3.80. Effect of the Cr(III) concentration on T5 chromium retention at several TMP

4.4. Membrane MWCO and composition effect on the iron(III) recovery with ceramic membranes

Several ceramic membranes were tested aiming at study the retention ability of ceramic UF membranes to recover iron ions. The MWCO (between 1 and 50 kDa) effect was tested with membranes of the same composition than T5. Moreover, membranes of different composition than T5 were tested. This experimental design allows investigating both the effect of the MWCO and the membrane nature on the filtration performance. In addition, the experiments are also useful to contrast the filtration mechanisms stated in the previous sections. With this goal, streaming potential characterisation through the membrane pores was carried out in order to identify the importance of the membrane charge on the retention of metals by ceramic UF membranes. A 0.90 mM Fe(III) solution at pH 2.00 was selected as model solution in all the filtration experiments.

The labelled T (including T1, T15 and T50) and F (including F5 and F10) membranes were manufactured by Tami Industries (Nyons, France). The T elements were InsideCéram model whilst the F elements were Filtanium model. M5 membrane was a Membralox® membrane manufactured by Pall Exekia (Tarbes, France) exhibiting a nominal MWCO of 5 kDa. The number accompanying the model letter (T, F or M) indicates the nominal MWCO of the membrane in kDa. Additional details on the composition, PWP and physical dimensions of the membranes can be found in Chapter 3.

4.4.1. Streaming potential characterisation

In this section, the streaming potential characterisation of the ceramic membranes used in this study is presented. Figure 4.27 shows the effect of the pH on the apparent zeta potential of T1, T15 and T50 membranes. It must be noted that, regardless of the membrane, charge changed from positive to negative at a pH between 4.5 and 5.0. Fievet et al. (2004) measured the streaming potential of a T membrane, made by the same supplier and with the same inorganic materials, having a MWCO of 1.5 kDa, using an 1 mM KCl solution for the streaming potential tests. They found that the isoelectric point was located at pH 6. Taking into account that the experimental set-up was not identical, the streaming potential results compares reasonably well. The streaming potential trends exhibited by these ceramic membranes as function of the pH can be explained by the equilibrium dissociation of the metal oxides forming the membrane (Moritz et al. 2001b). When metal oxides are exposed to an aqueous media, the amphoteric surface groups (MOH) may dissociate. Thus, the reactions shown in equations 4.4 and 4.5 can take place at acid or basic conditions, respectively.



As it can be deduced from equations 4.4 and 4.5, the dissociation of MOH surface groups is strongly related to the pH in the vicinity of the membrane surface. In addition, either when materials have no charge or when they have the same number of positive and negative charges, the surface charge becomes zero. Thus, the previous explanation serves to understand that ceramic membranes have positive apparent zeta potentials at low pH, but they become negative at high pH.

As Figure 4.27 shows, the MWCO of the membrane did not seem to noticeably affect the charge density when the pH was beyond around 5.2 because the apparent zeta potentials were quite close. However, when the membrane MWCO was raised, the charge density in the positive charge region increased.

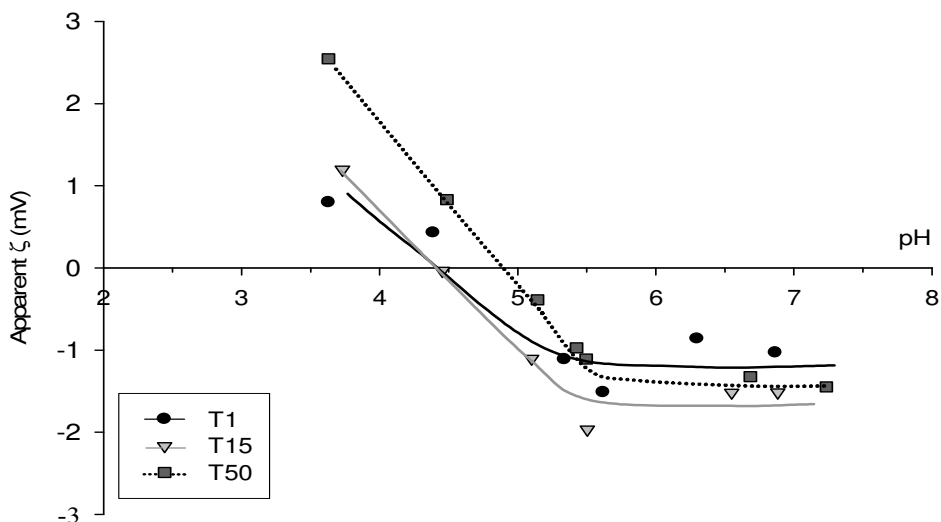


Figure 4.27. Apparent zeta potential of T1, T15 and T50 membranes at several pH

Figure 4.28 shows the evolution of the membrane charge at different pH for the F membranes. In the negative zone, i.e. at pH higher than about 5.5, membrane charges were smaller than those of T membranes.

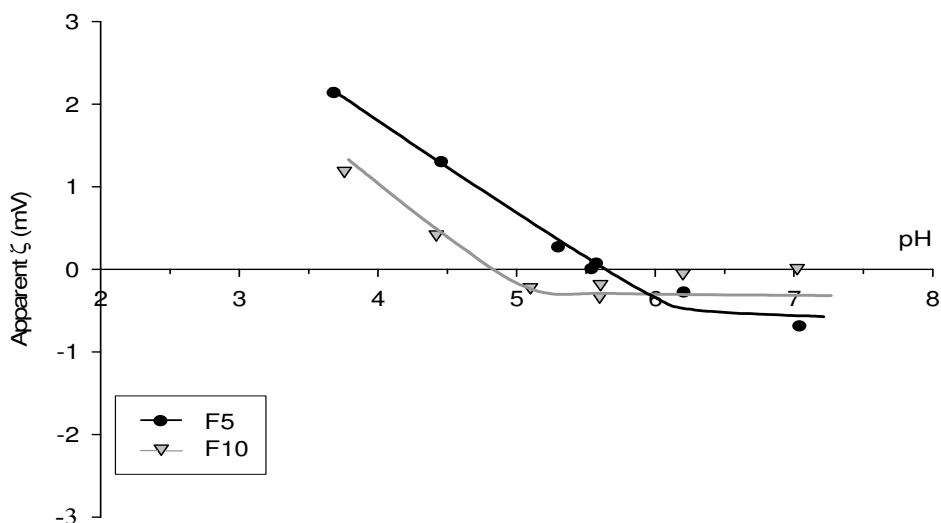


Figure 4.28. Apparent zeta potential of F5 and F10 membranes at several pH

It must be noted that F membranes are entirely made of titania, whereas T membranes are made of mixtures of alumina, titania and zirconia. In addition, F10 membrane had practically no charge after the isoelectric point. Labbez et al. (Labbez et al. 2002) found

that the isoelectric point of a titanium oxide membrane (also from Tami Industries) was at pH 6, which is in agreement with the presented characterisation. Unlike T membranes, the higher the MWCO, the lower the membrane charge density above pH 6. Thus, membrane material, configuration and/or manufacture seem to have a significant effect on the apparent zeta potential of the ceramic membranes.

The apparent zeta potential of M5 membrane was found to be similar to that obtained with T and F membranes. As it can be seen in Figure 4.29, the membrane has the isoelectric point at a pH of about 5.4. In addition, when comparing the apparent zeta potentials of this membrane to that observed with F5 membrane, which has the same MWCO, the values are quite similar. Overall, the isoelectric point was found to be at a pH between 4.5 and 5.5 for all the membranes. Moritz et al. (2001b) stated that the isoelectric point of titania, zirconia and alumina flat membranes was at pH 4.2, 4.6 and 4.3 respectively, which is mostly in agreement with the results obtained for the membranes used in the present study. The small differences between the isoelectric points presented in this study and those shown by Moritz et al. (2001b) may be due to the different manufacturing processes and membrane configurations, as demonstrated by the same authors in a previous work (Moritz et al. 2001a). In addition, membrane pre-treatment, history, ageing, storage and so on may lead to different streaming potential values. On the other hand, the isoelectric points of the oxides used in the composition of the tested membranes were found to be at pH 7-8.1 for alumina, pH 8 for zirconia and pH 5-6.1 for titania (Grün et al. 1996; Winkler and Marmé 2000). Hence, it is evident that the isoelectric point of titania, oxide found in the composition of all the selected membranes, is closer to the isoelectric point of the membranes than those of zirconia and alumina particles are.

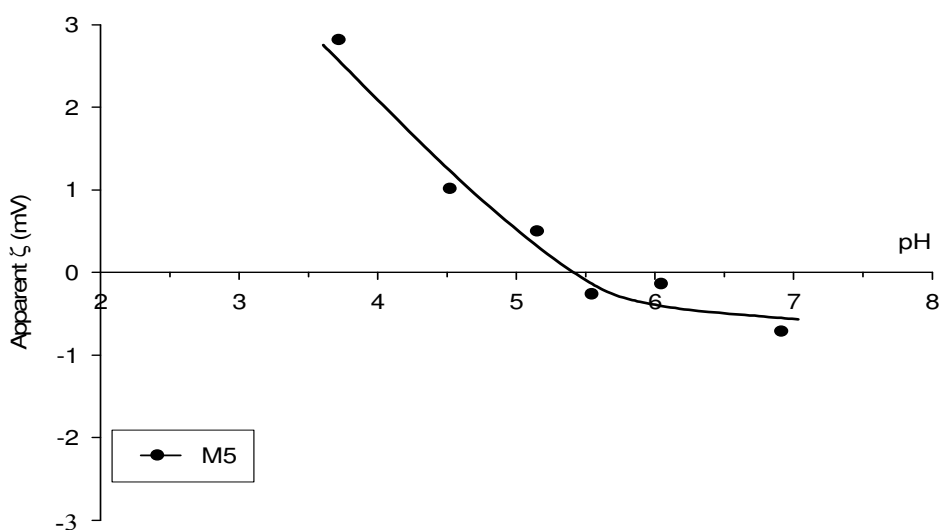


Figure 4.29. Apparent zeta potential of M5 membrane at several pH

4.4.2. Iron(III) filtration with T membranes

T1, T15 and T50 membranes exhibited a R_m of $2.06 \cdot 10^{16}$, $6.94 \cdot 10^{15}$ and $5.65 \cdot 10^{15} \text{ m}^{-1}$, respectively. The Fe(III) solution filtration results obtained with T membranes are presented in Figure 4.30, which shows the J_p evolution at several TMP. Regardless of the membrane, J_p decreased along the time. However, practically all the flux decline

occurred during the first thirty minutes of filtration and a steady-state could be observed beyond this point, as happened with T5 experiments.

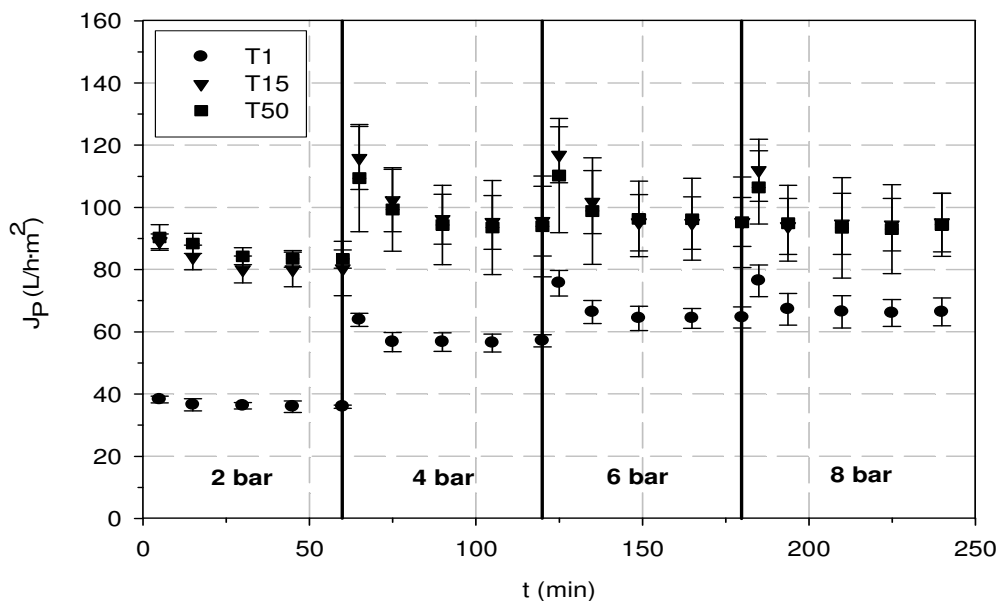


Figure 4.30. Filtration of 0.90 mM Fe(III) solution at pH 2.00.
 Permeate flux evolution of T membranes at several TMP

As it can be seen in Figure 4.30, permeate flux of T1 membrane was limited at around 65 L/h·m² whilst for T15 and T50 membranes, permeate flux was limited at around 95 L/h·m². In Table 4.4, it can be noted that for T1 membrane, R_a increased from $1.79 \cdot 10^{15}$ to $2.81 \cdot 10^{16} \text{ m}^{-1}$ when the TMP was raised from 2 to 8 bar. R_a/R_m values demonstrate that the contribution of the formed layer to the overall resistance became increasingly significant as the MWCO was higher. At 2 bar, R_a/R_m was 0.09 for T1, 0.39 for T15 and 0.78 for T50.

Table 4.4. Filtration of 0.90 mM Fe(III) solution at pH 2.00 with T membranes.
 Effect of the membrane on the additional resistance

TMP (bar)	$R_a \text{ (m}^{-1}\text{)}$			R_a/R_m		
	T1	T15	T50	T1	T15	T50
2	$1.79 \cdot 10^{15}$	$2.70 \cdot 10^{15}$	$4.42 \cdot 10^{15}$	0.09	0.39	0.78
4	$7.85 \cdot 10^{15}$	$1.03 \cdot 10^{16}$	$1.12 \cdot 10^{16}$	0.38	1.48	1.98
6	$1.70 \cdot 10^{16}$	$1.83 \cdot 10^{16}$	$1.98 \cdot 10^{16}$	0.82	2.64	3.50
8	$2.81 \cdot 10^{16}$	$2.76 \cdot 10^{16}$	$2.84 \cdot 10^{16}$	1.36	3.98	5.03

As shown in Figure 4.31, TMP did not exhibit almost any influence on the Fe(III) retention, which only depended on the membrane used. The retentions were quite significant, between 60 and 80%, and, as already stated, they could not be exclusively attributed to sieving mechanisms. This would reinforce the hypothesis that iron adsorption and formation of a layer of iron species on the ceramic material of the membrane is the key for its retention using UF ceramic elements. The adsorption of the hydrolysed species of Fe(III) onto the ceramic material of the membrane, forming a

deposit layer, is expected to be the first step once the filtration begins. After the initial adsorption, the retention may be enhanced by charge repulsions between the adsorbed positively charged hydrolysed Fe(III) species and those present in the bulk phase. In addition, the trend shown by the retention at several TMP using T1, T15 and T50 suggests that, at the steady-state, a size effect could be decisive on the rejection of iron species by ceramic UF membranes.

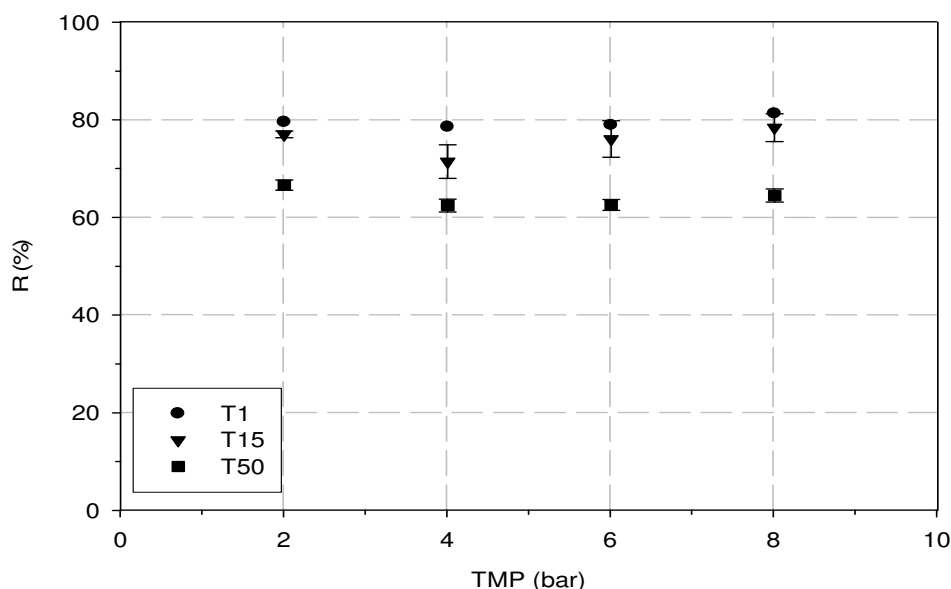


Figure 4.31. Filtration of 0.90 mM Fe(III) solution at pH 2.00. Iron retention of T membranes at several TMP

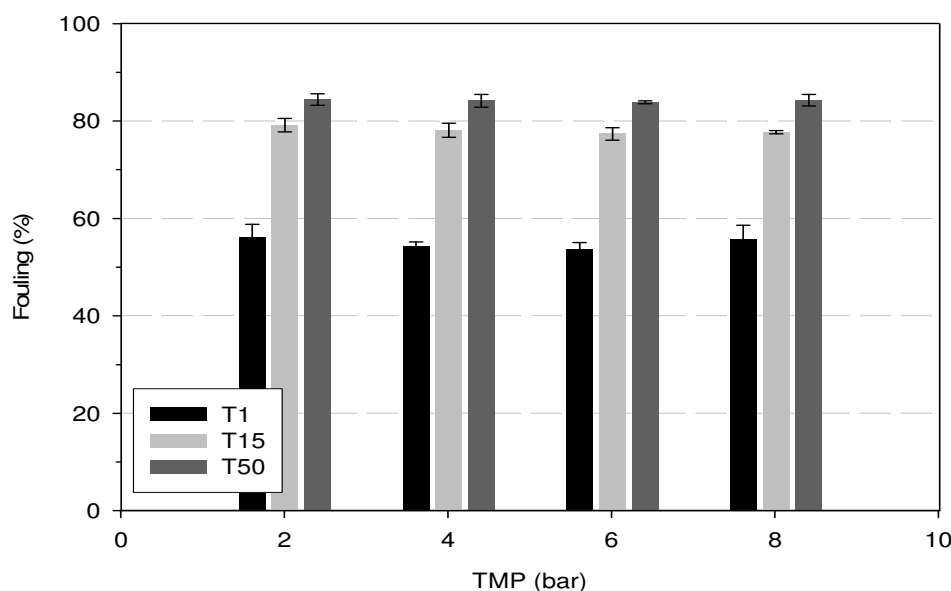


Figure 4.32. Filtration of 0.90 mM Fe(III) solution at pH 2.00. Fouling of T membranes at several TMP

An accumulation of iron soluble hydroxides, i.e. an increase of the local iron concentration, in the neighbourhood of the membrane, caused by concentration

polarisation and deposit layer formation, can be expected. Thus, the chemical properties of the ferric solution would change, allowing the formation of polynuclear species, which can be more easily retained by size-exclusion phenomena although charge repulsions and adsorption phenomena may simultaneously occur. In fact, polynuclear hydrolysed species are more easily adsorbed onto ceramic materials or yet they can directly grow on an inorganic material after the adsorption of their mononuclear predecessors.

The fouling percentage measured after rinsing the used membranes with deionised water is shown in Figure 4.32. As in all the previous experiments, the TMP did not affect the fouling extent. In addition, its values were very close to those measured during the filtration experiments, which indicates that formed layers were steady and rather resistant to water rinsing.

4.4.3. Iron(III) filtration with F and M5 membranes

Filtration of 0.90 mM Fe(III) solution at pH 2.00 was also tested using F membranes, which are fully made of TiO₂. Also, M5 membrane was tested for the same purpose. M5 membrane support is made of α-Al₂O₃ whereas its active layer is TiO₂. Thus, filtration results of these membranes are useful to ascertain the effect of the ceramic membrane material on the filtration performance.

Figure 4.33 shows the J_p evolution for F and M5 membranes at several TMP. As for the membranes explained earlier, J_p decreased during the first 30 min of operation after setting the TMP and a constant J_p was observed after this initial period. Thus, iron species instantaneously interacted with the membrane material from the beginning of the filtration. With F and M5 membranes, J_p became limited when the TMP was raised, as happened with T membranes. J_p of F5 and F10 membranes became limited at around 75 L/h·m². An increase on the TMP beyond the limiting flux only served to thicken and/or compact the deposit layer. M5 permeate flux was already limited at around 44 L/h·m², which was significantly lower than those observed for T and F membranes. Thus, higher adsorption density occurred when using M5 membrane, which is probably related to the different composition of the membrane, suggesting that the membrane material composition also affects the filtration performance.

Concerning the study of the resistances, the clean membrane resistances of F5, F10 and M5 membranes are 7.72·10¹⁵, 5.29·10¹⁵ and 6.58·10¹⁵ m⁻¹, respectively. Table 4.5 shows that, when TMP and MWCO were larger for F membranes, R_a/R_m was also greater. At 8 bar, R_a/R_m was 4.46 for F5 membrane whilst it was 7.15 for F10 membrane. In addition, Table 4.5 also indicates that the two membranes with the same MWCO but made of different materials (F5 and M5) showed different resistances. The R_a/R_m of M5 was always higher than that of F5 membrane, regardless of the TMP. For example, at 8 bar, R_a/R_m of M5 was about 2.3 times higher than that of F5. Thus, the composition of the ceramic membranes is proven to influence the filtration process.

Figure 4.34 shows that iron retentions slightly increased when the TMP was raised. Instead, no differences on iron retention were observed when changing the MWCO of F membranes. This effect could be attributed to the material of the membrane that would influence the adsorption of the soluble charged hydroxides onto the membrane material. Moreover, the retentions achieved with M5 membranes were slightly lower than those with F5. Once more, the influence of the membrane material and the manufacturing process on iron retention is demonstrated.

Comparing the apparent zeta potentials of M5 and F5 (Figures 4.28 and 4.29), the former has a slightly higher charge than the latter. Hence, if repulsion was the dominant retention factor, a significant difference on M5 iron retention should be expected. However, when inspecting Figure 4.34, M5 retentions were only slightly lower than F5 retentions. Thus, these results support that charge repulsion does not have an essential role on the Fe(III) retention by ceramic UF membranes, whereas hydrolysis undoubtedly has.

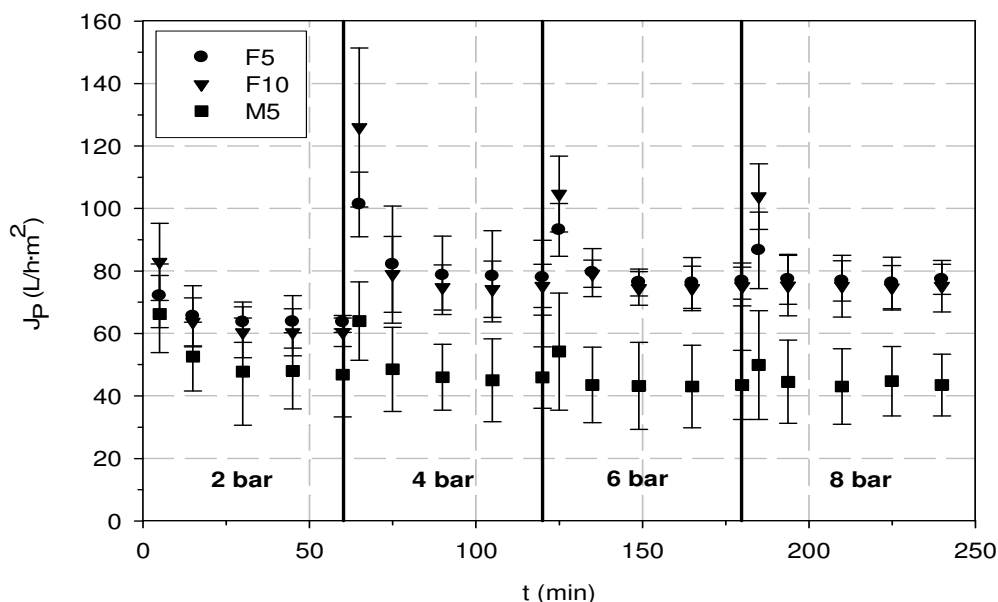


Figure 4.33. Filtration of 0.90 mM Fe(III) solution at pH 2.00. Permeate flux evolution of F and M5 membranes at several TMP

Table 4.5. Filtration of 0.90 mM Fe(III) solution at pH 2.00 with F and M5 membranes. Effect of the membrane on the additional resistance

TMP (bar)	R_a (m^{-1})			R_a/R_m		
	F5	F10	M5	F5	F10	M5
2	$4.96 \cdot 10^{15}$	$8.07 \cdot 10^{15}$	$1.04 \cdot 10^{16}$	0.64	1.53	1.58
4	$1.29 \cdot 10^{16}$	$1.63 \cdot 10^{16}$	$2.88 \cdot 10^{16}$	1.67	3.08	4.38
6	$2.40 \cdot 10^{16}$	$2.72 \cdot 10^{16}$	$4.94 \cdot 10^{16}$	3.11	5.14	7.51
8	$3.44 \cdot 10^{16}$	$3.78 \cdot 10^{16}$	$6.72 \cdot 10^{16}$	4.46	7.15	10.2

Figure 4.35 shows that fouling observed with F membranes was higher than that observed with T membranes, previously shown in Figure 4.32. Consequently, when using F membranes, more severe fouling remains after cleaning the membranes simply with deionised water. M5 membrane is the membrane showing the highest severe fouling degree (93%) as it could have been expected from its additional resistance values and J_p evolution, clear indication of high Fe(III) affinity for the inorganic membrane material.

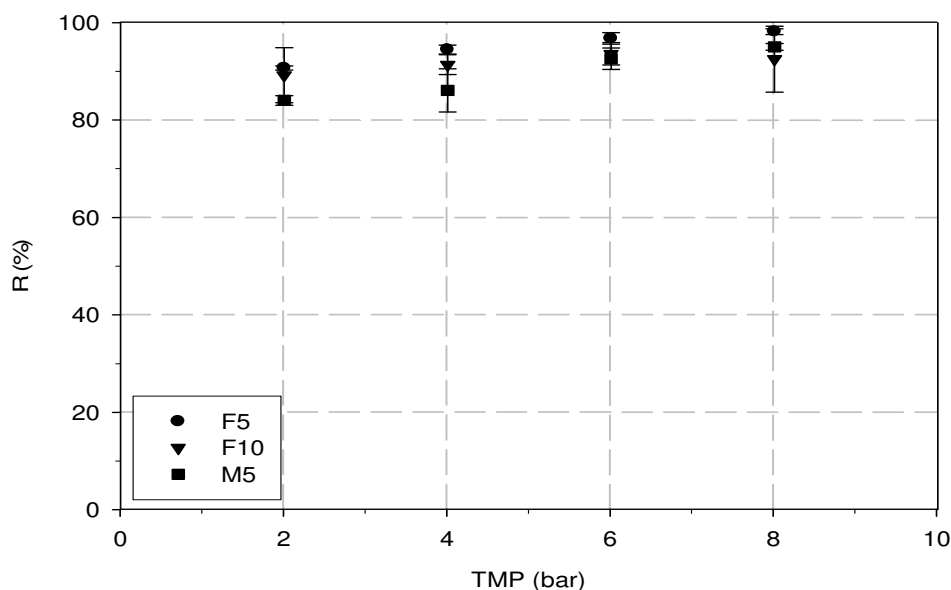


Figure 4.34. Filtration of 0.90 mM Fe(III) solution at pH 2.00. Iron retention of F and M5 membranes at several TMP

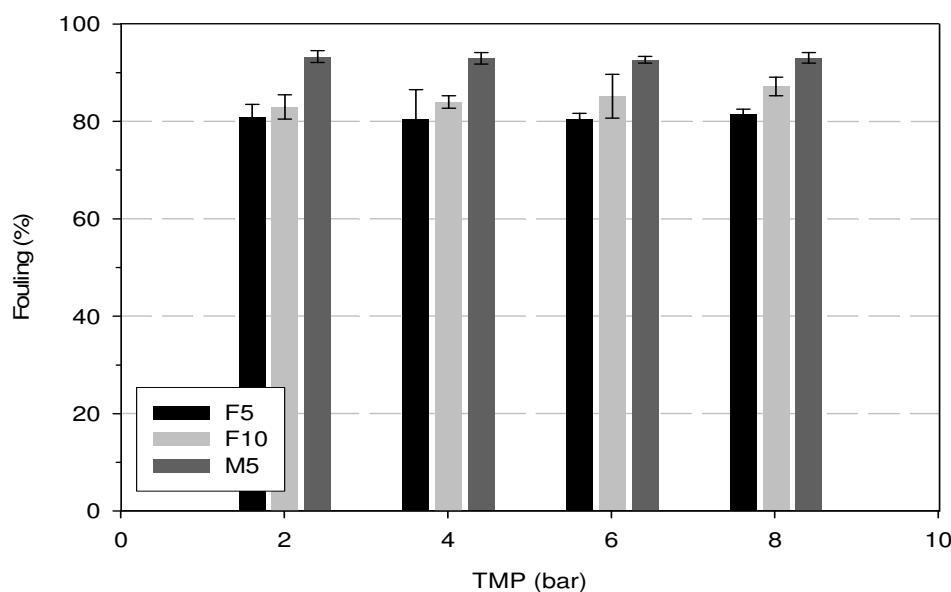


Figure 4.35. Filtration of 0.90 mM Fe(III) solution at pH 2.00. Fouling of F and M5 membranes at several TMP

4.5. Iron(III) recovery with polymeric UF membranes

In order to assess the key role of the ceramic nature of the membranes, the polymeric PT and ER membranes were used to filter 0.90 mM Fe(III) solutions at pH 2.00, as done for the other seven ceramic membranes tested. Previous streaming potential characterisation of polyethersulfone UF membranes, carried out with the same streaming potential device as in this study, showed that their surfaces were neutral in all the pH range (Weis et al. 2003; Delaunay et al. 2006). On the contrary, the

isoelectric point of polysulfone membranes was found at a pH between 3 and 4 (Kim et al. 2002; Weis et al. 2003; Martín et al. 2003). Furthermore, the surface charges of ER polysulfone membrane were higher than those observed with any of the ceramic membranes tested in this study (Weis et al. 2003). Thus, if repulsion was the dominant factor on the filtration of ferric solutions by UF membranes, significant rejection should be observed when dealing with ER membrane. However, no retention was observed at any TMP with PT membrane, whereas meagre retentions, below 3%, were achieved with ER membrane. The fact that the retention of iron species was almost nil when using polymeric membranes clearly indicates that the membrane charge has no effect on the rejection of iron species by UF. Hence, the membrane material affinity for adsorbing iron species is decisive for their retention, as explained in the previous sections. In fact, it has been proven that iron species are highly adsorbed onto ceramic materials and no iron adsorption is detected when polysulfone fibres are tested (Jones and Edwards 1993). Thus, because of the lack of inorganic oxides, there is no adsorption taking place in polymeric membranes and the subsequent formation of a deposit layer does not occur, which prevents polymeric membranes from being able to retain iron species. It is worth mentioning that, in this study, the ceramic membranes had to be cleaned, after the filtration tests, with an oxalic acid solution because it is an iron-complexing agent (as recommended by the membranes' manufacturers) and it was able to remove iron fouling. Hydrochloric acid and phosphoric acid were also tested as cleaners and no fouling removal was achieved. Thus, the necessity of using a complexing agent for the total removal of iron from the used ceramic membranes confirms that the layer formed over the ceramic material was significantly stable.

4.6. Conclusions

Ceramic UF membranes have been demonstrated to be an effective way for the recovery of hydrolysed heavy metals from aqueous solutions. Hydrolysable metals, Fe(III) and Cr(III), have shown to be efficiently retained by the ceramic membranes. On the contrary, Fe(II) and Cu(II) have not been retained by the same system due to the fact that they do not suffer from hydrolysis at the tested conditions.

The retention efficiency and filtration process performance is strongly related to both solution chemistry and membrane properties because of the crucial role that the adsorption of hydrolysed metal species on the membrane material has demonstrated to play. A retention mechanism based on the formation of a stable layer of iron species adsorbed on the membrane material seems to be the most adequate for explaining metals' retention. After the adsorbed layer formation, charge repulsions between the adsorbed iron species (positively charged) and the iron species present in the bulk solution (also positively charged) can coexist with adsorption phenomena. In addition, sieving effects could also contribute to the retention of hydrolysed species. Mononuclear hydrolysed species occurring at low pH may initiate the formation of polynuclear species, higher in molecular weight, in the vicinity of the membrane surface due to the local increase of the iron concentration in this zone. Despite the possible contribution of sieving effects and charge repulsions, they do not play a key role by itself in the filtration process as the adsorption of the species to filter on the membrane material do.

Thus, the affinity of the species to filter to adsorb on the membrane material probably governs the retention process. As a result, polymeric UF membranes are not able to retain neither non-hydrolysed nor hydrolysed metal species. Apart from metals' hydrolysis, solution chemistry variables such as pH, ionic strength, presence of

chelating agents and presence of non-hydrolysed species together with hydrolysed ones strongly affect filtration efficiency and performance.

Ceramic UF membranes have been shown to be a useful tool for the recovery of heavy metals from synthetic aqueous solutions. However, its application at real wastewater effluents' treatment needs to be tested in each application due to the sensitivity that this membrane process has demonstrated when solution chemistry or process variables are modified.

UNIVERSITAT ROVIRA I VIRGILI

TREATMENT OF BIOREFRACTORY WASTEWATER THROUGH MEMBRANE-ASSISTED OXIDATION PROCESSES

Xavier Bernat Camí

ISBN:978-84-693-1529-3/DL:T-652-2010

CHAPTER 5

Recovery of iron from aqueous solutions by nanofiltration

5.1. Introduction

UF has shown to be efficient to retain heavy metals from aqueous solutions. However, as shown in Chapter 4, its efficiency is strongly affected by process and solution chemistry variables. For example, when metal hydrolysis does not occur in solution, as happens when dealing with Fe(II), retention is marginal. The effluents from the Fenton oxidation are composed by, besides organic compounds, both Fe(II) and Fe(III) species due to the Fe(II)-Fe(III) redox cycle. Thus, the applicability of ceramic UF membranes as intermediate step between Fenton oxidation and biological degradation is limited. For this reason, NF has been tested with the same aim.

In this chapter, NF efficiency is explored in terms of permeate flux decline and iron retention when synthetic solutions of Fe(III) or Fe(II) are filtered. The experiments have allowed investigating the effect of the stirring rate, transmembrane pressure, the presence and concentration of a background electrolyte and the iron valence on the rejection efficiency and permeate flux decline when using three commercial NF membranes from DOW-Filmtec: NF-D, NF90 and NF270. In addition, due to the applicability of chelates such as EDTA, ethylenediaminedisuccinate (EDDA) or citrate, among many others, as chemical oxidation promoters (Sanchez et al. 2007; Laine et al. 2008; Rastogi et al. 2009), iron recovery from aqueous solutions containing Fe(III) species chelated by EDTA has also been thoroughly studied.

The filtration experiments were performed in dead-end mode until a VRF of around 6 was achieved. Both permeate flux evolution and iron concentration in the permeate as

well as initial feed and final concentrate were experimentally obtained. From the experimental measurements, both % J_P/J_w and iron retention were calculated in order to evaluate NF performance in the proposed scenarios. In addition, solute adsorption onto the membrane was estimated by mass balance, as previously reported by Plakas et al. (2006). For this, the initial feed concentration ($C_{f,initial}$), the final permeate concentration ($C_{P,final}$), the solute concentration in the final retentate ($C_{R,final}$), the feed solution volume (V_f), the total permeate volume (V_P) and the final retentate volume (V_R) are needed. Equation 5.1 is the general solute mass balance equation that can be used to obtain the mass of adsorbed solute onto the membrane (Ads). Equation 5.2, which is developed from equation 5.1, can be used to evaluate the solute adsorption onto the membrane in relative terms (%Ads).

$$C_{f,initial} \cdot V_f = C_{P,final} \cdot V_P + C_{R,final} \cdot V_R + Ads \quad (\text{eq. 5.1})$$

$$\%Ads = 100 \cdot \left[1 - \left(\frac{C_{P,final} \cdot V_P + C_{R,final} \cdot V_R}{C_{f,initial} \cdot V_f} \right) \right] \quad (\text{eq. 5.2})$$

All the experiments presented in this chapter showed a %Ads lower than 1.5%. Thus, no (or negligible) solute adsorption occurred onto the NF membranes at the tested experimental conditions.

5.2. Iron(III) and iron(II) recovery

A 0.90 mM Fe(III) solution was used as feed model solution to be filtered. When the effect of the variations on feed solution composition and/or on the filtration variables was tested, the results have been compared to those obtained with the 0.90 mM Fe(III) solution.

Initially, the NF-D membrane was selected for performing the filtration runs designed to test the effect of the filtration variables and solution chemistry on the process efficiency. Later, a screening of the three membranes to recover either Fe(III) or Fe(II) was carried out.

5.2.1. Influence of the stirring rate

The dead-end cell was continuously stirred during the filtration experiments in order to decrease concentration polarisation phenomena and membrane fouling. However, in order to optimise the filtration process, several stirring rates were tested and the obtained membrane filtration performance indicators accordingly compared. For this, a 0.90 mM Fe(III) solution adjusted at pH 2.00 was filtered through NF-D at 6 bar of TMP and at stirring rates ranging from 300 to 1200 rpm.

The effect of the stirring rate on the evolution of the % J_P/J_w , which indicates the permeate flux decrease, and on the iron retention is shown in Figure 5.1. The permeate flux decline was not influenced by the stirring rate between 300 and 900 rpm. Nevertheless, at 1200 rpm, the permeate flux suddenly dropped. After the filtration at 1200 rpm, the membrane was removed from the filtration cell and it presented an orange coloration in a narrow zone in the centre of the membrane disk. The colouration corresponded to the Fe(III) solution colour. Thus, as the rest of the membrane was completely colourless, the visual observation and the % J_P/J_w response seemed to

indicate that, at 1200 rpm, a vortex was formed as a result of the high stirring rate in the liquid filling the cell. The vortex prevented the areas of the membrane edges from being in contact with the bulk solution, decreasing the available filtration area, resulting in a decrease on the permeate flux. Vortex formation was visually corroborated by stirring a feed solution in the dead-end cell opened by the upper part. Thus, for hydrodynamic reasons, the cell had to be operated below 1200 rpm of stirring rate.

At stirring rates between 300 and 900 rpm, no significant changes were observed neither on permeate flux not on iron retention, as shown by Figure 5.1. $\%J_p/J_w$ was around 91% at a VRF of approximately 6, regardless of the stirring rate. This indicates that the increase on the iron concentration in the retentate side as long as the filtration proceeded, did not cause more than 9% of permeate flux reduction. Iron retention was around 99.5%, irrespective of the stirring rate and the VRF. Thus, NF-D membrane is capable of almost totally retaining Fe(III) species from aqueous solutions.

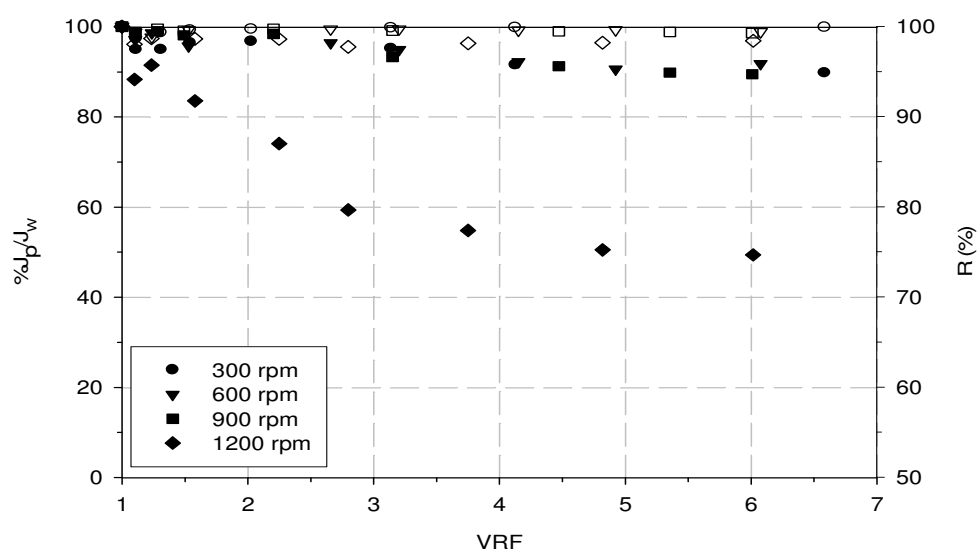


Figure 5.1. Filtration of 0.90 mM Fe(III) solution at pH 2.00 and 6 bar by NF-D. Effect of the stirring rate on the $\%J_p/J_w$ and iron retention evolution. Filled symbols represent $\%J_p/J_w$ and open symbols R(%)

Iron species present in solution at pH 2.00 are, as exposed in Chapter 4, positively-charged soluble hydroxides and free Fe(III) ions. Table 5.1 summarises these Fe(III) species present in the solution to be filtered at pH 2.00 together with their MW's. The MW's of the species, taking into account their hydration state, are not far away to those accepted as threshold for typical NF membranes (around 200 g/mol). However, as the species in solution are positively charged and NF-D at pH 2.00 exhibits a positive surface charge (Tanninen et al. 2006), charge repulsions between the species in solution and the membrane surface are expected to be the main rejection mechanism taking place.

After the iron filtration experiments were completed, the membranes (with the exception of that used at 1200 rpm) were flushed with deionised water and the permeate flux was measured again. All the membranes showed a complete restoration of the permeate flux, which clearly pointed out that permeate flux decline was due to concentration polarisation and reversible fouling. Hence, *a priori*, it seems that NF can be a robust membrane process candidate for Fe(III) recovery applications.

Table 5.1. 0.90 mM Fe(III) solution speciation at pH 2.00

Specie	Hydrated formula	MW (g/mol)
Fe ³⁺	Fe(H ₂ O) ₆ ³⁺	164
FeOH ²⁺	Fe(OH)(H ₂ O) ₅ ²⁺	163
Fe(OH) ₂ ⁺	Fe(OH) ₂ (H ₂ O) ₄ ⁺	162
Fe ₂ (HO) ₂ ⁴⁺	Fe ₂ (HO) ₂ (H ₂ O) ₈ ⁴⁺	290

5.2.2. Influence of the transmembrane pressure

The effect of the TMP was also assessed using NF-D membrane and a 0.90 mM Fe(III) solution at pH 2.00 as model single solution. Three TMP's were tested: 4, 6 and 8 bar. As Figure 5.2 shows, TMP did not affect the %J_p/J_w. In addition, only a slight decrease on %J_p/J_w was observed when VRF increased. This could be a result of the increase on the Fe(III) concentration in the feed side of the membrane as long as the filtration proceeded because of the high Fe(III) retention, which was around 99.5%, regardless of the TMP and VRF. The permeate flux of the membranes was completely restored after flushing them with deionised water once the filtration experiments finished, as happened when testing the effect of the stirring rate on the NF-D performance.

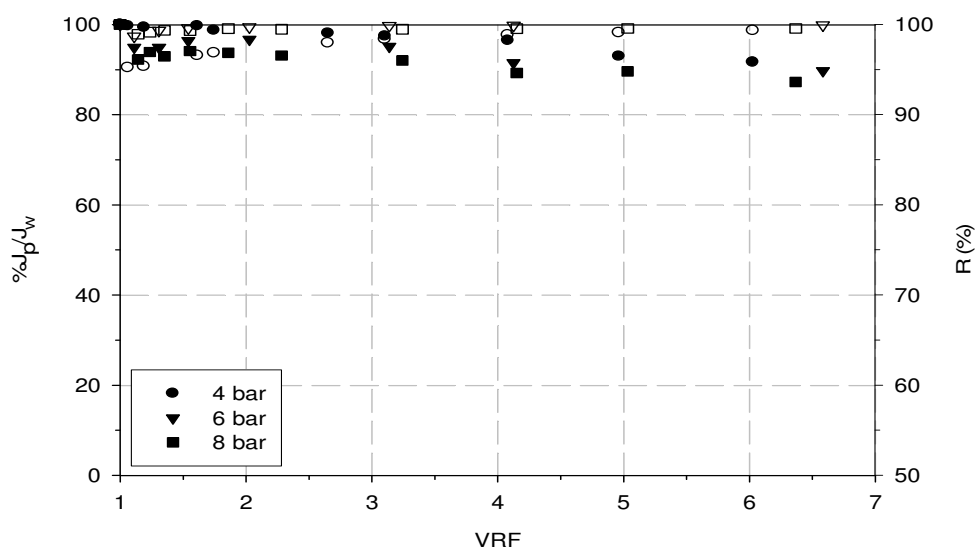


Figure 5.2. Filtration of 0.90 mM Fe(III) solution at pH 2.00 and 300 rpm by NF-D. Effect of the TMP on the %J_p/J_w and iron retention evolution. Filled symbols represent %J_p/J_w and open symbols R(%)

5.2.3. Influence of the background electrolyte

One of the main drawbacks of the Fe(III) separation with ceramic UF membranes was the drop on the retention efficiency when a background electrolyte (NaCl) was present in the Fe(III) feed solution. Thus, the influence of the presence and concentration of background electrolyte on the nanofiltration efficiency was considered. The filtration experiments were performed with NF-D membrane using a 0.90 mM Fe(III) aqueous

solution, whose pH had been adjusted at 2.00. The TMP and the stirring rate were fixed and kept constant during the experiment at 6 bar and 300 rpm, respectively. The effect of the background electrolyte was tested by adding NaCl together with Fe(III) in the feed solutions prepared. The NaCl concentrations tested were 10, 50 and 100 mM. The results obtained when testing the presence and concentration effect of NaCl on the $\%J_P/J_W$ and iron retention are shown in Figure 5.3. The blank experiment concerning the filtration of the Fe(III) solution without NaCl is also included in Figure 5.3.

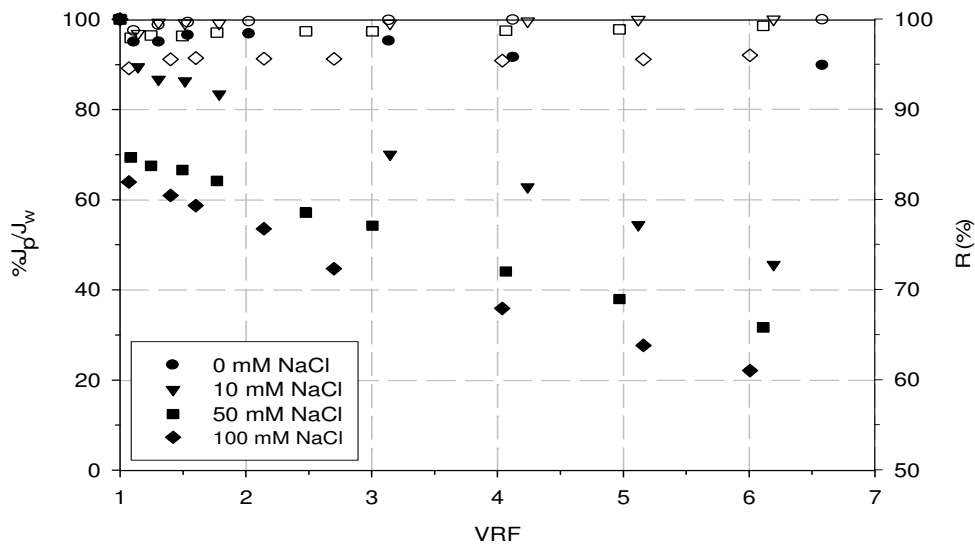


Figure 5.3. Filtration of 0.90 mM Fe(III) solution at pH 2.00, 6 bar and 300 rpm by NF-D. Effect of the NaCl concentration on the $\%J_P/J_W$ and iron retention evolution. Filled symbols represent $\%J_P/J_W$ and open symbols R(%)

The presence of NaCl in the feed solution decreased the $\%J_P/J_W$ and thus reduced the permeate flux. This decrease was enhanced as the NaCl concentration increased, i.e. when the ionic strength (IS) raised. This could be attributed to the fact that the charge of the membrane matrix has been found to decrease at high IS, increasing the proximity between the polymers that form the membrane, causing a permeate flux reduction (Braghetta et al. 1997). Moreover, an increase on the NaCl concentration results in an increase on the osmotic pressure (π), decreasing the effective TMP and, consequently, the permeate flux. In fact, by using the Van't Hoff law (Merten 1966), expressed by equation 5.3, and assuming that total dissociation of both $\text{Fe}(\text{NO}_3)_3$, used as Fe(III) source, and NaCl occurs ($\alpha=1$ in equation 5.4), π increases from 0.09 bar in absence of NaCl to 4.89 bar when 100 mM NaCl were present in the 0.90 mM Fe(III) feed solution.

$$\pi = i \cdot M \cdot R \cdot T \quad (\text{eq. 5.3})$$

$$\alpha = \frac{i-1}{n-1} \quad (\text{eq. 5.4})$$

where π is the osmotic pressure in bar, i is the Van't Hoff factor, M is the concentration in mol/L, R is the gas constant as 0.083 bar·L/K·mol (Perry et al. 1999), T is the temperature in K and α is the dissociation constant.

As Figure 5.3 shows, an increase on the NaCl concentration in the feed ferric solution slightly decreased the iron retention, which passed from 99.5% when no NaCl was present to 95.5% when 100 mM NaCl were present in the feed solution at the last-measured VRF. This minor retention decrease could be explained by the decrease on the thickness of the diffuse double layer at high IS, reducing the retention of charged solutes (Mulder 1997; Braghetta et al. 1997) such as Fe(III) species.

The permeate flux of the used membranes was totally restored after flushing them with deionised water. Thus, even though NaCl negatively affects membrane efficiency, it does not cause irreversible modifications on the membrane permeability.

5.2.4. Influence of the iron valence and membrane

In this section, the filtration of a 0.90 mM Fe(II) solution at pH 2.00 is presented. The filtration experiment was carried out using the NF-D membrane at 6 bar of TMP and at 300 rpm of stirring rate. The results obtained are compared to those found with the filtration of a 0.90 mM Fe(III) solution at the same experimental conditions. The filtration performance differences obtained when varying the valence of iron (III or II) are shown in Figure 5.4. The $\%J_P/J_W$ decrease was somewhat higher at the greater iron valence. This means that a lower permeate flux was found when filtering the Fe(III) solution than when filtering that of Fe(II). At a VRF of approximately 6, the $\%J_P/J_W$ was 90% and 94% for Fe(III) and Fe(II), respectively.

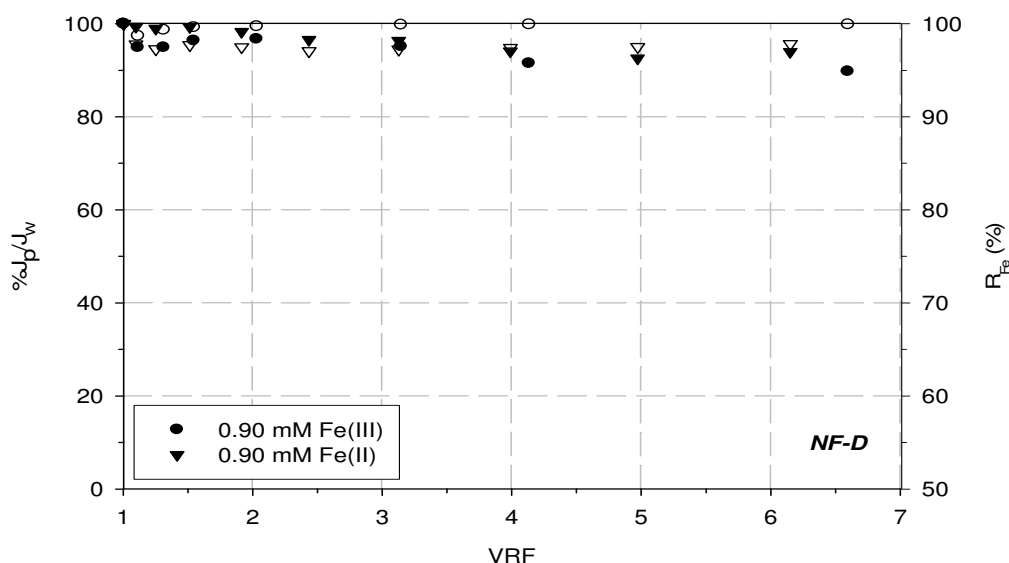


Figure 5.4. Filtration of 0.90 mM Fe solution at pH 2.00, 6 bar and 300 rpm by NF-D. Effect of the iron valence on the $\%J_P/J_W$ and iron retention evolution. Filled symbols represent $\%J_P/J_W$ and open symbols R_{Fe} (%)

In turn, an increase on the iron valence increased the iron retention, as it could be expected. When filtering Fe(II), contrarily to what happens when filtering Fe(III), no hydrolysed species with high MW are present. This may diminish sieving effects and accordingly retention. In addition, the charge of the species to recover is lower when dealing with Fe(II) because it exists as Fe^{2+} . Instead, when dealing with Fe(III), species in solution are 1+, 2+, 3+ and 4+ cations, which undoubtedly produce stronger repulsion between them and the positively-charged membrane surface, leading to a

higher iron retention. The positive charge of the membrane surface at pH 2.00 is demonstrated by its isoelectric point (IEP), which was found to be 5.1 (Tanninen et al. 2006), as mentioned in Chapter 3. Even though the iron retention was reduced when passing from Fe(III) to Fe(II), the difference is irrelevant because it only went from 99.5% to 97.5%, respectively.

The effect of the iron speciation was also tested using NF90 and NF270 membranes. The experimental conditions were the same than when testing NF-D membrane. Thus, TMP was 6 bar and the stirring rate 300 rpm. Regarding the solutions filtered, a 0.90 mM Fe(III) and a 0.90 mM Fe(II) solution, both prepared at pH 2.00, were used as feed model solutions.

The results obtained with the NF90 membrane are shown in Figure 5.5. As it can be seen, the permeate flux decrease of NF90 was significantly higher, i.e. $\%J_P/J_W$ was lower, than that observed with NF-D membrane. At a VRF of approximately 6, the $\%J_P/J_W$ was 70% for the Fe(III) solution and 71% for the Fe(II) one. However, the retention of both Fe(III) and Fe(II) was higher than that encountered with NF-D. 99.9% and 99.7% iron retentions were achieved when filtering Fe(III) and Fe(II) solutions with NF90, respectively. The retention mechanism can be explained, as with NF-D, by sieving effects and electrostatic repulsions between the species to retain, which were positively charged, and the membrane surface, which was also positively charged because its IEP was found to be at 4.0 (Nghiem et al. 2005), as exposed in Chapter 3.

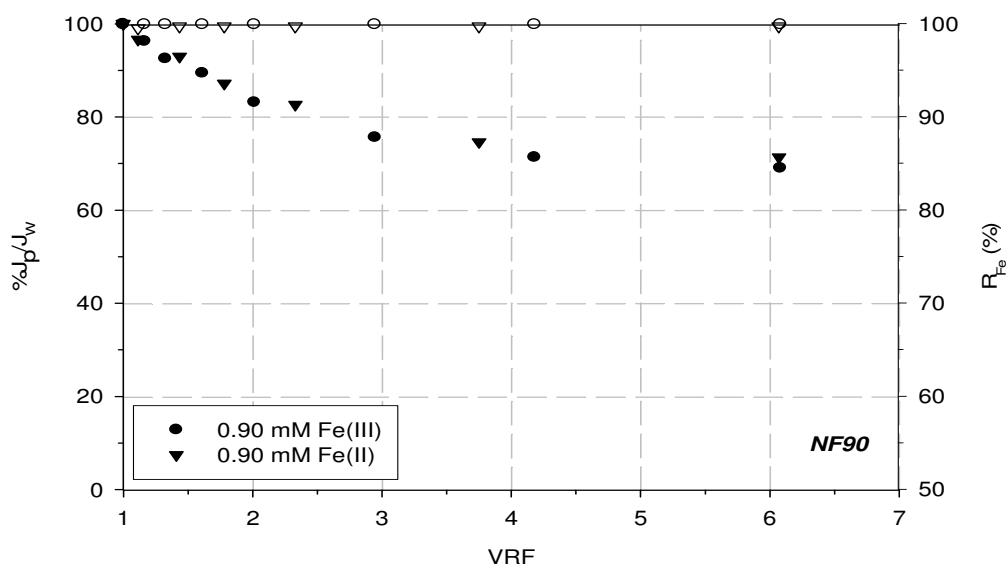


Figure 5.5. Filtration of 0.90 mM Fe solution at pH 2.00, 6 bar and 300 rpm by NF90. Effect of the iron valence on the $\%J_P/J_W$ and iron retention evolution. Filled symbols represent $\%J_P/J_W$ and open symbols R_{Fe} (%)

Used NF90 membranes recovered its initial permeate flux after rinsing with deionised water, as NF-D membranes. Hence, the permeate flux reduction measured during the filtration was due to concentration polarisation and reversible fouling. For these reasons, NF90 membrane could be used in applications needing very high iron retentions at moderate permeate flux. When permeate flux is more important that iron retention, NF-D would be recommended instead. As exposed in Chapter 3, both membranes have similar PWP's (NF-D: 5.9 L/h·m²·bar; NF90: 5.6 L/h·m²·bar) but

$\%J_P/J_W$ values measured for NF90 are quite lower than those for NF-D. Thus, obtained permeate flux would be higher with NF-D.

NF270 was also tested with the same purpose than NF-D and NF90. Thus, the membrane was again used for filtering a 0.90 mM Fe(III) and a 0.90 mM Fe(II) solution, both fixed at pH 2.00. The TMP was 6 bar and a 300 rpm stirring rate was set. The evolution of $\%J_P/J_W$ and iron retention along the VRF is presented in Figure 5.6. NF270 showed the poorest Fe(II) retention, which was around 95.5%. On the contrary, the Fe(III) retention was 99.5%. Iron retentions could be explained, as for NF-D and NF90, by sieving effects and especially by electrostatic solute-membrane repulsions because of the positive charge of the species to filter and the positive charge of the membrane surface, since its IEP is at pH 3.3 (Tanninen et al. 2006). The $\%J_P/J_W$ values were between those measured with NF-D and NF90. Around 76% and 78% of permeate flux remained at a VRF of about 6 when Fe(III) and Fe(II) solutions were filtered, respectively. NF-D and NF90 membranes have a PWP of 5.9 and 5.6 L/h·m²·bar, as explained in Chapter 3. Instead, NF270 has a PWP of 9.3 L/h·m²·bar, almost twice those of NF-D and NF90. Thus, despite NF270 membrane presented a permeate flux decline which was intermediate between that of NF-D and NF90, because its initial permeate flux was higher, the membrane still represents a better option than NF-D and NF90 in applications needing highly purified effluents' production at lower retentions than those obtained with NF-D and especially with NF90.

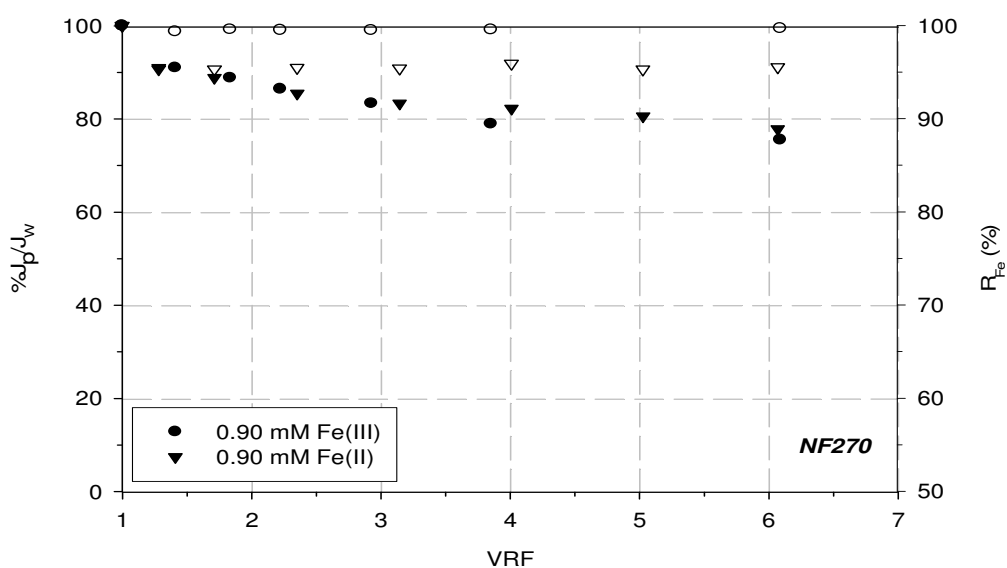


Figure 5.6. Filtration of 0.90 mM Fe solution at pH 2.00, 6 bar and 300 rpm by NF270. Effect of the iron valence on the $\%J_P/J_W$ and iron retention evolution. Filled symbols represent $\%J_P/J_W$ and open symbols R_{Fe} (%)

NF270 membrane instantaneously recovered its original PWP after being flushed with deionised water. Thus, like NF-D and NF90, permeate flux decline was due to concentration polarisation and reversible fouling phenomena. Therefore, NF-D, NF90 and NF270 do not need to be chemically cleaned after being used for the filtration of Fe(III) or Fe(II) species from synthetic aqueous solutions.

Table 5.2 summarises the $\%J_P/J_W$ and retentions obtained with the three tested membranes when filtering 0.90 mM Fe(III) or 0.90 mM Fe(II) solutions at pH 2.00, 6 bar of TMP and 300 rpm of stirring rate. As it can be observed, the lowest $\%J_P/J_W$ was

obtained with NF90, followed by NF270 and by NF-D. Iron(III) retention was 99.5% for NF-D and NF270 whilst it was 99.9% for NF90. Iron(II) retention was 95.5%, 97.5% and 99.7% for NF270, NF-D and NF90 membranes, respectively. Overall, NF90 seems to be the most suitable NF membrane for retaining almost completely iron(III) and (II) from aqueous synthetic solutions at pH 2.00.

Table 5.2. $\%J_P/J_W$ and iron retention by NF-D, NF90 and NF270. Filtration of 0.90 mM Fe(III) or Fe(II) solution at pH 2.00, 6 bar and 300 rpm

Membrane	Fe(III) solution		Fe(II) solution	
	$\%J_P/J_W$ (VRF~6)	R(%)	$\%J_P/J_W$ (VRF~6)	R(%)
NF-D	90	99.5	94	97.5
NF90	70	99.9	71	99.7
NF270	76	99.5	78	95.5

5.3. Iron(III)-EDTA recovery

Iron(III) speciation is strongly influenced by the presence of chelating agents, as demonstrated in Chapter 4. In addition, in Chapter 4, it was found that the Fe(III) chelation degree affected its retention by ceramic UF membranes. The NF of a 0.90 mM Fe(III) solution containing EDTA at the stoichiometric ratio (1:1) was studied using NF-D, NF90 and NF270 membranes. Three pH levels were tested to highlight the effect of the pH on the filtration performance as a result of its influence on the chelated iron speciation. The pH ranges are identified as low (pH~2.5), intermediate (pH~4.3) and high (pH~8.4). The exact pH of the feed solutions is reported below and can be found in the figures showing the results obtained with each membrane (Figures 5.8, 5.9 and 5.10). The speciation diagram of a 0.90 mM Fe(III)+0.90 mM EDTA solution is given in Figure 5.7. At low pH, neutral chelates coexist with (1-) charged chelates. At intermediate pH, only (1-) charged chelates exist and at high pH, (1-) and (2-) mononuclear chelates coexist with binuclear (4-) charged ones. Thus, at the three tested pH levels, the fraction and nature of the chelates vary.

The first membrane tested was NF-D, whose performance results are shown in Figure 5.8. $\%J_P/J_W$ was around 98%, indicating that only 2% permeate flux reduction occurred during the filtration of the iron chelates, regardless of the solution pH. Chelating agents such as EDTA are efficient membrane cleaners usually recommended by membrane manufacturers for scaling removal among other fouling removal applications (Al-Almoudi and Lovitt 2007). In consequence, the low permeate flux decline observed agrees with the nature of the solutions filtered which are expected not to foul membranes. Liikanen et al. (2002) detected that, when a membrane was cleaned with an alkaline cleaner based on NaOH and EDTA, its PWP after cleaning was higher than that of the virgin membrane. They attributed this response to an increase on the membrane negative charge in EDTA alkaline environment, which made the membrane more open (Liikanen et al. 2002). In this work, the $\%J_P/J_W$ was found to be always below 100% when filtering Fe(III)-EDTA solutions, which indicates that, if membrane pores were opened during the filtration, the permeate flux decline was balanced by the membrane fouling. However, this is not expected to take place because no permeate flux changes were observed after flushing the used NF-D membranes with water.

Iron average retentions were, as shown in Figure 5.8, 92.5%, 95.0% and 96.5% when the solution pH was 2.52, 4.22 and 8.19, respectively. This slight retention increase could be explained by the raise on the positive charge of the dissolved species. This would enhance iron retention by increasing the iron chelates-membrane charge repulsions. In addition, iron retentions were not found to vary as the VRF increased. EDTA retentions, evaluated from TOC analyses, were 91.3%, 93.8% and 95.5% when the feed pH was 2.52, 4.22 and 8.19, respectively. Thus, iron and EDTA retentions can be practically considered equal. This suggests that chelation was complete and that iron and EDTA concentrations increased at the same rate in the feed (retentate) side of the membrane as the filtration proceeded, which allowed keeping constant the membrane retention regardless of the VRF.

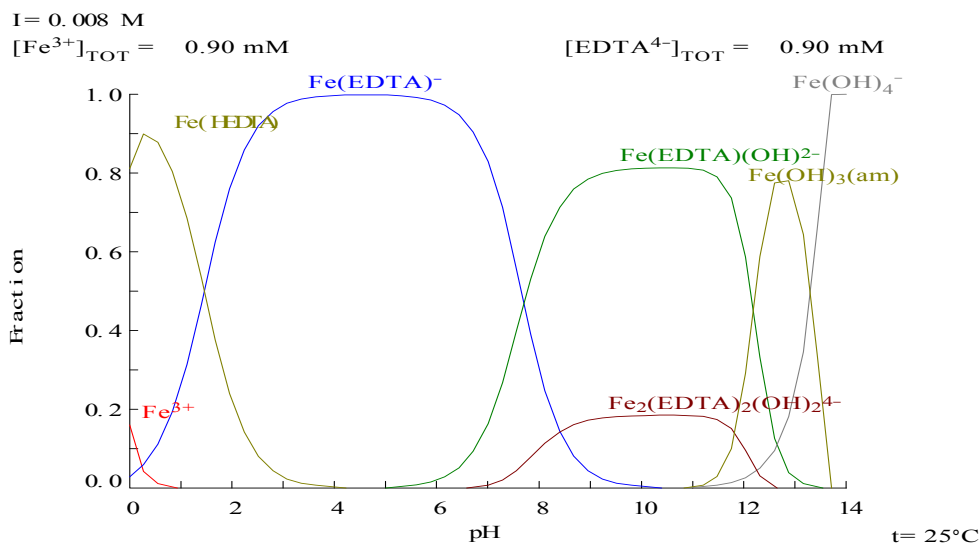


Figure 5.7. Chemical speciation diagram of a 0.90 mM Fe(III)+0.90 mM EDTA solution

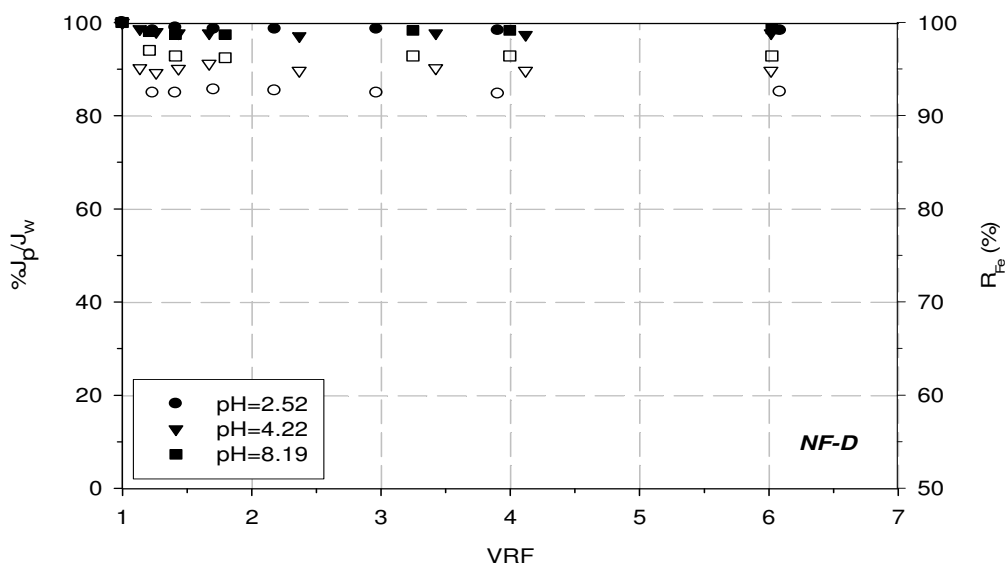


Figure 5.8. Filtration of 0.90 mM Fe(III)+0.90 mM EDTA solution at 6 bar and 300 rpm by NF-D. Effect of the pH on the $\%J_P/J_W$ and iron retention evolution. Filled symbols represent $\%J_P/J_W$ and open symbols $R_{Fe}(\%)$

Figure 5.9 shows the $\%J_P/J_W$ and iron retention evolution when NF90 membrane was selected to study the retention of Fe(III)-EDTA chelates. As NF-D, the effect of the pH was studied at three levels. The $\%J_P/J_W$ was constant at any VRF and no significant differences were observed when the feed solution pH was varied, as happened with NF-D. Nonetheless, the average $\%J_P/J_W$ was 94%, which is a higher, although still low, permeate flux decline in comparison to that of NF-D (98%). The permeate flux was totally restored after flushing the used membranes with deionised water, indicating that only concentration polarisation and soft fouling occurred.

NF90 iron retentions, also represented in Figure 5.9, increased with solution pH, like for NF-D. This can be explained, as abovementioned, by the increase on the positive charge of the species to filter when the feed pH increases, which raises the electrostatic interactions occurring between the solutes and the membrane, allowing their retention. Iron retentions were 94.5%, 97.1% and 98.7% when the feed pH was 2.44, 4.34 and 8.41, respectively. The comparison of the NF90 retentions to those obtained with NF-D allows stating that NF90 membrane retains iron at a higher extent than NF-D. NF90 EDTA retentions were 93.0%, 95.8% and 96.4% at pH 2.44, 4.34 and 8.41, respectively. Thus, as when NF-D was examined, total iron chelation occurred and retention was kept constant as VRF increased because retentate (feed) iron and EDTA concentrations increased at the same rate, avoiding chelation changes which could affect retention.

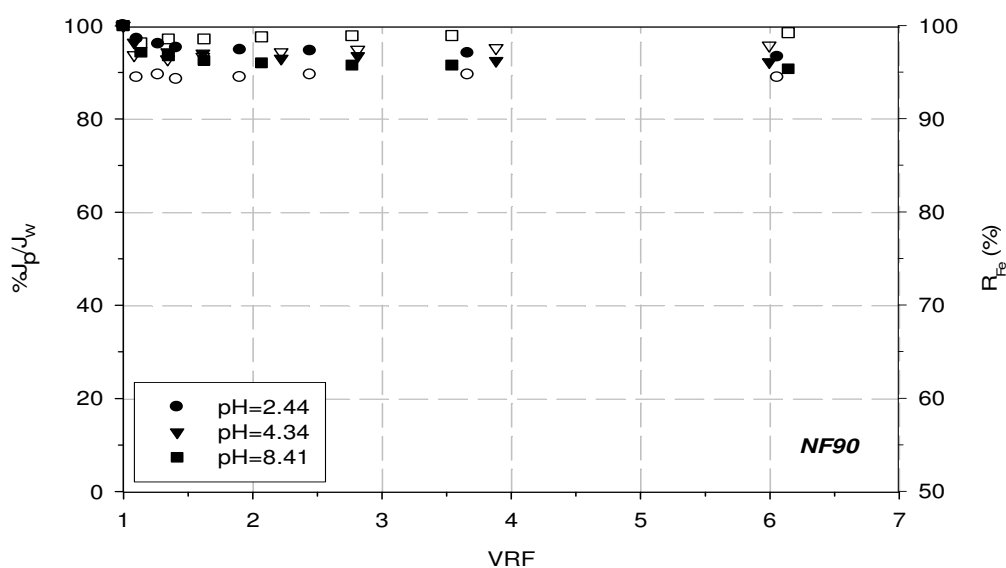


Figure 5.9. Filtration of 0.90 mM Fe(III)+0.90 mM EDTA solution at 6 bar and 300 rpm by NF90. Effect of the pH on the $\%J_P/J_W$ and iron retention evolution. Filled symbols represent $\%J_P/J_W$ and open symbols $R_{Fe}(\%)$

Finally, NF270 was also tested to recover Fe-EDTA at several pH. The filtration results including both $\%J_P/J_W$ and iron retention are presented in Figure 5.10. The $\%J_P/J_W$ was not affected by VRF, which agrees with the NF-D and NF90 observed behaviour. In addition, a pH independency of the permeate flux decline was detected because, irrespective of the feed pH, a practically constant $\%J_P/J_W$ of 94% was measured. This value is equal to that obtained with NF90 membrane. However, as the initial PWP of NF270 is almost twofold higher than that of NF90, a higher permeate production would be obtained with NF270 than with NF90. As for NF-D and NF90, no permeate flux loss

remained after flushing the membranes with deionised water, which undoubtedly indicated the reversibility of fouling phenomena.

NF270 iron retention, shown in Figure 5.10, followed the same trends than NF-D and NF90. A pH increase, which causes a raise of the solute-membrane charge repulsions, enhances iron retention. The average iron retention was 91.8%, 94.8% and 95.4% when the feed pH was 2.81, 4.44 and 8.54, respectively. The average EDTA retentions were 90.3%, 93.7% and 94.3% for the same pH values. This indicates that iron and EDTA retentions were almost equal due to the fact that chelation degree remained unchanged in the concentrate at any VRF, at least at the tested conditions.

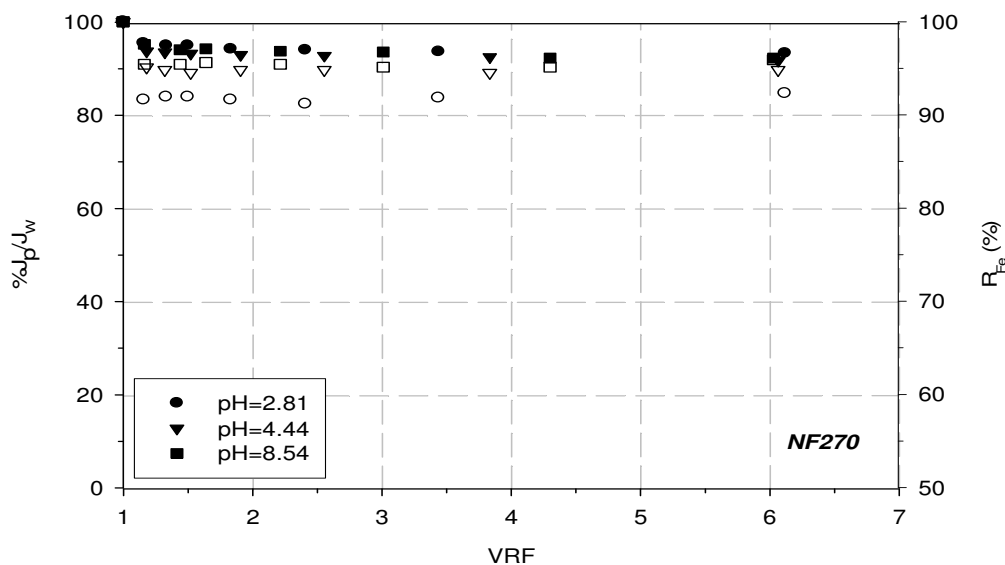


Figure 5.10. Filtration of 0.90 mM Fe(III)+0.90 mM EDTA solution at 6 bar and 300 rpm by NF270. Effect of the pH on the $\%J_p/J_w$ and iron retention evolution. Filled symbols represent $\%J_p/J_w$ and open symbols $R_{Fe}(\%)$

Table 5.3 summarises the $\%J_p/J_w$ and iron retentions obtained with NF-D, NF90 and NF270 when 0.90 mM Fe(III)+0.90 mM EDTA solutions were filtered at the three pH levels, 6 bar of TMP and 300 rpm of stirring rate. The $\%J_p/J_w$ values demonstrate that NF-D is the membrane with the lowest permeate flux decline and that NF90 and NF270 display approximately the same permeate flux reduction.

Table 5.3. $\%J_p/J_w$ and iron retention by NF-D, NF90 and NF270. Filtration of 0.90 mM Fe(III)+0.90 mM EDTA solution at 6 bar and 300 rpm

Membrane	Low pH (~2.5)		Intermediate pH (~4.3)		High pH (~8.4)	
	$\%J_p/J_w$ (average)	$R_{Fe}(\%)$	$\%J_p/J_w$ (average)	$R_{Fe}(\%)$	$\%J_p/J_w$ (average)	$R_{Fe}(\%)$
NF-D	98	92.5	98	95.0	98	96.5
NF90	95	94.5	94	97.1	93	98.7
NF270	94	91.8	93	94.8	94	95.4

As exposed in Chapter 3, the PWP of NF270 ($9.3 \text{ L/h}\cdot\text{m}^2\cdot\text{bar}$) is almost the double of that of NF-D ($5.9 \text{ L/h}\cdot\text{m}^2\cdot\text{bar}$) and NF90 ($5.6 \text{ L/h}\cdot\text{m}^2\cdot\text{bar}$). Thus, this indicates that, although NF-D shows the highest $\%J_P/J_W$, NF270 permeate flux is still higher than that of NF-D and NF90. NF90 shows the highest iron retention followed by NF-D and by NF270, as shown in Table 5.3. Thus, although NF90 exhibits a high permeate flux decline, it also possess the highest iron retention, regardless of the feed solution pH. In fact, NF90 also showed the highest iron retention when filtering single solutions of Fe(III) and Fe(II). Thus, NF90 membrane seems to be a promising membrane to obtain purified effluents from synthetic solutions containing iron species including iron chelates.

5.4. Conclusions

NF has demonstrated to be an effective membrane technology to purify iron-containing synthetic effluents either in its free (or hydrolysed) form or in its chelated one. Iron retention is slightly decreased when filtering Fe(II) solutions instead of Fe(III) ones at acid pH due to the decrease of the iron-membrane electrostatic repulsions, which have been identified as the main NF rejection mechanism. Iron retention is practically unaffected by TMP and stirring rate (if adequate hydrodynamic conditions are guaranteed). The presence and concentration of a background electrolyte, such as NaCl, strongly affects the normalised permeate flux, which decreases when the NaCl content in the feed solution increases. This behaviour can be explained by the reduction of the membrane charge at high ionic strength, increasing the proximity between the membrane polymers, causing an increase on the permeate flux decline. Besides this physical phenomenon, an increase on the salt content raises the osmotic pressure and thus the net TMP decreases, lessening the permeate flux. Concerning the Fe(III) retention, an increase on the salt content in the feed solution reduces the rejection owing to the lowered thickness of the diffuse double layer. Thus, the salinity is the only variable, among those tested, strongly affecting the permeate flux and the Fe(III) retention.

The three tested commercial membranes from DOW-Filmtec: NF-D, NF90 and NF270 are adequate candidates for retaining dissolved Fe(III) or Fe(II) from acidic synthetic solutions. Moreover, they successfully retain Fe(III)-EDTA chelates from synthetic aqueous solutions. In terms of iron retention, NF90 is the most-attractive membrane for the given application. In terms of permeate flux, NF270 could be chosen instead of NF90 because of its higher permeate flux.

NF seems to have potential to retain homogeneous catalysts commonly used in AOP's. However, in this chapter, the membrane efficiency has been evaluated using synthetic model solutions. The efficiency of NF as purification unit of Fenton pre-treated effluents is presented in Chapters 6 and 7.

UNIVERSITAT ROVIRA I VIRGILI

TREATMENT OF BIOREFRACTORY WASTEWATER THROUGH MEMBRANE-ASSISTED OXIDATION PROCESSES

Xavier Bernat Camí

ISBN:978-84-693-1529-3/DL:T-652-2010

CHAPTER 6

Treatment of phenol effluents coupling Fenton process and nanofiltration

6.1. Introduction

Phenols are non-biodegradable compounds (Dojilido and Best 1993) that cannot be directly driven to a biological treatment unit due to their inherent toxicity (González 1993) unless a pre-treatment is previously conducted. The Fenton process is one of the possible pre-treatments that could be used when dealing with phenol effluents, as exposed in Chapter 1. However, the Fenton process presents a limitation associated to the homogeneous nature of the Fe(II) salts used as catalyst: their continuous loss within the effluent. Thus, an environmental and economic constraint exists if combined Fenton oxidation and biological treatment is considered.

In this chapter, the feasibility of coupling an intermediate membrane separation unit between the Fenton oxidation and the subsequent biological treatment is presented using synthetic phenol solutions as model industrially-polluted effluents. Phenol has been chosen as model pollutant because it is often present in industrial effluents of the chemical industry and also because it is an oxidation intermediate of higher molecular weight aromatic compounds (Rivas et al. 2001). NF has been selected as the coupled membrane process because of its superior iron retention efficiency, described in Chapter 5, if compared to UF, presented in Chapter 4. The efficiency of the Fenton oxidation and of the NF of pre-oxidised effluents is presented. Concretely, the effect of the hydrogen peroxide and Fe(II) initial concentration on the phenol oxidation was considered. In addition, the effect of these variables on the filtration efficiency of three commercial NF membranes was also investigated. Several parameters describing the effluents' quality were determined in order to assess the efficiency of both processes.

These include the concentration of phenol and of its oxidation intermediates, the iron content, TOC and COD and the colour of the effluents. In order to study the membrane process efficiency, permeate flux parameters were also evaluated. In addition, the biodegradability of both Fenton and NF effluents was measured by respirometry.

A 2500 mg/L phenol solution was tested as model polluted effluent and its oxidation was studied batchwise at 30°C and 300 rpm of stirring rate for 90 min. The oxidised effluents were nanofiltered for 360 min at 6 bar of TMP and at a constant temperature of 30°C. In order to test the effect of the H₂O₂ and Fe(II) concentration, their doses used in the Fenton reaction were varied depending on the goal of each experiment. When testing the effect of the oxidant concentration, 7.0 mg/L Fe(II) were used as catalyst in all the experiments. When the effect of the Fe(II) concentration wanted to be investigated, 12500 mg/L H₂O₂ were employed. This concentration corresponds to the theoretical stoichiometric concentration of oxidant needed for completely mineralising, according to equation 6.1, initial phenol (2500 mg/L).



6.2. Phenol oxidation pathway by the Fenton process

Fenton and Fenton-like processes, among other AOP's, have been frequently chosen to partially oxidise effluents polluted with phenol compounds (Eisenhauer 1964; Kwon et al. 1999; Esplugas et al. 2002; Pera-Titus et al. 2004). Figure 6.1 exposes the Fenton oxidation route for phenol published by Zazo et al. (2005). This oxidation pathway has been employed in this thesis to understand and explain the results obtained in the Fenton oxidation experiments. In addition, the oxidation intermediates identified in this route were determined by HPLC, as explained in Chapter 3. However, o-benzoquinone appeared at the same retention time than p-benzoquinone. For this reason, o-benzoquinone was not calibrated and p-benzoquinone concentrations analysed could also include o-benzoquinone.

As Figure 6.1 shows, phenol is degraded to other ring compounds during the first stage of the oxidation process. Those organics, called quinone-like compounds are non-readily biodegradable and can be, depending on their concentration, even more toxic than phenol itself (Suárez-Ojeda et al. 2007a).

Condensation products, which also appear in the first stage of the oxidation process, consist of two (or more)-ring structures (Basu and Wei 2000) and iron-aromatic complexes (Eisenhauer 1964). Figure 6.2 shows some condensation products, identified by Mijangos et al. (2006), which can appear during the Fenton oxidation of phenol. In that work, a direct correlation between the oxidised solution colour and the aromatic intermediates present in solution was presented. The authors identified that phenol is firstly degraded forming colourless dihydroxilated ring compounds (catechol, resorcinol and hydroquinone) which are further degraded into o-benzoquinone (red) and p-benzoquinone (yellow). Their findings agreed with the phenol oxidation pathway presented by Zazo et al. (2005), above depicted in Figure 6.1. Mijangos et al. (2006) stated that, on the one hand, condensation products can be produced through the reaction of the dihydroxilated ring compounds with their own quinones, forming quinhydrone. This is the case of hydroquinone and p-benzoquinone, which react forming quinhydrone (brown, very coloured), as Figure 6.2 shows. On the other hand, the authors identified that ferric ion, generated during the Fenton process, could react with dihydroxilated ring compounds, forming green metal-aromatic complexes (Mijangos et al. 2006).

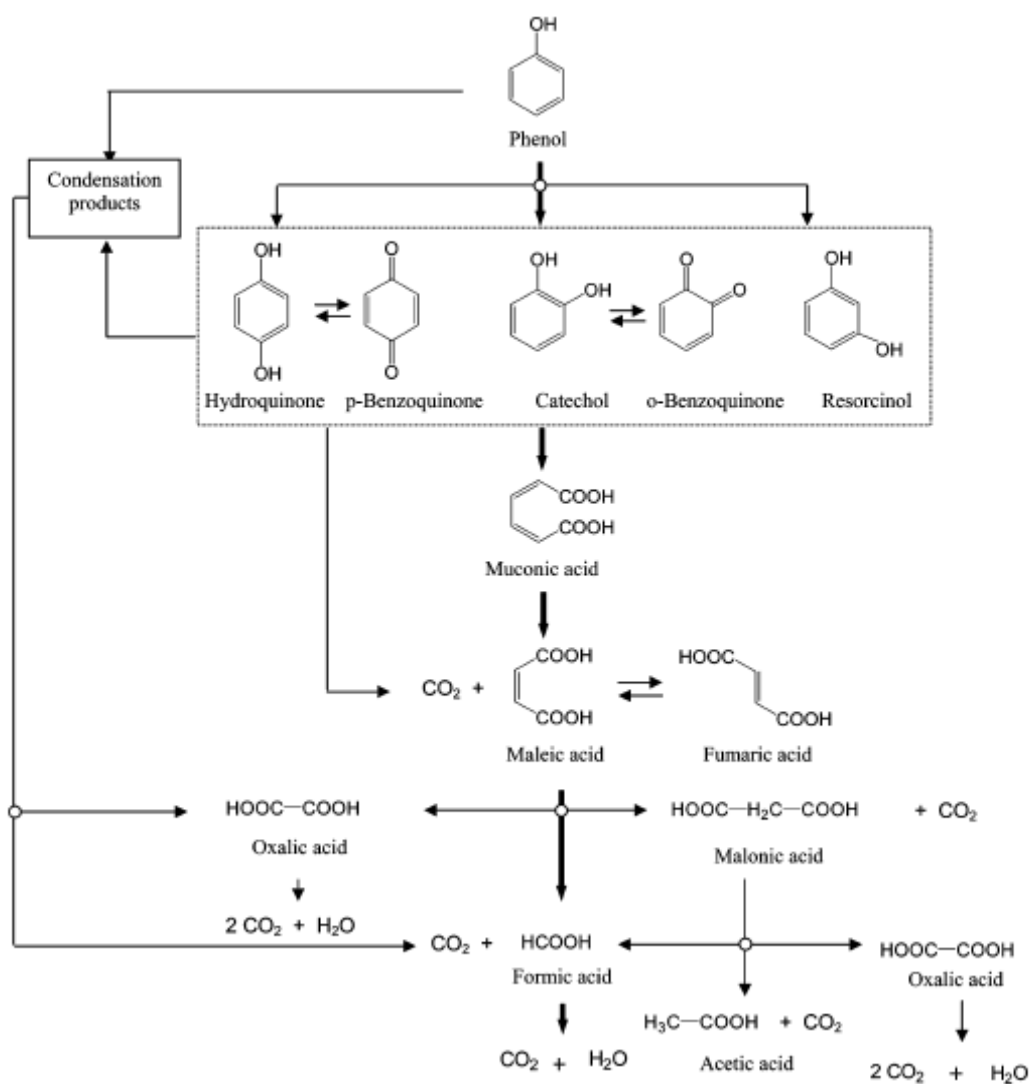


Figure 6.1. Fenton oxidation pathway of phenol (Zazo et al. 2005)

Carboxylic acids, which have been classified by respirometric techniques as non-toxic for microorganisms (Suárez-Ojeda et al. 2007a), are obtained as a result of the oxidation of quinone-like and condensation products. Acetic and oxalic acids have been identified as refractory compounds to the Fenton attack by several authors (Bigda 1995; Kwon et al. 1999; Kavitha and Palanivelu 2005a; Zazo et al. 2005; Martínez et al. 2007; Pignatello et al. 2006). Carbon dioxide and water production occurs from the oxidation of low-chain carboxylic acids. However, as explained in Chapter 1, total mineralisation is not the goal when coupling oxidation and biological processes because of the high associated treatment cost. In the proposed approach, polluted effluents want to be pre-treated only until its composition guarantees an adequate operation of the subsequent biological treatment.

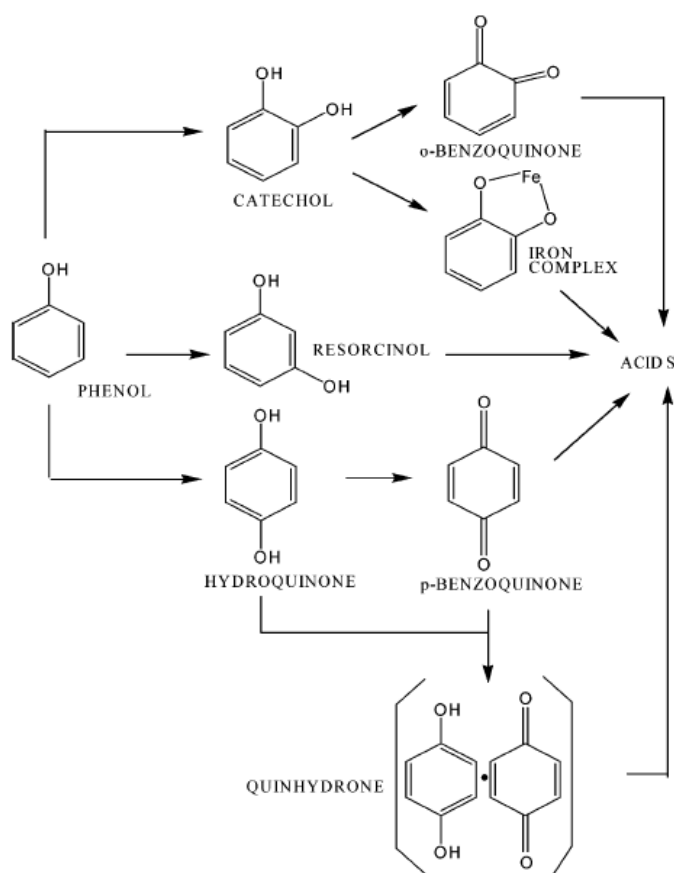


Figure 6.2. Possible condensation products formed in the Fenton oxidation of phenol (Mijangos et al. 2006)

Table 6.1 collects selected properties of phenol and its oxidation intermediates identified in this study. The properties of the compounds will be helpful to understand and investigate possible NF retention mechanisms from the obtained experimental data in filtration experiments.

Table 6.1. Properties of the organic compounds identified

Family	Compound	MW (g/mol)	pK _{a1} at 25°C ^(a)	pK _{a2} at 25°C ^(a)	logK _{ow} ^(b)	Colour
Carboxylic acids	Acetic	60.05	4.76	-	-0.17	colourless
	Formic	46.03	3.75	-	-0.54	colourless
	Oxalic	90.03	1.25	4.27	-2.22	colourless
	Malonic	104.06	2.85	5.70	-0.81	colourless
	Maleic	116.08	1.91	6.33	-0.48	colourless
	Fumaric	116.08	3.05	4.49	0.46	colourless
	t,t-muconic	142.11	3.10 ^(c)	4.70 ^(c)	-0.20	colourless
Quinone-like compounds	Resorcinol	110.11	9.30	11.06	0.80	colourless
	Catechol	110.11	9.40	12.80	0.88	colourless
	p-benzoquinone	108.10	10.16 ^(d)	-	0.20	yellow
	Hydroquinone	110.11	10.90 ^(b)	-	0.59	colourless
Phenol	Phenol	94.11	9.89	-	1.46	colourless

^(a) CurTiPot Database, unless otherwise noted

^(b) PhysProp Database Demo

^(c) Marrubini et al. 2001

^(d) Roberts and Caserio 1977

6.3. Influence of the hydrogen peroxide dose on the Fenton process and NF efficiency

The effect of the hydrogen peroxide dose on the efficiency of the Fenton reaction and of the subsequent NF is presented in this section. Its effect on the Fenton process performance is initially discussed. Then, the results of the screening of NF membranes at selected oxidation conditions are shown. Finally, the effect of the H₂O₂ dose on the NF efficiency is described.

6.3.1. Effect of the hydrogen peroxide dose on the Fenton process efficiency

The influence of the oxidant dose on the degradation of phenol was assessed through the evaluation of phenol, TOC and COD conversion. Table 6.2 summarises the conversion, X(%), of phenol, TOC and COD at several H₂O₂ concentrations. In addition, Table 6.2 collects the pre-oxidised effluents' absorbance (Abs), spectrophotometrically measured at 455 nm of wavelength (λ). This wavelength was selected because it was observed that oxidised effluents showed a maximum in the

absorbance spectrum at this value, as Figure 6.3 demonstrates. The spectrum shown in Figure 6.3 corresponds to a phenol effluent oxidised during 90 min with 12500 mg/L H_2O_2 and 7.0 mg/L Fe(II). The same maximum wavelength was found in a previous work dealing with phenol oxidation by the Fenton's reagent (Mijangos et al. 2006).

Table 6.2. Effect of the H_2O_2 dose on the conversion and colour formation after 90 min oxidation. 2500 mg/L phenol ; 7.0 mg/L Fe(II) ; 30°C ; 300 rpm

[H_2O_2] (mg/L)	X_{phenol} (%)	X_{TOC} (%)	X_{COD} (%)	Abs at 455 nm	%ID
2500	85.0±0.9	12.8±0.5	51.4±2.6	1.75±0.10	37.2±1.6
5000	86.5±1.5	13.8±0.7	57.4±3.2	1.65±0.06	37.9±2.1
7500	87.1±1.8	14.9±0.8	61.6±3.0	1.59±0.04	36.4±2.0
10000	88.2±1.6	15.7±0.8	60.6±3.5	1.56±0.07	36.4±2.0
12500	89.4±1.1	15.9±0.9	62.3±3.2	1.52±0.03	35.1±1.9
15000	88.7±2.0	15.4±0.8	61.8±3.1	1.48±0.13	35.8±2.0

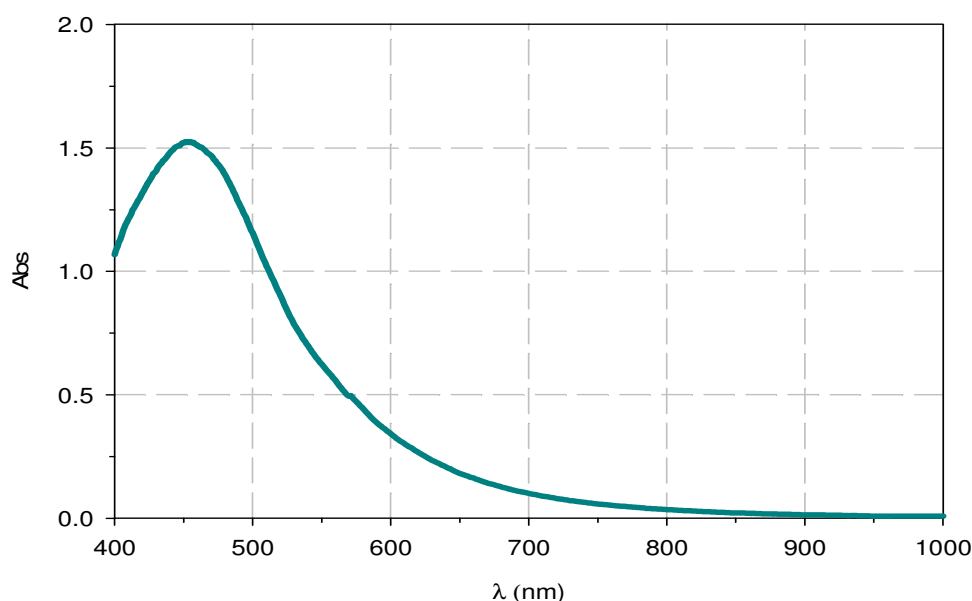


Figure 6.3. Absorbance spectrum of an oxidised phenol effluent after 90 min. 2500 mg/L phenol ; 12500 mg/L H_2O_2 ; 7.0 mg/L Fe(II) ; 30°C ; 300 rpm

As Table 6.2 shows, an increase on the H_2O_2 dose between 2500 and 12500 mg/L improved the Fenton process efficiency because phenol, TOC and COD conversions increased. Between 2500 and 12500 mg/L H_2O_2 , phenol conversion increased from 85.0% to 89.4%, TOC conversion from 12.8% to 15.9% and COD conversion from 51.4% to 62.3%, respectively. This response can be explained by a higher generation of oxidative radicals when hydrogen peroxide content increases (Ciotti et al. 2009). The higher amount of available radicals can attack more phenol molecules, increasing phenol conversion. X_{TOC} increase can be explained by the higher attack of formed

intermediates at high H_2O_2 concentrations, increasing mineralisation degree, as reported in previous works (Kwon et al. 1999; Arslan-Alaton et al. 2008). Likewise, the increase on the X_{COD} as long as H_2O_2 dose was raised can be explained by the production of intermediates with a lower number of carbon atoms in their molecule than those produced at low H_2O_2 concentration. This would decrease the number of oxygen moles required for chemically oxidising them and, accordingly, COD. As Table 6.2 shows, at 15000 mg/L H_2O_2 , a slight reduction on phenol, TOC and COD conversions is observed. This can indicate that, at very-high hydrogen peroxide dose, oxidative radicals are scavenged and/or hydrogen peroxide is autodecomposed, as explained in Chapter 1, decreasing the oxidation efficiency.

Table 6.2 shows the percentage of sample identification (%ID). As explained in Chapter 3, the % ID is defined as the ratio of theoretical TOC estimated from the concentration of organic compounds calculated from HPLC analyses to the measured TOC. Thus, the percentage gives an idea of the fraction of sample which has not been directly identified. In fact, this carbon balance can be used as an estimation of the non-identified products which include, at least, condensation products present in the analysed waters (Melero et al. 2007; Zazo et al. 2005). Since all phenol oxidation intermediates have been analysed by HPLC, the %ID will be considered in this study as an indirect indicator of the amount of condensation products. As Table 6.2 shows, the %ID remained almost constant at around 36%, regardless the H_2O_2 concentration. This indicates that around 64% of the carbon contained in the oxidised effluents can come from condensation products. This value is not distinct to those published in previous oxidation studies (Suárez-Ojeda et al. 2007b).

The effect of the H_2O_2 dose on the oxidation efficiency was also studied analysing the phenol oxidation intermediates after 90 min of oxidation. Figure 6.4 shows the distribution of intermediates obtained when oxidising the 2500 mg/L phenol solution with 7.0 mg/L Fe(II) at several H_2O_2 concentrations. Figure 6.4 demonstrates that the tendency of the intermediates' concentration when increasing the oxidant dose is broken between 12500 and 15000 mg/L H_2O_2 , regardless of the organic observed, as happened with phenol, TOC and COD conversion. This behaviour reinforces the fact that, at 15000 mg/L, there is a waste of oxidant. The trends observed between 2500 and 12500 mg/L H_2O_2 are explained below.

Acetic acid was not detected in the oxidised effluents at any hydrogen peroxide concentration. As abovementioned, acetic acid is considered to be refractory to the Fenton treatment. Thus, the absence of acetic acid in the oxidised effluents indicates that the acid was not generated during the experiments. Formic acid concentration decreased when the H_2O_2 dose was raised, which agrees with the increase on the X_{TOC} , indicating that formic acid oxidation results in mineralisation. As Figure 6.4 shows, an increase on the H_2O_2 caused a raise of the oxalic acid concentration. In fact, as this acid is refractory to the Fenton oxidation, an increase on the hydrogen peroxide dose increased its concentration because of the higher degradation of the intermediates appearing before it.

Malonic acid is, as shown in Figure 6.1, the precursor of acetic acid and is in turn generated from maleic and fumaric acid oxidation. Thus, the absence of both malonic and acetic acids probably indicates that maleic and fumaric acids, present in the oxidised effluents, were preferentially oxidised at the tested conditions forming oxalic and formic acid, both found in the oxidised effluents. In a previous work, malonic acid was only encountered in certain experimental conditions but not for every experimental run (Zazo et al. 2005), which agrees with the results presented.

Maleic and fumaric acids, which are isomers, had opposite responses when the H_2O_2 dose was varied. The former increased its concentration when the oxidant dose was raised whilst the latter decreased it. As those acids are located in the middle of the phenol oxidation pathway, it is difficult to predict their behaviour against a process variable modification. However, their concentrations were quite lower than those measured for formic and oxalic acid. Finally, t,t-muconic acid was present at a lower content than the other acids and its concentration decreased as long as the oxidant concentration was raised as result of a higher radical attack.

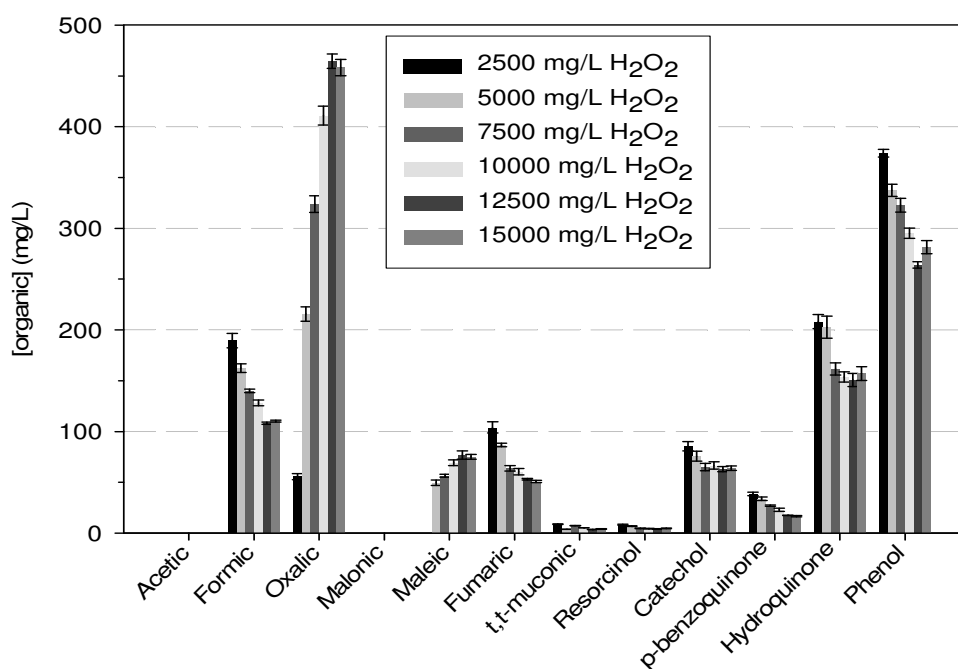


Figure 6.4. Effect of the H_2O_2 dose on the concentration of intermediates after 90 min oxidation. 2500 mg/L phenol ; 7.0 mg/L Fe(II) ; 30°C ; 300 rpm

As shown in Figure 6.4, quinone-like compounds and phenol decreased their concentration when the H_2O_2 dose was increased between 2500 and 12500 mg/L H_2O_2 . It is worth mentioning that hydroquinone concentration was higher than that analysed for the rest of quinone-like compounds. Hydroquinone and p-benzoquinone have been respirometrically classified as highly toxic (Suárez-Ojeda et al. 2007a). Thus, the need of installing an intermediate treatment between the Fenton oxidation and the aerobic biological treatment seems evident. The biodegradability characterisation of the oxidised effluents will be presented later in order to show it together with that measured in NF permeates.

The residual H_2O_2 dose after 90 min of oxidation was below 3 mg/L, regardless of the initial oxidant dose. This could indicate that a high fraction of the initial hydrogen peroxide was converted to hydroxyl radicals. However, it has to be taken into account that part of the converted H_2O_2 could have not been invested in producing radicals but wasted through its decomposition into molecular oxygen and water. In addition, part of the converted H_2O_2 could also have contributed to scavenge oxidative radicals. In this thesis, neither radical quantification nor balance was done. Thus, the only conclusion that can be drawn from H_2O_2 measurements is that initial oxidant reacted almost totally at the tested experimental conditions.

6.3.2. Effect of the membrane on the NF efficiency

Three NF membranes (NF-D, NF90 and NF270 from DOW-Filmtec) were selected to filter Fenton effluents. A 2500 mg/L phenol effluent was oxidised with 5000 mg/L H_2O_2 and 7.0 mg/L Fe(II) at 30°C and 300 rpm for 90 min. The oxidised effluent was filtered through the three NF membranes at 30°C and at TMP of 6 bar for 360 min. This study was designed to choose the most adequate membrane in terms of iron and organic compounds' retention. In order to test membranes' suitability, permeate flux decline and fouling were quantified besides retention. In addition, respirometry was used to assess the biodegradability, toxicity and inhibition of the permeates.

Figure 6.5 represents the $\%J_p/J_w$ evolution monitored with the three tested membranes. As it can be observed, all the membrane lost part of their initial permeate flux since the filtration started. Thus, both concentration polarisation and fouling phenomena probably occurred. As it can be seen in Figure 6.5, NF90 exhibited the highest permeate flux decline followed by NF270 and NF-D.

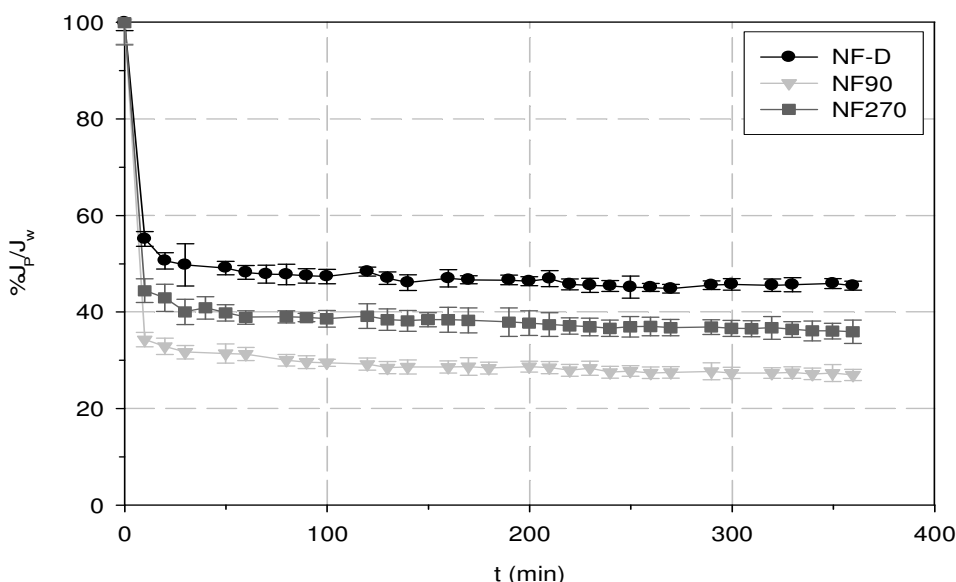


Figure 6.5. Effect of the membrane on the $\%J_p/J_w$ evolution when pre-oxidised effluents are filtered at 6 bar and 30°C. Fenton conditions: 2500 mg/L phenol ; 5000 mg/L H_2O_2 ; 7.0 mg/L Fe(II) ; 30°C ; 300 rpm ; 90 min

Figure 6.6, which shows the normalised permeate fluxes of the virgin membranes, after 360 min filtration and after rinsing the used membranes with deionised water, corroborates that fouling occurred. As it can be seen, NF90 showed the highest remaining fouling fraction (lowest normalised permeate flux after water rinsing) when compared to NF-D and NF270. Despite NF90 membrane showed the highest permeate flux loss, it also exhibited the highest retention of organic compounds, as shown in Figure 6.7. In fact, NF90 membrane is considered as a tight NF membrane (Nghiem et al. 2004) because its MWCO is below 200 g/mol (López-Muñoz et al. 2009). Thus, the membrane can in principle remove small organics at a higher extent than typical NF membranes would do. For this reason, a significant difference exists between the retentions obtained with NF90 and those with NF and NF270. From now on, the retentions obtained with NF90 are explained in detail. In order to consider charge interactions between the membrane and the organics, it is worth mentioning that the

Fenton effluents had a pH of around 2 and that NF90 membrane IEP was found to be at pH 4.0 (Nghiem et al. 2005), as exposed in Chapter 3.

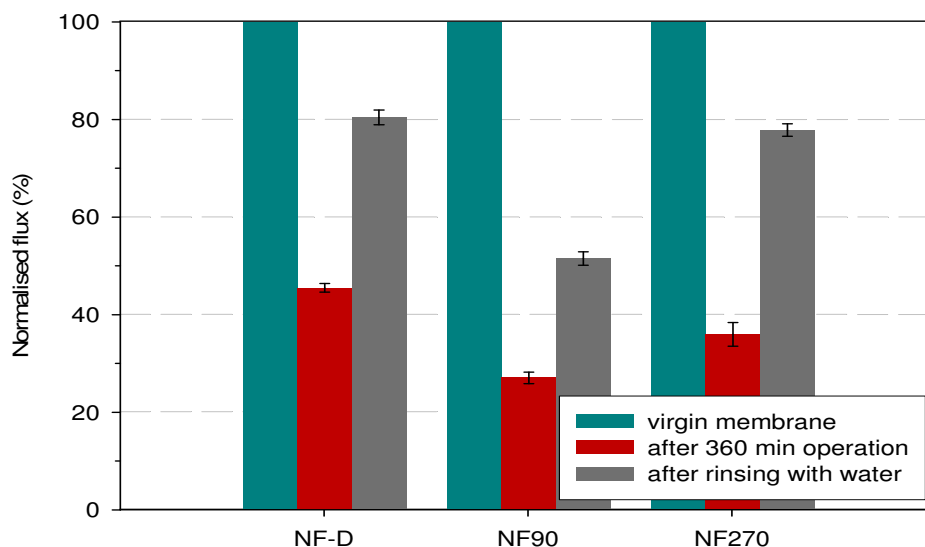


Figure 6.6. Effect of the membrane on the normalised fluxes when pre-oxidised effluents are filtered at 6 bar and 30°C. Fenton conditions: 2500 mg/L phenol ; 5000 mg/L H₂O₂ ; 7.0 mg/L Fe(II) ; 30°C ; 300 rpm ; 90 min

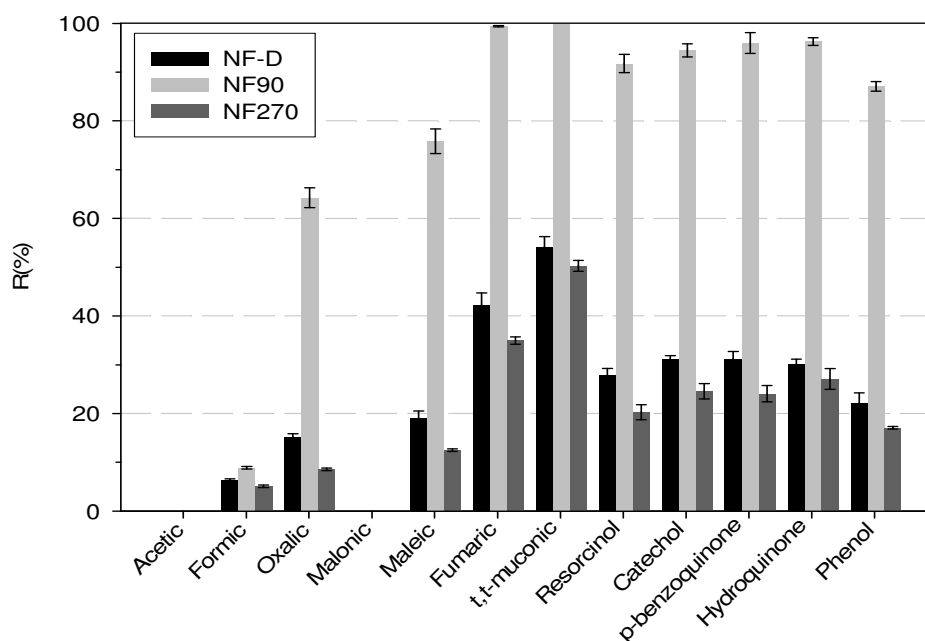


Figure 6.7. Effect of the membrane on the retention of organics when pre-oxidised effluents are filtered at 6 bar and 30°C. Fenton conditions: 2500 mg/L phenol ; 5000 mg/L H₂O₂ ; 7.0 mg/L Fe(II) ; 30°C ; 300 rpm ; 90 min

Formic acid, with a MW of 46 g/mol, was retained only 8.9±0.3% because of its very low MW. Instead, oxalic acid retention was 64.3±2.0%. This acid has a low MW (90 g/mol) and is dissociated at the effluent pH because of its also low pK_{a1} (1.25). Thus, if sieving effects and repulsions between the acid and the membrane were the

dominant retention factor, low oxalic acid retention would be expected. However, oxalic acid has demonstrated to form complexes with iron, having higher MW's, in Fenton conditions (Alegría et al. 2003). The high-MW complexes could be retained easily through sieving mechanisms. Thus, oxalic acid retention could be understood by iron complexation and sieving mechanisms.

Maleic and fumaric acids, which are isomers, were retained in a different extent. Maleic acid retention ($75.9 \pm 2.5\%$) was lower than that of fumaric acid ($99.5 \pm 0.1\%$). Sieving effects cannot explain the retention of these isomers because their MW's are obviously equal. However, membrane-solute charge interactions seem to be the most reasonable way for explaining maleic and fumaric acid retention differences. Maleic acid is negatively charged at the effluents' pH whilst fumaric acid molecules are neutral. As NF90 is positively charged at these conditions, maleic acid could be attracted towards its surface and easily transported through the membrane, decreasing its retention when compared to fumaric acid.

The only acid which was not detected in the NF90 permeate was t,t-muconic acid, which possess the highest MW (142 g/mol) when compared to the other organics chromatographically analysed. Due to its pK_{a1} (3.10), only around 5% of the acid is negatively charged and the rest is in its neutral form at the effluents' pH. Thus, sieving effects are expected to be responsible of its rejection.

The retention of quinone-like compounds was around 95%. As these compounds were not in their ionised form at pH around 2, they are expected to be retained by sieving effects. Phenol retention, which was $87.1 \pm 1.0\%$, could be explained by the same retention mechanism.

The previous retention mechanisms have not considered the adsorption of solutes onto the membranes. Molecules with $\log K_{OW}$ values beyond 2 are considered hydrophobic and are consequently more easily adsorbed onto membranes, decreasing their retention, than hydrophilic (or less-hydrophobic) ones (Kimura et al. 2003; Verliefde 2008). Hydrophobic-hydrophobic solute-membrane interactions, resulting in solute adsorption, are not expected to occur because $\log K_{OW}$ values of the analysed organics are all below 2, as shown in Table 6.1.

In addition to the previously explained likely retention mechanisms, condensation products, not directly characterised in this thesis, could contribute and even govern the retention phenomena. Condensation products have polymer-like structures (Zazo et al. 2007) that could accumulate and affect retention mechanisms. This could be achieved throughout the narrowing of the "hypothetic" pore size of the membranes or by modifying the electrostatic interactions and/or hydrophobic-hydrophobic ones between the solutes studied and the membranes. In fact, it has been previously published that the retention of phenol and resorcinol from aqueous synthetic solutions by using NF90 membrane at 5.5 bar of TMP and at pH of around 2 was negligible (López-Muñoz et al 2009). Therefore, it is evident that, when dealing with real pre-oxidised effluents, retentions are affected by the effluents' composition. Both the presence of other directly-identified organic compounds and condensation products could explain the differences on the retentions obtained in this work with those obtained when filtering synthetic single model solutions. This observation clearly indicates that it is highly valuable to test the efficiency of membrane processes with the real effluents to purify.

The retention of the organic compounds present in the pre-oxidised effluents can be grouped by families. Figure 6.8 brings together the retention of the organic compounds grouped by families (carboxylic acids, quinone-like compounds and phenol) with the iron, TOC, COD and colour retention. As it can be observed in Figure 6.8, when NF90

was used, higher retentions were achieved, regardless of the parameter examined. Iron retention was $94.2 \pm 1.5\%$ whilst TOC, COD and colour ones were $92.2 \pm 0.8\%$, $94.4 \pm 0.6\%$ and $99.1 \pm 0.1\%$, respectively. As the previous values indicate, very high rejections are achieved when using NF90.

Colour abatement can be explained by the fact that condensation products were partially retained by the membrane, as %ID values, shown in Table 6.3, demonstrate. The %ID after the Fenton oxidation was $37.9 \pm 2.1\%$ whilst it increased up to $82.2 \pm 2.2\%$ after filtering the oxidised effluent through NF90. As abovementioned, condensation products and p-benzoquinone are highly coloured and its partial removal would reduce the effluent colour. In addition, the high removal of total iron, which includes both Fe(III) and Fe(II), could also contribute to the decrease of the colour when the effluents are nanofiltered because Fe(III) ions give a dark orange colouration to the solutions where they are dissolved. For now on, the retention results will be presented grouped by families of organics and general parameters because the individual intermediates' and phenol retentions can be explained in all the experiments with the previously-proposed rejection mechanisms.

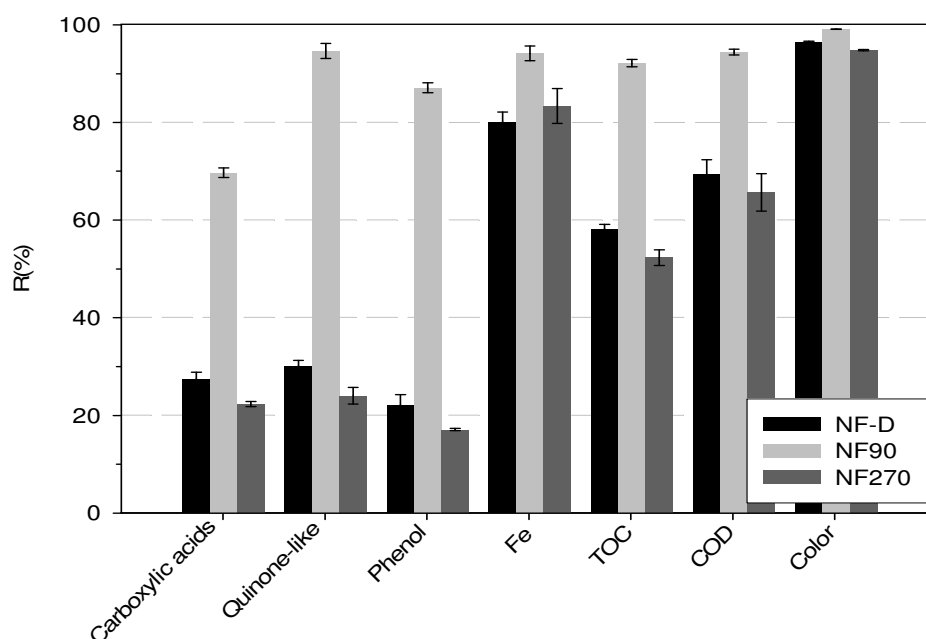


Figure 6.8. Effect of the membrane on the retention of general parameters when pre-oxidised effluents are filtered at 6 bar and 30°C. Fenton conditions: 2500 mg/L phenol ; 5000 mg/L H₂O₂ ; 7.0 mg/L Fe(II) ; 30°C ; 300 rpm ; 90 min

Table 6.3 summarises the biodegradability parameters obtained from respirometric measurements. As it can be deduced from the analysis of the data presented, regardless of the membrane, biodegradability was clearly enhanced when NF was coupled to Fenton process compared to the pre-oxidised effluent characteristics. In fact, the toxicity of the Fenton effluent was 42.2% whilst this value was reduced at least to one half when NF was carried out, regardless of the membrane. The same happened with the inhibition character of the oxidised effluents, which was reduced after filtering them through NF membranes. Even though the three membranes tested enhanced the effluent biodegradability, NF90 membrane was that showing the highest improvement. This can be assigned to the higher retention of organics, especially quinone-like and condensation intermediates, which were probably responsible of the

poor biodegradability of the Fenton effluent. A phenol respirometry showed that the %COD_{rb} was 0.0%, which is quite lower than the values obtained in the oxidised and nanofiltered effluents. Nevertheless, the %toxicity and %inhibition of the phenol respirometry were found to be 3.8% and 17.2%, respectively. Phenol behaviour fits with the results published by Suárez-Ojeda et al. (2007a), who found that 8 mg/L of COD coming from phenol was non-biodegradable, non-toxic and caused inhibition. Thus, it can be stated that non-filtered oxidised phenol effluents are even more biorefractory than phenol itself, which agrees with Zazo et al. (2007) who confirmed that some intermediates such as p-benzoquinone and hydroquinone showed higher toxicity levels than phenol. NF90 effluents showed higher %COD_{rb} and lower %toxicity and %inhibition than the others. Thus, oxidation and NF optimisation is needed in order to improve the biodegradability of the effluents. The study of the effect of the process variables on the final effluents' characteristics is presented in the following sections.

Table 6.3. %ID and biodegradability parameters of the effluents after Fenton and after NF. Pre-oxidised effluents filtered at 6 bar and 30°C. Fenton conditions: 2500 mg/L phenol ; 5000 mg/L H₂O₂ ; 7.0 mg/L Fe(II) ; 30°C ; 300 rpm ; 90 min

After Fenton				
Membrane	%ID	%COD _{rb}	%toxicity	%inhibition
NF-D				
NF90	37.9±2.1	12.6	42.2	47.2
NF270				
After NF				
Membrane	%ID	%COD _{rb}	%toxicity	%inhibition
NF-D	68.5±4.0	20.1	16.2	18.1
NF90	82.2±2.2	25.7	15.3	10.1
NF270	64.0±4.1	18.2	20.4	20.1

6.3.3. Effect of the hydrogen peroxide dose on the NF efficiency

The concentration of H₂O₂ strongly affects the composition of the oxidised effluents, as explained in Section 6.3.1. In order to study its influence on the NF efficiency, Fenton effluents treated with H₂O₂ concentrations ranging between 2500 and 15000 mg/L were filtered with NF90 at a TMP of 6 bar and 30°C for 360 min.

The effect of the H₂O₂ dose used for performing the phenol oxidation on the NF90 permeate flux decline is presented in Figure 6.9. As it can be seen, the H₂O₂ dose did not affect the permeate flux evolution although the effluent composition varied with it (as Figure 6.4 showed). In addition, the oxidant dose did not cause a significant modification on the permeate flux loss remaining after rinsing the used membranes with deionised water, which was around 52% irrespective of the H₂O₂ dose. These results can be seen in Figure 6.10, where the normalised fluxes measured with the virgin membranes, the %J_p/J_w after 360 min of filtration and those measured after softly rinsing the membranes (indicators of the severe fouling) are represented. Remaining

permeate flux loss after membrane rinsing would thus need to be chemically recovered in order to use the membranes more than once. Membrane cleaning and reusability experiments are presented later.

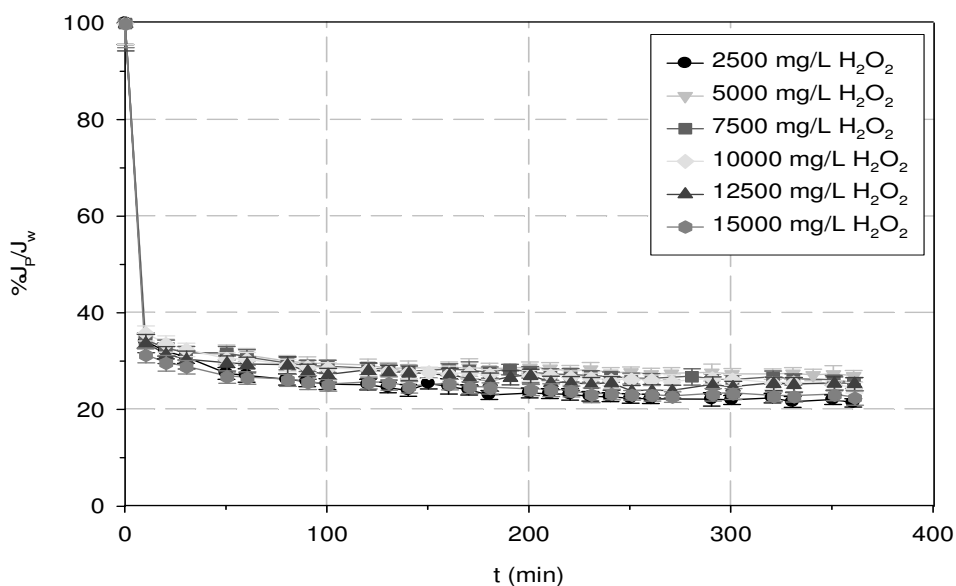


Figure 6.9. Effect of the H₂O₂ dose on the %J_p/J_w evolution when pre-oxidised effluents are filtered with NF90 at 6 bar and 30°C. Fenton conditions: 2500 mg/L phenol ; 7.0 mg/L Fe(II) ; 30°C ; 300 rpm ; 90 min

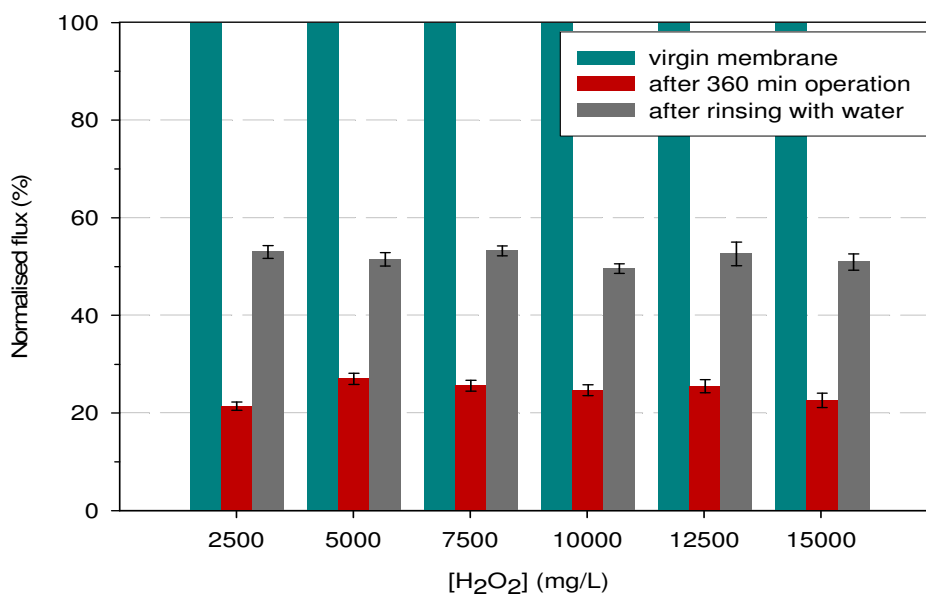


Figure 6.10. Effect of the H₂O₂ dose on the normalised fluxes when pre-oxidised effluents are filtered with NF90 at 6 bar and 30°C. Fenton conditions: 2500 mg/L phenol ; 7.0 mg/L Fe(II) ; 30°C ; 300 rpm ; 90 min

The retentions achieved with NF90 when filtering effluents pre-oxidised with several H₂O₂ concentrations, shown in Figure 6.11, did not vary with the oxidant dose as happened with the permeate flux evolution and the permeate flux loss. Thus, it can be

concluded that hydrogen peroxide dose strongly influences the composition of the pre-oxidised effluents with the Fenton process but it does not modify NF90 membrane efficiency in terms of rejection, permeate flux and fouling.

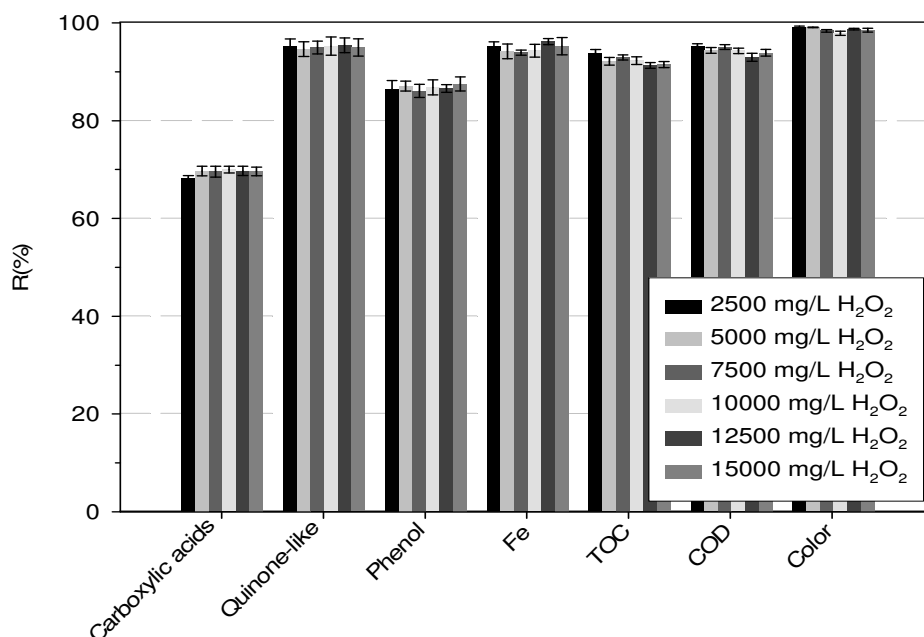


Figure 6.11. Effect of the H₂O₂ dose on the retention of general parameters when pre-oxidised effluents are filtered with NF90 at 6 bar and 30°C. Fenton conditions: 2500 mg/L phenol ; 7.0 mg/L Fe(II) ; 30°C ; 300 rpm ; 90 min

Table 6.4 summarises the effect of the H₂O₂ dose on the %ID and biodegradability parameters of the effluents after the Fenton oxidation and after being filtered with NF90. %ID values demonstrate that, in all the tested conditions, condensation products were highly retained by NF90 membrane. For instance, at 12500 mg/L H₂O₂, the %ID passed from 35.1±1.9% after oxidation to 78.0±7.1% after nanofiltration. This indicates that around 22% of the permeate stream was formed by condensation products whilst, in the effluent fed to the membrane, this percentage was around 65%. Despite the clear benefit (in terms of %ID increase) of using an intermediate NF step in all the tested conditions, the %ID after NF90 varied significantly depending on the H₂O₂ dose and did not follow a clear trend. This could be attributed to the possible changes on the nature of the unidentified compounds occurring when the H₂O₂ dose is varied, which would affect the %ID values.

Biodegradability parameters are also summarised in Table 6.4. As it can be observed, the %COD_{rb} increased and the %toxicity decreased both in Fenton effluents and in NF90 permeates as the dose of H₂O₂ was raised. These results indicate that a favourable effect on the biodegradability is achieved when the H₂O₂ dose is increased in the Fenton process. This may be linked to the fact that an increase on the H₂O₂ dose decreased the concentration of toxic compounds such as p-benzoquinone and hydroquinone. It is worth mentioning that beyond 12500 mg/L, as happened with the concentration of quinone-like compounds, the COD_{rb} was worsened and the %toxicity as well. This clearly shows that quinone-like compounds are probably responsible of the effluents' toxicity. The %inhibition varied when the H₂O₂ was modified. However, there is not a clear tendency on the %inhibition data, as happens with the %ID.

Concerning the biodegradability of the nanofiltered effluents, it is doubtless that there is always a biodegradability enhancement compared to the oxidised effluents. This is probably associated to the decrease of the toxic intermediates and to the increase on the biodegradable or inert compounds when the effluents are filtered with NF90. Thus, it seems logical to expect that the integration of the Fenton process with an aerobic biological reactor would be enhanced if an intermediate NF step was installed. Nevertheless, the integration of the three systems has not been studied in this thesis.

Table 6.4. Effect of the H₂O₂ dose on the %ID and biodegradability parameters of the effluents after Fenton and after NF. Pre-oxidised effluents filtered with NF90 at 6 bar and 30°C. Fenton conditions: 2500 mg/L phenol ; 7.0 mg/L Fe(II) ; 30°C ; 300 rpm ; 90 min

After Fenton				
[H ₂ O ₂] (mg/L)	%ID	%COD _{rb}	%toxicity	%inhibition
2500	37.2±1.6	8.1	46.3	48.1
5000	37.9±2.1	12.6	42.2	47.2
7500	36.4±2.0	16.3	41.6	46.2
10000	36.4±2.0	19.3	39.8	48.1
12500	35.1±1.9	20.2	37.1	46.1
15000	35.8±2.0	18.9	40.1	46.3
After NF				
[H ₂ O ₂] (mg/L)	%ID	%COD _{rb}	%toxicity	%inhibition
2500	95.9±1.3	22.1	21.2	22.1
5000	82.2±2.2	25.7	17.1	20.2
7500	97.3±1.4	27.2	13.0	21.7
10000	90.1±5.1	29.1	9.9	19.8
12500	78.0±7.1	30.8	9.3	20.1
15000	80.9±7.8	28.1	9.8	22.0

6.4. Influence of the iron(II) concentration on the Fenton process and NF efficiency

Iron(II) actively participates in the generation of oxidative radicals from hydrogen peroxide in the Fenton process, as explained in Chapter 1. For this reason, its effect on the Fenton and NF efficiency has been investigated. A 2500 mg/L phenol solution was oxidised with the theoretical stoichiometric dose of H₂O₂ needed for completely mineralising phenol. Thus, according to equation 6.1, 12500 mg/L H₂O₂ were used. Oxidation experiments were carried out for 90 min at 30°C and 300 rpm of stirring rate.

The Fe(II) concentration ranged between 7 and 56 mg/L. Nanofiltration experiments consisted in filtering the pre-oxidised effluents at 6 bar of TMP and 30°C for 360 min.

6.4.1. Effect of the iron(II) concentration on the Fenton process efficiency

The results of the oxidation at several Fe(II) concentrations are shown in Figure 6.12, which shows the analysed concentrations of organic compounds present in the oxidised effluents. As it can be observed, all the organic compounds follow the same trend when Fe(II) concentration is increased than when H₂O₂ dose is raised (results shown in Figure 6.4). However, the changes on the organic compounds' concentration are more marked than when H₂O₂ dose effect is studied. An increase on the Fe(II) concentration is invested in increasing the concentration of carboxylic acids, mainly composed by oxalic acid, and in decreasing the content of phenol and quinone-like compounds. Thus, an increase on the Fe(II) would enhance the expected biodegradability of the oxidised effluents. The biodegradability characterisation of the oxidised effluents is shown below together with that of the nanofiltered effluents.

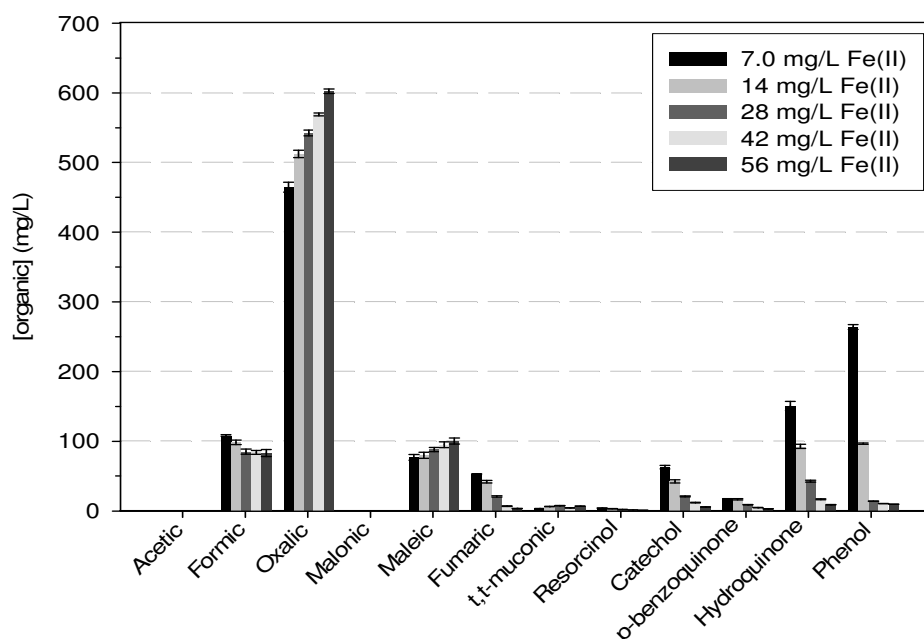


Figure 6.12. Effect of the Fe(II) concentration on the concentration of intermediates after 90 min oxidation. 2500 mg/L phenol ; 12500 mg/L H₂O₂ ; 30°C ; 300 rpm

When testing the effect of the H₂O₂ dose on the Fenton efficiency, an almost complete H₂O₂ decomposition was observed. Besides, when increasing the Fe(II) concentration at constant H₂O₂ dose, a deeper oxidation was achieved, as shown by the organic compounds' concentration. However, the residual H₂O₂ concentrations were in the same range (between 2.2 and 2.5 mg/L) than when testing the effect of the oxidant dose (between 2.2 and 2.7 mg/L). These observations indicate that a clear waste of oxidant occurs during the Fenton reaction. Otherwise, when increasing the Fe(II) concentration, no oxidation improvement would be observed as the residual oxidant concentration is practically the same, no matter the experimental conditions.

Phenol, TOC, and COD conversions achieved at several Fe(II) concentrations are summarised in Table 6.5 together with the colour of the oxidised effluents measured at 455 nm and the %ID. As Table 6.5 shows, an increase on the Fe(II) concentration enhanced phenol oxidation (i.e. increase on the X_{phenol}), mineralisation degree (i.e. increase on the X_{TOC}) and appearance of low-chain intermediates (i.e. increase on the X_{COD} and corroborated by the concentrations of organics represented in Figure 6.12). Furthermore, as Table 6.5 demonstrates, an increase of the Fe(II) concentration decreased the colour of the oxidised effluents. The %ID also decreased when the Fe(II) concentration was raised. It could be expected that a decrease on the %ID, caused by a raise on the Fe(II) concentration, would imply the formation of more-coloured effluents because of the higher iron association with quinone-like compounds. Nevertheless, the %ID decrease does not necessarily imply an increase on the colour formation because different condensation products (giving different colours) might be generated depending on the oxidation conditions.

Table 6.5. Effect of the Fe(II) concentration on the conversion and colour formation after 90 min oxidation. 2500 mg/L phenol ; 12500 mg/L H₂O₂ ; 30°C ; 300 rpm

[Fe(II)] (mg/L)	X_{phenol} (%)	X_{TOC} (%)	X_{COD} (%)	Abs at 455 nm	%ID
7.0	89.4±1.1	15.9±0.9	62.3±3.2	1.52±0.03	35.1±1.9
14	96.1±0.9	21.0±0.8	64.6±1.9	1.45±0.05	25.9±1.0
28	99.4±0.2	22.2±1.4	65.5±1.6	1.38±0.06	18.5±1.2
42	99.6±0.2	24.0±1.0	69.6±2.7	1.08±0.04	17.2±0.7
56	99.6±0.2	24.2±1.0	70.5±2.5	0.86±0.02	17.2±0.8

6.4.2. Effect of the iron(II) concentration on the NF efficiency

The influence of the Fe(II) concentration on the NF90 efficiency was tested like when the H₂O₂ dose effect was studied. Thus, the effect of the Fe(II) concentration used for oxidising effluents on the nanofiltration efficiency was investigated. For this, phenol synthetic effluents were oxidised with five different Fe(II) concentrations ranging from 7.0 to 56 mg/L. Those effluents were oxidised with 12500 mg/L H₂O₂ at 30°C and 300 rpm for 90 min. The subsequent filtration of the pre-oxidised effluents was carried out at 6 bar of TMP and 30°C for 360 min.

The Fe(II) concentration did not cause any detrimental effect on the permeate flux evolution as Figure 6.13 shows. This behaviour was already observed when the influence of the H₂O₂ dose on the NF efficiency was studied. An average % J_p/J_w of 28% was measured after 360 min filtration, regardless of the Fe(II) concentration used in the oxidation. Figure 6.14, which shows the effect of the Fe(II) concentration on the normalised permeate fluxes, demonstrates that an increase on the Fe(II) concentration resulted in a decrease on the % J_a/J_w although the catalyst concentration did not affect the % J_p/J_w evolution. This indicates that, when the concentration of iron increases, the remaining fouling after membrane rinsing also does. Stronger fouling could occur as result of the higher iron concentration in the membrane feed and/or the higher concentration of condensation products in it, demonstrated by the decrease on the %ID of the oxidised effluents as the Fe(II) concentration increased.

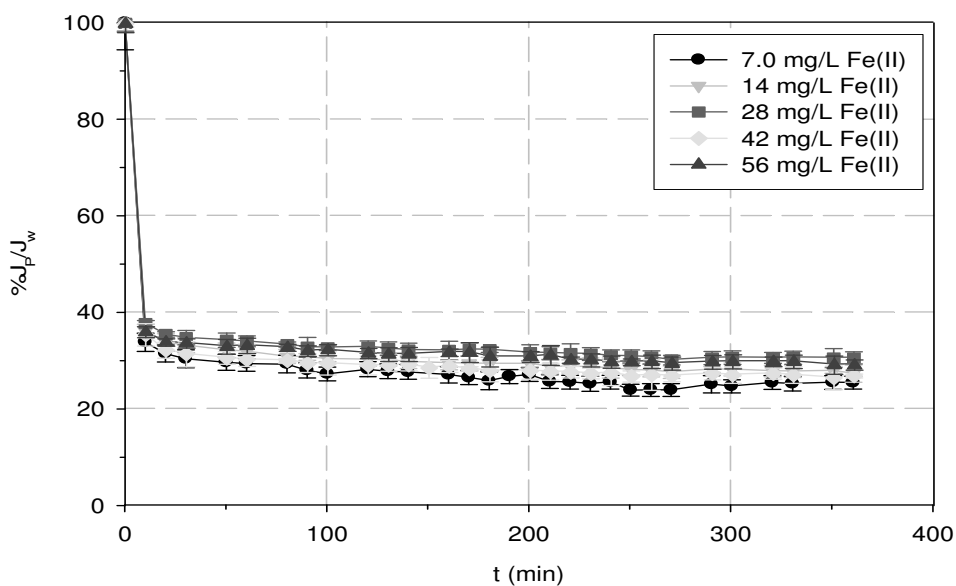


Figure 6.13. Effect of the Fe(II) concentration on the $\%J_p/J_w$ evolution when pre-oxidised effluents are filtered with NF90 at 6 bar and 30°C. Fenton conditions: 2500 mg/L phenol ; 12500 mg/L H_2O_2 ; 30°C ; 300 rpm ; 90 min

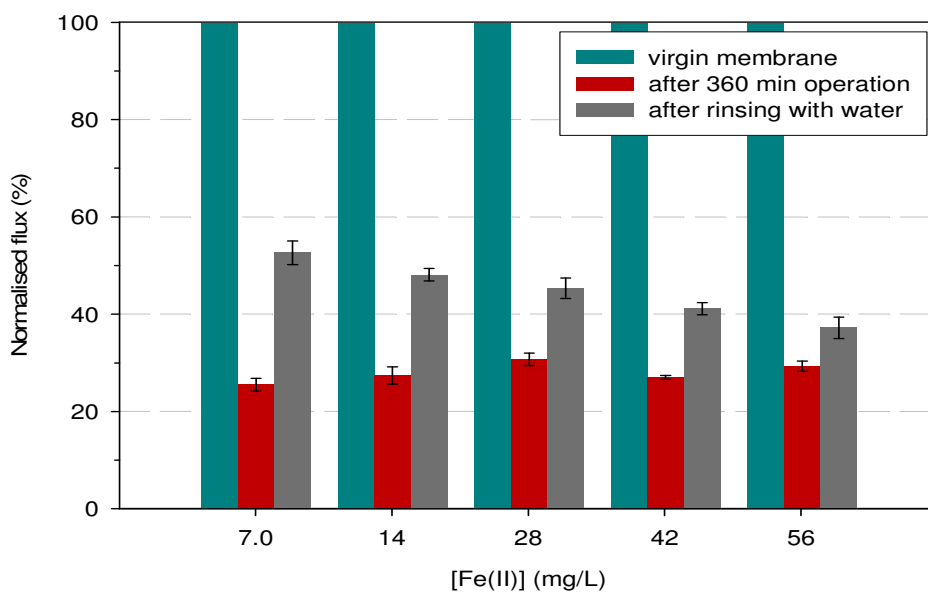


Figure 6.14. Effect of the Fe(II) concentration on the normalised fluxes when pre-oxidised effluents are filtered with NF90 at 6 bar and 30°C. Fenton conditions: 2500 mg/L phenol ; 12500 mg/L H_2O_2 ; 30°C ; 300 rpm ; 90 min

The Fe(II) concentration influenced the retention of some compounds achieved with NF90. This behaviour can be observed in Figure 6.15, where the retentions of the organics, grouped by families, and those of TOC, COD and colour are plotted in function of the Fe(II) concentration. As it can be observed, carboxylic acids', COD, TOC and colour retentions were not influenced by the Fe(II) concentration. However, quinone-like compounds' and phenol retentions increased when the iron concentration

was raised. Thus, iron concentration somehow favours the retention of ring compounds. This could be explained by the decrease on the intermediates' feed concentration when the iron concentration increases, which would reduce their diffusion through the membrane and thus increase their retention. The retention improvement at high Fe(II) concentrations could also be due to the higher content of condensation products, which would favour the retention of ring compounds by the formation of an additional polymeric layer over the membrane. Finally, iron itself could somehow improve the retention of quinone-like compounds and phenol. All three previous explanations could participate in increasing ring compounds' retention. However, the existence and contribution of each one has not been distinguished.

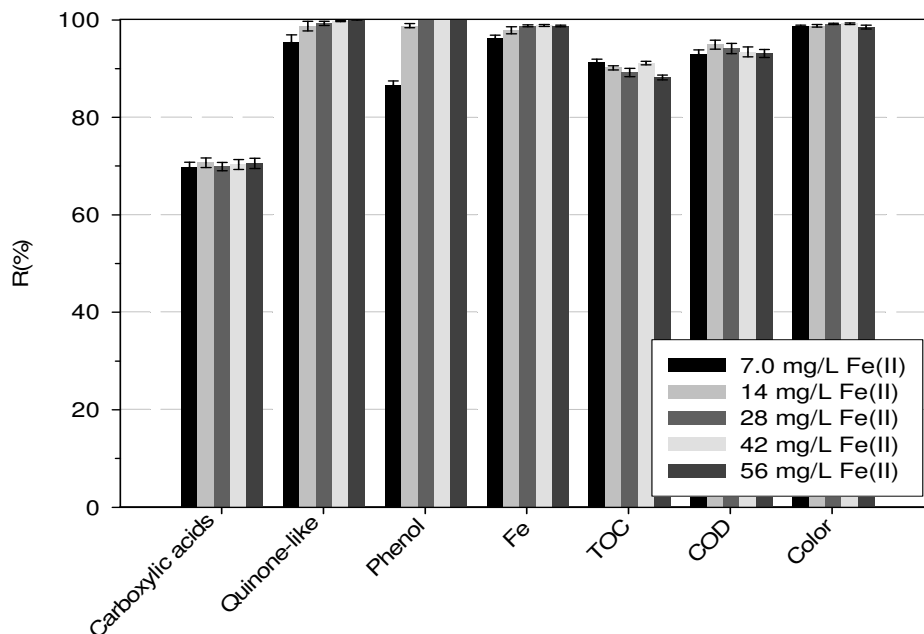


Figure 6.15. Effect of the Fe(II) concentration on the retention of general parameters when pre-oxidised effluents are filtered with NF90 at 6 bar and 30°C. Fenton conditions: 2500 mg/L phenol ; 12500 mg/L H₂O₂ ; 30°C ; 300 rpm ; 90 min

Table 6.6 collects the %ID and biodegradability characterisation of the effluents oxidised with the Fenton process and of the permeates of their subsequent filtration with NF90. As it could have been expected, regardless of the Fe(II) concentration, the intermediate NF step allowed partially-removing unidentified oxidation intermediates. Furthermore, NF increased the biodegradability of the effluents as most of the retained species were identified as toxic or inhibitory.

The %ID of the oxidised effluents decreased when the Fe(II) concentration increased. However, beyond 42 mg/L Fe(II), no further %ID gain was observed. It is worth mentioning that the variations on the %ID are not only due to the possible oxidation of condensation products but also to their changes in nature when the process variables are altered. The %ID increased when the oxidised effluents were nanofiltered as result of the retention of condensation products. However, %ID after NF90 did not follow a clear tendency. As condensation products' nature may vary depending on the oxidation conditions, their retention would be directly affected as it depends on the properties of the solutes studied. %COD_{rb} and %toxicity were enhanced when the Fe(II) concentration was increased. As Table 6.6 shows, pre-oxidised effluents' %COD_{rb} increased from 20.2% to 42.3% when the Fe(II) concentration was increased from 7.0

to 56 mg/L. At the same Fe(II) concentrations, the %toxicity decreased from 37.1% to 10.1%. The %inhibition did not show a clear tendency when the Fe(II) concentration was changed, as happened when the H₂O₂ dose influence was studied. Thus, inhibition seems to be more complex and probably partially linked to the unidentified compounds. When the characteristics of the oxidised effluents are compared to those measured after nanofiltration, all of them showed an enhancement in terms of biodegradation. Thus, integrated chemical and biological processes can be enhanced by an intermediate purification step such as nanofiltration.

Table 6.6. Effect of the Fe(II) concentration on the %ID and biodegradability parameters of the effluents after Fenton and after NF. Pre-oxidised effluents filtered with NF90 at 6 bar and 30°C. Fenton conditions: 2500 mg/L phenol ; 12500 mg/L H₂O₂ ; 30°C ; 300 rpm ; 90 min

After Fenton				
[Fe(II)] (mg/L)	%ID	%COD _{rb}	%toxicity	%inhibition
7.0	35.1±1.9	20.2	37.1	46.1
14	25.9±1.0	28.6	22.2	42.1
28	18.5±1.2	33.1	15.3	44.1
42	17.2±0.7	38.4	12.4	43.2
56	17.2±0.8	42.3	10.1	40.1
After NF				
[Fe(II)] (mg/L)	%ID	%COD _{rb}	%toxicity	%inhibition
7.0	78.0±7.1	30.8	9.3	20.1
14	53.4±3.6	38.6	5.1	17.3
28	49.7±5.1	46.2	0.0	16.8
42	63.2±4.1	52.6	0.0	17.1
56	49.5±3.7	57.2	0.0	15.4

6.5. Membrane cleaning and reusability assessment

The results presented in the previous sections demonstrate that there is always a fraction of permeate flux loss remaining after rinsing the used membranes with water, no matter the experimental conditions. Thus, a fraction of fouling remains on the membranes after their use and rinsing. In this case, it is doubtless that the NF process suffers from an inherent limitation. Consequently, it is necessary to assess the possibility of completely removing fouling and use the membranes for several times.

The membranes used in the filtration experiments were characterised with ESEM-EDS. In addition, virgin membranes were analysed in order to know the differences in the elemental composition due to the operation. Figure 6.16 shows the micrographies of a

virgin NF90 membrane and of a NF90 membrane used for filtering an effluent pre-oxidised with 12500 mg/L H_2O_2 and 56 mg/L Fe(II). As it can be seen, no apparent morphology differences are observed between the virgin and used membrane.

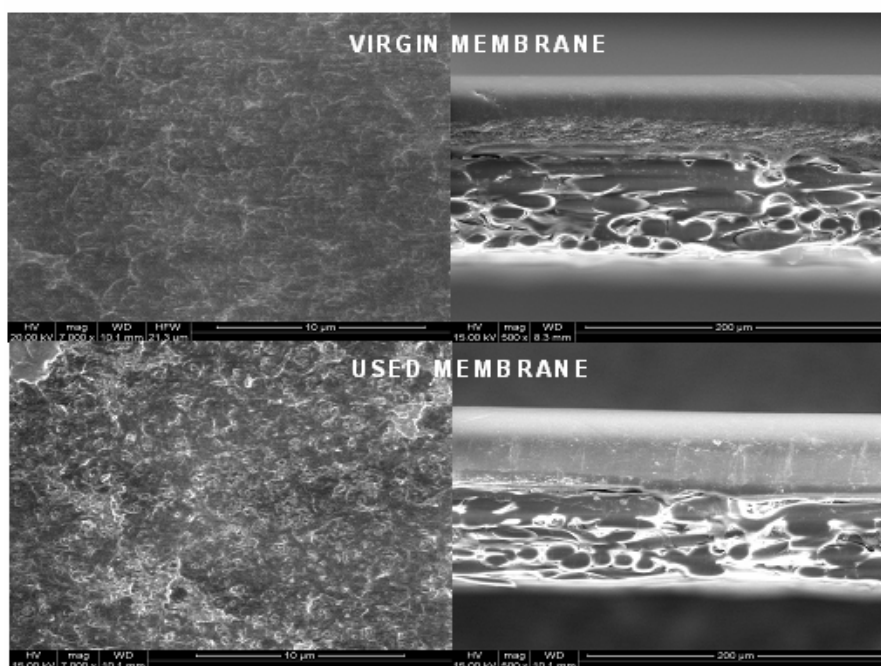


Figure 6.16. Micrographies of virgin and used NF90 membrane. Pre-oxidised effluents filtered at 6 bar and 30°C. Fenton conditions: 2500 mg/L phenol ; 12500 mg/L H_2O_2 ; 56 mg/L Fe(II) ; 30°C ; 300 rpm ; 90 min

As Table 6.7 shows, no iron was detected in the elemental analysis performed by EDS. This can be due to the fact that EDS analysis was carried out only in one point and not in the whole membrane or due to the small amount of iron present over the membrane (if any). The %weight C increased about 2% due to the membrane use. Thus, it could be expected that fouling was mainly organic. However, this percentage change can be considered to fall within the experimental error. Therefore, the selected technique is not the most appropriate for investigating fouling characteristics in the presented application. Thus, other analyses would be needed for this purpose. In this thesis, no other advanced characterisations were performed and thus no information on fouling nature and morphology has been acquired. However, from a process operation point of view, fouling percentages were obtained (as shown before) from permeate flux measurements. In addition, membrane cleaning and reusability studies were carried out to assess fouling removal and membrane response when used several times for the same application.

The membranes used for filtering the effluent giving the highest fouling extent were cleaned and reused in four subsequent filtration runs. The effluent filtered corresponded to that oxidised with the highest Fe(II) concentration tested: 56 mg/L and with 12500 mg/L H_2O_2 . The used NF90 membranes were cleaned with 1% wt. EDTA at pH 12 (adjusted with NaOH) for one hour, applied after membrane rinsing with deionised water. The cleaning solution was selected according to the membrane manufacturer recommendations (FILMTEC Reverse Osmosis Membranes Technical Manual). After cleaning, the membranes were rinsed again with deionised water in order to achieve a neutral pH both in the retentate and permeate. Membrane rinsing was carried out for 10 min at room temperature followed by a 5 min deionised water

filtration at 30°C and 6 bar of TMP. In all the cleaning tests, no more than one cleaning cycle was needed to completely restore the permeate flux of the membranes at its initial value, i.e. that of the virgin membranes.

Table 6.7. Elemental composition of virgin and used NF90 membrane. Pre-oxidised effluents filtered with NF90 at 6 bar and 30°C. Fenton conditions: 2500 mg/L phenol ; 12500 mg/L H₂O₂ ; 56 mg/L Fe(II) ; 30°C ; 300 rpm ; 90 min

Virgin membrane		
%weight C	%weight O	%weight S
55.35±1.59	29.93±1.50	14.72±0.60
Used membrane		
%weight C	%weight O	%weight S
57.46±1.55	27.76±1.47	14.78±0.70

The %J_P/J_w evolution for the four subsequent runs is plotted in Figure 6.17. As it can be seen, the four filtration runs showed identical %J_P/J_w trend. Thus, besides the permeate flux restoration with the aforementioned cleaning strategy, the membranes did not show any permeate flux modification due to its continuous use, at least for four runs.

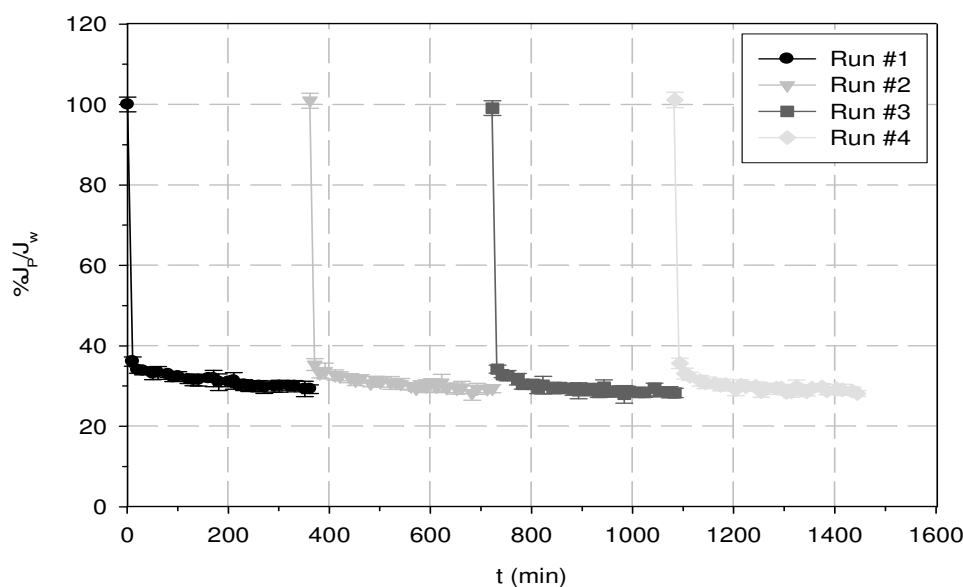


Figure 6.17. Effect of the membrane reusability on the %J_P/J_w evolution when pre-oxidised effluents are filtered with NF90 at 6 bar and 30°C. Fenton conditions: 2500 mg/L phenol ; 12500 mg/L H₂O₂ ; 56 mg/L Fe(II) ; 30°C ; 300 rpm ; 90 min

Figures 6.18 and 6.19 corroborate that the membrane process efficiency was not affected by the reusability of the membranes because the four runs showed practically the same normalised permeate fluxes and, what is even more important, the same retention. Thus, it can be claimed that both the cleaning strategy proposed was

effective and the NF90 membrane showed to be a suitable membrane for the studied application. The deviation on the %ID and on the biodegradability parameters was a meagre 1.2% in the worst case. Thus, from these data, it can be asserted that membrane reuse did not cause adverse effects on NF performance.

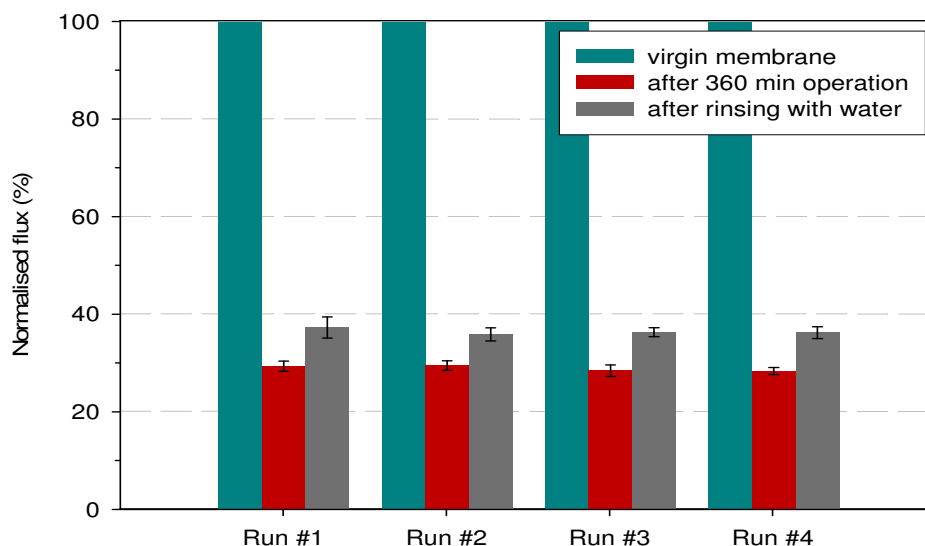


Figure 6.18. Effect of the membrane reusability on the normalised fluxes when pre-oxidised effluents are filtered with NF90 at 6 bar and 30°C. Fenton conditions: 2500 mg/L phenol ; 12500 mg/L H₂O₂ ; 56 mg/L Fe(II) ; 30°C ; 300 rpm ; 90 min

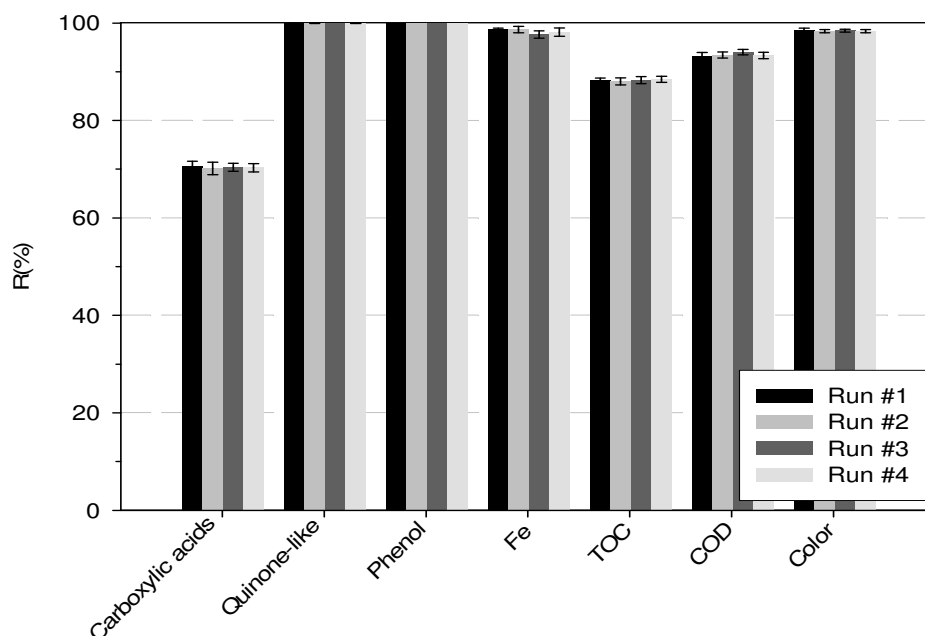


Figure 6.19. Effect of the membrane reusability on the retention of general parameters when pre-oxidised effluents are filtered with NF90 at 6 bar and 30°C. Fenton conditions: 2500 mg/L phenol ; 12500 mg/L H₂O₂ ; 56 mg/L Fe(II) ; 30°C ; 300 rpm ; 90 min

It is important to note that, although Fenton oxidation has been reported to attack membranes and negatively affect their properties (Causserand et al. 2008), the tested membranes did not show any symbol of damage. However, it has to be highlighted that the membranes were used with pre-oxidised effluents where H_2O_2 concentrations were always lower than 3 mg/L. When a tentative was made on coupling Fenton process and NF in one single unit, the membrane was damaged and the permeate flux increased along the time since the very beginning of the experiment. Thus, for this application, oxidant-resistant membranes would be needed. Kim et al. (2008) proposed an intensified Fenton-like oxidation and NF to treat bisphenol-A model effluents and no polyamide membrane damages were reported. However, the authors used a continuous H_2O_2 addition strategy that prevented the membrane from being oxidised because the oxidant concentration was thus kept at low concentration. Therefore, this process design could also be an attractive configuration when the intensified scheme wants to be selected.

6.6. Conclusions

Coupling Fenton process and NF to deal with phenol effluents allows total phenol abatement and obtaining effluents free of quinone-like compounds. For this, operation conditions need to be optimised, especially hydrogen peroxide and iron concentrations used in the Fenton oxidation. In general, an increase on hydrogen peroxide and iron concentration enhances the quality of the oxidised effluents. This means that phenol, TOC and COD conversions are higher and that effluent biodegradability is improved. However, when the oxidant dose is increased beyond the stoichiometric concentration needed for achieving complete phenol mineralisation, a slight worsening on the oxidation performance is observed. This behaviour can be ascribed to the possible autodecomposition of hydrogen peroxide at high concentrations or even to its radical scavenging character.

NF90 membrane showed the best performance in terms of purification of the pre-oxidised effluents. The retention of the parameters describing the effluents' quality has been explained through electrostatic solute-membrane interactions and sieving effects. The membrane has shown to be able not only to purify the pre-oxidised wastewater in terms of chemical parameters but also in biodegradability terms. By adequately tuning the oxidation variables, NF90 permeates can show nil toxicity despite high toxicity did exist before the filtration.

Overall, coupling Fenton and biological treatment can be clearly enhanced through the installation of a NF step as intermediate unit between the two treatments. NF can warrant an adequate operation of the subsequent biological treatment because it is able to completely eliminate toxicity of the pre-oxidised effluents. In addition to the biodegradation parameters, iron is completely removed from the oxidation effluent, which ensures its recycling back to the reaction unit. For achieving high retentions, not only the membrane properties need to be optimised but also the oxidation variables. Thus, the coupled process is a complex three-step configuration in series where every process unit affects the efficiency of the subsequent one.

UNIVERSITAT ROVIRA I VIRGILI

TREATMENT OF BIOREFRACTORY WASTEWATER THROUGH MEMBRANE-ASSISTED OXIDATION PROCESSES

Xavier Bernat Camí

ISBN:978-84-693-1529-3/DL:T-652-2010

CHAPTER 7

Treatment of phenol effluents by surfactant-assisted Fenton process and nanofiltration

7.1. Introduction

The remediation of effluents composed by phenol and a surfactant was studied and is presented in this chapter. Concretely, the Fenton oxidation of phenol with SDS or phenol with CPC solutions was investigated. This research was conducted for two main reasons. The first one is because of the interest on investigating the degradation of binary phenol effluents composed also by common pollutants such as surfactants. Surfactants have been found to affect the fate, transport and transformation of contaminants in the environment (Jia et al. 2005), which reinforces the importance of studying the degradation of phenol in presence of surfactant. The second reason is because confining iron ions in surfactant micelles, which would be subsequently used as Fenton-like catalyst, wanted to be studied.

SDS was selected as model anionic surfactant because it has been commonly used in micellar-enhanced ultrafiltration (MEUF) to host cations and organic compounds in its micelles, which are further retained by UF (Dunn et al. 1989; Reiller et al. 1996; Adamczak et al. 1999; Talens-Alession et al. 2001; Witek et al. 2006). This property wanted to be employed in this study to complex iron ions on surfactant micelles, which would represent an alternative to the support of the Fenton catalyst on solid matrixes. The confined iron species would be, in principle, easily retained by MF or UF (Lobo et al. 2006; Pan et al. 2007; Chakrabarty et al. 2008) and feasible to be reused in the oxidation step. CPC, a cationic surfactant, was selected to understand the influence of the surfactant charge on the Fenton degradation efficiency. This surfactant has also been typically employed to confine anions and organic compounds from aqueous

media (Jadhav et al. 2001; Sabaté et al. 2002; Beolchini et al. 2006; Zeng et al. 2008). For testing the feasibility of this application, the effect of the surfactant presence on phenol degradation, the possible surfactant degradation, the ability of the micelles to host homogeneous iron species among many other aspects need to be thoroughly studied. The first part of this chapter covers the effect of the presence of surfactants on the Fenton efficiency. For this, the effect of the oxidation operation variables (oxidant, catalyst and surfactant concentrations) on the Fenton efficiency was considered. The second part covers the assessment of nanofiltration as subsequent treatment unit after the Fenton oxidation. In this part, the influence of the oxidant, catalyst and surfactant concentration as well as of the membrane on the NF efficiency was studied. For the nanofiltration feasibility studies, phenol+SDS mixtures were chosen as initial polluted effluents.

7.2. Fenton oxidation of effluents polluted by phenol and SDS or phenol and CPC

Only few works have dealt with the degradation of surfactants by AOP's. Most of these studies have employed photolysis and photocatalysis as oxidation motor (Cuzzola et al. 2002; Arslan-Alaton and Erdinc 2006; Arslan-Alaton et al. 2007). Furthermore, due to the high diversity and nature of surfactants, oxidation processes and conditions, published results are strongly dependant on the particular conditions tested (Méndez-Díaz et al. 2009). Hence, it is difficult to correlate and extrapolate them for the application proposed in this thesis. The degradation of SDS by the dark Fenton oxidation was studied by Lin et al. (1999) and Bandala et al. (2008) and, as indicated by the latter, their results were quite diverse. It is worth mentioning that the studies dealt with different oxidation conditions, pH and initial SDS concentrations. Lin et al. (1999) obtained a 95% SDS conversion when 10 mg/L SDS solutions were oxidised at pH 3 at a mass ratio Fe(II):H₂O₂ and H₂O₂:SDS of around 0.193 and 5.984, respectively. 63% SDS conversion was measured by Bandala et al. (2008) when 1000 mg/L SDS were oxidised at free pH at a mass ratio Fe(II):H₂O₂ and H₂O₂:SDS of around 0.411 and 1.360, respectively. Bandala et al. (2008) stated that their observed conversion was lower due to the higher initial SDS content and unfixed pH conditions. However, it must be noted that they used Fe(II):H₂O₂ and H₂O₂:SDS ratios different than those selected by Lin et al (1999). Hence, it is unreliable to make comparisons between the two works. For these evidences, the feasibility of Fenton oxidation to degrade binary phenol and surfactant solutions was experimentally studied in this thesis.

Three main process variables were considered: the oxidant, catalyst and surfactant concentration. The first two variables are related to the Fenton chemistry. The last one was tested in order to investigate the effect of the surfactant morphology on the Fenton process efficiency. As surfactants form micelles, the effect of their state as monomers or micelles is thus considered when testing the effect of the surfactant concentration. This section presents the effect of the abovementioned variables on phenol, surfactant and TOC conversion as well as on the concentration of phenol oxidation intermediates and colour formation. In order to understand the effect of the surfactant presence on the Fenton efficiency, the results are compared to those obtained when oxidising single phenol solutions (without surfactant), discussed in Chapter 6. All the experiments presented were performed batchwise at 30°C and stirring the reaction mixture at 300 rpm. The initial phenol concentration was 2500 mg/L in all the experiments, whose total duration was 90 min.

7.2.1. Influence of the hydrogen peroxide dose on the Fenton process efficiency

The effect of the oxidant dose on the Fenton efficiency when dealing with binary effluents composed by phenol and SDS or phenol and CPC was studied. In order to test the effect of the presence of surfactant, initial phenol+SDS and phenol+CPC solutions contained 2500 mg/L phenol and a concentration of surfactant equal to its critical micellar concentration (cmc). The cmc of SDS and CPC were found to be 2307 mg/L (Fernández et al. 2005) and 299 mg/L (Mukerjee and Mysels 1999), respectively. Part of the surfactant molecules associates to form micelles, which coexist with surfactant molecules (monomers), at a concentration equal and higher than its cmc. Micelles are amphiphilic aggregates where the surfactant hydrophilic groups are oriented towards the bulk solution and the hydrophobic tails remain inside the micelle (Fernández et al. 2005). Depending on their properties, surfactants are able to attract metal ions towards their surface and dissolve organic compounds in their core (Tung et al. 2002). Obviously, apart from the surfactant characteristics, the properties of the metal ions and organics are crucial for their attraction or dissolution in surfactant micelles (Jadhav et al. 2001; Bielska and Szymanowski 2004).

The H_2O_2 doses tested ranged from 2500 to 15000 mg/L in intervals of 2500 mg/L. The Fe(II) concentration was kept constant in all the experiments at 7.0 mg/L. Temperature and stirring rate were fixed and controlled at 30°C and 300 rpm, respectively. The oxidation runs had a total duration of 90 min and regular sample withdrawal was carried out in order to analyse phenol concentrations. The rest of the parameters defining oxidised effluents' quality was analysed after 90 min oxidation.

Phenol conversions are plotted in Figure 7.1, which shows the effect of the presence and nature of surfactant on them at several oxidant concentrations. As the data show, the presence of surfactant strongly decreases phenol conversion. For instance, at 12500 mg/L H_2O_2 , X_{phenol} was 89.4% when phenol was alone in the solution to oxidise. This value decreased down to 66.4% and 48.5%, respectively, when SDS and CPC were present at its cmc. This results could be explained by the fact that SDS and CPC micelles have been found to host phenol molecules (Dunn et al. 1989; Syamal et al. 1997; Suratkar and Mahapatra 2000; Jadhav et al. 2001). Thus, it would be in principle less easy for hydroxyl radicals to attain phenol molecules and attack them when they are solubilised in the micelles' core. Moreover, oxidative radicals could also attack surfactant molecules that compete for the radicals. In fact, this agrees with previous works dealing with surfactants' oxidation by the Fenton process showing that surfactant molecules can be attacked by oxidative radicals (Lin et al. 1999; Bandala et al. 2008). Finally, iron ions, attracted by the micelles, could decrease their catalytic activity due to the interaction with the surfactant. This would cause a decrease on the generation of oxidative radicals and less phenol molecules would be accordingly degraded. As it can be observed in Figure 7.1, when dealing with phenol+CPC solutions, lower phenol conversions than when dealing with single phenol or phenol+SDS solutions were achieved. Therefore, if the last hypothesis would be dominant, higher phenol conversion would be observed when CPC is present than when SDS is because CPC is a cationic surfactant that should not attract iron ions towards the micellar interface. Hence, it seems that the first two possible mechanisms are the main responsible of the X_{phenol} decrease when surfactants are present. In fact, previous works have demonstrated that the degradation of organic contaminants by oxidative processes is inhibited by the presence of surfactants because of their degradation and due to micellar solubilisation of the target organics (Fabbri et al. 2006; Kong and Lemley 2007). Fabbri et al. (2006) showed that phenol degradation was decreased when hexadecyltrimethylammonium bromide, a cationic surfactant, was present in the

solutions to oxidise. This occurred when surfactant concentrations were both below and above the cmc (Fabbri et al. 2006). Kong and Lemley (2007) studied the degradation of carbaryl in presence of a non-ionic surfactant, Triton X-100. From this study, it can be only concluded that the presence of Triton X-100 reduced the carbaryl degradation rate because all the experiments presented achieved complete destruction of carbaryl and thus no comparison could be made. Nonetheless, the article valuably stated that carbaryl-Fe-surfactant complexes and surfactant molecules were attacked by oxidative radicals, which were found to be the cause of the decrease on the carbaryl degradation rate when surfactant was present (Kong and Lemley 2007).

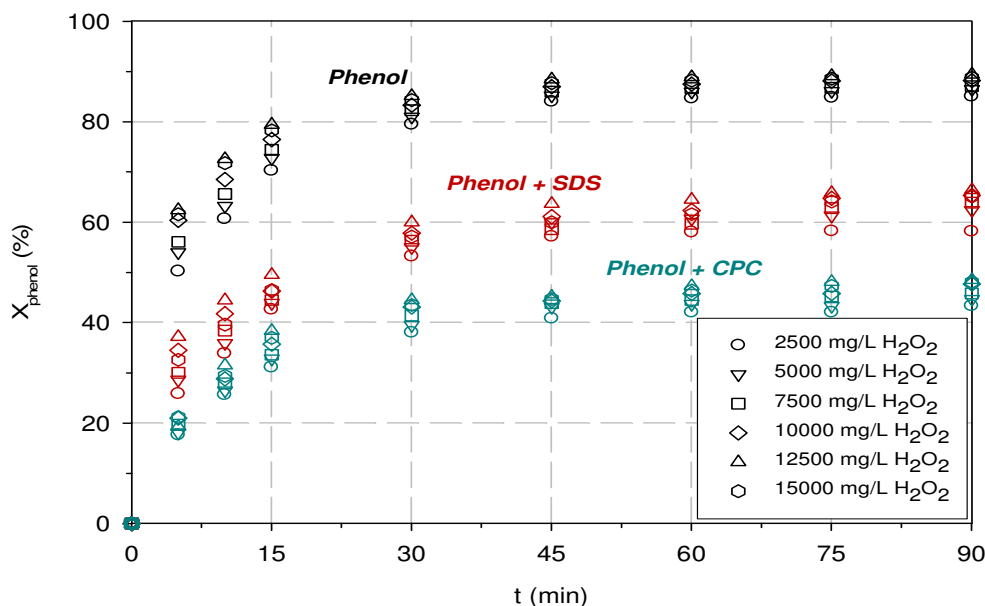


Figure 7.1. Effect of the H_2O_2 dose and surfactant presence on phenol conversion. 2500 mg/L phenol ; 2307 mg/L SDS (when present) ; 299 mg/L CPC (when present); 7.0 mg/L Fe(II) ; 30°C ; 300 rpm

In order to discriminate between the possible mechanisms responsible of the reduction of phenol conversion when surfactants were present in the solutions to oxidise, surfactants' concentration was analysed and their conversions subsequently calculated. Phenol oxidation intermediates, TOC conversion and colour (absorbance at 455 nm) were also determined. %ID was estimated from TOC values and the carbon balance from the analysed oxidation intermediates. When surfactants were present, as their oxidation intermediates were neither identified nor quantified, %ID accounted not only the phenol condensation products formed but also the surfactants' intermediates. Table 7.1 reviews the abovementioned data at the tested oxidant concentrations both in absence and presence of surfactant. Table 7.1 demonstrates that, as happened with phenol conversion, X_{TOC} strongly decreased down to almost nil conversion when surfactant was present regardless of the oxidant dose. This indicates that mineralisation does not occur when surfactants are present in the phenol solution. As concluded before, degradation could be limited by the phenol molecules hosted in micelles and/or surfactant codegradation. The latter is corroborated by the $X_{surfactant}$ values, which are between 54 and 74% for SDS and between 71 and 86% for CPC, as Table 7.1 shows. CPC conversion could be higher than the SDS one because CPC absolute concentration (299 mg/L) was around ten times lower than that of SDS (2307 mg/L). Thus, assuming that oxidative radicals were produced in the same degree than when SDS was present, more CPC molecules and/or micelles could be attacked than when SDS was considered. In addition, it is important to note that surfactant

conversion increased with H_2O_2 dose only until a certain oxidant level was reached, as observed with phenol single solutions. Again, this could be attributed to the autodecomposition of hydrogen peroxide and its radical scavenging effect occurring at high oxidant doses. By inspecting X_{phenol} data, when no surfactant was present, this effect was observed between 12500 and 15000 mg/L as it happened when SDS or CPC were present in the initial phenol solution.

Table 7.1. Effect of the H_2O_2 dose and surfactant presence on phenol, surfactants' and TOC conversion after 90 min oxidation. 2500 mg/L phenol ; 2307 mg/L SDS (when present) ; 299 mg/L CPC (when present) ; 7.0 mg/L Fe(II) ; 30°C ; 300 rpm

	$[H_2O_2]$ (mg/L)	X_{phenol} (%)	X_{TOC} (%)	$X_{surfactant}$ (%)	Abs at 455 nm	%ID
Phenol	2500	85.0±0.9	12.8±0.5	-	1.75±0.10	37.2±1.6
	5000	86.5±1.5	13.8±0.7	-	1.65±0.06	37.9±2.1
	7500	87.1±1.8	14.9±0.8	-	1.59±0.04	36.4±2.0
	10000	88.2±1.6	15.7±0.8	-	1.56±0.07	36.4±2.0
	12500	89.4±1.1	15.9±0.9	-	1.52±0.03	35.1±1.9
	15000	88.7±2.0	15.4±0.8	-	1.48±0.13	35.8±2.0
Phenol + SDS	$[H_2O_2]$ (mg/L)	X_{phenol} (%)	X_{TOC} (%)	$X_{surfactant}$ (%)	Abs at 455 nm	%ID
	2500	58.1±2.1	1.1±0.0	54.4±0.4	1.61±0.00	44.9±1.0
	5000	62.4±2.5	1.6±0.0	71.6±1.7	1.59±0.00	36.1±1.0
	7500	63.9±2.1	1.3±0.0	70.6±0.5	1.55±0.00	36.8±0.8
	10000	65.3±2.8	1.3±0.0	74.2±1.1	1.53±0.00	35.0±1.0
	12500	66.4±2.1	1.6±0.0	73.1±1.3	1.50±0.00	35.3±0.7
15000	65.1±2.2	1.7±0.0	72.7±1.0	1.48±0.00	36.4±0.8	
Phenol + CPC	$[H_2O_2]$ (mg/L)	X_{phenol} (%)	X_{TOC} (%)	$X_{surfactant}$ (%)	Abs at 455 nm	%ID
	2500	43.3±1.2	2.1±0.0	70.5±1.1	n.m.	57.7±1.5
	5000	44.7±1.2	2.4±0.0	82.8±2.4	n.m.	56.1±1.4
	7500	45.8±2.2	2.4±0.0	83.5±1.6	n.m.	55.8±2.4
	10000	47.7±1.2	1.9±0.0	85.6±1.8	n.m.	54.5±1.3
	12500	48.5±1.1	2.1±0.0	86.1±2.2	n.m.	54.5±1.1
15000	48.1±0.9	2.2±0.0	85.1±2.1	n.m.	55.3±1.0	

n.m.: not measured

The colour of the oxidised effluents was slightly higher, although visually equal, when phenol solutions did not contain SDS. This was probably related to the lower

concentration of quinone-like compounds, as explained below. Condensation products influence cannot be discussed because, as abovementioned, when surfactants are present, %ID cannot be considered as their indirect indicator. As Table 7.1 shows, %ID of oxidised single phenol and binary phenol+SDS solutions were practically equal. However, %ID seemed to increase when CPC was present in the phenol effluents to oxidise. This was unexpected because, when CPC was present, the X_{TOC} values were approximately the same than when SDS was present and the $X_{\text{surfactant}}$ was higher. Hence, it could have been expected that a lower %ID would be found due to the formation of more CPC oxidation intermediates, unidentified in this thesis. Nevertheless, as CPC molecules have an aromatic ring in their structure, %ID can be increased because radicals can attack this ring and form some of the intermediates appearing in the phenol oxidation pathway, identified in this thesis. Anyway, as explained in the previous chapter, it is difficult to predict the behaviour of %ID because of its relation with unidentified compounds that can be formed and further oxidised by numerous and unpredictable ways.

Figure 7.2 shows the effect of the H_2O_2 dose and surfactant type on the organic compounds' concentration measured after 90 min oxidation. Carboxylic acids' concentration was quite lower when SDS and CPC were present than when dealing with phenol single effluents. The concentration of carboxylic acids was higher when CPC was present than for SDS. For instance, at 12500 mg/L H_2O_2 and 7.0 mg/L Fe(II), when no surfactant was present, carboxylic acids' concentration was 706 ± 8 mg/L whilst when SDS and CPC were present at their cmc, the concentration decreased down to 375 ± 11 mg/L and 431 ± 18 mg/L, respectively. The higher concentration of acids when CPC was tested can be due to its higher decomposition, which could lead to the formation of a higher amount of carboxylic acids. Quinone-like compounds' concentration was significantly lower when surfactants were present in the solutions to oxidise. Figure 7.2 scaling does not allow reading the exact concentration of quinone-like compounds when surfactant was present because it was lower than 1.5 mg/L and 0.5 mg/L when SDS and CPC were present, respectively. Their concentration when only phenol was present ranged between 341 ± 8 mg/L and 235 ± 7 mg/L depending on the H_2O_2 dose, as exposed in Chapter 6. It is worth mentioning that, when dealing with phenol+surfactant solutions, carboxylic acids were composed only by oxalic and maleic acids. Quinone-like compounds were formed by catechol and hydroquinone when phenol+SDS solutions were considered while only catechol was present when phenol+CPC solutions were oxidised.

Residual hydrogen peroxide concentration was below 3 mg/L when phenol was alone and below 2 mg/L when either SDS or CPC were present in the phenol effluents. Thus, it could be expected that oxidative radicals are more efficiently used for oxidation of the target contaminants when surfactants are present because their conversions are quite significant. However, this cannot be stated because oxidation intermediates' concentration as well as phenol and TOC conversion are diverse depending on the initial effluents' composition. On the contrary, it can be clearly stated that Fenton process, operated at the same conditions than when only phenol was present, is able to partially attack other organic contaminants such as SDS and CPC. Hence, the goal of using surfactants to confine iron species used as catalyst in the Fenton process is demonstrated to be inefficient because of their partial oxidation. If implemented, the process would imply a continuous injection of surfactants to the reaction system, increasing costs. Moreover, a phenol degradation reduction would occur. Despite the inherent inefficiency of the proposed process scheme, the study of coupling Fenton and membrane filtration was continued because the results could be helpful when polluted binary phenol+surfactant effluents need to be managed.

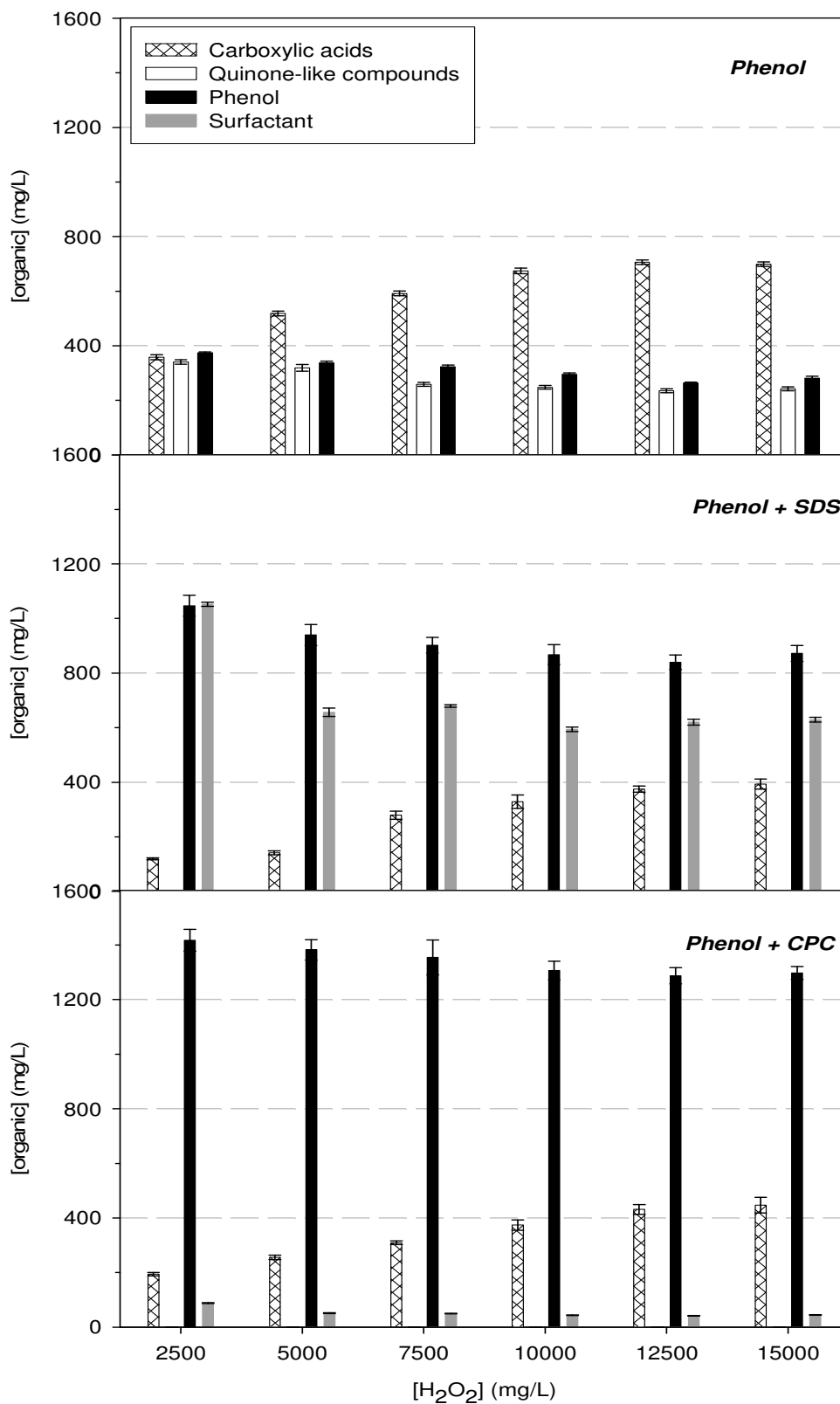


Figure 7.2. Effect of the H_2O_2 dose on the organic compounds' concentration after 90 min oxidation. 2500 mg/L phenol ; 2307 mg/L SDS (when present) ; 299 mg/L CPC (when present) ; 7.0 mg/L Fe(II) ; 30°C ; 300 rpm

7.2.2. Influence of the iron(II) concentration on the Fenton process efficiency

Iron(II) actively participates in the Fenton oxidation and, as found in Chapter 6, its concentration strongly affects the process efficiency. In this section, the effect of the Fe(II) concentration on the oxidation efficiency when dealing with phenol solutions containing either SDS or CPC at their cmc is presented. In all the experiments, the H_2O_2 dose was 12500 mg/L, which corresponds to the theoretical stoichiometric concentration needed for totally mineralising all phenol contained in the initial effluent (2500 mg/L). The oxidation results were obtained through batch experiments performed at 30°C and 300 rpm for 90 min.

As Figure 7.3 shows, the presence of surfactant reduces phenol conversion. However, an increase on the Fe(II) concentration can result in an almost complete removal of phenol. When dealing with single phenol solutions, at 12500 mg/L H_2O_2 and 56 mg/L Fe(II), X_{phenol} was $99.6 \pm 0.2\%$ whilst when SDS or CPC were present in the phenol solution at its cmc, X_{phenol} was $98.2 \pm 1.1\%$ and $99.7 \pm 0.2\%$, respectively, as Table 7.2 shows. Moreover, $X_{surfactant}$ was not negligible at all because, at the same oxidant conditions, it was $98.9 \pm 0.5\%$ and $99.5 \pm 0.3\%$ when SDS or CPC were present in the phenol solution, respectively. These results indicate that, by using the same oxidation conditions than when phenol alone was treated, SDS and CPC can be almost completely destructed. This could be partially due to the decrease on the mineralisation degree and to a lower degradation of the intermediates occurring when surfactants are present. As when discussing the effect of the H_2O_2 dose, the colour of the oxidised effluents was slightly higher when no surfactant was present. This could be related, as explained below, to the lower concentration of quinone-like compounds present in the oxidised effluents when surfactants were present.

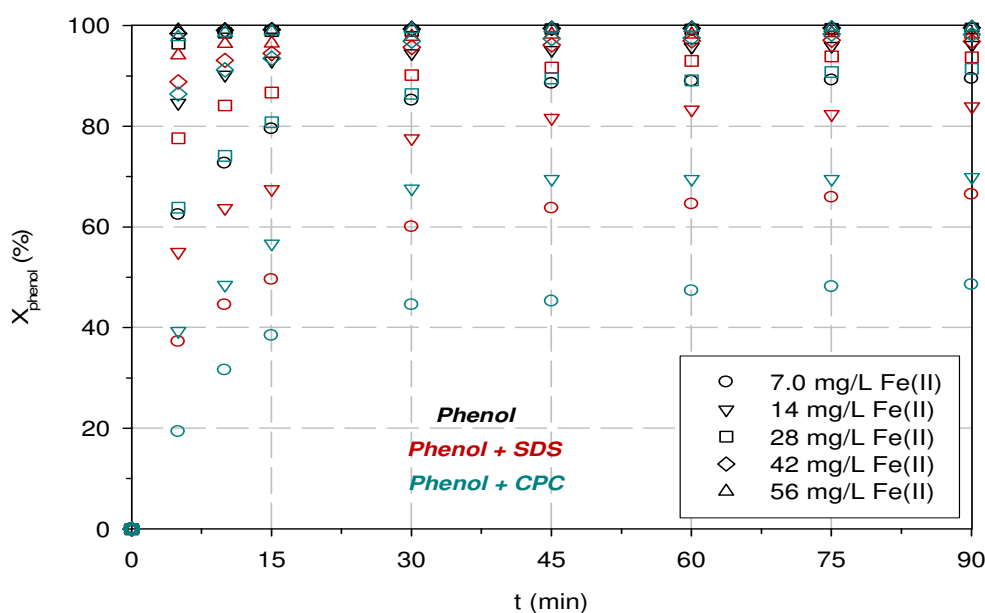


Figure 7.3. Effect of the Fe(II) concentration and surfactant presence on phenol conversion. 2500 mg/L phenol ; 2307 mg/L SDS (when present) ; 299 mg/L CPC (when present); 12500 mg/L H_2O_2 ; 30°C ; 300 rpm

Table 7.2. Effect of the Fe(II) concentration and surfactant presence on phenol, surfactants' and TOC conversion after 90 min oxidation. 2500 mg/L phenol ; 2307 mg/L SDS (when present) ; 299 mg/L CPC (when present) ; 12500 mg/L H₂O₂ ; 30°C ; 300 rpm

	[Fe(II)] (mg/L)	X _{phenol} (%)	X _{TOC} (%)	X _{surfactant} (%)	Abs at 455 nm	%ID
Phenol	7.0	89.4±1.1	15.9±0.9	-	1.52±0.03	35.1±1.9
	14	96.1±0.9	21.0±0.8	-	1.45±0.05	25.9±1.0
	28	99.4±0.2	22.2±1.4	-	1.38±0.06	18.5±1.2
	42	99.6±0.2	24.0±1.0	-	1.08±0.04	17.2±0.7
	56	99.6±0.2	24.2±1.0	-	0.86±0.02	17.2±0.8
	[Fe(II)] (mg/L)	X _{phenol} (%)	X _{TOC} (%)	X _{surfactant} (%)	Abs at 455 nm	%ID
Phenol + SDS	7.0	66.4±2.1	1.6±0.0	73.1±1.3	1.50±0.00	35.3±0.7
	14	83.9±3.5	1.2±0.0	87.2±0.7	1.43±0.00	19.5±0.7
	28	93.7±2.3	0.9±0.0	94.2±0.5	1.33±0.00	10.8±0.2
	42	96.8±2.2	1.0±0.0	99.2±0.7	1.15±0.00	7.3±0.2
	56	98.2±1.1	0.8±0.0	98.9±0.5	0.82±0.00	6.9±0.2
	[Fe(II)] (mg/L)	X _{phenol} (%)	X _{TOC} (%)	X _{surfactant} (%)	Abs at 455 nm	%ID
Phenol + CPC	7.0	48.5±1.1	2.1±0.0	86.1±2.2	n.m.	54.5±1.1
	14	69.9±2.5	1.7±0.0	94.1±1.2	n.m.	34.3±1.1
	28	91.4±2.3	1.9±0.0	97.8±2.1	n.m.	14.8±0.3
	42	98.2±1.2	2.1±0.0	99.1±0.2	n.m.	9.3±0.4
	56	99.7±0.2	2.2±0.0	99.5±0.3	n.m.	8.3±0.4

n.m.: not measured

It has to be pointed out that, as Table 7.2 shows, the effluents composed by phenol and surfactant, once oxidised, were poorly identified (as %ID demonstrate). As neither surfactant degradation intermediates' identification nor biodegradability assessment measurements were carried out, the effluents could also have a toxic character to the biomass used in the subsequent step. Thus, biodegradability characterisation would be needed to determine the feasibility of the integrated process configuration.

The strong effect of the Fe(II) concentration on the final concentration of organic compounds is illustrated in Figure 7.4. As it can be observed, an increase on the Fe(II) concentration leads to a raise on the carboxylic acids' concentration and to a reduction of phenol, surfactant (when present) and quinone-like compounds' concentration. The most marked influence was observed on the concentration of quinone-like compounds. Their concentration when phenol was the only contaminant present in the solutions to oxidise passed from 235 ± 7 mg/L, when 7.0 mg/L Fe(II) were used, to 19 ± 0 mg/L when 56 mg/L Fe(II) were employed. When SDS or CPC were present in the initial phenol effluents, quinone-like compounds' concentration was, regardless of the Fe(II) concentration, below 1.5 mg/L and 0.5 mg/L, respectively. As Figure 7.4 demonstrates, when mixed phenol+SDS solutions were oxidised, residual surfactant concentrations decreased from 620 ± 11 mg/L to 24 ± 0 mg/L when Fe(II) concentration was increased from 7.0 mg/L to 56 mg/L, respectively. When phenol+CPC effluents were oxidised, residual surfactant concentration passed from 41 ± 1 mg/L to 2 ± 0 mg/L when Fe(II) concentration was increased from 7.0 to 56 mg/L.

Residual hydrogen peroxide concentration remaining after 90 min oxidation was always below 2.5 mg/L when the oxidation of single phenol solutions was tested. When SDS and CPC were present in the initial phenol solutions at its cmc, the remaining hydrogen peroxide concentration was below 1.5 mg/L, irrespective of the surfactant and oxidation conditions. Thus, residual hydrogen peroxide content was practically unaffected by the target contaminants studied, whose conversion could be almost complete depending on the oxidation conditions. Table 7.2 and Figure 7.4 show that %ID and intermediates identified significantly varied depending on whether phenol was alone in the initial effluents to oxidise or mixed with surfactant. Thus, the differences on the residual hydrogen peroxide concentration cannot be employed to predict the oxidant fraction used for the degradation of organics and that lost due to its autodecomposition and/or radical scavenging effects. For this purpose, radical quantification, which was not carried out in this thesis, would be useful.

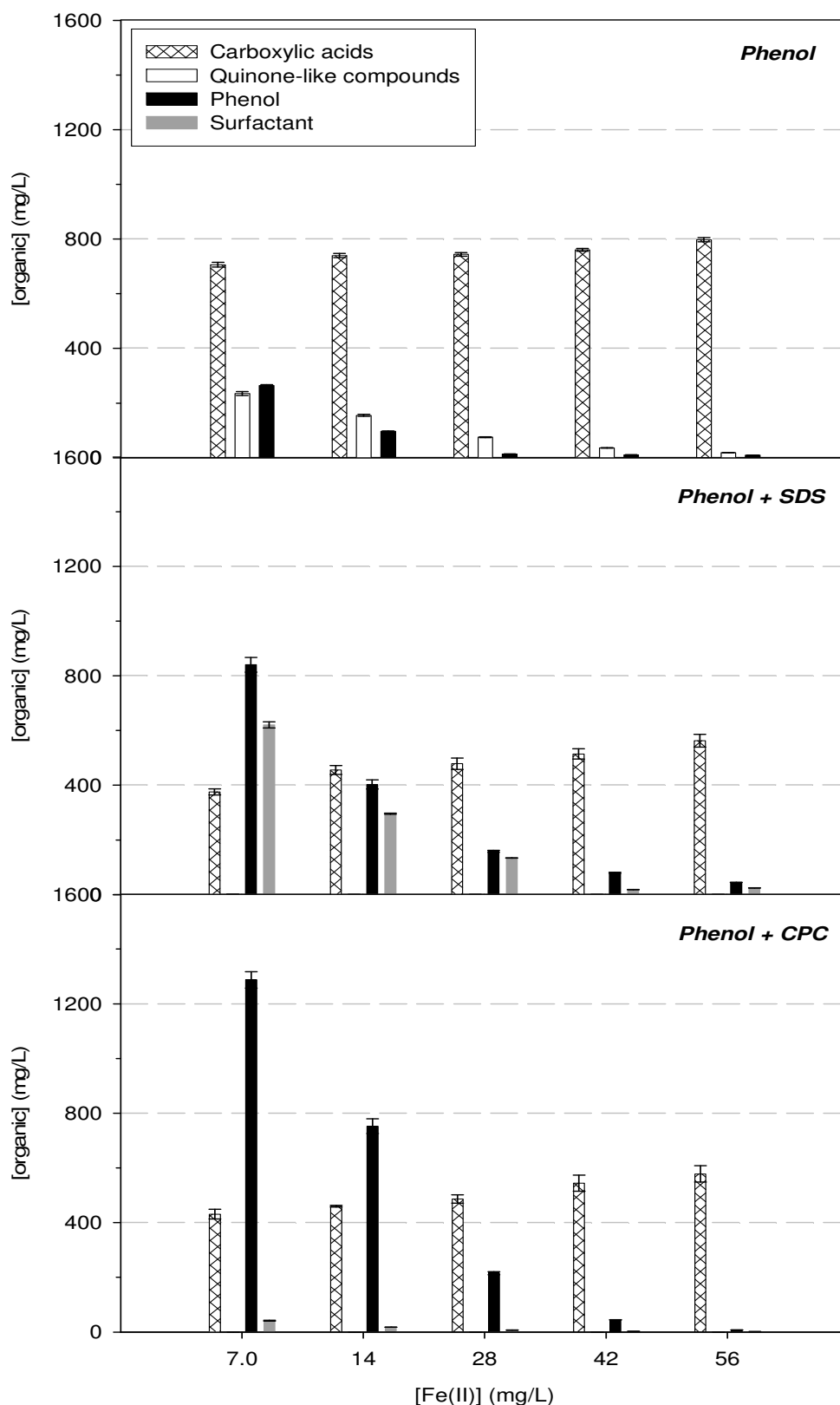


Figure 7.4. Effect of the Fe(II) concentration on the organic compounds' concentration after 90 min oxidation. 2500 mg/L phenol ; 2307 mg/L SDS (when present) ; 299 mg/L CPC (when present) ; 12500 mg/L H₂O₂ ; 30°C ; 300 rpm

7.2.3. Influence of the surfactant:cmc ratio on the Fenton process efficiency

The decrease on phenol conversion in presence of surfactants has been attributed to the possible competition of the surfactant for the hydroxyl radicals and/or to the phenol solubilisation in the surfactant micelles' nucleus. This solubilisation would decrease availability of phenol to be attacked by the radicals generated in the bulk phase. The degradation of surfactant molecules has already been confirmed in the previous sections. Phenol solubilisation effect on its conversion decline when surfactant is present has not been yet checked. It is expected that, when surfactants are present, mainly in micellar form (above the cmc), high phenol solubilisation occurs. Below the cmc, although lower organics' solubilisation occurs, their solubility is enhanced compared to when no surfactant is present (Li et al. 2007). Phenol has demonstrated to solubilise in micelles of both anionic and cationic surfactants. Nevertheless, it has been proven that phenol is better solubilised in micelles of surfactants containing ammonium groups in their structure such as CPC (Adamczak et al. 1999). This would agree with the previously-presented results, which indicated that phenol degradation was lower when cationic CPC surfactants were present. Thus, phenol solubilisation seems to have some unfavourable influence on phenol degradation by Fenton reaction.

In order to study the effect of the surfactant state (monomeric or micellar) on the oxidation efficiency, several oxidation experiments at variable surfactant concentration were carried out. The concentration of surfactant ranged between below and above their cmc. The ratio surfactant concentration:cmc ([surf]:cmc) was varied between 0.3 and 1.8. In all the experiments, the initial phenol, H₂O₂ and Fe(II) concentrations were 2500 mg/L, 12500 mg/L and 7.0 mg/L, respectively. The temperature was fixed at 30°C and the stirring rate at 300 rpm. As in all the experiments performed, the oxidation reaction lasted 90 min.

Table 7.3 shows phenol, TOC and surfactant conversion after 90 min of oxidation at variable [surf]:cmc ratio. As Table 7.3 clearly demonstrates, phenol and surfactant conversions decreased when [surf]:cmc passed from 0.3 to 1.0. Beyond 1.0, both phenol and surfactant conversions remained constant with a further increase of [surf]:cmc. Hence, phenol conversion is strongly influenced by the surfactant state (monomer or micelle). In addition, surfactant degradation itself is influenced by its condition, indicating that surfactant monomers are more easily degraded than micelles. Micelles are probably more robust and resistant to degradation because they are clusters of monomer units. As Table 7.3 reveals, CPC is degraded in a higher degree than SDS, regardless of the [surf]:cmc. This can be explained by the presence of the aromatic structure in its molecule that, in principle, can be more easily attacked by hydroxyl radicals. The attack could be favoured by its orientation in the micelles because the linear hydrocarbon tail is oriented towards the micelle core and the aromatic head to the bulk solution, where radicals are expected to be generated. As abovementioned, phenol can be easily solubilised in the micelles of CPC because of its ammonium group. Thus, the lower phenol conversion obtained when CPC was studied could be explained by the higher phenol solubilisation into the CPC micelles.

The distribution of organic compounds measured after 90 min of oxidation when surfactants are present is represented in Figure 7.5. As it can be seen, carboxylic acids' concentration was higher when dealing with phenol+CPC solutions than when with phenol+SDS, irrespective of the [surf]:cmc. This could be explained by the aromatic ring present in the molecule of CPC, which could give similar intermediates, when oxidised, than phenol. Carboxylic acids' concentration decreased as long as the [surf]:cmc increased from 0.3 to 1.0. Nonetheless, as happened with phenol and

surfactant conversions (summarised in Table 7.3), any further increase of this ratio beyond 1.0, did not affect their concentration. Thus, carboxylic acids' concentration follows the trends of both phenol and surfactants' degradation.

Table 7.3. Effect of the [surf]:cmc on phenol, surfactants' and TOC conversion after 90 min oxidation. 2500 mg/L phenol ; 12500 mg/L H₂O₂ ; 7.0 mg/L Fe(II) ; 30°C ; 300 rpm

	[surf]:cmc	X _{phenol} (%)	X _{TOC} (%)	X _{surfactant} (%)	Abs at 455 nm	%ID
Phenol + SDS	0.3	85.1±2.3	1.3±0.0	92.1±1.1	1.52±0.00	20.8±0.7
	0.6	73.0±2.7	1.1±0.0	86.2±1.4	1.54±0.00	28.7±0.8
	1.0	66.4±2.1	1.6±0.0	73.1±1.3	1.50±0.00	35.3±0.7
	1.4	66.1±1.9	1.8±0.0	70.6±0.9	1.53±0.00	35.5±0.6
	1.8	67.7±1.5	1.2±0.0	71.6±0.8	1.54±0.01	33.5±0.9
	[surf]:cmc	X _{phenol} (%)	X _{TOC} (%)	X _{surfactant} (%)	Abs at 455 nm	%ID
Phenol + CPC	0.3	60.9±1.8	2.2±0.0	95.7±2.1	n.m.	46.5±1.5
	0.6	55.5±2.4	2.8±0.0	90.9±1.7	n.m.	53.0±2.0
	1.0	48.5±1.1	2.1±0.0	86.1±2.2	n.m.	54.5±1.1
	1.4	47.7±2.5	1.8±0.0	85.8±1.3	n.m.	53.4±2.5
	1.8	47.3±3.1	2.2±0.0	85.0±1.2	n.m.	52.6±3.1

n.m.: not measured

Quinone-like products analysed in the phenol+SDS oxidation decreased from 3.6 to below 0.5 mg/L when the [surf]:ratio passed from 0.3 to 1.8. However, at ratios of 1.4 and 1.8, the same concentration values were found as a result of the unchanged phenol conversion. Concerning the oxidation of phenol+CPC, quinone-like compounds' concentration remained unchanged (around 0.5 mg/L) regardless of the [surf]:ratio. Thus, in this case, it is not observed the same tendency than with phenol and CPC conversion. The difference could be attributed to the fact that, contrarily to what happens when the phenol+SDS is studied, CPC can form quinone-like compounds from the degradation of its aromatic ring, which would sum up to those from phenol. Thus, it is difficult to know the individual influence of phenol and CPC degradation on quinone-like compounds' formation and therefore on overall quinone-like compounds' content.

Surfactant concentration analysed after oxidation was higher when dealing with SDS than with CPC. This is mostly due to the higher initial concentration of this surfactant, whose cmc is around ten times higher than that of the CPC. Residual hydrogen peroxide concentration was below 1.6 mg/L regardless of the surfactant present in the initial phenol solution. Thus, almost complete transformation of the initial oxidant was achieved, as happened in the experiments concerning the effect of the H₂O₂ and Fe(II) concentrations on the Fenton process efficiency.

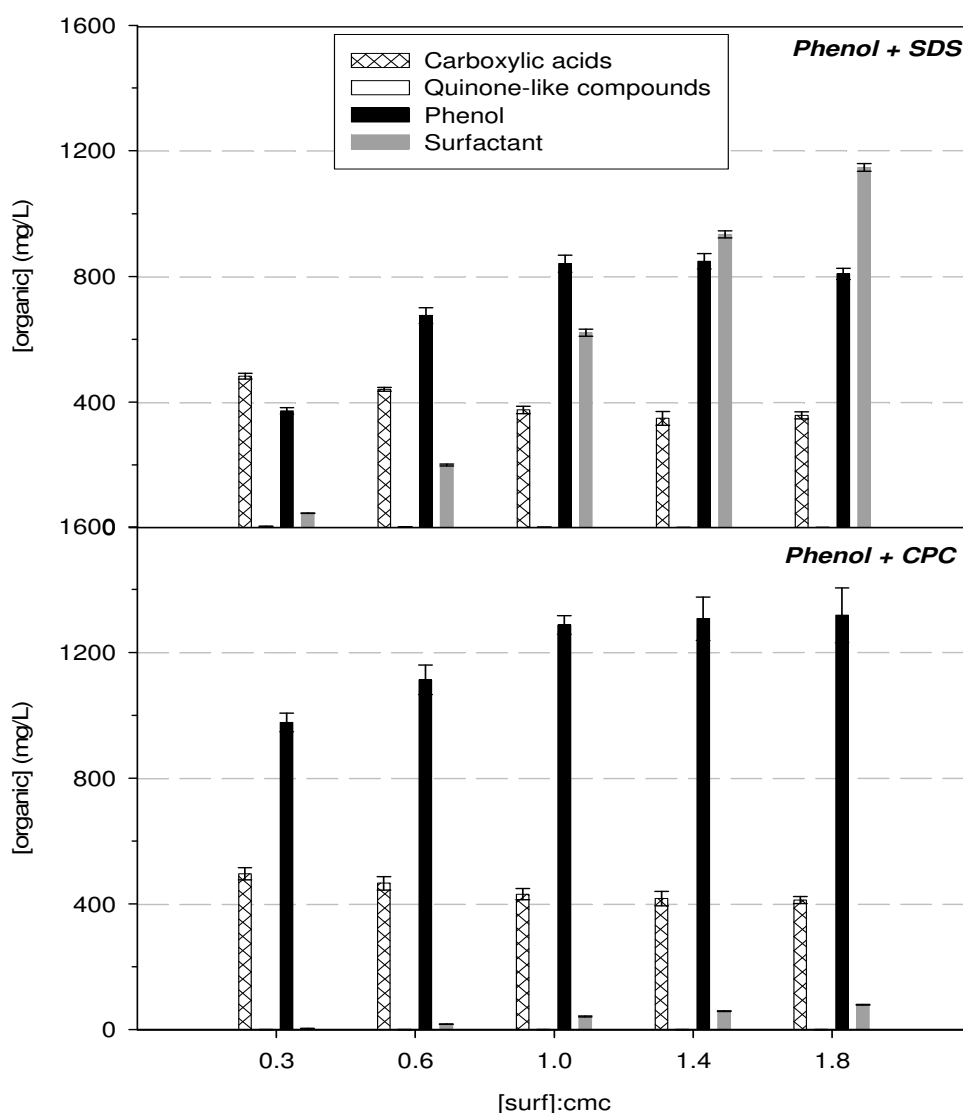


Figure 7.5. Effect of the [surf]:cmc on the organic compounds' concentration after 90 min oxidation. 2500 mg/L phenol ; 12500 mg/L H₂O₂ ; 7.0 mg/L Fe(II) ; 30°C ; 300 rpm

7.3. Coupling of Fenton process and NF: treatment of effluents containing phenol and SDS

Coupling Fenton process and NF has shown to be an efficient process design to treat single phenol effluents before sending them to a biological treatment unit. In this section, the applicability of the same process scheme when phenol effluents are also polluted with SDS is presented. In the preceding sections, the effect of the H₂O₂ dose, Fe(II) concentration and [surf]:cmc on the Fenton oxidation efficiency has been discussed. In order to study the effect of those operation variables on the NF efficiency, some of the oxidised effluents were subsequently filtered to evaluate membrane performance. In addition to the study of the influence of the three abovementioned variables on the permeate flux decline evolution, retention of compounds and fouling percentages, the NF study also included testing three commercial NF membranes from DOW-Filmtec (NF-D, NF90 and NF270).

First of all, the membrane giving the highest efficiency was selected. Then, the effect of the hydrogen peroxide dose, Fe(II) concentration and ratio [surf]:cmc on the separation efficiency of the selected membrane was investigated. All the filtration runs had a total duration of 360 min and were carried out at a TMP of 6 bar and at 30°C. In order to assess the membranes' efficiency, permeate flux parameters and retention of organic compounds, TOC, iron and colour were evaluated. Furthermore, the %ID after NF was also obtained and compared to that assessed in the pre-oxidised effluents.

7.3.1. Influence of the membrane on the NF efficiency

NF-D, NF90 and NF270 membranes were selected for filtering the effluents of the oxidation of 2500 mg/L phenol and 2307 mg/L SDS with 12500 mg/L H₂O₂ and 7.0 mg/L Fe(II). The %J_p/J_w evolution monitored with the three membranes is represented in Figure 7.6. As it can be noted, the highest permeate flux decline was observed for NF90 membrane followed by NF270 and NF-D. Nevertheless, the three membranes exhibited a permeate flux decline higher than around 70%, which can be due to concentration polarisation but particularly to fouling.

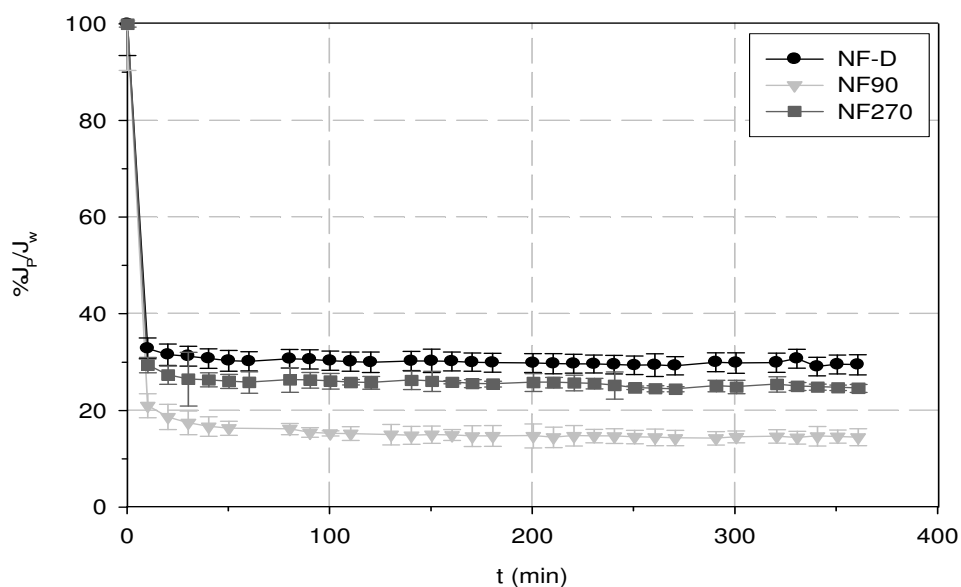


Figure 7.6. Effect of the membrane on the %J_p/J_w evolution when pre-oxidised effluents are filtered at 6 bar and 30°C. Fenton conditions: 2500 mg/L phenol ; 2307 mg/L SDS ; 12500 mg/L H₂O₂ ; 7.0 mg/L Fe(II) ; 30°C ; 300 rpm ; 90 min

Normalised permeate fluxes of all the tested membranes, shown in Figure 7.7, evidence that, part of the permeate flux loss occurred during the filtration was restored by rinsing the membranes with water. For instance, the %J_p/J_w of NF90 was 15±2% whilst its %J_a/J_w (after membrane rinsing) increased up to 34±1%. Regardless of the membrane, a loss of permeate flux still remained after rinsing. Hence, chemical cleaning would be needed to totally restore the membrane flux as happened when pre-oxidised phenol-alone solutions were filtered with the same membranes.

Membrane purification efficiency was also evaluated in terms of general parameters' retention. The results of the membranes' screening are represented in Figure 7.8. The highest retentions were achieved, as Figure 7.8 shows, with NF90, regardless of the

parameter observed. From now on, the efficiency of NF90 is explained. Figure 7.8 evidences that carboxylic acids' retention was lower than any of the rest of parameters. In addition, the rejection of carboxylic acids was around 30% lower than when filtering pre-oxidised effluents initially composed by only phenol (see Chapter 6). This significant decrease could be explained by the possible iron complexation in surfactant micelles, which would prevent iron complexation with the acid. As explained in Chapter 6, iron complexation is considered to be responsible of the oxalic acid retention through sieving effects. As oxalic acid was the major acid found in phenol and phenol+SDS oxidised effluents, its lower retention, observed when SDS was present, directly decreases the global retention of carboxylic acids.

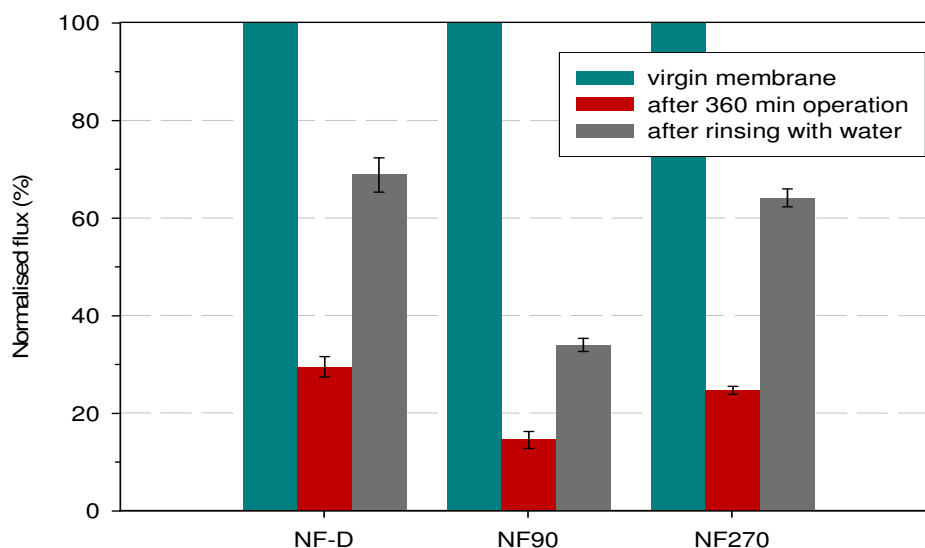


Figure 7.7. Effect of the membrane on the normalised fluxes when pre-oxidised effluents are filtered at 6 bar and 30°C. Fenton conditions: 2500 mg/L phenol ; 2307 mg/L SDS ; 12500 mg/L H₂O₂ ; 7.0 mg/L Fe(II) ; 30°C ; 300 rpm ; 90 min

The retention of quinone-like compounds, also depicted in Figure 7.8, was almost complete. This suggests that, when SDS was present in the effluents to be oxidised and in the oxidised effluents, as result of its only partial degradation, the retention of aromatic compounds is increased. This response is also valid for phenol, which was also undetected in the NF90 permeate. The increase on the retention of quinone-like compounds and phenol could be attributed to their solubilisation in surfactant micelles, which are retained by NF. Furthermore, the formation of a gel layer of surfactant on the membrane surface, giving an additional resistance to permeation and probably an enhanced separation selectivity, could also help increasing their retentions.

Surfactants were completely rejected by NF90, which could be possibly explained by their high MW's and thus by sieving effects. SDS is not expected to be the only surfactant in the pre-oxidised effluents because it could have been degraded into other lower-chain surfactants. The method selected for analysing anionic surfactants did not distinguish between surfactant molecules and thus only gave a global concentration of surfactants. However, although other surfactants can have been generated, they are also expected to have considerable MW's and thus be easily retained by the membranes. Iron retention was around 98.2±0.1%, implying that almost all Fenton catalyst could be presumably recycled and reused in the oxidation reactor. Permeate TOC was only 124±7 mg/L as a result of its high retention, which was 95.9±0.2%. The

NF90 permeate was visually colourless, which is corroborated by the almost complete colour removal. From an effluents' purification perspective, NF90 has shown to be a potential membrane to eliminate iron and to completely remove non-reacted phenol, surfactant and generated quinone-like compounds, which are expected to put in danger the operation of the subsequent biological treatment.

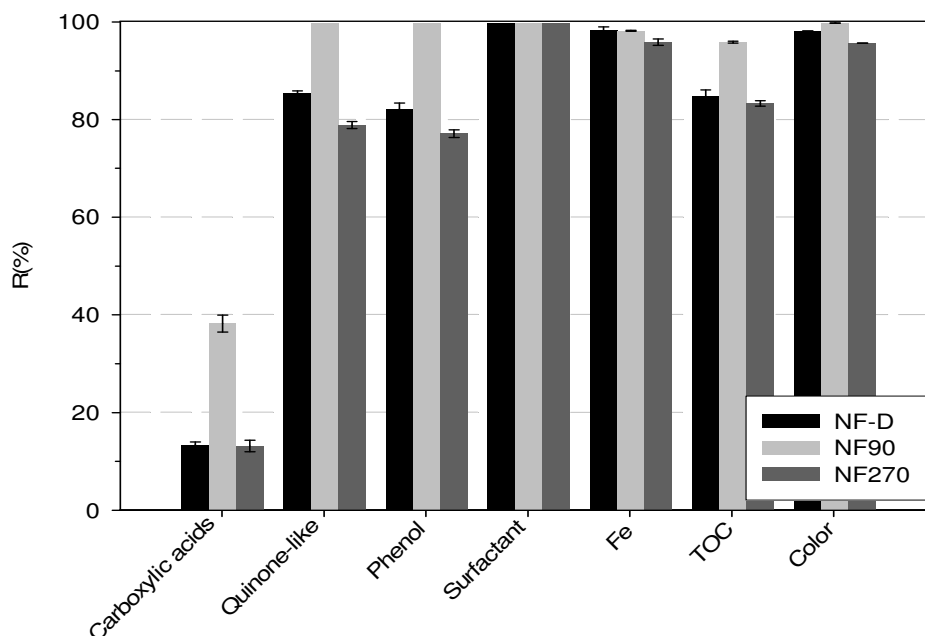


Figure 7.8. Effect of the membrane on the retention of general parameters when pre-oxidised effluents are filtered at 6 bar and 30°C. Fenton conditions: 2500 mg/L phenol; 2307 mg/L SDS ; 12500 mg/L H₂O₂ ; 7.0 mg/L Fe(II) ; 30°C ; 300 rpm ; 90 min

The %ID values after Fenton and after NF are shown in Table 7.4. As it can be seen, the NF90 permeate had more identified compounds than those from the other two membranes, which had similar %ID among them. The fact that permeate streams are more identified than feed ones indicate that the membranes partially retain unidentified compounds. However, it has to be noted that even when NF90 was selected, around 30% of the permeate composition was still unidentified. Thus, biodegradability assessment would be needed in order to know whether the nanofiltered effluents could be safely driven or not to a biological treatment unit.

Table 7.4. %ID of the effluents after Fenton and after NF. Pre-oxidised effluents filtered at 6 bar and 30°C. Fenton conditions: 2500 mg/L phenol ; 2307 mg/L SDS ; 12500 mg/L H₂O₂ ; 7.0 mg/L Fe(II) ; 30°C ; 300 rpm ; 90 min

Membrane	%ID	
	After Fenton	After NF
NF-D		47.2±3.9
NF90	35.3±0.7	69.1±3.7
NF270		49.6±1.7

7.3.2. Influence of the hydrogen peroxide dose on the NF efficiency

The effect of the hydrogen peroxide dose used in the Fenton reaction on the NF efficiency was studied by filtering through NF90 three effluents pre-oxidised at different H_2O_2 doses. The initial phenol concentration in the solution to oxidise was 2500 mg/L whereas that of SDS was 2307 mg/L, corresponding to the surfactant cmc. The Fe(II) concentration used as oxidation catalyst was 7.0 mg/L. The temperature and stirring rate were set constant for the 90 min oxidations at 30°C and 300 rpm, respectively. The filtration experiments were carried out with NF90 membrane working at a TMP of 6 bar and at a constant temperature of 30°C.

As Figure 7.9 shows, the $\%J_p/J_w$ evolution is not affected by the H_2O_2 dose used in the Fenton reaction. These results follow the same behaviour observed when the filtration of oxidised phenol effluents (without SDS) was studied. In addition, the effect of the hydrogen peroxide dose on the membrane fouling, represented by the normalised permeate fluxes, can be considered negligible, as Figure 7.10 proves. As Figure 7.10 shows, the same recovery of permeate flux is achieved when rinsing the membrane with deionised water, no matter the oxidant concentration employed in the oxidation. Thus, even though the concentration of organics in the pre-oxidised effluents varies with the oxidant dose, this does not affect membrane fouling.

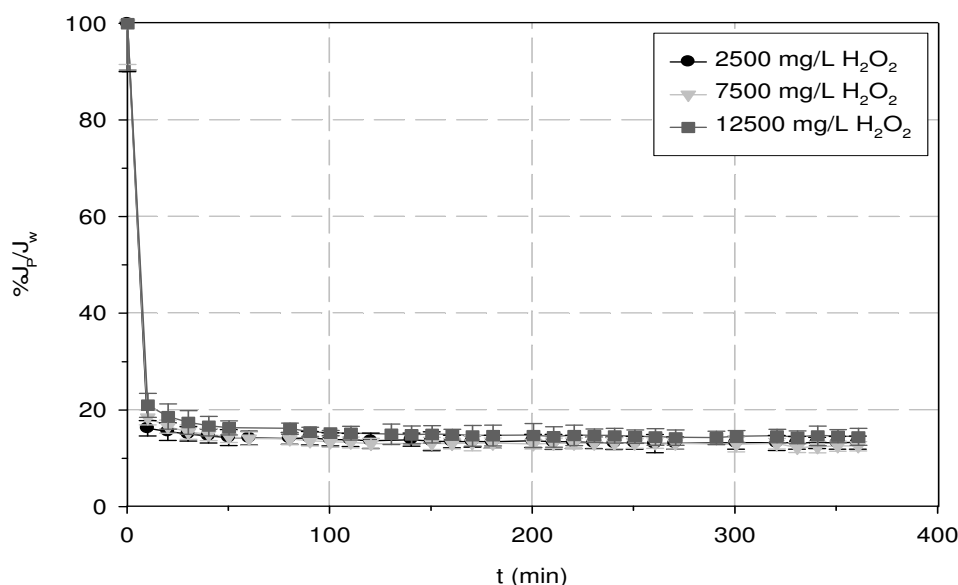


Figure 7.9. Effect of the H_2O_2 dose on the $\%J_p/J_w$ evolution when pre-oxidised effluents are filtered with NF90 at 6 bar and 30°C. Fenton conditions: 2500 mg/L phenol ; 2307 mg/L SDS ; 7.0 mg/L Fe(II) ; 30°C ; 300 rpm ; 90 min

The influence of the oxidant dose used in the oxidation reaction on the retention of general parameters can be observed in Figure 7.11. No significant hydrogen peroxide dose impact is seen on the rejection of any of the parameters analysed. This behaviour was already observed when investigating the filtration of oxidised phenol-alone effluents. Nevertheless, when the initial effluents contained SDS, carboxylic acids' retention decreased. This can be due, as explained before, to the fact that Fe is trapped by the surfactant, restricting (or avoiding) its complexation with oxalic acid, which is expected to be the key of the oxalic acid retention mechanism by NF90, as explained in Chapter 6. Carboxylic acids present in oxidised phenol+SDS effluents

were mainly composed by oxalic acid. Thus, the decrease of its complexation with Fe when SDS is present would explain the reduction of the carboxylic acids' family retention.

Phenol and quinone-like substances are, as Figure 7.11 shows, completely removed from pre-oxidised effluents, regardless of the H_2O_2 dose used in the Fenton oxidation. This can be attributed to their solubilisation in the remaining micelles, which are totally retained by the membrane, after the oxidation and/or to the formation of a concentrated layer of surfactant over the membrane surface. This layer could represent an additional selective barrier to these compounds and also be able to form new micelles, which would host them in their core, due to the surfactant accumulation in this zone. Fe and TOC retentions were practically unaffected by the oxidant dose used in the oxidation of the polluted effluents. The colour of the effluents was almost completely removed, which agrees with the also high retention of quinone-like compounds and iron, mainly responsible of the colour formation.

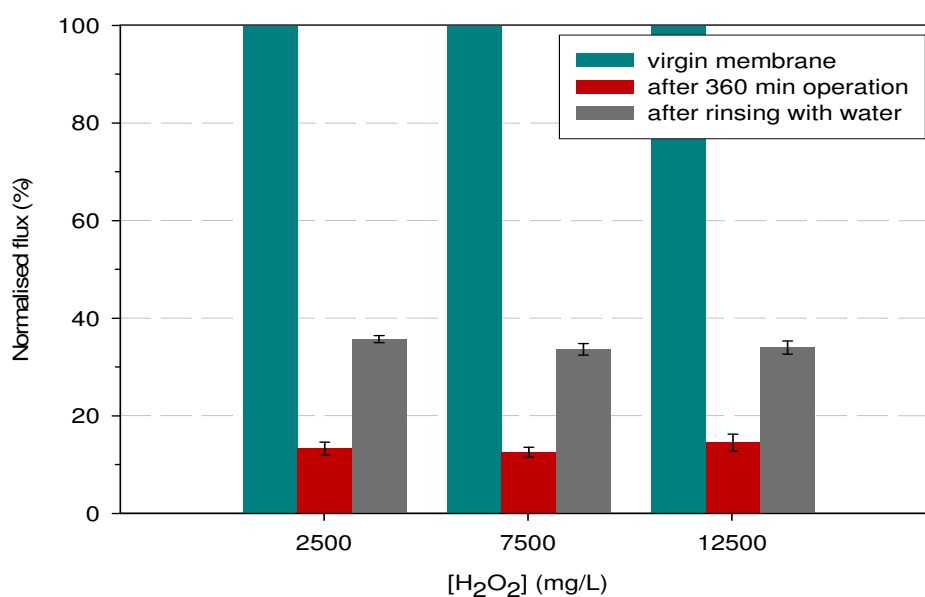


Figure 7.10. Effect of the H_2O_2 dose on the normalised fluxes when pre-oxidised effluents are filtered with NF90 at 6 bar and 30°C. Fenton conditions: 2500 mg/L phenol ; 2307 mg/L SDS ; 7.0 mg/L Fe(II) ; 30°C ; 300 rpm ; 90 min

The %ID of the pre-oxidised effluents and those calculated after their filtration through NF90 are summarised together in Table 7.5. As Table 7.5 shows, the %ID after filtration does not follow a clear dependency on the hydrogen peroxide dose. In fact, this result was already observed when filtering pre-oxidised phenol-alone effluents, presented in Chapter 6, whose %ID was not found to have a direct relation with the oxidation conditions. It is worthy that this percentage is sensitive to the changes on the unidentified intermediates' nature that can occur when the oxidant doses or other oxidation condition are varied. In general, regardless of the hydrogen peroxide concentration, the %ID of the effluents increases when they are filtered, which indicates that some of the unidentified intermediates are indeed retained by NF90.

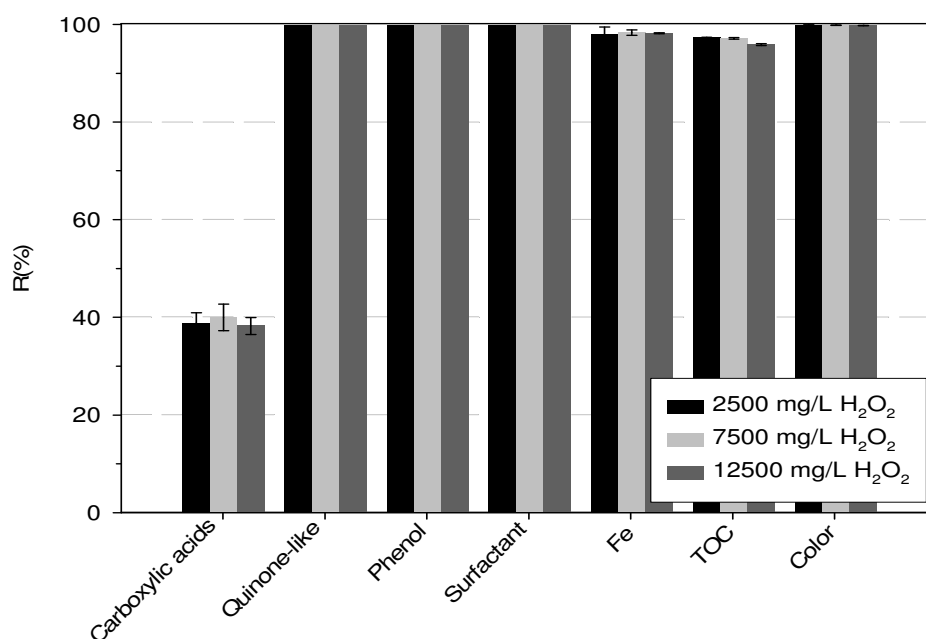


Figure 7.11. Effect of the H₂O₂ dose on the retention of general parameters when pre-oxidised effluents are filtered with NF90 at 6 bar and 30°C. Fenton conditions: 2500 mg/L phenol ; 2307 mg/L SDS ; 7.0 mg/L Fe(II) ; 30°C ; 300 rpm ; 90 min

Table 7.5. Effect of the H₂O₂ dose on the %ID of the effluents after Fenton and after NF. Pre-oxidised effluents filtered with NF90 at 6 bar and 30°C. Fenton conditions: 2500 mg/L phenol ; 2307 mg/L SDS ; 7.0 mg/L Fe(II) ; 30°C ; 300 rpm ; 90 min

[H ₂ O ₂] (mg/L)	%ID	
	After Fenton	After NF
2500	44.9±1.0	35.6±1.6
7500	36.8±0.8	75.9±4.9
12500	35.3±0.7	69.1±3.7

7.3.3. Influence of the iron(II) concentration on the NF efficiency

The iron(II) concentration was found to have a significant influence on the Fenton process efficiency either when phenol-alone or binary phenol+surfactant effluents were oxidised. Concretely, an increase on the Fe(II) concentration, resulted in an improvement of the oxidation efficiency. Due to its demonstrated influence on the Fenton effluents, it is important to test its impact on the filtration efficiency. The filtration of three effluents pre-oxidised at three Fe(II) concentrations was carried out. For the preparation of such effluents, initial solutions containing 2500 mg/L phenol and 2307 mg/L SDS were oxidised with 12500 mg/L H₂O₂ for 90 min at 30°C and 300 rpm. The solutions were then nanofiltered through NF90 for 360 min at 6 bar of TMP and 30°C.

Figure 7.12 demonstrates that the Fe(II) concentration used in the Fenton oxidation does not affect the evolution of the $\%J_P/J_w$, as happened when investigating the effect of the oxidant concentration. Thus, an increase of the Fe(II) concentration in the oxidation reactor and consequently in the membrane feed does not affect the permeate flux at least at the tested range of Fe(II) concentrations and experimental conditions.

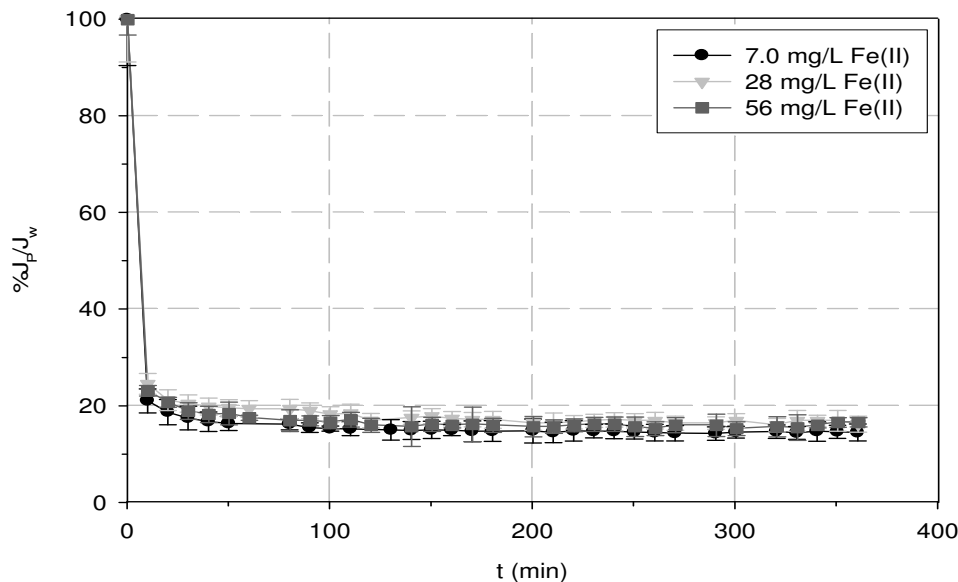


Figure 7.12. Effect of the Fe(II) concentration on the $\%J_P/J_w$ evolution when pre-oxidised effluents are filtered with NF90 at 6 bar and 30°C. Fenton conditions: 2500 mg/L phenol ; 2307 mg/L SDS ; 12500 mg/L H_2O_2 ; 30°C ; 300 rpm ; 90 min

Normalised permeate fluxes measured after 360 min of filtration and after rinsing the membranes with deionised water are not affected by the iron concentration, as Figure 7.13 shows. This behaviour was not found when pre-oxidised phenol-alone effluents were filtered. In that case, membrane fouling increased ($\%J_a/J_w$ decreased) when the iron concentration in the Fenton oxidation was raised. This was attributed to the possible fouling caused by condensation products, quinone-like compounds and/or iron species itself. The difference on fouling is probably eliminated when filtering mixed phenol+SDS oxidised effluents because the presence and deposition of surfactant molecules and/or micelles predominates and finally governs fouling. In addition, the concentration of quinone-like compounds, which could contribute to fouling, was found to be lower in phenol+SDS pre-oxidised effluents than in phenol-alone pre-oxidised ones. Moreover, iron was possibly associated with surfactants, when present. Hence, fouling due to quinone-like compounds and free iron would be reduced when phenol+SDS pre-oxidised effluents are considered. Nevertheless, it can be noted that, when dealing with pre-oxidised phenol+SDS effluents, significantly higher fouling was observed (lower $\%J_a/J_w$) than when dealing with pre-oxidised phenol-alone streams. This can be linked, as explained below, to the presence and deposition of surfactants on the membrane which could govern fouling phenomena.

The effect of the Fe(II) concentration on the retention of general parameters can be found in Figure 7.14. This figure shows that carboxylic acids' retention was unaltered by the Fe(II) concentration. Their retention was almost 40%, which is quite lower than when the effect of the Fe(II) concentration was tested in pre-oxidised phenol-alone solutions. At those conditions, carboxylic acids' rejection was almost 70%. As explained above, this retention decline can be due to the non complexation (or less complexation)

of iron ions with oxalic acid, which has been considered to be directly related to the sieving effects responsible of the retention of this acid.

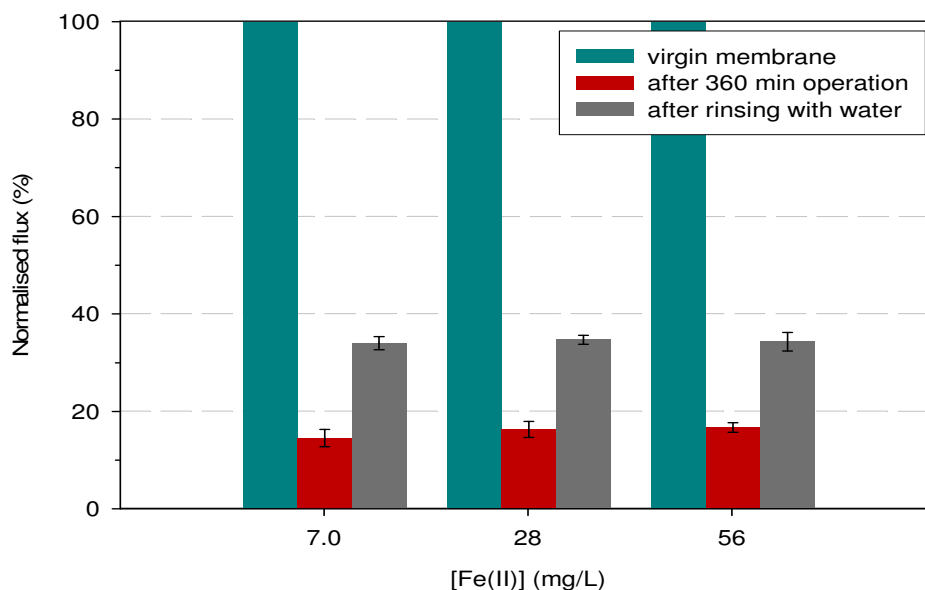


Figure 7.13. Effect of the Fe(II) concentration on the normalised fluxes when pre-oxidised effluents are filtered with NF90 at 6 bar and 30°C. Fenton conditions: 2500 mg/L phenol ; 2307 mg/L SDS ; 12500 mg/L H₂O₂ ; 30°C ; 300 rpm ; 90 min

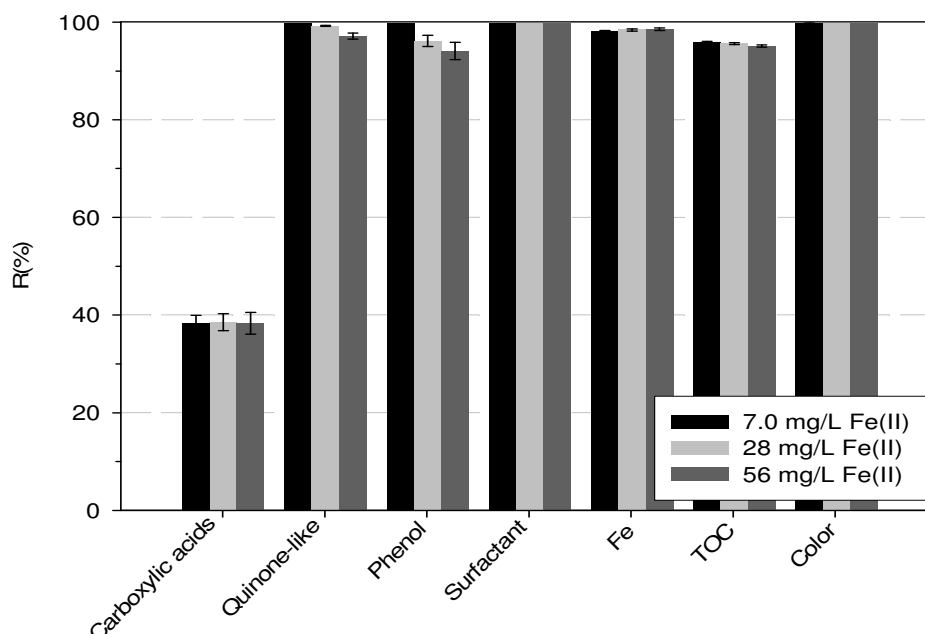


Figure 7.14. Effect of the Fe(II) concentration on the retention of general parameters when pre-oxidised effluents are filtered with NF90 at 6 bar and 30°C. Fenton conditions: 2500 mg/L phenol ; 2307 mg/L SDS ; 12500 mg/L H₂O₂ ; 30°C ; 300 rpm ; 90 min

Surfactant, iron, TOC and colour retentions do not practically change when iron concentration varies, as shown by Figure 7.14. Nonetheless, quinone-like compounds

and phenol are strongly affected by iron concentration. Their rejection diminished when the iron concentration was raised. This result could be explained by the lower concentration of surfactant present in the pre-oxidised effluents when the Fe(II) concentration increased as result of its partial degradation. This would confirm the importance of the surfactant concentration on the removal of these organic compounds. As abovementioned, surfactants could help the retention of aromatics by sequestering them in the micelles or even by the additional surfactant layer formed on the membrane.

Table 7.6 summarises the %ID calculated after Fenton oxidation and after filtration. As the data indicate, regardless of the Fe(II) concentration, there is always a gain on the effluents' identification after their filtration through NF90.

Table 7.6. Effect of the Fe(II) concentration on the %ID of the effluents after Fenton and after NF. Pre-oxidised effluents filtered with NF90 at 6 bar and 30°C. Fenton conditions: 2500 mg/L phenol ; 2307 mg/L SDS ; 12500 mg/L H₂O₂ ; 30°C ; 300 rpm ; 90 min

[Fe(II)] (mg/L)	%ID	
	After Fenton	After NF
7.0	35.3±0.7	69.1±3.7
28	10.8±0.2	87.1±3.7
56	6.9±0.2	89.2±4.8

7.3.4. Influence of the surfactant:cmc ratio on the NF efficiency

The study of the surfactant:cmc ratio on the Fenton efficiency has demonstrated that this variable significantly affects it. An increase on the [surf]:cmc below the cmc mainly caused an increase on the final phenol and surfactant concentration. In this section, the effect of the [surf]:cmc on the NF efficiency is presented. The influence was assessed through the filtration of pre-oxidised phenol+SDS solutions initially containing different ratios [surf]:cmc. In order to prepare the pre-oxidised effluents, the Fenton oxidation of the effluents was performed for 90 min at 30°C and 300 rpm of stirring rate. The phenol, oxidant and catalyst concentrations were set constant and equal to 2500 mg/L, 12500 mg/L and 7.0 mg/L Fe(II) in all the experiments, respectively. The pre-oxidised effluents were filtered for 360 min with NF90 at 6 bar of TMP and at 30°C.

The effect of the [surf]:cmc on the permeate flux decline evolution is presented in Figure 7.15. As this figure shows, the %J_p/J_w was around 15%, regardless of the [surf]:cmc. Thus, from this result and those describing the effect of the membrane, hydrogen peroxide dose and iron concentration, it can be concluded that, none of those variables affected the permeate flux evolution. In addition, as Figure 7.16 demonstrates, no significant changes neither on %J_p/J_w nor on %J_a/J_w were detected when the [surf]:cmc was varied. It must be pointed out that the permeate flux after rinsing the membrane with deionised water was around twofold that instantaneously measured at the end of filtration. Thus, a fraction of the occurred fouling could be easily eliminated. However, the remaining fouling would need to be removed by stronger rinsing conditions or by chemical means, as happened with the membranes fouled by pre-oxidised phenol-alone solutions.

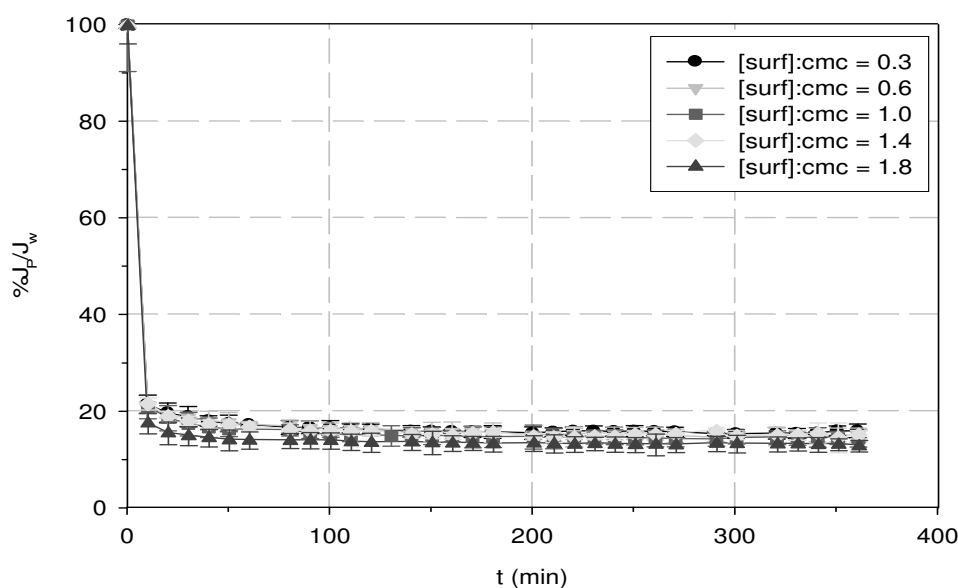


Figure 7.15. Effect of the [surf]:cmc on the $\%J_p/J_w$ evolution when pre-oxidised effluents are filtered with NF90 at 6 bar and 30°C. Fenton conditions: 2500 mg/L phenol ; 12500 mg/L H_2O_2 ; 7.0 mg/L Fe(II) ; 30°C ; 300 rpm ; 90 min

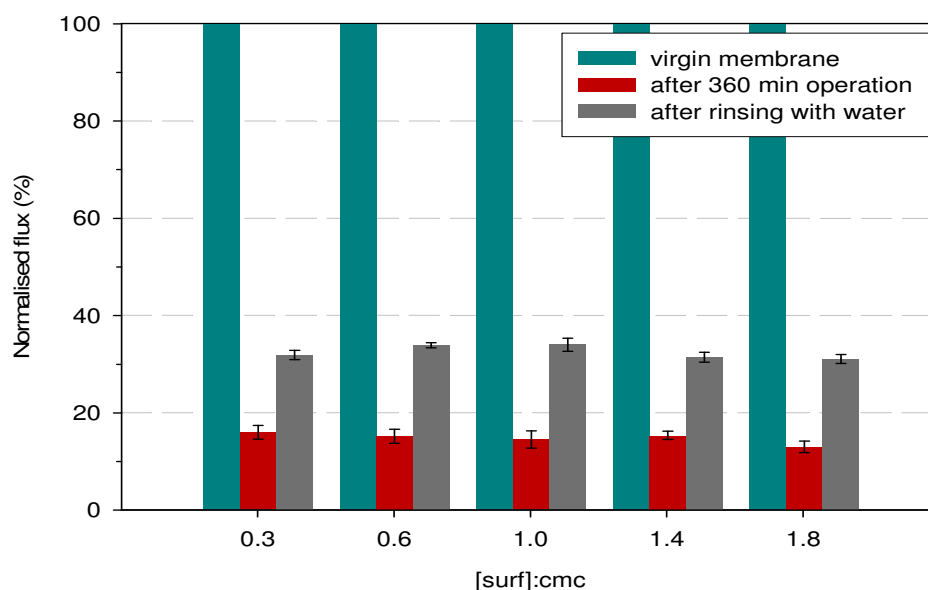


Figure 7.16. Effect of the [surf]:cmc on the normalised fluxes when pre-oxidised effluents are filtered with NF90 at 6 bar and 30°C. Fenton conditions: 2500 mg/L phenol ; 12500 mg/L H_2O_2 ; 7.0 mg/L Fe(II) ; 30°C ; 300 rpm ; 90 min

The results showing the influence of the [surf]:cmc on the retention of general parameters are displayed in Figure 7.17. This figure shows that the retention of phenol and quinone-like products was increased when the [surf]:cmc was raised. This rejection gain could be explained by their solubilisation in surfactant micelles that would be formed in the membrane vicinities due to the surfactant accumulation. In addition, the surfactant layer formation, favoured when the surfactant concentration is large (at high

[surf]:cmc), could also contribute to increase the retention of these compounds at high [surf]:cmc. As the Figure 7.17 shows, the retentions of the rest of parameters analysed (carboxylic acids, surfactant, iron, TOC and colour) were unaltered by the [surf]:cmc ratio.

The %ID values calculated after Fenton oxidation and after NF when dealing with solutions containing phenol+SDS are summarised in Table 7.7. As it can be observed, the effluents' %ID was always higher after filtration than after oxidation. However, there was still a fraction of the NF effluents' composition which was unidentified. Thus, the evaluation of biodegradability parameters of the NF effluents would be recommended in order to predict their behaviour in an aerobic biological treatment unit.

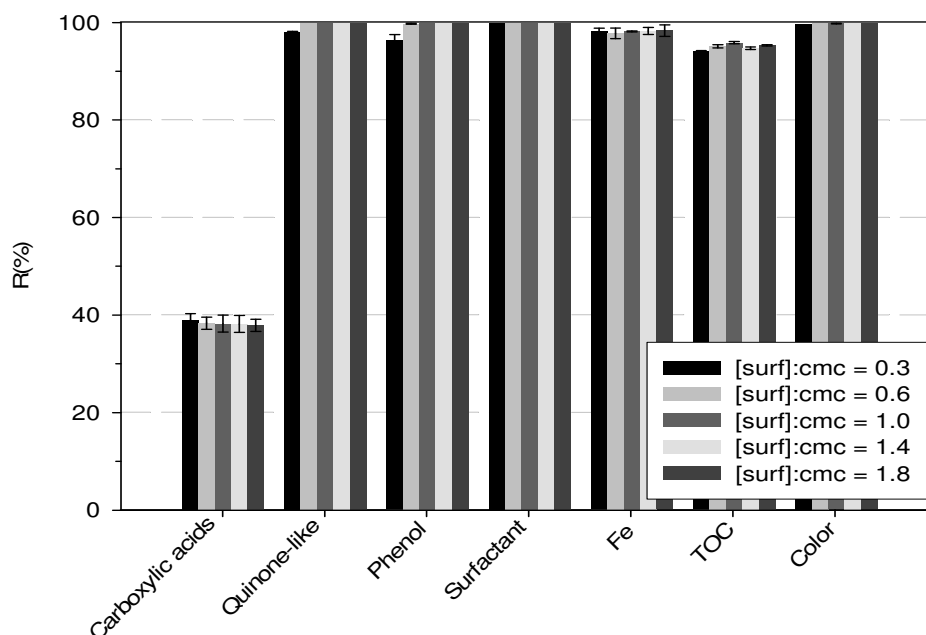


Figure 7.17. Effect of the [surf]:cmc on the retention of general parameters when pre-oxidised effluents are filtered with NF90 at 6 bar and 30°C. Fenton conditions: 2500 mg/L phenol ; 12500 mg/L H₂O₂ ; 7.0 mg/L Fe(II) ; 30°C ; 300 rpm ; 90 min

Table 7.7. Effect of the [surf]:cmc on the %ID of the effluents after Fenton and after NF. Pre-oxidised effluents filtered with NF90 at 6 bar and 30°C. Fenton conditions: 2500 mg/L phenol ; 12500 mg/L H₂O₂ ; 7.0 mg/L Fe(II) ; 30°C ; 300 rpm ; 90 min

[surf]:cmc	%ID	
	After Fenton	After NF
0.3	20.8±0.7	93.6±3.4
0.6	28.7±0.8	69.3±4.9
1.0	35.3±0.7	69.1±3.7
1.4	35.5±0.6	43.9±2.0
1.8	33.5±0.9	45.1±1.8

7.4. Conclusions

The degradation of phenol has also been found to take place when the pollutant coexists with SDS or CPC surfactants. High phenol degradation in mixed effluents can be achieved when the Fenton process variables are properly selected. However, CPC and SDS have been found to be simultaneously degraded through the Fenton reaction. Thus, the feasibility of using surfactant micelles as iron support has been discarded because the process would imply a continuous addition of surfactants into the reactor, which would increase costs and decrease environmental suitability. However, although the presence of surfactants has not allowed ensuring iron confining, the oxidation results have indicated that mixed phenol+surfactant effluents can be efficiently managed by the Fenton process.

Coupling Fenton oxidation with NF90 membrane as subsequent separation step allows overcoming, depending on the operation conditions, the release of iron, quinone-like intermediates and non-reacted phenol and surfactants to the subsequent biological treatment. Thus, the pair Fenton oxidation-NF seems to be an attractive configuration to decrease (or avoid) operational drawbacks in the subsequent aerobic biological treatment. Nevertheless, as nanofiltered effluents' composition was not totally determined, assessing their biodegradability would be needed to guarantee the safe operation of the subsequent biological treatment unit.

CHAPTER 8

Treatment of phenol effluents with ferrous emulsions formulated by membrane emulsification

8.1. Introduction

The feasibility of using O/W emulsions, prepared by membrane emulsification, as support of Fe(II) ions was tested in order to prepare potential Fenton catalysts to be used for the treatment of phenol effluents. The advantage of designing this catalytic system would be its expected easy recovery through MF or UF, both low-pressure membrane processes.

In order to test the viability of the proposed alternative, several experimental steps were programmed. The first one consisted in the formulation of stable O/W emulsions without Fe(II) presence in order to investigate the influence of the membrane emulsification variables on the properties of the obtained emulsions. Once the flexibility and characteristics of the system studied were established, the preparation of Fe(II)-containing emulsions was carried out. This part included, as explained in Chapter 3, not only the preparation of emulsions with Fe(II)-containing continuous phases but also the further support of iron onto emulsions prepared without Fe(II) dissolved in the continuous phase. In this case, the original continuous phase of the emulsions (W_o) was replaced by Fe(II) aqueous solutions, acting as the new continuous phase (W_n). The third and last step consisted in testing the efficiency of the emulsions to treat phenol aqueous solutions. The protocol designed for the preparation of the emulsions and their use as Fenton catalyst is explained in detail in Chapter 3 although some additional remarks are given in the following sections.

8.2. Formulation of O/W emulsions

8.2.1. Effect of the stirring rate and membrane pore size on the emulsion properties

The study of the effect of the stirring rate on the properties of the prepared emulsions was carried out with 2% SDS aqueous solution as W_o . The percentage of oil-in-water (%O/W) was 10% in all experiments and the tested stirring rates varied from 583 to 2333 rpm. Two metallic membranes (10 and 20 μm) were used to test the effect of the membrane pore size on the final characteristics and stability of the obtained emulsions.

Figure 8.1 shows the effect of the stirring rate on the mean droplet diameter. In particular, Figure 8.1 illustrates the $D[3,2]$, $D[4,3]$ and Span of the recently prepared emulsions obtained with the stirred cell using the two metallic membranes. As it can be seen, for both membrane pore sizes, the higher the stirring rate, the lower the mean droplet diameter. This can be ascribed to the higher shear stress at the vicinities of the membrane, causing a higher degree of detachment of the oil droplets per time unit. The Span is slightly higher at lower stirring rate, which indicates that droplet distribution was widened at these conditions. The emulsion stability was evaluated by comparing initial $D[3,2]$, $D[4,3]$ and Span with those measured after 7 days. Table 8.1 shows the ESI for emulsions obtained using 10 μm and 20 μm metallic membranes. The results show that emulsions prepared at stirring rate equal or higher than 1750 rpm were very stable when the 10 μm membrane was used. For lower stirring rate, the values of $\text{ESI} > 1$ and $\text{ESI} < 1$ indicate that emulsions are destabilised. In fact, ESI values higher than 1.10 and lower than 0.90 have been considered representative of emulsion instability. The effect is more severe for 20 μm membrane pore size. The prepared emulsions with this membrane were stable at 2333 rpm because, at 1750 rpm, ESI values obtained one week after the preparation of the emulsions were slightly higher than 1.1. However, no phase separation occurred in the observed time. 1750 rpm of stirring rate and the 10 μm metallic membrane were selected for carrying out the rest of experiments presented in the following sections.

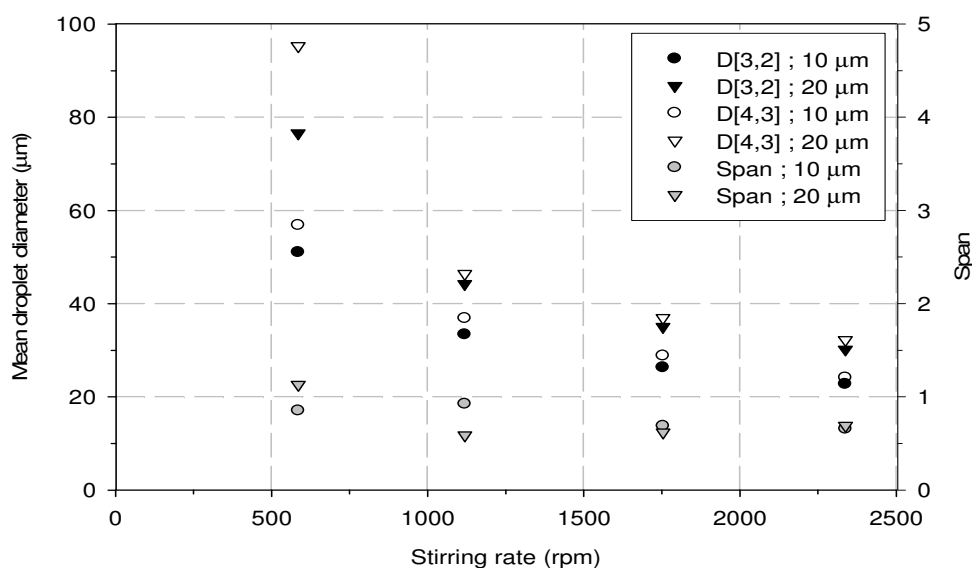


Figure 8.1. Effect of the stirring rate and membrane pore size on the $D[3,2]$, $D[4,3]$ and Span. 10% O/W ; 2% SDS in W_o

Table 8.1. Effect of the stirring rate and membrane pore size on ESI.
 10% O/W ; 2% SDS in W_o

Stirring rate (rpm)	10 μm membrane		
	ESI _{D[3,2]}	ESI _{D[4,3]}	ESI _{Span}
583	0.92	0.97	1.04
1116	1.01	1.11	1.06
1750	0.99	0.95	0.92
2333	1.00	1.00	1.00

Stirring rate (rpm)	20 μm membrane		
	ESI _{D[3,2]}	ESI _{D[4,3]}	ESI _{Span}
583	1.01	1.16	1.54
1116	1.06	1.19	1.50
1750	1.05	1.11	1.08
2333	1.01	1.02	1.02

8.2.2. Effect of the SDS concentration on the emulsion properties

This section shows the emulsions' characteristics as a function of the SDS weight percentage (%SDS) in the W_o . The %SDS was varied from 0.2 to 2%. 10 %O/W emulsions were prepared using the 10 μm metallic membrane in the stirred cell at 1750 rpm of stirring rate. Figure 8.2 shows the effect of the %SDS on the D[3,2], D[4,3] and Span of the formulated emulsions.

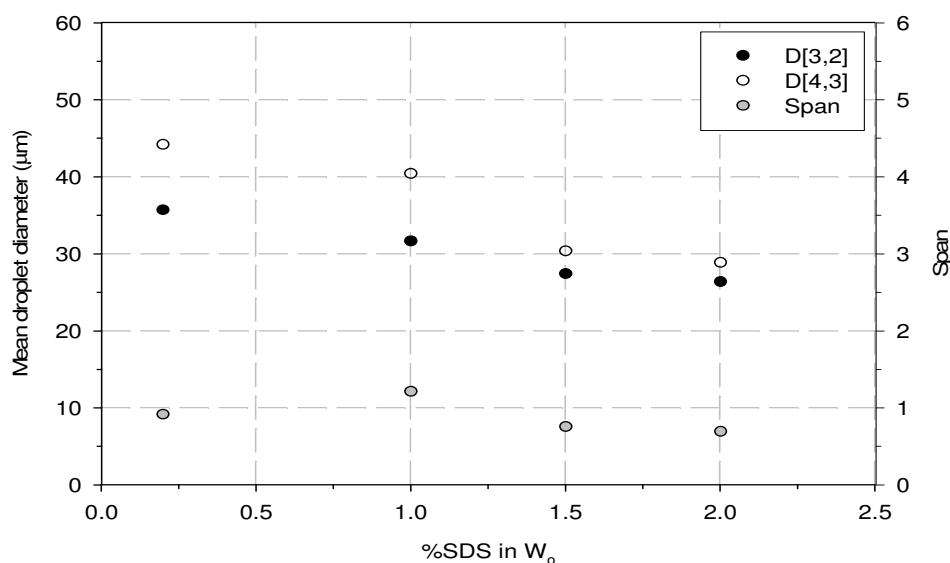


Figure 8.2. Effect of the %SDS in W_o on the D[3,2], D[4,3] and Span.
 10% O/W ; 10 μm metallic membrane ; 1750 rpm

As it can be seen in Figure 8.2, the mean droplet diameter decreases when the emulsifier concentration is increased. In particular, the major change is obtained between 0.2 and 1.5% SDS while, between 1.5 and 2%, the droplet properties are quite similar. This behaviour is due to the decrease of interfacial tension with increasing the emulsifier concentration (Joscelyne and Trägårdh 2000). In fact, the emulsion droplet formation and detachment is governed by the balance between the interfacial tension force and the shear force exerted by the continuous phase. Since in these experiments the shear force was constant, droplet size distribution changed due to the interfacial tension decrease. This effect is more significant at 0.2% SDS, when separation of oil phase after emulsion preparation was observed. This behaviour can be mainly due to the fact that a SDS concentration lower than its critical micellar concentration (0.24% w/w) was used (Joscelyne and Trägårdh 2000; Gasparini et al. 2008). As shown in Table 8.2, the emulsion prepared with 2% SDS was the most stable compared the others because its ESI values are closer to 1.

*Table 8.2. Effect of the %SDS in W_o on ESI.
 10% O/W ; 10 μ m metallic membrane ; 1750 rpm*

%SDS in W_o	ESI _{D[3,2]}	ESI _{D[4,3]}	ESI _{Span}
0.2	0.97	0.88	0.71
1	0.97	0.88	0.77
1.5	0.96	0.92	0.83
2	0.99	0.95	0.92

8.2.3. Effect of the %O/W on the emulsion properties

2% SDS in W_o was employed to prepare O/W emulsions at different %O/W in the stirred cell at 1750 rpm. Figure 8.3 shows the D[3,2], D[4,3] and Span of the prepared emulsions as a function of the %O/W.

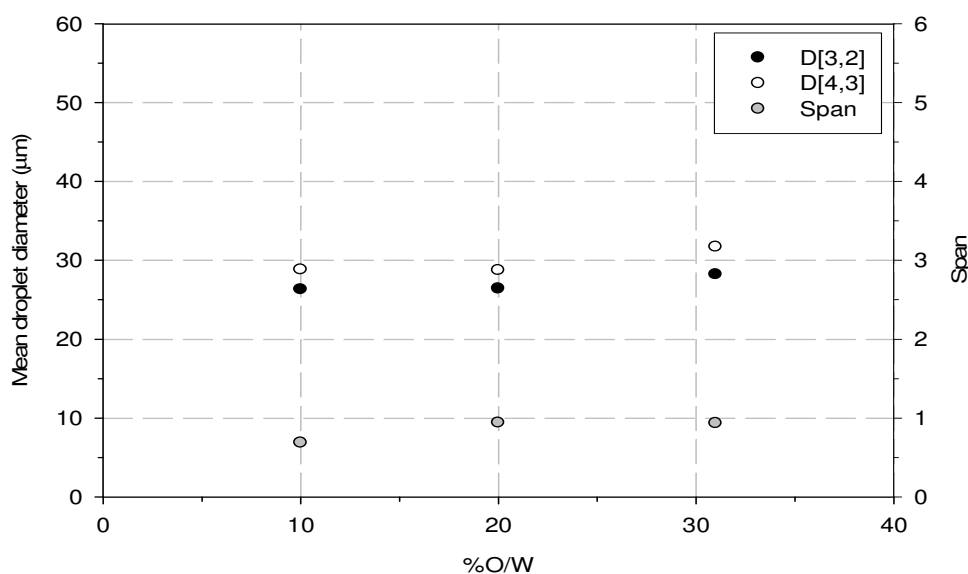


*Figure 8.3. Effect of the %O/W on the D[3,2], D[4,3] and Span.
 2% SDS ; 10 μ m metallic membrane ; 1750 rpm*

As Figure 8.3 illustrates, an increase on the %O/W from 10 to 20% does not significantly modify the $D_{[3,2]}$ and $D_{[4,3]}$ of the obtained emulsions while they are slightly higher for the 31% O/W emulsion. Contrarily, the Span increases when passing from 10 to 20% O/W remaining almost constant afterwards. Less SDS is available per oil volume unit at higher %O/W and, consequently, larger droplets are produced, which agrees with literature data (Berot et al. 2003). Even though $D_{[3,2]}$, $D_{[4,3]}$ and Span are slightly increased at high %O/W, none of the emulsions was found to be broken during one week of observation. Table 8.3 shows that ESI values slightly increase with the %O/W. However, they are inside 1.00 ± 0.10 , which has not been considered a destabilisation indicator, as abovementioned. This agrees with the fact that emulsions' instability was not visually observed regardless of the %O/W.

Table 8.3. Effect of the %O/W on ESI.
 2% SDS ; 10 μm metallic membrane ; 1750 rpm

%O/W	ESI _{D[3,2]}	ESI _{D[4,3]}	ESI _{Span}
10	0.99	0.95	0.92
20	0.99	0.99	0.94
31	1.02	1.09	1.09

8.3. Formulation of ferrous O/W emulsions

Two operation modes have been explored to investigate the effect of the presence of Fe(II) in the final properties of O/W emulsions. The first methodology deals with the addition of Fe(II) in the initial continuous phase (W_o) together with 2% SDS. The second one is devoted to replace the separated aqueous phase of a previously prepared emulsion for a new Fe(II) aqueous solution (W_n). Both strategies were tested and the results obtained are presented and discussed in Sections 8.3.1 and 8.3.2.

8.3.1. Formulation of emulsions with iron-containing W_o

The emulsions presented in this section were prepared with the stirred cell emulsification set-up at a constant stirring rate of 1750 rpm and employing the 10 μm metallic membrane. The %SDS was 2% and the %O/W 10%, unless otherwise noted. Thus, the only variable changed during the experiments was the Fe(II) concentration ([Fe(II)]) in W_o .

Figure 8.4 shows the behaviour of $D_{[3,2]}$, $D_{[4,3]}$ and Span as a function of time for emulsions prepared with different [Fe(II)]. This figure also includes the properties of the emulsion prepared without Fe(II) in the W_o , identified by a dashed line. Table 8.4 summarises the ESI values and the actual %O/W for one week-aged emulsions as well as the final [Fe(II)] in the continuous phase of the prepared emulsions.

The emulsion prepared with a W_o containing the highest [Fe(II)] tested, this is 133 mg/L, broke just in few hours after its formulation. After one week, the existing %O/W of the remaining emulsion was only 1.4%, as shown in Table 8.4. Figure 8.4 shows that, at this [Fe(II)] in W_o , $D_{[3,2]}$ increased from 30.1 to 33.8 μm and $D_{[4,3]}$ increased from 35.9 to 53.5 μm in one week. Similarly, Span increased from 1.2 to 3.3.

When no Fe(II) was present in the W_o , $D[3,2]$, $D[4,3]$ and Span were $26.1 \mu\text{m}$, $28.0 \mu\text{m}$ and 0.65 , respectively. This difference on the emulsions' behaviour can be explained by the charge interactions between Fe(II) ions and the negatively charged emulsion droplets, made of SDS, which is an anionic surfactant. Mei et al. (1998) demonstrated, by using zeta potential measurements, that Fe(II) and Fe(III) ions were associated with emulsion droplets prepared with SDS as emulsifier due to the electrostatic attractions occurring between them and the charged interface of the emulsion droplets. Similarly, other studies have dealt with the association of calcium ions with emulsion droplets, causing similar destabilisation phenomena (Ríos et al. 1998; Keowmaneechai and McClements 2006). Thus, the results obtained can be explained by partial charge neutralisation of the emulsion droplets, which causes their destabilisation.

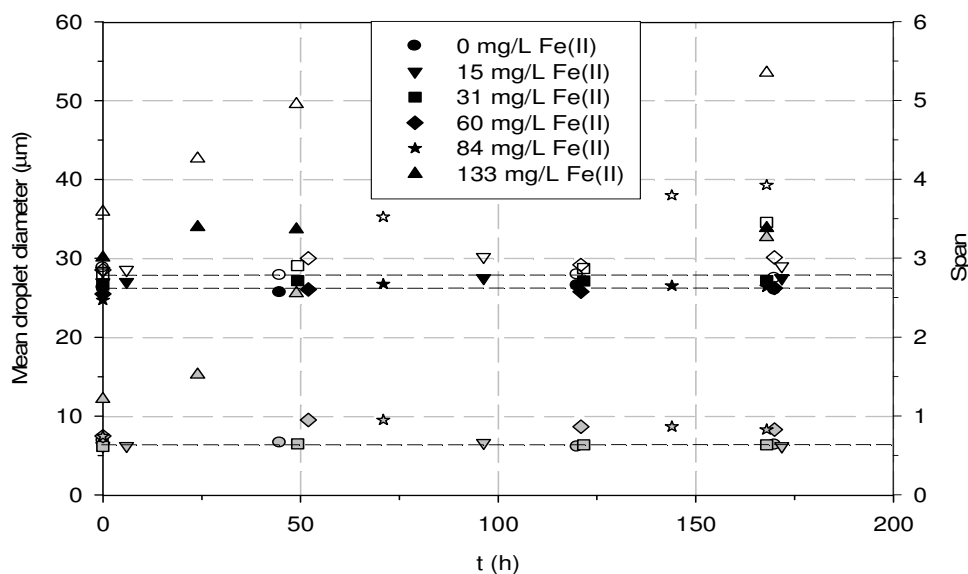


Figure 8.4. Effect of the $[Fe(II)]$ in W_o on the $D[3,2]$, $D[4,3]$ and Span evolution. 10% O/W ; 2% SDS ; $10 \mu\text{m}$ metallic membrane ; 1750 rpm. Black symbols represent $D[3,2]$, open symbols $D[4,3]$ and grey symbols Span

Table 8.4. Effect of the $[Fe(II)]$ in W_o on ESI, remaining %O/W and final $[Fe(II)]$ in W . 10% O/W ; 2% SDS ; $10 \mu\text{m}$ metallic membrane ; 1750 rpm

$[Fe(II)]$ in W_o (mg/L)	$ESI_{D[3,2]}$	$ESI_{D[4,3]}$	ESI_{Span}	Emulsion breakage?	%O/W	$[Fe(II)]$ (mg/L)
0	0.99	0.95	0.92	No	10	0
15	1.02	1.02	1.00	No	10	12
31	1.02	1.02	1.03	No	10	28
60	1.03	1.06	1.11	7 th day	7.1	n.m.
84	1.07	1.45	1.11	6 th day	3.2	n.m.
133	1.12	1.49	2.60	1 st day	1.4	n.m.

n.m.: not measured due to emulsion destabilisation

When 84 mg/L Fe(II) or 60 mg/L Fe(II) were present in W_o , the resultant emulsions were also broken six and seven days after their formulation, respectively. The remaining %O/W was 3.2 and 7.1% when 84 and 60 mg/L Fe(II) were present in W_o , respectively, as shown in Table 8.4. In both emulsions, $D[3,2]$ remained practically invariable along the time and very close to the $D[3,2]$ of the emulsion prepared without Fe(II) in W_o . Nonetheless, Span and $D[4,3]$ values slightly increased along the observation time, being the indicator of emulsion destabilisation. ESI values, summarised in Table 8.4, were higher than 1.10, which agrees with the emulsion destabilisation observed.

For 31 and 15 mg/L Fe(II), the emulsions remained stable and their droplet size distributions unchanged along one week. As Table 8.4 shows, the %O/W of both emulsions was constant and equal to 10% and the [Fe(II)] in the prepared emulsions after one week was 28 and 12 mg/L, respectively. Thus, even though Fe(II) destabilises the emulsions, it is possible to obtain stable emulsions in presence of Fe(II) below 31 mg/L. Taking into account the differences between the initial and final [Fe(II)], summarised in Table 8.4, around 27 mg Fe(II) per litre of emulsified oil were linked to the emulsion droplets' interface.

The effect of the presence of Fe(II) in W_o was also studied at several %O/W. During the preparation of the emulsions, [Fe(II)] in W_o was 15 mg/L and the rest of the emulsification variables remained constant and equal to those used for performing the previous experiments. Thus, 2% SDS was present in W_o together with Fe(II), the stirred emulsification cell was selected for preparing the emulsions at 1750 rpm of stirring rate and the 10 μm metallic membrane was chosen. $D[3,2]$, $D[4,3]$ and Span of the prepared emulsions are shown in Figure 8.5. As it can be seen, their behaviour is similar to that observed for experiments carried out without iron in the continuous phase, whose results were shown in Figure 8.3. However, in the present case, the change on $D[4,3]$ and Span is more evident.

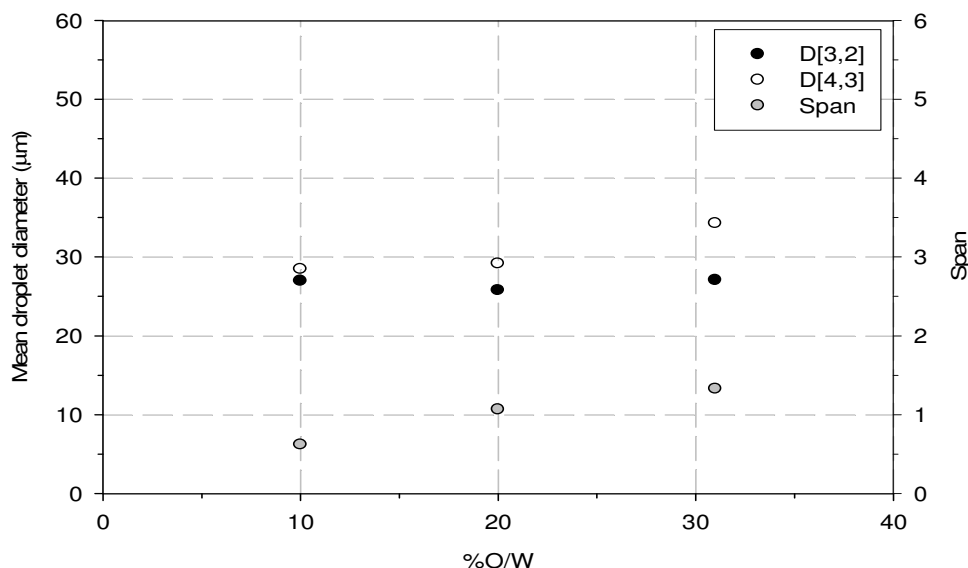


Figure 8.5. Effect of the %O/W on the $D[3,2]$, $D[4,3]$ and Span of emulsions prepared with Fe(II) in W_o . 10% O/W ; 2% SDS ; 15 mg/L Fe(II); 10 μm metallic membrane ; 1750 rpm

Table 8.5 reports ESI values of the emulsions after one week. Neither D[3,2], D[4,3] nor Span underwent significant changes along one week but, when 31% emulsion was produced, three days after the emulsion formulation, free oil was visually detected. As the droplets of the 31% O/W emulsion were originally larger, they were more sensitive to be destabilised by coalescence and, finally, breakage, giving a final %O/W of 18%. Therefore, even though ESI is practically 1, the emulsion was actually not stable, as %O/W indicates. On the other hand, as Table 8.5 shows, neither 10% nor 20% O/W emulsions containing 15 mg/L Fe(II) in the W_o were destabilised and their properties remained unaltered (ESI~1 and %O/W constant) at least during the observation period. Regarding the remaining [Fe(II)] in the emulsion continuous phase, Table 8.5 demonstrates that, for the 10% and 20% O/W emulsions, 12 and 9.3 mg/L Fe(II) remained in the continuous phase after one week. For 10% O/W emulsion, this represents a presence of 27 mg Fe(II) per litre of emulsified oil, as exposed before. For 20% O/W emulsion, this ratio slightly decreases to 26 mg Fe(II) per litre of emulsified oil. Thus, the mass of Fe(II) linked to the emulsion droplets per litre of emulsified oil can be assumed to be between 26 and 27 mg/L.

Table 8.5. Effect of the %O/W on ESI, remaining %O/W and final [Fe(II)] in W_o . 10% O/W ; 2% SDS ; 15 mg/L Fe(II) ; 10 μ m metallic membrane ; 1750 rpm

%O/W	ESI _{D[3,2]}	ESI _{D[4,3]}	ESI _{Span}	Emulsion breakage?	%O/W	[Fe(II)] (mg/L)
10	1.02	1.02	1.00	No	10	12
20	0.96	0.94	0.97	No	20	9.3
31	1.05	1.01	1.02	3 rd day	18	n.m.

n.m.: not measured due to emulsion destabilisation

8.3.2. Addition of iron to previously-prepared emulsions

The effect of the presence of Fe(II) and its concentration on the stability and properties of previously-produced O/W emulsions is discussed in this section. In the experiments presented, the initial emulsions were prepared without Fe(II) in W_o . After this, the emulsions were left to separate and the continuous phase was replaced by an Fe(II) aqueous solution (W_n). The difference between this type of experiments and those carried out with Fe(II) in W_o is that, replacing the continuous phase by W_n , almost no free SDS remained in the continuous phase and the Fe(II) could not be thus trapped by free negatively-charged SDS molecules. Hence, the effect of the presence of free SDS molecules (or micelles) is also considered in this section. In addition, some of the emulsions were obtained by crossflow membrane emulsification with a 0.5 μ m ceramic membrane. This way, the effect of the [Fe(II)] in W_n was examined with emulsions having smaller mean droplet diameters. The replacement of the emulsions' continuous phase was also carried out when no Fe(II) was present in the new continuous phase (W_n). For this, the original continuous phases of the prepared emulsions were removed and replaced by ultrapure water. Hence, the effect of the intrinsic instability, which might arise from the elimination of the emulsifier from the continuous phases, was considered. This blank experiment allowed discussing the destabilisation phenomena occurring when W_o is replaced by Fe(II)-containing W_n . All the emulsions prepared had a %O/W equal to 10% and the %SDS in W_o was 2%. The emulsions prepared in the

stirred cell were made at 1750 rpm and those obtained in the crossflow membrane emulsification set-up were formulated at 760 mL/min of continuous phase flowrate. This flowrate corresponds to a continuous phase tangential velocity in the membrane lumen of 0.33 m/s.

Figure 8.6 shows the $D[3,2]$, $D[4,3]$ and Span evolution in front of time at several $[Fe(II)]$ in W_n and it also includes those of the virgin emulsion, therefore, when no continuous phase replacement was performed. As it can be seen, when the W_n did not contain $Fe(II)$ (blank experiment) or contained 0.44 mg/L $Fe(II)$, neither $D[3,2]$, $D[4,3]$ nor Span differed from the values of the virgin emulsion, represented by a dashed line. Thus, no instabilities were observed when removing surfactant molecules from the continuous phase and when this was carried out in parallel with the addition of $Fe(II)$ at low concentration. However, when 5.1 or 15 mg/L $Fe(II)$ were present in W_n , $D[3,2]$ and $D[4,3]$ decreased during the first hours after the continuous phase replacement. Span values remained practically unchanged after the substitution of the continuous phase by an $Fe(II)$ -containing W_n , regardless of the $[Fe(II)]$ in W_n .

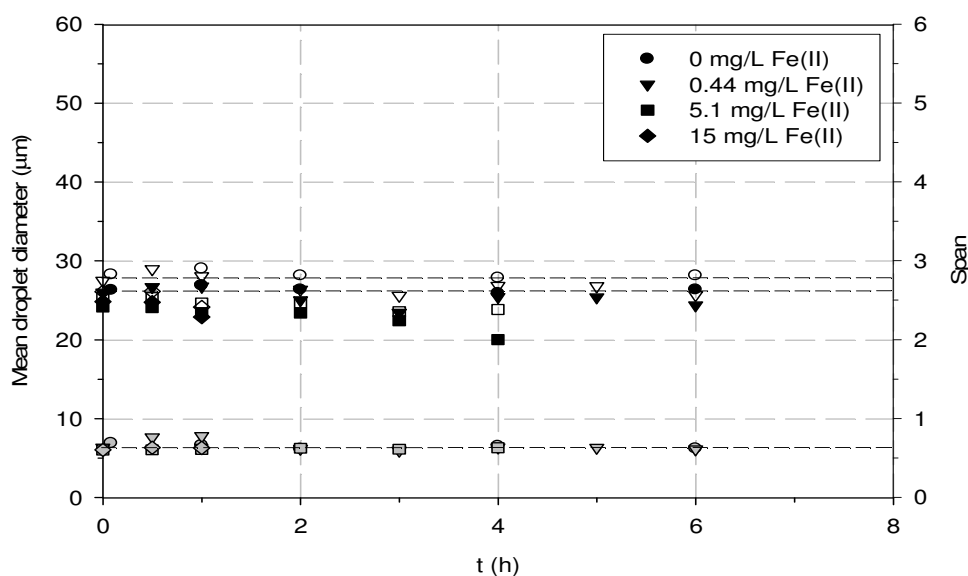


Figure 8.6. Effect of the $[Fe(II)]$ in W_n on the $D[3,2]$, $D[4,3]$ and Span evolution. 10% O/W ; 2% SDS in W_o ; 10 μ m metallic membrane ; 1750 rpm. Dashed lines represent mean values of the virgin emulsions. Black symbols represent $D[3,2]$, open symbols $D[4,3]$ and grey symbols Span

Figure 8.7 shows the evolution of the %O/W along the time as an indicator of the emulsion breakage due to the presence of $Fe(II)$ in W_n . It can be noticed that, when no $Fe(II)$ was present in W_n (blank experiment), no emulsion destabilisation occurred and the emulsion behaved as the virgin one. However, no matter the $[Fe(II)]$ in W_n , %O/W reduction occurred during the first hours after the continuous phase exchange and, therefore, emulsion breakage was observed. These results suggest that $Fe(II)$ cations were linked to the emulsion droplets causing an increase on their instability due to the reduction of the repulsion forces existing between them, as explained in the previous section. Figure 8.7 demonstrates that, as the $[Fe(II)]$ in W_n increased, emulsion breakage occurred earlier. For instance, at 0.44 mg/L $Fe(II)$ in W_n , the %O/W decreased down to around 7.5% during the first six hours after the continuous phase exchange. After one week, the %O/W of this emulsion was 5.9%. At 5.1 and 15 mg/L $Fe(II)$ in W_n , total breakage of the emulsion occurred five and one hour after the continuous phase exchange, respectively. Thus, $[Fe(II)]$ in W_n strongly affects the

stability of previously-formulated O/W emulsions. Comparing the previous results to those of the stability of O/W emulsions produced with Fe(II)-containing W_o , at the same [Fe(II)], these latter were more stable than the former. SDS molecules (or micelles), present in the continuous phase when Fe(II) was dissolved in W_o , could attract Fe(II) cations. However, when Fe(II) was dissolved in W_n , where nearly no free SDS molecules were present, Fe(II) cations were more available to be attracted by the droplets' interface and, in consequence, lessen emulsion stability.

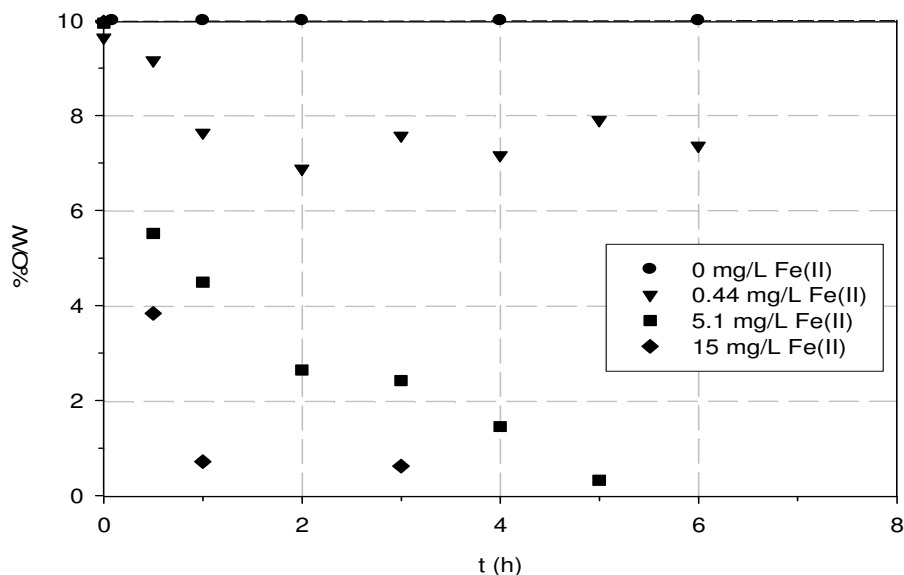


Figure 8.7. Effect of the [Fe(II)] in W_n on the %O/W evolution. 10% O/W ; 2% SDS in W_o ; 10 μm metallic membrane ; 1750 rpm. Dashed line represents mean values of the virgin emulsions

Emulsions obtained in the crossflow membrane emulsification device, equipped with a 0.5 μm ceramic membrane were also prepared without Fe(II) in W_o . The emulsions' continuous phases were replaced by Fe(II)-containing aqueous solutions so that the effect of the [Fe(II)] in W_n on the emulsions' stability could be evaluated in emulsions having smaller mean droplet diameter. The original emulsions obtained in crossflow mode had a D[3,2] of 5.8 μm , a D[4.3] of 7.9 μm and a Span of 1.6. The obtained emulsions remained stable during one week because the previous parameters and the %O/W stayed constant. The same values of [Fe(II)] in W_n than with the emulsions obtained in the stirred emulsification cell were considered, this is, 0.44, 5.1 and 15 mg/L Fe(II). The evolution of D[3,2], D[4.3], Span and %O/W were followed along the time to characterise the changes in the emulsion properties and stability. Figure 8.8 shows that the replacement of W_o by a W_n without Fe(II) (blank experiment) did not cause any modification on the mean droplet diameter and Span compared to the virgin emulsion. Thus, the removal of SDS from the W_o (and its replacement by ultrapure water) did not induce destabilisation on the emulsions. This was not observed in the emulsions where their W_o was replaced by Fe(II)-containing W_n , which indicates that destabilisation phenomena occur only when Fe(II) is present.

Figure 8.9 shows the %O/W evolution at the three tested [Fe(II)] in W_n together with the virgin (represented by a dashed line) and blank emulsion. Figure 8.9 demonstrates that the emulsions, after the replacement of their original continuous phases by Fe(II)-containing ones suffered from destabilisation, regardless of the [Fe(II)]. The remaining %O/W one week after the continuous phase replacement was 6.6, 7.5 and 8.3% when

15, 5.1 and 0.44 mg/L Fe(II) aqueous solutions were employed as W_n , respectively. Emulsions' destabilisation may be explained by, as aforementioned, the lower droplet-droplet repulsion forces occurring when Fe(II) is present in the system and thus attracted by the interface of the emulsion droplets.

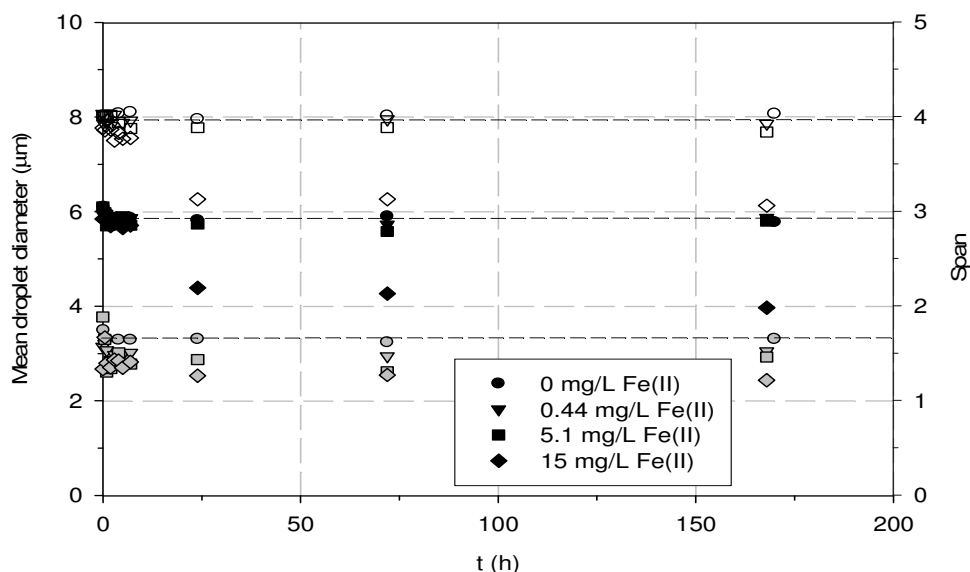


Figure 8.8. Effect of the $[\text{Fe(II)}]$ in W_n on the $D[3,2]$, $D[4,3]$ and Span evolution. 10% O/W ; 2% SDS in W_o ; 0.5 μm ceramic membrane. Dashed lines represent mean values of the virgin emulsions. Black symbols represent $D[3,2]$, open symbols $D[4,3]$ and grey symbols Span

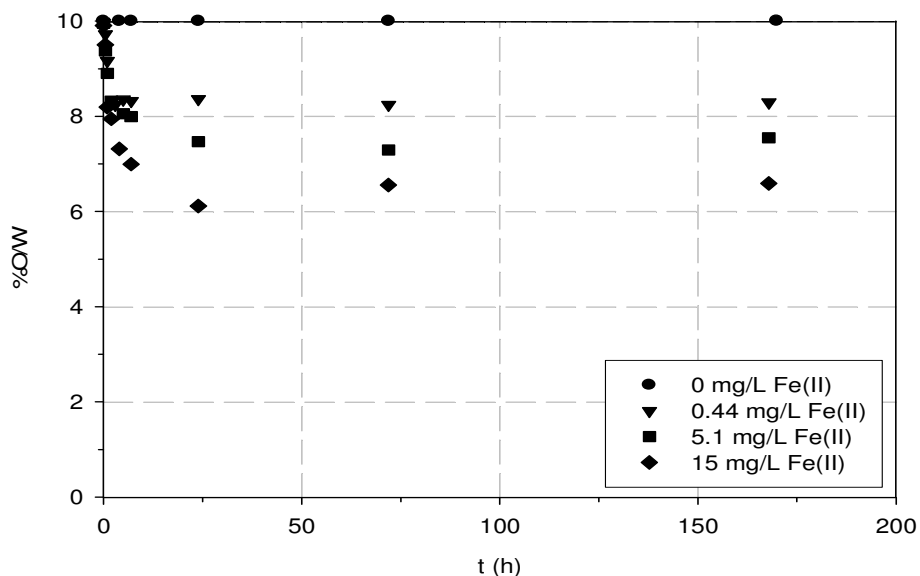
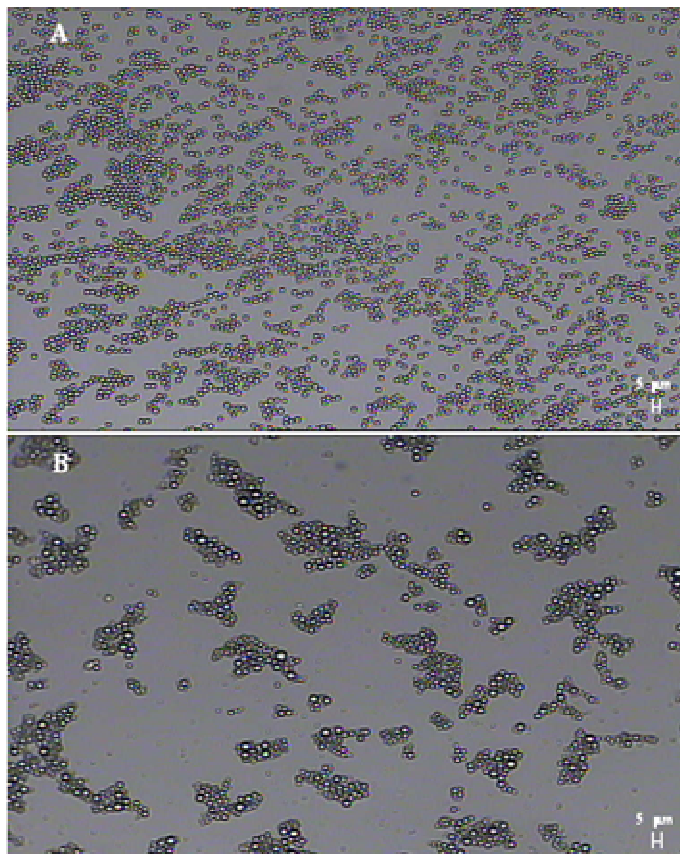


Figure 8.9. Effect of the $[\text{Fe(II)}]$ in W_n on the %O/W evolution. 10% O/W ; 2% SDS in W_o ; 0.5 μm ceramic membrane. Dashed line represents mean values of the virgin emulsions

Figure 8.10 shows optical micrographs of both the virgin emulsion obtained in crossflow mode (Figure 8.10A) and after replacing its continuous phase by a 15 mg/L W_n (Figure 8.10B). It is evident that, when Fe(II) is present, droplets agglomerate due

to the lower charge repulsion between them, which can be the starting point for coalescence and result, at the end, in emulsion rupture. Instead, when no Fe(II) is present, agglomeration between droplets is not observed. Thus, the observations support the proposed destabilisation mechanism based on the decrease on the droplets' charge and, consequently, on the droplet-droplet repulsions when Fe(II) is present due to its electrostatic attraction towards the droplets' interface. Comparing the response of the larger-droplet-size emulsions to that of the smaller ones, it can be deduced that, the former are more negatively affected by Fe(II) ions and thus easily broken at the same [Fe(II)] in W_n than the latter. Hence, not only the [Fe(II)] in W_n is an important parameter affecting the emulsion stability but also the original droplet size plays a crucial role on it.



*Figure 8.10. Optical micrographies at 20x of a virgin emulsion (A) and after replacing its continuous phase by a 15 mg/L Fe(II) solution (B).
10% O/W ; 2% SDS in W_o ; 0.5 μ m ceramic membrane*

8.4. Oxidation of phenol effluents with ferrous emulsions

The emulsions formulated with iron in their initial continuous phase were tested as catalysts for the oxidation of phenol solutions. The concentrations of iron (II) in W_o ranged from 15 to 84 mg/L. The emulsions were prepared in the stirred membrane emulsification device at 10%O/W, with 2%SDS in W_o and at 1750 rpm. Additionally, an emulsion without iron was formulated. The properties of the prepared emulsions were presented in Section 8.3.1. The oxidation of 1000 mg/L phenol was carried out using 5000 mg/L H_2O_2 in a batch reactor at 20°C and 50 rpm of stirring rate for 120 min, as explained in Chapter 3. A %O/W equal to 10% was ensured in the reactor in order to

avoid possible instabilities arising from %O/W variations. Figure 8.11 represents the average phenol removal when the emulsions prepared at several $[Fe(II)]$ in W_o were used as catalyst. In addition, this figure shows the results obtained with the blank emulsion test (represented by a dashed line) that consisted on subjecting an emulsion prepared without $Fe(II)$ at the same reaction protocol than when $Fe(II)$ -containing emulsions were tested.

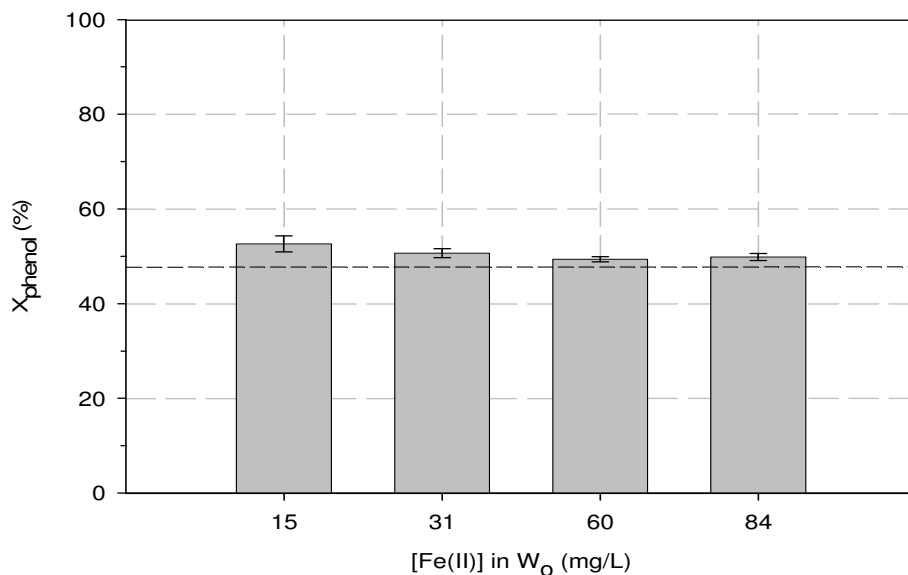


Figure 8.11. Effect of the $[Fe(II)]$ in W_o on the average phenol removal. 10% O/W ; 2% SDS in W_o ; 10 μm metallic membrane ; 1750 rpm. Fenton conditions: 1000 mg/L phenol ; 5000 mg/L H_2O_2 ; 20 $^{\circ}C$; 50 rpm ; 120 min. Dashed line represents the blank experiment results

As Figure 8.11 shows, phenol removal measured at several $Fe(II)$ concentrations in W_o was independent of the $Fe(II)$ content in the continuous phase used to formulate the emulsions. It must be pointed out that $47.7 \pm 0.4\%$ phenol removal was achieved when no $Fe(II)$ was present in the emulsion droplets (blank test). This indicates that, at these conditions, phenol was partially transferred from the bulk solution to the oil phase. When $Fe(II)$ was present in the emulsions, no significant differences on the phenol removal percentage were observed compared to the blank test. Thus, it cannot be distinguished whether phenol degradation took place or phenol removal was simply due to its partition between phases. In fact, additional experiments would be needed to investigate if phenol removal would be enhanced at higher $Fe(II)$ concentrations in W_o as result of the Fenton oxidation. For this, it would be necessary to develop other emulsion systems able to remain stable at higher $Fe(II)$ concentrations. Anyway, in the present system, taking into account that around 27 mg $Fe(II)$ per litre of emulsified oil were confined in emulsion droplets, around 2.7 mg/L $Fe(II)$ were used as catalyst in the oxidation tests. Thus, a mass ratio $Fe(II):H_2O_2$ of $5.4 \cdot 10^{-4}$ was used for the oxidation experiments with Fe -containing emulsions. As shown in Chapter 6, when phenol effluents were oxidised in homogeneous phase at the stoichiometric hydrogen peroxide concentration needed to completely mineralise initial phenol, a ratio $Fe(II):H_2O_2$ of $5.6 \cdot 10^{-4}$ was selected. Thus, the oxidation conditions used with Fe -containing emulsions are not far away from those used in homogeneous mode. However, as Fe -emulsion droplets are heterogeneous-like catalysts, its activity is expected to decrease compared to the homogeneous conditions. Thus, experiments conducted at higher $Fe(II)$ concentration in W_o would be needed and, as abovementioned, this would imply

working with emulsions exhibiting higher stability and capacity for Fe(II) confining than those developed in this thesis.

The stability of the emulsions subjected to oxidation and that of the blank one was assessed. The ESI values calculated after the oxidation was completed are summarised in Table 8.6. This table also collects the characterisation of the original emulsions without performing over them neither phase separation nor oxidation.

Table 8.6. Effect of the [Fe(II)] in W_o on ESI of emulsions tested for phenol oxidation. 10% O/W ; 2% SDS ; 10 μ m metallic membrane ; 1750 rpm. Fenton conditions: 1000 mg/L phenol ; 5000 mg/L H_2O_2 ; 20 $^\circ$ C ; 50 rpm ; 120 min

Emulsion stability after 7 days (no oxidation)				
[Fe(II)] in W_o (mg/L)	ESI_{D[3,2]}	ESI_{D[4,3]}	ESI_{Span}	Emulsion breakage?
0	0.99	0.95	0.92	No
15	1.02	1.02	1.00	No
31	1.02	1.02	1.03	No
60	1.03	1.06	1.11	7 th day
84	1.07	1.45	1.11	6 th day
Emulsion stability after oxidation (120 min)				
[Fe(II)] in W_o (mg/L)	ESI_{D[3,2]}	ESI_{D[4,3]}	ESI_{Span}	Emulsion breakage?
0 (blank)	0.96	0.94	0.91	No
15	1.12	1.18	1.26	No
31	1.14	1.23	1.54	No
60	1.21	2.92	3.84	Yes
84	1.42	3.21	4.80	Yes

As Table 8.6 demonstrates, the instability of the emulsions which showed to be unstable seven days after their formulation, i.e. those prepared with 60 and 84 mg/L Fe(II) in W_o , was worsened when the emulsions were used in oxidation experiments. For the emulsions containing iron in their W_o which were stable in its original state even seven days after their preparation, corresponding to those prepared with 15 and 31 mg/L Fe(II) in W_o , their stability was also worsened when they were used in oxidation tests because their ESI values differed from those exhibited when they were not used as catalysts. For instance, the emulsion prepared with 31 mg/L Fe(II) in W_o was found to have an ESI_{Span} of 1.03. This value was increased to 1.54 after use in oxidation. In general, with the exception of the blank emulsion, whose stability was unaffected during the test, all the emulsions decreased their stability, even if, in some of them, no visual instability was observed. In fact, the results agree with what could have been expected from phenol+surfactant Fenton oxidations experiments presented

in Chapter 7. As the tested emulsions are composed of SDS, a degradable compound by the Fenton process, emulsion droplets are susceptible to be degraded and thus destabilised during the oxidation of phenol solutions.

8.5. Conclusions

Membrane emulsification, operated in a dispersion cell or in a crossflow set-up, has demonstrated to be an efficient technology to formulate stable O/W emulsions. Parameters such as surfactant percentage, stirring speed (when the dispersion cell set-up was used), percentage of O/W and membrane pore size have been found to significantly affect the final droplet size distribution and emulsion stability.

The stability of O/W emulsions is strongly affected by the presence of Fe(II) dissolved in the continuous phase. It was found that the maximal tested Fe(II) concentration that did not cause emulsion breakage during one week was 31 mg/L with a 10% O/W emulsion prepared with 2% SDS. Destabilisation occurring in presence of Fe(II) cations is probably due to the attraction of Fe(II) towards the negatively-charged emulsion droplets' interface. The interfacial charge of emulsion droplets is then decreased and charge repulsions between emulsion droplets accordingly diminished, causing coalescence and even rupture. Free negatively-charged SDS molecules and/or micelles in the emulsions' continuous phase have been found to be possible Fe(II) attractors. Experiments based on the removal of free SDS from the continuous phase and subsequent addition of Fe(II)-containing solutions demonstrated that the absence of free SDS caused an increase on the emulsions' instability. On the contrary, the absence of free SDS in emulsions formulated without Fe(II) did not destabilize the droplets. Thus, it is evident that free SDS can act as emulsion breakage retardant (or even evader) when Fe(II) is present in the continuous phase.

The droplet size of the emulsions also plays a crucial role on their stability when Fe(II) is present in the continuous phase. Emulsions with larger droplet diameters are more sensitive to be broken in presence of Fe(II) in the continuous phase. Thus, not only the Fe(II) concentration and presence of free SDS molecules (or micelles) in the continuous phase are important variables affecting the stability of O/W emulsions but also the droplet diameter.

Emulsions prepared with Fe(II) dissolved in the initial continuous phase were selected for oxidising 1000 mg/L phenol solutions with 5000 mg/L H₂O₂ for 120 min at 20°C. The results showed that phenol removal occurred at the same degree, regardless of the Fe(II) concentration in the original continuous phase. A blank oxidation test, carried out with an emulsion prepared without Fe(II), demonstrated that a negligible increase on phenol removal from the bulk solution occurred when Fe(II) was present in the emulsion droplets. Hence, the results seem to indicate that phenol is not removed by an oxidative mechanism at the tested conditions but as result of its partition between the continuous and dispersed phase. The emulsions containing Fe(II) which were used as phenol degradation catalyst were all destabilised during the oxidation tests. This can be due to the possible simultaneous degradation of the emulsifier (SDS) by the Fenton process, as proven in Chapter 6, which would cause emulsion destabilisation. To sum up, seeking alternative emulsifiers with increased resistance to be oxidised and higher Fe(II) confining capacity is needed for assuring the feasibility of using catalytic emulsions for the degradation of phenol effluents by the Fenton process.

UNIVERSITAT ROVIRA I VIRGILI

TREATMENT OF BIOREFRACTORY WASTEWATER THROUGH MEMBRANE-ASSISTED OXIDATION PROCESSES

Xavier Bernat Camí

ISBN:978-84-693-1529-3/DL:T-652-2010

CHAPTER 9

Fenton treatment of phenol effluents in an inert membrane reactor

9.1. Introduction

One of the drawbacks of the Fenton process is the waste of hydrogen peroxide through its self-decomposition and radical scavenging effect occurring at high oxidant concentration. Some authors have attempted to solve this problem by performing periodical additions of oxidant along the process. This process configuration has shown to increase hydrogen peroxide usage and the oxidation efficiency has been found to be related to the frequency of the oxidant injections and their concentration (Bremmer et al. 2006; Guimarães et al. 2008; Monteagudo et al. 2009; Zazo et al. 2009).

In this thesis, in order to increase the H_2O_2 usage in the treatment of phenol effluents by means of the Fenton oxidation, a tubular reactor with lateral injections of oxidant was designed and its efficiency assessed. A tubular ceramic UF membrane was selected as reactor because its porous structure allowed continuously feeding the oxidant through its wall. The hydrogen peroxide entered from the shell to the lumen of the membrane, where phenol and iron(II) flowed through. Thus, in the membrane lumen, the Fenton oxidation took place. As a result, hydrogen peroxide was kept at low concentration because the oxidant was step by step consumed as the effluent progressed through the membrane lumen and accordingly added in a continuous mode. Thus, the efficiency of the hydrogen peroxide usage was expected to be higher than if the oxidant was totally introduced in the reactor inlet together with the pollutant and iron(II).

The feasibility of the membrane reactor configuration was evaluated by considering the influence of several operation variables on the process performance. The impact of the hydrogen peroxide dose, iron(II) concentration and Reynolds number on phenol conversion, TOC conversion and distribution of the intermediates in the reactor effluent was assessed. The oxidation performance in a tubular reactor without lateral injection of hydrogen peroxide was compared to that exhibited by the described membrane reactor. Last but not least, the degradation of effluents composed by phenol oxidation intermediates alone was tested in order to corroborate the phenol oxidation pathway and the refractory nature of each intermediate to the Fenton process.

In all the experiments, the initial phenol concentration in the polluted stream was 5000 mg/L which corresponded, as the flowrates of the oxidant and polluted solution were equal, to an apparent phenol concentration of 2500 mg/L. When the oxidation of an intermediate was tested, its initial apparent concentration was 100 mg/L. From now on, initial concentrations of phenol, intermediate, hydrogen peroxide and iron(II) refers to apparent concentrations and not to their actual value in the reactor inlets. The range of flowrates tested gave always a laminar regime in the reactor. Reynolds number, calculated considering the reactor outlet stream flowrate (Re_{out}), was chosen to describe the flow conditions in the reactor. The reaction tests were performed for 240 min when phenol solutions were oxidised and for 120 min when the oxidation of phenol oxidation intermediates was investigated. In all the experiments performed, after 5 min of oxidation, the steady-state was achieved because all the parameters analysed in the reactor effluents were constant with respect to time on stream in all the following samples. The results presented in this chapter are the average of all the samples withdrawn along the run with the exception of the distribution of phenol oxidation intermediates which was calculated only from the analysis of the last sample of the reactor outlet stream.

9.2. Influence of the hydrogen peroxide dose on the membrane reactor performance

The effect of the hydrogen peroxide dose on the degradation efficiency achieved in the membrane reactor configuration was tested by oxidising 2500 mg/L phenol with 28 mg/L Fe(II) at several hydrogen peroxide doses ranging from 2500 to 25000 mg/L.

Figure 9.1 shows the effect of the oxidant dose on phenol and TOC conversion. As expected, an increase on the hydrogen peroxide dose improved the efficiency of the oxidation process in terms of phenol abatement and mineralisation. Nevertheless, an increase of the oxidant dose between 12500 mg/L and 25000 mg/L only improved phenol conversion from $91.3 \pm 0.9\%$ to $92.3 \pm 0.5\%$, respectively. TOC conversion remained practically constant beyond 7500 mg/L H_2O_2 . It could be accordingly expected that phenol intermediates were deeply oxidised when these oxidant concentrations were overcome because neither phenol nor TOC concentration was further reduced.

The effect of the H_2O_2 dose on the concentration of each family of intermediates over the TOC concentration of the reactor effluent can be seen in Figure 9.2. Figure 9.2 reveals that carboxylic acids' fraction increased as long as the hydrogen peroxide dose was raised. The increase on the carboxylic acids' content could result from the deeper phenol degradation, which would generate a higher fraction of low-chain organic acids. Quinone-like compounds were unaffected by the H_2O_2 dose and they were around 0.6% of the total effluents' TOC regardless of the oxidant dose. The fraction of unidentified compounds increased, as Figure 9.2 shows, with the hydrogen peroxide

dose. The increase of the fraction of unidentified compounds could be due to a raise on the generation of condensation products, which have not been analysed in this thesis, resulting from a higher phenol degradation (Zazo et al. 2005). When the oxidation of phenol in batch mode was studied, which was presented in Chapter 6, the %ID remained practically constant when the hydrogen peroxide dose was increased. The difference on the %ID behaviour cannot be directly compared to those results because the reactors' configuration are not the same (continuous versus batch) and the flow regimes are markedly different (laminar versus perfectly mixed).

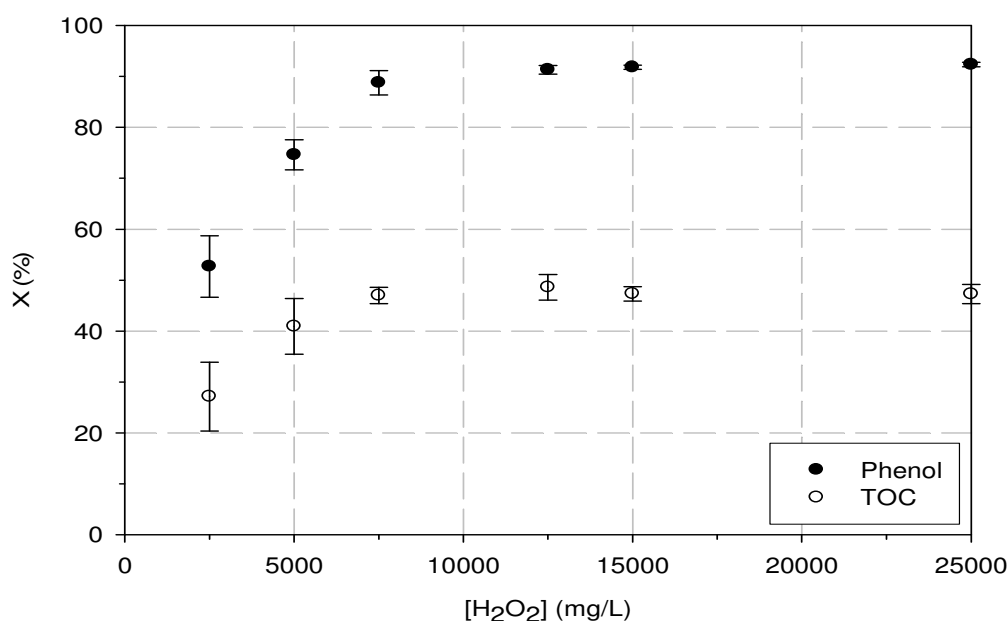


Figure 9.1. Effect of the H₂O₂ dose on phenol and TOC conversion. 2500 mg/L phenol ; 28 mg/L Fe(II) ; Re_{out}=2.5

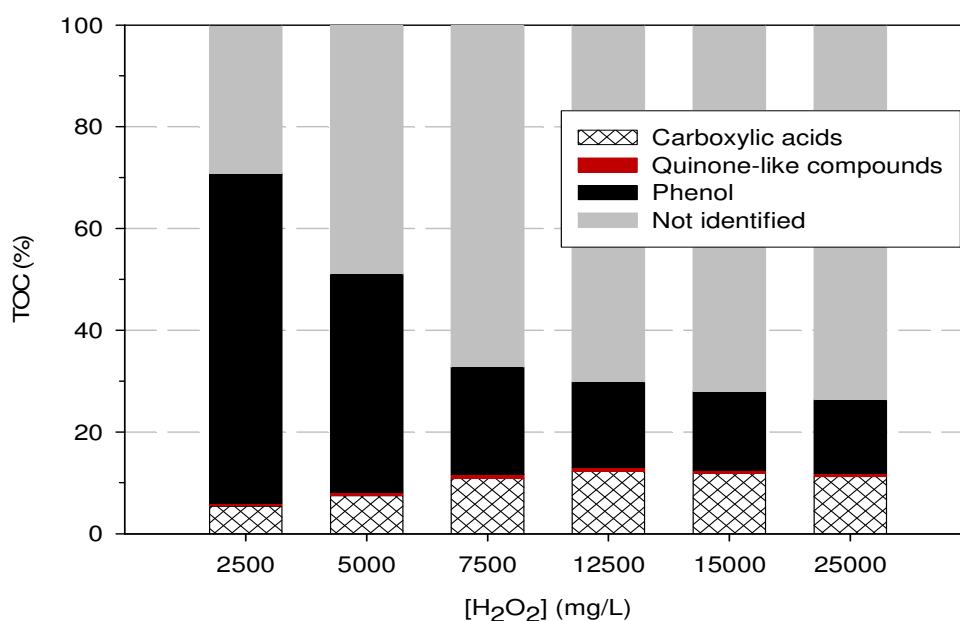


Figure 9.2. Effect of the H₂O₂ dose on the distribution of intermediates. 2500 mg/L phenol ; 28 mg/L Fe(II) ; Re_{out}=2.5

9.3. Influence of the iron(II) concentration on the membrane reactor performance

The influence of the Fe(II) concentration on phenol and TOC conversion was examined by oxidising 2500 mg/L phenol with 12500 mg/L H₂O₂ at several Fe(II) concentrations. As Figure 9.3 demonstrates, an increase on the Fe(II) concentration enhanced the Fenton process efficiency in terms of both phenol and TOC abatement. For instance, when the Fe(II) concentration was increased from 7.0 to 70 mg/L, phenol conversion increased from 45.8±3.2% to 98.1±0.4%, respectively. TOC conversion, at the same range of Fe(II) concentrations, increased from 18.5±3.1% to 56.7±1.9%, respectively. These results must be assigned to a higher generation of oxidative radicals, responsible of the organic molecules' attack, when the Fe(II) concentration was higher. Nevertheless, as it can be observed in Figure 9.3, beyond 28 mg/L Fe(II), phenol and TOC abatement was not significantly improved and only slight conversion increases were measured.

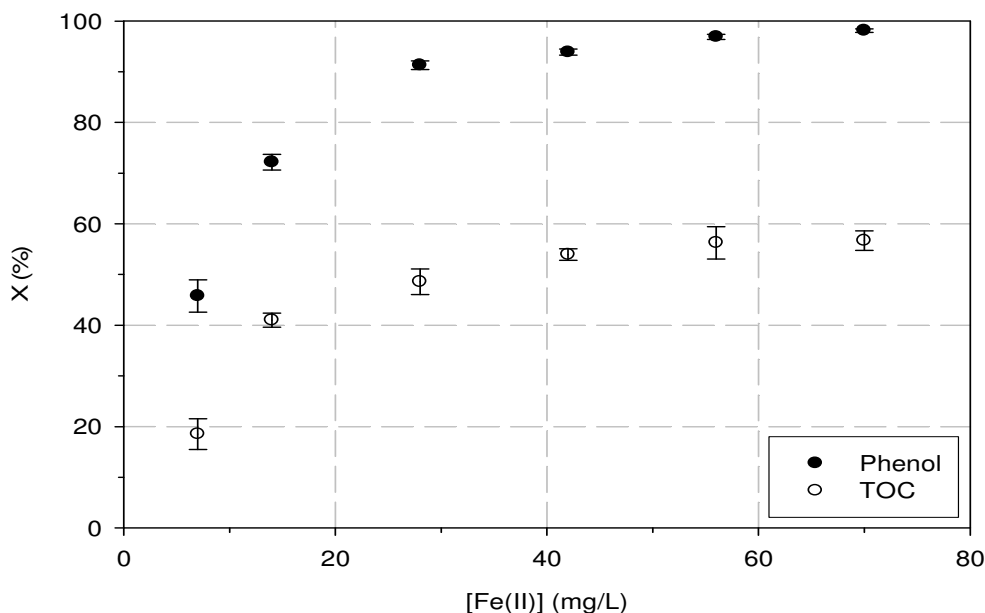


Figure 9.3. Effect of the Fe(II) concentration on phenol and TOC conversion. 2500 mg/L phenol ; 12500 mg/L H₂O₂ ; Re_{out}=2.5

The influence of the Fe(II) concentration on the distribution of families of intermediates is shown in Figure 9.4. As it can be seen, an increase on the Fe(II) concentration reduced the final phenol fraction, as a result of the increase on its conversion, already explained above. An increase on the iron(II) concentration also reduced the quinone-like compounds' fraction and increased the content of carboxylic acids and of non-identified intermediates. For instance, when increasing the Fe(II) concentration from 7.0 to 70 mg/L, the fraction of phenol decreased from 66.6% to 4.3% and that of carboxylic acids increased from 8.4% to 21.3%. In the same concentration range, the fraction of quinone-like compounds decreased from 0.7% to 0.0% and the fraction of unidentified compounds increased from 24.3% to 74.3%. The higher fraction of carboxylic acids and the decrease on the fraction of quinone-like compounds and phenol can be explained by the expected higher production of oxidative radicals at high Fe(II) concentrations that would generate stronger oxidation conditions. The increase on the fraction of unidentified compounds when the Fe(II) concentration was raised

could be explained both by probable changes on the nature of the condensation products formed and by the increased phenol conversion, which may generate a higher amount of condensation products, not analysed in this study. In addition, as non-identified condensation products also include Fe-complexes (Eisenhauer 1964), the increase on the iron concentration, could favour their formation and thus their content.

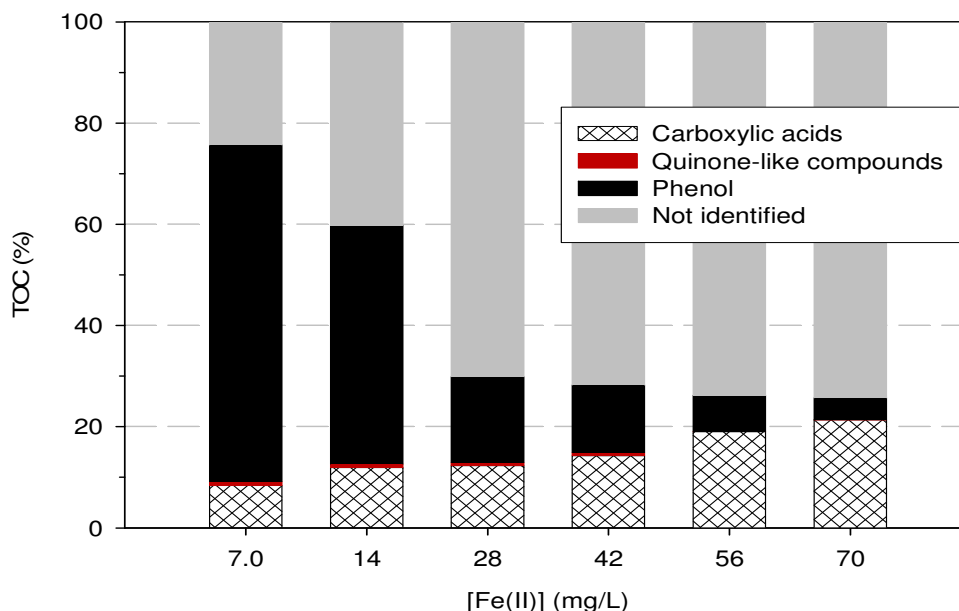


Figure 9.4. Effect of the Fe(II) concentration on the distribution of intermediates. 2500 mg/L phenol ; 12500 mg/L H₂O₂ ; Re_{out}=2.5

9.4. Influence of the Reynolds number on the membrane reactor performance

The effect of the effluents' flowrate was assessed by changing the inlets' flowrate, which directly affects the Re_{out}. However, the flowrates of the two separated reactor influents were always kept equal. Thus, the oxidant and the polluted flowrates were exactly the same and only the total reactor effluent flowrate was varied. Particularly, the effect of the Reynolds number (i.e. flowrate) on the membrane reactor performance was evaluated at three Re_{out} values which, as abovementioned, were calculated considering the reactor outlet flowrate. The experiments designed for evaluating the influence of the Re_{out} were carried out oxidising 2500 mg/L phenol with 12500 mg/L H₂O₂ and 28 mg/L Fe(II).

The influence of the Re_{out} on phenol and TOC conversion is shown in Figure 9.5. As this figure proves, an increase on the Re_{out} produced a decrease on both phenol and TOC abatement. Thus, the Fenton process performance was worsened as long as the Re_{out} was raised. This behaviour could be explained by the decrease on the contact (residence) time between the organic molecules to oxidise and the generated oxidative radicals, which occurred when the Re_{out} was raised.

The response of phenol and TOC conversion was in agreement with the effect of the Re_{out} on the distribution of families of intermediates, shown in Figure 9.6. As this figure reveals, an increase on the Re_{out} caused a decrease on the carboxylic acids' and non-identified fraction. On the contrary, a raise on the Re_{out} increased the final phenol and

quinone-like compounds' fraction. These results agree with the hypothesis that an increase on the Re_{out} decreases the contact time between organics and oxidative radicals.

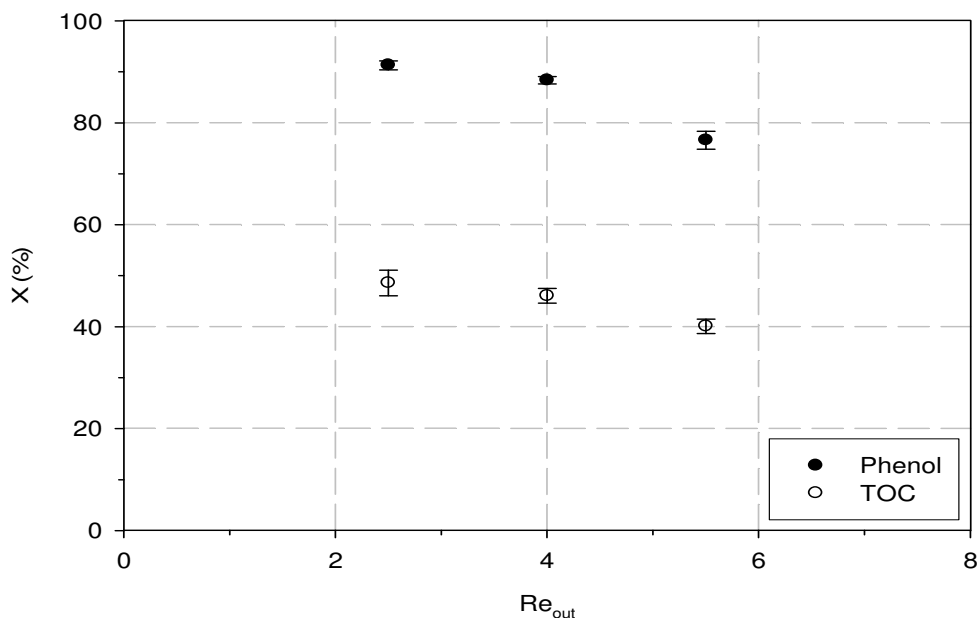


Figure 9.5. Effect of the Re_{out} on phenol and TOC conversion.
 2500 mg/L phenol ; 12500 mg/L H_2O_2 ; 28 mg/L Fe(II)

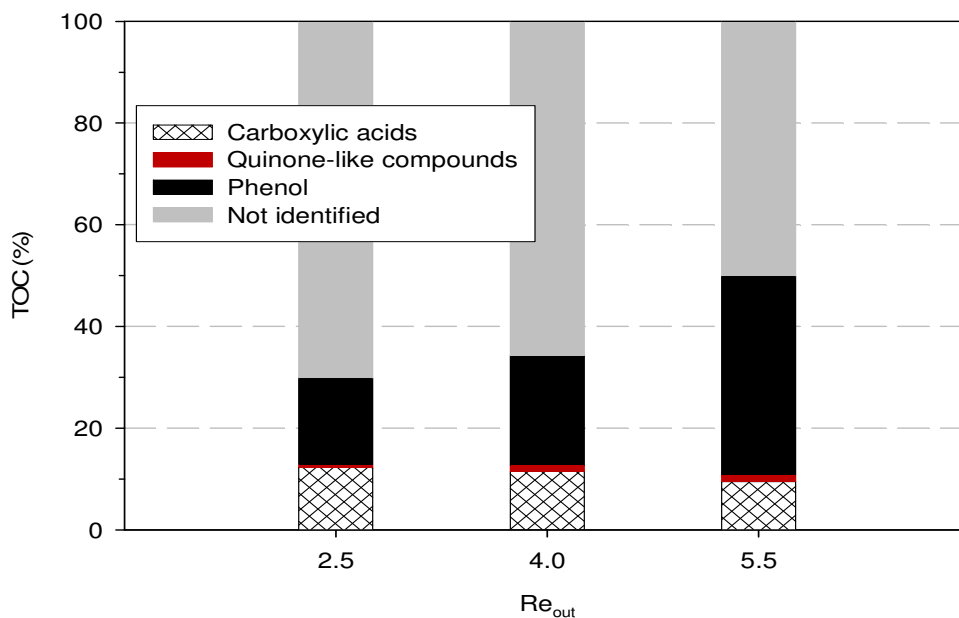


Figure 9.6. Effect of the Re_{out} on the distribution of intermediates.
 2500 mg/L phenol ; 12500 mg/L H_2O_2 ; 28 mg/L Fe(II)

9.5. Oxidation efficiency of tubular versus membrane reactor

The performance of a tubular reactor without lateral injection of hydrogen peroxide was tested in order to compare it to the efficiency of the novel reactor configuration presented above. In the classical tubular reactor experiments, the oxidant solution was introduced together with the polluted solution in the inlet of a tubular reactor of the same dimensions than the membrane reactor. The initial phenol apparent concentration was 2500 mg/L and that of H₂O₂ and Fe(II) was 12500 mg/L and 28 mg/L, respectively. The Re_{out} was 2.5 regardless of the reactor configuration.

The influence of the reactor configuration on phenol and TOC conversion is summarised in Table 9.1. As the data shows, the membrane reactor configuration allowed increasing around 20% both phenol and TOC conversions. Thus, membrane reactor configuration improves the oxidation performance probably as consequence of the enhancement on the hydrogen peroxide conversion towards effective oxidative radicals. Hence, hydrogen peroxide is probably less self-decomposed and/or causes lower radical scavenging effects because the membrane reactor configuration allows keeping its concentration in a low level inside the reactor. The hydrogen peroxide conversion achieved with both configurations is also included in Table 9.1. As it can be seen, the conversion of hydrogen peroxide was slightly higher when the membrane reactor design was selected. No difference between hydrogen peroxide conversion for oxidant radicals' production or due to its self-decomposition/scavenging effect can be stated because radicals were neither detected nor quantified in this thesis.

Table 9.1. Effect of the reactor configuration on phenol, TOC and H₂O₂ conversion. 2500 mg/L phenol ; 12500 mg/L H₂O₂ ; 28 mg/L Fe(II) ; $Re_{out}=2.5$

Reactor configuration	X _{phenol} (%)	X _{TOC} (%)	X _{H₂O₂} (%)
Tubular reactor	69.2±1.3	27.3±1.0	97.8±0.0
Membrane reactor	91.3±0.9	48.6±2.5	98.4±0.0

The effect of the reactor configuration on the distribution of families of phenol intermediates is shown in Figure 9.7. As this figure shows, the tubular reactor effluents had a higher fraction of non-reacted phenol and quinone-like compounds. On the other hand, the fraction of carboxylic acids was lower in the tubular reactor effluent than in that of the membrane reactor. These results agree with the lower phenol conversion achieved in the former than in the latter. Thus, as indicated by phenol and TOC conversion, the membrane reactor configuration increases the efficiency of the Fenton oxidation in terms of higher target compound destruction and lower quinone-like compounds' production. The fraction of unidentified reaction by-products increased in the membrane reactor configuration. As deeper oxidation occurred in the membrane reactor, more condensation products could be produced from the oxidation of phenol and quinone-like compounds. It is worth mentioning that the nature of the condensation products could change depending on the oxidation conditions and thus on the reactor configuration. Despite the effluent identification was higher in the tubular reactor than in the membrane reactor, the biodegradability (or toxicity) of the effluents was not assessed. Hence, a direct relation between the unidentified fraction and process efficiency in terms of biodegradation cannot be given.

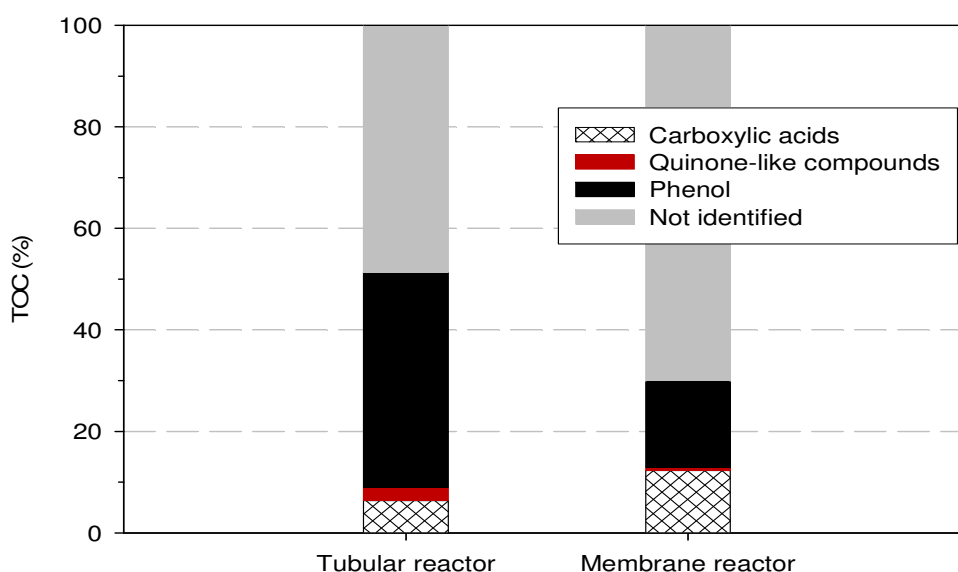


Figure 9.7. Effect of the reactor configuration on the distribution of intermediates. 2500 mg/L phenol ; 12500 mg/L H_2O_2 ; 28 mg/L Fe(II) ; $Re_{out}=2.5$

9.6. Degradation of phenol oxidation intermediates in an inert membrane reactor

The membrane reactor configuration was selected to study the oxidation of phenol oxidation intermediates in model compound-alone effluents. In all the oxidation tests, the initial intermediate apparent concentration was 100 mg/L and that of hydrogen peroxide and iron(II) was 12500 mg/L and 28 mg/L, respectively. The total duration of the experiments and the Re_{out} were 120 min and 2.5 regardless of the experiment.

Figure 9.8 shows the conversion of the intermediates and TOC in all the experiments carried out. As the figure demonstrates, quinone-like compounds were completely abated at the tested conditions although the TOC conversion achieved when their degradation was evaluated was around 30% regardless of the quinone-like compound examined. These results allow understanding the low fraction of quinone-like products present in the membrane reactor effluents of the phenol oxidation.

Maleic and fumaric acids' conversion was $88.2 \pm 0.5\%$ and $68.0 \pm 2.7\%$, respectively. The TOC conversion achieved in the oxidation of these acids was $15.6 \pm 2.6\%$ and $23.9 \pm 1.2\%$, respectively. T,t-muconic acid conversion was $93.5 \pm 1.3\%$ whilst the TOC conversion measured in its oxidation was $19.3 \pm 1.9\%$. Formic acid conversion was $34.5 \pm 1.1\%$ whilst TOC conversion achieved in its degradation was $33.4 \pm 1.2\%$. Assuming a possible experimental error and the presence of only one carbon atom in the molecular structure of formic acid, it can be stated that this acid was totally mineralised, so no derived compounds were generated in its oxidation, as published by Zazo et al. (2005).

Malonic, oxalic and acetic acids' conversions were below 2% which indicate that those acids were mostly refractory at the tested conditions. The absence of malonic and acetic acids in the oxidation effluents when phenol degradation experiments were

carried out confirms that the oxidation of phenol by the Fenton process did not occur through malonic-acetic acids' pathway. The nil conversion exhibited by oxalic acid confirms its well-known refractory nature to the Fenton oxidation (Bigda 1995; Kwon et al. 1999; Kavitha and Palanivelu 2005a; Pignatello et al. 2006).

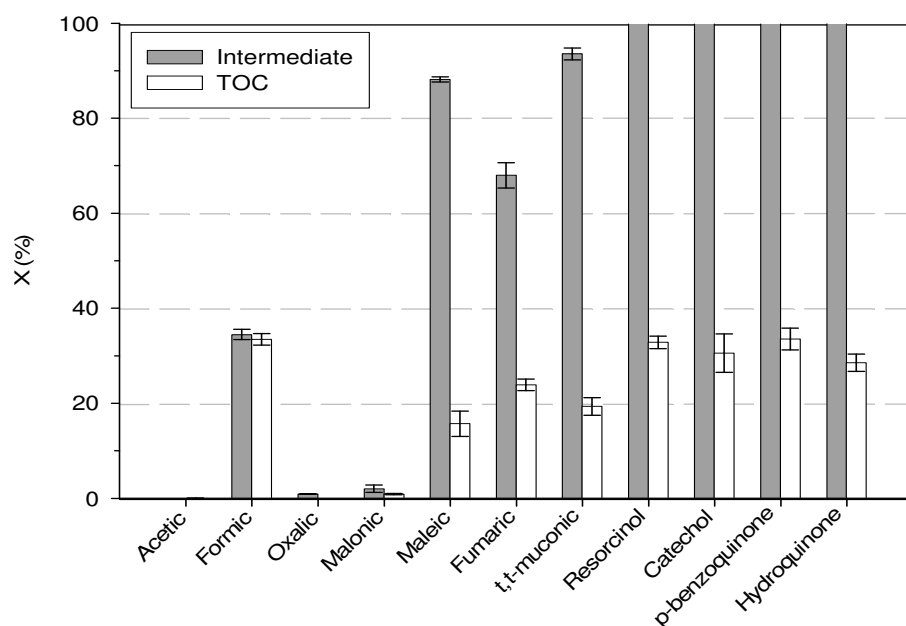


Figure 9.8. Oxidation of phenol intermediates in an inert membrane reactor. 100 mg/L organic ; 12500 mg/L H_2O_2 ; 28 mg/L Fe(II) ; $Re_{out}=2.5$

The detailed distribution of organic products (intermediates) of the oxidation of phenol intermediates is summarised in Table 9.2. As this table shows, the effluents of the acetic, oxalic and malonic acid oxidation, which were not degraded at the tested conditions, were obviously composed only by them. As converted formic acid was mineralised, no other intermediate was accordingly detected in the oxidation effluent.

Maleic acid oxidation effluent was formed by its unreacted fraction and by formic and oxalic acids. Fumaric acid, which is the isomer of maleic acid, was also degraded into the same acids. This indicates that the isomers are degraded forming the same oxidation by-products. The oxidation of t,t-muconic produced mainly formic, maleic and fumaric acid as well as a small fraction of oxalic acid. Thus, this acid appears before formic, oxalic, maleic and fumaric acids in the phenol oxidation pathway.

Quinone-like compounds were, as abovementioned, all totally oxidised and thus they were absent in their oxidation effluents. Quinone-like compounds were converted to oxalic, formic, maleic and fumaric acids. The non-identified fraction in this case was between 55 and 61%, which is quite higher than the values obtained when the rest of the phenol intermediates were degraded. This could be due to the formation of condensation products, which have not been analysed in this thesis.

The organic analyses presented in Table 9.2 show that the oxidation of intermediates in the membrane reactor agrees with the phenol oxidation pathway published by Zazo et al. (2005). The only difference with that route is that, in the present case, phenol oxidation scheme seemed not to pass through the malonic-acetic acids' route.

Table 9.2. Distribution of by-products of the oxidation of phenol intermediates in an inert membrane reactor. 100 mg/L organic ; 12500 mg/L H₂O₂ ; 28 mg/L Fe(II) ; Re_{out}=2.5

		Intermediate fraction in the reactor effluent as TOC (%)											
		Acetic	Formic	Oxalic	Malonic	Maleic	Fumaric	t,t-muconic	Resorcinol	Catechol	p-benzoquinone	Hydroquinone	Not identified
Phenol intermediate oxidised	Acetic	99.9											0.1
	Formic	0.0	98.4										1.6
	Oxalic	0.0	0.0	99.1									0.9
	Malonic	0.0	0.0	0.0	98.8								1.2
	Maleic	0.0	31.5	37.5	0.0	14.0							17.0
	Fumaric	0.0	33.4	14.1	0.0	0.0	42.1						10.4
	t,t-muconic	0.0	23.8	7.0	0.0	24.8	28.5	8.0					7.9
	Resorcinol	0.0	7.8	30.9	0.0	4.2	2.0	0.0	0.0				55.1
	Catechol	0.0	6.9	27.9	0.0	3.2	1.1	0.0	0.0	0.0			60.9
	p-benzoquinone	0.0	6.8	25.7	0.0	4.2	2.0	0.0	0.0	0.0	0.0		61.3
	Hydroquinone	0.0	8.8	28.9	0.0	5.5	2.1	0.0	0.0	0.0	0.0	0.0	54.7

9.7. Conclusions

Phenol oxidation by the Fenton process in an inert ceramic membrane reactor increases the degradation efficiency both in terms of phenol abatement and mineralisation degree. At the same oxidation conditions, phenol and TOC conversions in the membrane reactor are around 20% higher than those achieved in the tubular reactor. Hence, it can be expected that hydrogen peroxide autodecomposition or its radical scavenging effect, both occurring at high oxidant concentrations, are reduced in the membrane reactor configuration.

Phenol and TOC conversions are affected by the classical Fenton process variables such as hydrogen peroxide dose and iron(II) concentration. An increase on the hydrogen peroxide dose or on the iron(II) concentration benefits phenol abatement and mineralisation. However, there is a limit value beyond which an increase of these concentrations does not enhance anymore the process efficiency in terms of phenol and TOC conversion but still improves the degradation of phenol oxidation intermediates. For instance, at high iron(II) concentration, quinone-like compounds' content, associated to toxic character, is minimised. On the other hand, an increase on the Reynolds number decreases the conversion of phenol and TOC, which can be

attributed to the lower contact time, i.e. residence time, between the generated oxidative radicals and the organic compounds to be attacked. In addition, an increase on the Reynolds number worsens the quality of the oxidised effluents because the concentration of phenol and quinone-like compounds is increased whilst the carboxylic acids' fraction is reduced.

The degradation of phenol oxidation intermediates has confirmed that the chemical oxidation pathway of phenol by the Fenton process proposed by Zazo et al. (2005) matches that from the oxidation tests performed. The only variation is that, in this thesis, phenol oxidation was not found to pass through the malonic-acetic acids' route because these acids were neither identified in phenol oxidation effluents nor in the effluents from the oxidation of phenol intermediates.

UNIVERSITAT ROVIRA I VIRGILI

TREATMENT OF BIOREFRACTORY WASTEWATER THROUGH MEMBRANE-ASSISTED OXIDATION PROCESSES

Xavier Bernat Camí

ISBN:978-84-693-1529-3/DL:T-652-2010

CHAPTER 10

Conclusions and future work

10.1. Conclusions

This thesis has dealt with the design and application of membrane-based strategies to solve Fenton process drawbacks. The identified drawbacks are the continuous loss of iron in the reactor effluent and the waste of oxidant due to its self-decomposition and/or radical scavenging effect.

The recoverability of iron was first assessed by studying the retention efficiency of UF and NF. Then, coupling of the Fenton process and NF was evaluated by selecting phenol as model compound. The feasibility of using surfactant micelles to confine iron ions and use them as Fenton catalyst for phenol oxidation was also investigated. Finally, iron-containing oil-in-water emulsions, formulated by membrane emulsification, were tested as Fenton catalyst for phenol oxidation.

In a different approach, an inert ceramic membrane reactor was tested to increase the hydrogen peroxide use. The membrane operated as a hydrogen peroxide diffuser feeding it from the shell to the lumen of a ceramic membrane, where phenol oxidation by the Fenton reaction took place. The reactor behaviour was compared to a conventional tubular configuration in order to quantify the degradation efficiency enhancement.

The main conclusions derived from each subject investigated in this thesis, corresponding to the previous membrane-based strategies, are exposed below.

Surprisingly, ceramic UF membranes were able to retain iron(III) species without the need of complexing agents. Contrarily, iron(II) was not retained at the same conditions. This difference allowed postulating a retention mechanism that mostly depends on the hydrolysis of the species and the interactions with the membrane material. The retention of hydrolysed species such as iron(III) was explained by their adsorption onto the inorganic membrane material. Charge repulsions between the adsorbed iron species and those present in the bulk solution can coexist with adsorption phenomena. Furthermore, sieving effects could result from the adsorption of metal species and from the formation of polynuclear species from their mononuclear predecessors, too. These high molecular weight species can be more easily rejected by sieving effects and/or adsorbed into the membrane. The adsorption of hydrolysed species is the initiator of the retention of iron species and its absence, when no hydrolysis occurs, gives nil retention. This was also proved for other different metals undergoing or not hydrolysis. The membrane material was also shown to be a key variable. When polymeric membranes with close MWCO's to those of the ceramic ones were tested, no iron(III) rejection was found. As the polymeric membranes did not adsorb iron species, this proves the critical role of adsorption on the iron retention by UF. Anyway, as ferrous species are not hydrolysed and thus were not rejected by UF, the process is not useful for this particular application, i.e. the recovery of iron species from Fenton effluents.

Polymeric NF membranes showed increased retention of iron species. In addition, for the three commercial membranes tested, only a slight difference on the iron retention was observed between ferric and ferrous species. The membrane exhibiting the highest iron retention was NF90 from Dow-Filmtec, whose iron retention was higher than 99% regardless of the iron species filtered. Thus, as NF demonstrated to be an adequate filtration range for iron recovery, it was selected for testing its efficiency to filter pre-oxidised effluents.

The efficiency of the Fenton process for degrading phenolic effluents was evaluated in order to understand the influence of several oxidation variables. In general, an increase on the concentration of hydrogen peroxide and iron(II) enhanced the effluent quality. The concentration of phenol and quinone-like compounds decreased whilst the carboxylic acids' content rose when the Fenton conditions were more severe. This resulted into an enhancement of the biodegradable fraction of the effluent and into a reduction of its toxicity. However, at the highest iron(II) concentration tested, i.e. 56 mg/L, the effluent still exhibited a toxicity of around 10%.

NF tests were carried out by filtering effluents from the Fenton process at several oxidation conditions. This allowed investigating the effect of the Fenton process variables on the NF performance. The retention of phenol and its oxidation intermediates was explained through electrostatic solute-membrane interactions and sieving effects. Among the three NF membranes tested, NF90 from Dow-Filmtec was found to be that giving the highest effluent purification. When 2500 mg/L phenol were oxidised with 12500 mg/L H₂O₂ and 28 mg/L Fe(II) (or higher), the toxicity of the NF90 permeate was nil. All the tested membranes suffered from fouling, which was shown to be partially removed by rinsing the membranes just with water and totally removed after chemical cleaning. Cleaned membranes were reused in four subsequent runs and no performance loss was observed. Hence, coupling Fenton process and NF is an attractive process configuration to ensure a proper operation of the subsequent biological degradation.

The feasibility of using surfactant micelles to confine iron(II) ions and subsequently use them as Fenton catalyst for the phenol degradation was assessed. The effect of the presence of surfactant (SDS or CPC) on the phenol degradation by the Fenton reaction was investigated. The presence of surfactant decreased phenol degradation because

phenol solubilisation inside the surfactant micelles made it less available to be attacked by oxidant radicals. In addition, surfactants were codegraded in Fenton conditions, thus competing for the radicals. Surfactant oxidation would imply a continuous addition of surfactant to the reactor, increasing treatment costs. Hence, it does not seem to be recommendable the application of iron-containing surfactant micelles as Fenton catalyst.

Despite the use of surfactant micelles to confine iron species and use them as Fenton catalyst is not recommended, the NF of the effluents of the oxidation of phenol and SDS binary solutions was still studied. This would allow assessing the possibility of dealing with wastewater containing both phenol and surfactant. The effect of the oxidation variables was not found to affect the membrane permeate flux and fouling. In addition, NF was found to be an effective process to remove residual surfactant and phenol as well as quinone-like intermediates from the pre-oxidised effluents. NF also satisfactorily retained iron species (around 98%) from Fenton effluents. Thus, as when dealing with single phenol effluents, NF can be a potential intermediate unit between oxidation and biological treatment.

Emulsions formulated by membrane emulsification were prepared at several emulsification conditions. Among other variables, iron presence was found to decrease the stability of the emulsions. Destabilisation was attributed to the decrease on the charge of the emulsion droplets due to the attraction of iron ions towards their interface. The charge decrease probably caused lower droplet-droplet repulsions and thus promoted coalescence and even emulsion breakage. The removal of the original continuous phase of a prepared emulsion, containing free emulsifier molecules, and its replacement by water did not cause emulsion destabilisation. However, when the emulsion continuous phase was replaced by an iron-containing solution, the destabilisation was higher than when the same concentration of iron was initially present in the continuous phase together with the emulsifier. Thus, free emulsifier molecules or micelles were found to act as emulsion destabilisation retardant or evader because a fraction of iron ions was possibly bound to them and thus less iron ions were attracted towards the droplets' interface.

Emulsions containing iron in their original continuous phase were tested as catalysts of the Fenton oxidation of phenol. Irrespective of the emulsion selected, no phenol conversion was observed. Any phenol disappearance was due to its distribution between the continuous and oil phase. Due to its partition, phenol molecules were less available to be attacked by oxidative radicals. The emulsions containing iron were all destabilised during the reaction because the degradation of SDS molecules used as emulsifier probably occurred. Therefore, iron-containing emulsions cannot be used as Fenton catalysts at the tested conditions and with the emulsion ingredients considered in this thesis.

Phenol conversion and mineralisation increased around 20% when phenol solutions were oxidised in an inert ceramic membrane reactor instead of in a conventional tubular reactor. Hence, a membrane reactor where the oxidant is continuously fed through the membrane wall, from the shell to the lumen, can help to increase phenol degradation by the Fenton reaction. The proposed reactor configuration is accordingly a potential design to enhance the efficiency of the Fenton process in terms of oxidant use.

10.2. Future work

The results obtained and the conclusions derived must serve to design future research guidelines that would improve the knowledge gained in this thesis. Below, some observations about possible future research are given.

The combination of Fenton process, NF and biological treatment seems a powerful alternative to avoid damages on the microorganisms used in the last unit. The influents of the biological treatment can be absent of toxic compounds and iron species because NF retain them. However, the biological treatment efficiency was not deeply assessed in this thesis and only respirometric analyses were performed. Thus, it would be necessary to test the efficiency of the combined treatment including the aerobic biological treatment. A long-term operation of the three-step process would indicate the benefits and limitations of each step in the global process scheme.

Designing and manufacturing oxidant-resistant membranes would allow performing the Fenton reaction and the separation in one single process unit. The membranes selected in this thesis cannot be used in the intensified configuration because, when this was evaluated, they were damaged due to the high concentration of oxidant present in the reactor liquor of the intensified configuration. Instead, the membranes were used in the two-step configuration without troubles because only minimal residual hydrogen peroxide concentration was present in the reactor effluent. Thus, it would be worth researching into new-generation nanofiltration membranes resistant to the oxidation and able to operate in oxidation membrane reactors for environmental applications.

Iron concentration was observed to exert positive effects on its retention, but also on that of ring compounds. In addition, it was found that an increase on iron concentration raised membrane fouling. However, this behaviour was not completely explained. Hence, filtration experiments of synthetic effluents prepared with the same composition of identified compounds than those analysed in Fenton oxidation effluents need to be carried out. This would allow assessing the effect of the unidentified compounds on the filtration efficiency. The same experiments but with effluents without iron would allow highlighting the effect of iron on the retention efficiency. From those experiments, the mechanisms taking place in the filtration of oxidised phenol effluents would be clarified.

The catalysis of the Fenton process by iron-containing emulsions caused emulsion destabilisation. In addition, the target contaminant was not degraded. Research into other emulsifiers would be thus required. Those emulsifiers could be enzymes which have shown activity to degrade phenol and behave as emulsifiers. Once the formulation of stable and catalytically-active emulsions was achieved, the integration of the Fenton reaction with MF or UF to retain and recycle the emulsions would need to be studied.

The operation of an inert membrane reactor showed that phenol degradation was higher than when a conventional tubular reactor was tested. It would be worth to model the reactor operation in order to predict oxidation results in this configuration for a wide range of operation variables. In addition, developing and testing a membrane reactor with catalyst or enzymes loaded in the membrane material would be recommended. This would avoid installing a separation unit after the membrane reactor to recover and reuse the catalyst or enzymes.

References

- Adamczak, H.; Materna, K.; Urbański, R.; Szymanowski, J. Ultrafiltration of micellar solutions containing phenol, *J. Colloid Interface Sci.* 218 (1999) 359-368.
- AGUA Programme, Actuaciones para la Gestión y la Utilización del Agua, Ministerio de Medio Ambiente, based on the actuations exposed in the Spanish Water Act 2/2004 of 18th June 2004.
- Ahn, K.-H.; Song, K.-G. ; Cha, H.-Y.; Yeom, I.-T. Removal of ions in nickel electroplating rinse water using low-pressure nanofiltration, *Desalination* 122 (1999) 77-84.
- Akata, A. and Gurol, M. Photocatalytic oxidation processes in the presence of polymers, *Ozone Sci. Eng.* 14 (1992) 367-380.
- Al-Almoudi, A. and Lovitt, R.W. Fouling strategies and the cleaning system of NF membranes and factors affecting cleaning efficiency, *J. Membr. Sci.* 303 (2007) 4-28.
- Alcaina-Miranda, M.I.; Barredo-Damas, S.; Bes-Pía, A.; Iborra-Clar, M.I.; Iborra-Clar, A.; Mendoza-Roca, J.A. Nanofiltration as final step towards textile wastewater reclamation, *Desalination* 240 (2009) 290-297.
- Alegría, Y.; Liendo, F.; Nuñez, O. On the Fenton degradation mechanism. The role of oxalic acid. *Arkivoc* 10 (2003) 538-549.
- Alghoul, M.A.; Poovanaesvaran, P.; Sopian, K.; Sulaiman, M.Y. Review of brackish water reverse osmosis (BWRO) system designs, *Renewable Sustainable Energy Rev.* 13 (2009) 2661-2667.

- Al-Hayek, N. and Doré, M. Oxidation of phenols in water by hydrogen peroxide on alumina-supported iron, *Water Res.* 24 (1990) 973-982.
- Al Momani, F.; González, O.; Sans, C.; Esplugas, S. Combining photo-Fenton process with biological sequencing batch reactor for 2,4-dichlorophenol degradation, *Water Sci. Technol.* 49 (2004) 293-298.
- Al Momani, F.; Sans, C.; Contreras, S.; Esplugas, S. Degradation of 2,4-dichlorophenol by combining photo-assisted Fenton reaction and biological treatment, *Water Environ. Res.* 78 (2006) 590-597.
- Anderson, M.A. and Rubin, A. Adsorption of Inorganics at Solid-Liquid Interfaces, Ann Arbor Science, MI, 1981.
- Anderson, J.V.; Link, H.; Bohn, M.; Gupta, B. Development of US solar detoxification technology: An introduction, *Sol. Energy Mater.* 24 (1991) 538-549.
- Aoustin, E.; Schäfer, A.I.; Fane, A.G.; Waite, T.D. Ultrafiltration of natural organic matter, *Sep. Purif. Technol.* 22-23 (2001) 63-78.
- Arkhangelsky, E. and Gitis, V. Effect of transmembrane pressure on rejection of viruses by ultrafiltration membranes, *Sep. Purif. Technol.* 62 (2008) 619-628.
- Arslan-Alaton, I.; Erdinc, E. Effect of the photochemical treatment on the biocompatibility of a commercial nonionic surfactant used in the textile industry, *Water Res.* 40 (2006) 3409-3418.
- Arslan-Alaton, I.; Cokgor, E.U.; Koban, B. Integrated photochemical and biological treatment of a commercial textile surfactant: Process optimization, process kinetics and COD fractionation, *J. Hazard. Mater.* 146 (2007) 453-458.
- Arslan-Alaton, I.; Gursoy, B.H.; Schmidt, J.-E. Advanced oxidation of acid and reactive dyes: Effect of Fenton treatment on aerobic, anoxic and anaerobic processes, *Dyes Pigm.* 78 (2008) 117-130.
- Assessment of alternative water supply options. Final summary report, VITO, 2008.
- Assessment of the risks and impacts of four alternative water supply options, Task 1 Report, VITO, 2008.
- Ates, N.; Yilmaz, L.; Kitis, M.; Yetis, U. Removal of disinfection by-product precursors by UF and NF membranes in low-SUVA waters, *J. Membr. Sci.* 328 (2009) 104-112.
- Azrague, K.; Aimar, P.; Benoit-Marquié, F.; Maurette, M.T. A new combination of a membrane and a photocatalytic reactor for the depollution of turbid water, *Appl. Catal. B* 72 (2007) 197-204.
- Baes, C.F. and Mesmer, R.E. The Hydrolysis of Cations, John Wiley & Sons, New York, 1976.
- Bandala, E.R.; Peláez, M.A.; Salgado, M.J.; Torres, L. Degradation of sodium dodecyl sulphate in water using solar-driven Fenton-like advanced oxidation processes, *J. Hazard. Mater.* 151 (2008) 578-584.
- Barb, W.G.; Baxendale, J.H.; George, P.; Hargrave, K.R. Reactions of ferrous and ferric ions with hydrogen peroxide, *Nature* 163 (1949) 692-694.
- Barb, W.G.; Baxendale, J.H.; George, P.; Hargrave, K.R. Reactions of ferrous and ferric ions with hydrogen peroxide. Part I. – The ferrous ion reaction. *Trans. Faraday Soc.* 47 (1951a) 462-500.

- Barb, W.G.; Baxendale, J.H.; George, P.; Hargrave, K.R. Reactions of ferrous and ferric ions with hydrogen peroxide. Part II. – The ferric ion reaction. *Trans. Faraday Soc.* 47 (1951b) 591-616.
- Basu, S. and Wei, I.W. Mechanism and kinetics of oxidation of 2,4,6-trichlorophenol by Fenton's reagent, *Environ. Eng. Sci.* 17 (2000) 279-289.
- Bautista, P.; Mohedano, A.F.; Gilarranz, M.A.; Casas, J.A.; Rodriguez, J.J. Application of Fenton oxidation to cosmetic wastewaters treatment, *J. Hazard. Mater.* 143 (2007) 128-134.
- Bautista, P.; Mohedano, A.F.; Casas, J.A.; Zazo, J.A.; Rodríguez, J.J. An overview of the application of Fenton oxidation to industrial wastewaters treatment, *J. Chem. Technol. Biotechnol.* 83 (2008) 1323-1338.
- Belfort, G.; Davies, R.H.; Zydney, A.L. The behaviour of suspensions and macromolecular solutions in crossflow microfiltration, *J. Membr. Sci.* 96 (1994) 1-58.
- Bellona, C.; Drewes, J.E.; Xu, P.; Amy, G. Factors affecting the rejection of organic solutes during NF/RO treatment – a literature review, *Water Res.* 38 (2004) 2795-2809.
- Bellona, C. and Drewes, J.E. Viability of a low-pressure nanofilter in treating recycled water for water reuse applications: A pilot-scale study, *Water Res.* 41 (2007) 3948-3958.
- Benatti, C.T.; da Costa, A.C.S.; Tavares, C.R.G. Characterisation of solids originating from the Fenton's process, *J. Hazard. Mater.* 163 (2009) 1246-1253.
- Benítez, F.J.; Acero, J.L.; Leal, A.I.; Real, F.J. Ozone and membrane filtration based strategies for the abatement of cork processing wastewaters, *J. Hazard. Mater.* 152 (2008a) 373-380.
- Benítez, F.J.; Acero, J.L.; Leal, A.I. Treatment of wastewaters from the cork process industry by using ultrafiltration membranes, *Desalination* 229 (2008b) 156-159.
- Beolchini, F.; Pagnanelli, F.; De Michellis, I.; Vegliò, F. Micellar enhanced ultrafiltration for Arsenic (V) removal: Effect of main operating conditions and dynamic modelling, *Environ. Sci. Technol.* 40 (2006) 2746-2752.
- Berot, S.; Giraudet, S.; Riaublanc, A.; Anton, M.; Popineau, Y. Key factors in membrane emulsification, *Chem. Eng. Res. Des.* 81 (2003) 1077-1082.
- Bielska, M. and Szymanowski, J. Micellar enhanced ultrafiltration of nitrobenzene and 4-nitrophenol, *J. Membr. Sci.* 243 (2004) 273-281.
- Bigda, R. Consider Fenton's chemistry for wastewater treatment, *Chem. Eng. Prog.* 91 (1995) 62-66.
- Blesa, M.A. Phase transformations of iron oxides, oxohydroxides and hydrous oxides in aqueous media, *Adv. Colloid Interface Sci.* 29 (1989) 173-221.
- Boschke, E.; Böhmer, U.; Lange, J.; Constapel, M.; Schellenträger, M.; Bley, T. The use of respirometric measurements to determine the toxicity of textile dyes in aqueous solution and after oxidative decolourisation process, *Chemosphere* 67 (2007) 2163-2168.
- Bossmann, S.H.; Oliveros, E.; Göb, S.; Siegwart, S.; Dahlen, E.P.; Payawan, L.; Straub, M.; Wörner M.; Braun, A. New evidence against hydroxyl radicals are reactive intermediates in the thermal and photochemically enhanced Fenton reactions, *J. Phys. Chem. A* 102 (1998) 5542-5550.

- Bowen, W.R.; Mukhtar, H. Characterisation and prediction of separation performance of nanofiltration membranes, *J. Membr. Sci.* 112 (1996) 263-274.
- Bowen, W.R.; Mohammad, A.W.; Hilal, N. Characterisation of nanofiltration membranes for predictive purposes – use of salts, uncharged solutes and atomic force microscopy, *J. Membr. Sci.* 126 (1997) 91-105.
- Braghetta, A.; Di Giano, F.A.; Ball, W.P. Nanofiltration of Natural Organic Matter: pH and Ionic Strength Effects, *J. Environ. Eng.* 123 (1997) 628-641.
- Bremmer, D.H.; Burgess, A.E.; Houlemare, D.; Namkung, K.-C. Phenol degradation using hydroxyl radicals generated from zero-valent iron and hydrogen peroxide, *Appl. Catal., B* 63 (2006) 15-19.
- Brouwer, H.; Klapwijk, A.; Kessman, K.J. Identification of activated sludge and wastewater characteristics using respirometric batch-experiments, *Water Res.* 32 (1998) 1240-1254.
- Brown, R.F.; Jamison, S.E.; Pandit, U.K.; Pinkus, J.; White, G.R.; Braendlin, H.P. The reaction of Fenton's reagent with phenoxyacetic and some halogen-substituted phenoxyacetic acids, *J. Org. Chem.* 29 (1964) 146-153.
- Buxton, G.V.; Greenstock, C.L.; Helman, W.P.; Ross, A.B. Critical review of rate constants for reactions of hydrated electrons, hydrogen atoms and hydroxyl radicals ($\cdot\text{OH}/\cdot\text{O}$) in aqueous solution, *J. Phys. Chem. Ref. Data* 17 (1988) 513-886.
- Castro, I.U.; Stüber, F.; Fabregat, A.; Font, J.; Fortuny, A.; Bengoa, C. Supported Cu(II) polymer catalysts for aqueous phenol oxidation, *J. Hazard. Mater.* 163 (2009) 809-815.
- Catalan Water Act 130/2003 of 13th May 2003.
- Causserand, C.; Rouaix, S.; Lafaille, J.-P.; Aimar, P. Ageing of polysulfone membranes in contact with bleach solution: Role of radical oxidation and of some dissolved metal ions, *Chem. Eng. Process.* 47 (2008) 48-56.
- CESIO News - June 2008, CESIO, 2008. In www.cefic.be/files/Downloads. Last time accessed August 2008.
- CESIO Recommendation for the classification of and labelling of surfactants as "dangerous for the environment", CESIO, Brussels, 2003.
- CESIO Statistics 2006-2007, CESIO, 2008. In www.cefic.be. Last time accessed March 2009.
- Chai, X.; Chen, G.; Yue, P.-L.; Mi, Y. Pilot scale membrane separation of electroplating waste water by reverse osmosis, *J. Membr. Sci.* 123 (1997) 235-242.
- Chakrabarty, B.; Ghoshal, A.K.; Purkait, M.K. Effect of molecular weight of PEG on membrane morphology and transport properties, *J. Membr. Sci.* 309 (2008) 209-221.
- Chamarro, E.; Marco, A.; Prado, J.; Espulgas, S. Tratamiento de aguas y aguas residuales mediante utilización de procesos de oxidación avanzada, *Química & Industria*, Sociedad Chilena de Química, 1-2 (1996) 28-32.
- Chang, B.V.; Chiang, F.; Yuan, S.Y. Biodegradation of nonylphenol in sewage sludge, *Chemosphere* 60 (2005) 1652-1659.
- Charpentier, J.-C. Market demand versus technological development: the future of chemical engineering, *Int. J. Chem. React. Eng.* 1 (2003) 1-30.

- Chemical Economics Handbook, Marketing Research Abstract – November 2007, 2007.
- Chemical Industries Newsletter – July 2008, SRI Consulting, 2008.
- Chen, R.; Pignatello, J.J. Role of quinone intermediates as electron shuttles in Fenton and photoassisted Fenton oxidations of aromatic compounds, *Environ. Sci. Technol.* 31 (1997) 2399-2406.
- Choi, J.-H.; Fukushi, K.; Yamamoto, K. A study on the removal of organic acids from wastewaters using nanofiltration membranes, *Sep. Purif. Technol.* 59 (2008) 17-25.
- Ciotti, C.; Baciocchi, R.; Tuhkanen, T. Influence of the operating conditions on highly oxidative radicals generation in Fenton's systems, *J. Hazard. Mater.* 161 (2009) 402-408.
- Clesceri, L.S.; Greenberg, A.E.; Trusel, R.R.; Franson, M.A. Standard Methods for the Examination of Water and Wastewater, 17th Ed., American Public Health Association and American Water Works Association, Washington, DC, 1989.
- Comninellis, C.; Kapalka, A.; Malato, S.; Parsons, S.A.; Poulios, I.; Mantzavinos, D. Advanced oxidation processes for water treatment: advances and trends for R&D, *J. Chem. Technol. Biotechnol.* 83 (2008) 769-776.
- Conditions for the sustainable development of alternative water supply options. Task 3 Report, VITO, 2008.
- Condom, S.; Cretin, M.; Persin, M.; Sarrazin, J.; Larbot, A. Characterization of three low UF mineral membranes by streaming potential measurements, *Desalination* 149 (2002) 447-451.
- Condom, S.; Larbot, A.; Alami-Younssi, S.; M. Persin. Use of ultra- and nanofiltration ceramic membranes for desalination, *Desalination* 168 (2004) 207-213.
- Contreras, S.; Rodriguez, M.; Al Momani, F.; Sans, C.; Esplugas, S. Contribution of the ozonation pre-treatment to the biodegradation of aqueous solutions of 2,4-dichlorophenol, *Water Res.* 37 (2003) 3164-3171.
- CurTiPot Database, Version 3.4.1 option i (nov/2008), Prof. I.G.R. Gutz, 2008. In http://www2.iq.usp.br/docente/gutz/Curtipot_.htm. Last time accessed March 2009.
- Cuzzola, A.; Bernini, M.; Salvadori, P. A preliminary study on iron species as heterogeneous catalysts for the degradation of linear alkylbenzene sulphonic acids by H₂O₂, *Appl. Catal., B* 36 (2002) 231-237.
- Dalzell, D.J.B.; Alte, S.; Aspichueta, E.; de la Sota, A.; Etxebarria, J.; Gutiérrez, M.; Hoffmann, C.C.; Sales, D.; Obst, U.; Christofi, N. A comparison of five rapid direct toxicity assessment methods to determine toxicity of pollutants to activated sludge, *Chemosphere* 47 (2002) 535-545.
- Dantas, T.L.P.; Mendonca, V.P.; Jose, H.J.; Rodrigues, A.E.; Moreira, R.F.P.M. Treatment of textile wastewater by heterogeneous Fenton process using a new composite Fe₂O₃/carbon, *Chem. Eng. J.* 118 (2006) 77-82.
- Delaunay, D.; Rabiller-Baudry, M.; Paugam, L.; Pihlajamäki, A.; Nyström, M. Physico-chemical characterisations of a UF membrane in dairy application to estimate chemical efficiency of cleaning, *Desalination* 200 (2006) 189-191.
- Deng, Y. Physical and oxidative removal of organics during Fenton treatment of mature municipal landfill leachate, *J. Hazard. Mater.* 146 (2007) 334-340.

- Dojilido, R. and Best, G.A. Chemistry of waters and water pollution, Ellis Horwood, New York, 1993.
- Drioli, E.; Fontananova, E.; Bonchio, M.; Carraro, M.; Gardan, M.; Scorrano, G. Catalytic membranes and membrane reactors: an integrated approach to catalytic process with a high efficiency and a low environmental impact, *Chin. J. Catal.* 29 (2008) 1152-1158.
- Du, Y.; Zhou, M.; Lei, L. The role of the intermediates in the degradation of phenolic compounds by Fenton-like process, *J. Hazard. Mater.* 136 (2006) 859-865.
- Du, Y.; Zhou, M.; Lei, L. The role of oxygen in the degradation of p-chlorophenol by Fenton system, *J. Hazard. Mater.* 139 (2007) 108-115.
- Dunn, R.O.; Scamehorn, J.F.; Christian, S.D. Simultaneous removal of dissolved organics and metal cations from water using micellar-enhanced ultrafiltration, *Colloids Surf.* 35 (1989) 49-56.
- EC 1179/94, OJ L131, 26.5.94, p.3. Regulation 793/93.
- Effectiveness of urban wastewater treatment policies in selected countries: an EEA pilot study, EEA Report No 2/2005, European Environment Agency, Copenhagen, 2005.
- Eisenhauer, H.R. Oxidation of phenolic wastes, *J. Water Pollut. Contr. Fed.* 36 (1964) 1116-1128.
- Environmental performance reviews: Spain, Paris, OECD, 2004.
- EPER, European Pollutant Emission Register. In www.eper.eea.eu.int. Last time accessed June 2006.
- Erdei, L.; Arecrachakul, N.; Vigneswaran, S. A combined photocatalytic slurry reactor-immersed membrane module system for advanced wastewater treatment, *Sep. Purif. Technol.* 62 (2008) 382-388.
- Esplugas, S.; Giménez, J.; Contreras, S.; Pascual, E.; Rodríguez, M. Comparison of different advanced oxidation processes for phenol degradation, *Water Res.* 36 (2002) 1034-1042.
- Essam, T.; Amin, M.A.; El Tayeb, O.; Mattiasson, B.; Guieysse, B. Sequential photochemical-biological degradation of chlorophenols, *Chemosphere* 66 (2007) 2201-2209.
- EU Water Saving Potential - Part 1. Report, Ecologic – Institute for International and Environmental Policy, Berlin, 2007.
- European Environment Outlook, EEA Report No 4/2005, European Environment Agency, Copenhagen, 2005.
- Fabbri, D.; Bianco Prevot, A.; Pramauro, E. Effect of surfactant microstructures on photocatalytic degradation of phenol and chlorophenols, *Appl. Catal., B* 62 (2006) 21-27.
- Feng, J.; Hu, X.; Yue, P.L. Novel bentonite clay-based Fe-nanocomposite as a heterogeneous catalyst for photo-Fenton discoloration and mineralization of Orange II, *Environ. Sci. Technol.* 38 (2004) 269-275.
- Fenton, H.J.H. Oxidation of tartaric acid in presence of iron, *J. Chem. Soc. Trans.* 65 (1894) 899-910.
- Fernández, E.; Benito, J.M.; Pazos, C.; Coca, C. Ceramic membrane ultrafiltration of anionic and nonionic surfactant solutions, *J. Membr. Sci.* 246 (2005) 1-6.

- Fievet, P.; Sbaï, M.; Szymczyk, A.; Magnenet, C.; Labbez, C.; Vidonne, A. A new tangential streaming potential setup for the electrokinetic characterization of tubular membranes, *Sep. Sci. Technol.* 39 (2004) 2931-2949.
- FILMTEC Reverse Osmosis Membranes Technical Manual. Dow Water & Process Solutions, In www.dow.com. Last time accessed September 2009.
- Fortuny, A.; Bengoa, C.; Font, J.; Castells, F.; Fabregat, A. Water pollution abatement by catalytic wet air oxidation in a trickle bed reactor, *Catal. Today* 53 (1999) 107-114.
- Fritzmann, C.; Löwenberg, J.; Wintgens, T.; Melin, T. State-of-the-art of reverse osmosis desalination, *Desalination* 216 (2007) 1-76.
- Garcia, F.; Ciceron, D.; Saboni, A.; Alexandrova, S. Nitrate ions elimination from drinking water by nanofiltration: Membrane choice, *Sep. Purif. Technol.* 52 (2006) 196-200.
- Gasparini, G.; Kosvintsev, S.R.; Stillwell, M.T.; Holdich, R.G. Preparation and characterization of PLGA particles for subcutaneous controlled drug release by membrane emulsification, *Colloids Surf., B* 61 (2008) 199-207.
- Giorno, L.; D'Amore, E.; Mazzei, R.; Piacentini, E.; Zhang, J.; Drioli, E.; Cassano, R.; Picci, N. An innovative approach to improve the performance of a two separate phase enzyme membrane reactor by immobilising lipase in presence of emulsion, *J. Membr. Sci.* 295 (2007) 95-101.
- Giorno, L.; Piacentini, E.; Mazzei, R.; Drioli, E. Membrane emulsification as novel method to distribute phase-transfer biocatalysts at the oil/water interface in bioorganic reactions, *J. Membr. Sci.* 317 (2008) 19-25.
- Glaze, W.H.; Kang, J.W.; Chapin, D.H. The chemistry of Water Treatment Processes involving Ozone, Hydrogen Peroxide and UV-Radiation, *Ozone Sci. Eng.* 9 (1987) 335-352.
- Glaze, W.H. and Kang, J.W. Advanced oxidation processes. Test of a kinetic model for the oxidation of organic compounds with ozone and hydrogen peroxide in a semibatch reactor, *Ind. Eng. Chem. Res.* 28 (1989) 1580-1587.
- Goi, A. and Trapido, M. Hydrogen peroxide photolysis, Fenton reagent and photo-Fenton for the degradation of nitrophenols: a comparative study, *Chemosphere* 46 (2002) 913-922.
- González, V. Estudios de biodegradabilidad de efluentes industriales, *Ingeniería Química* 260 (1993) 97-101.
- Grün, M.; Kurganov, A.A.; Schacht, S.; Schüth, F.; Unger, K.K. Comparison of an ordered mesoporous aluminosilicate, silica, alumina, titania and zirconia in normal-phase high-performance liquid chromatography, *J. Chromatogr. A* 40 (1996) 1-9.
- Guimarães, O.L.C.; Filho, D.N.V.; Siqueira, A.F.; Filho, H.J.I.; Silva, M.B. Optimization of the AZO dyes decoloration process through neural networks: Determination of the H₂O₂ addition critical point, *Chem. Eng. J.* 141 (2008) 35-41.
- Guisasola, A.; Baeza, J.A.; Carrera, J.; Casas, C.; Lafuente, J. An off-line respirometric procedure to determine inhibition and toxicity of biodegradable compounds in biomass from an industrial WWTP, *Water Sci. Technol.* 48 (2003) 267-275.
- Gutiérrez, M.; Etxebarria, J.; de las Fuentes, L.; Evaluation of wastewater toxicity: comparative study between Microtox® and activated sludge oxygen uptake inhibition, *Water Res.* 36 (2002) 919-924.

- Haber, F. and Weiss, J. The catalytic decomposition of hydrogen peroxide by iron salts, *J. Proc. R. Soc. London A* 147 (1934) 332-351.
- Huang, X.; Meng, Y.; Liang, P.; Qian, Y. Operational conditions of a membrane filtration reactor coupled with photocatalytic oxidation, *Sep. Purif. Technol.* 55 (2007) 165-172.
- Human Development Report 2007/2008, United Nations Development Program, New York, 2007.
- Into, M.; Jönsson, A.-S.; Lengdén, G. Reuse of industrial wastewater following treatment with reverse osmosis, *J. Membr. Sci.* 242 (2004) 21-25.
- lojoiu, E.E.; Landrison, E.; Raeder, H.; Torp, E.G.; Miachon, S.; Dalmon, J.-A. The "Watercatox" process: Wet air oxidation of industrial effluents in a catalytic membrane reactor. First report on contactor CMR up-scaling to pilot plant, *Catal. Today* 118 (2006) 246-252.
- Jadhav, S.R.; Verma, N.; Sharma, A.; Bhattacharya, P.K. Flux and retention analysis during micellar enhanced ultrafiltration for the removal of phenol and aniline, *Sep. Purif. Technol.* 24 (2001) 541-557.
- James, R.O. and Healy, T.W. Adsorption of hydrolyzable metal ions at the oxide-water interface. I. Co(II) adsorption on SiO₂ and TiO₂ as model systems, *J. Colloid Interface Sci.* 40 (1972a) 42-52.
- James, R.O. and Healy, T.W. Adsorption of hydrolyzable metal ions at the oxide-water interface. III. A thermodynamic Model of Adsorption, *J. Colloid Interface Sci.* 40 (1972b) 65-81.
- James, R.O.; Stiglich, P.J.; Healy, T.W. Analysis of models of adsorption of metal ions at oxide/water interfaces, *Faraday Discuss. Chem. Soc.* 52 (1975) 142-156.
- Jansen, R.H.S.; de Rijk, J.W.; Zwijnenburg, A.; Mulder, M.H.V.; Wessling, M. Hollow fiber membrane contactors – A means to study the reaction kinetics of humic substance ozonation, *J. Membr. Sci.* 257 (2005) 48-59.
- Jia, L.Q.; Ou, Z.Q.; Yang, Z.Y. Ecological behaviour of linear alkylbenzene sulphonate (LAS) in soil-plant systems, *Pedosphere* 15 (2005) 216-224.
- Jones, D.L. and Edwards, A.C. Evaluation of polysulfone hollow fibres and ceramic suction samplers as devices for the in situ extraction of soil solution, *Plant Soil* 150 (1993) 157-165.
- Joscelyne, S.M. and Trägårdh, G. Membrane emulsification – a literature review, *J. Membr. Sci.* 169 (2000) 107-117.
- Judd, S. *The MBR Book: Principles and Applications of Membrane Bioreactors in Water and Wastewater Treatment*, Elsevier, Oxford, 2006.
- Kang, Y.W.; Cho, M.-J.; Hwang, K.I. Correction of hydrogen peroxide interference on standard chemical oxygen demand test, *Water Res.* 33 (1999) 1247-1251.
- Karnik, B.S.; Davies, S.H.; Baumann, M.J.; Masten, S.J. The effects of combined ozonation and filtration on disinfection by-product formation, *Water Res.* 39 (2005) 2839-2850.
- Kavitha, V. and Palanivelu, K. The role of ferrous ion in Fenton and photo-Fenton processes for the degradation of phenol, *Chemosphere* 55 (2004) 1235-1243.
- Kavitha, V. and Palanivelu, K. Destruction of cresols by Fenton oxidation process, *Water Res.* 39 (2005a) 3062-3072.

- Kavitha, V. and Palanivelu, K. Degradation of nitrophenols by Fenton and photo-Fenton processes, *J. Photochem. Photobiol., A* 170 (2005b) 83-95.
- Keowmaneechai, E. and McClements, D.J. Influence of EDTA and citrate on thermal stability of whey protein stabilized oil-in-water emulsions containing calcium chloride, *Food Res. Int.* 39 (2006) 230-239.
- Kim, K.S.; Lee, K.H.; Cho, K.; Park, C.E. Surface modification of polysulfone ultrafiltration membrane by oxygen plasma treatment, *J. Membr. Sci.* 199 (2002) 135-145.
- Kim, H.; Baek, K.; Lee, J.; Iqbal, J.; Yang, J.-W. Comparison of separation methods of heavy metal from surfactant micellar solutions for the recovery of surfactant, *Desalination* 191 (2006) 186-192.
- Kim, J.-H.; Park, P.-K.; Lee, C.-H.; Kwon, H.-H.; Lee, S. A novel hybrid system for the removal of endocrine disrupting chemicals: Nanofiltration and homogeneous catalytic oxidation, *J. Membr. Sci.* 312 (2008) 66-75.
- Kimura, K.; Amy, G.; Drewes, J.E.; Heberer, T.; Kim, T.-U.; Watanabe, Y. Rejection of organic micropollutants (disinfection by-products, endocrine disrupting chemicals and pharmaceutically active compounds) by NF/RO membranes, *J. Membr. Sci.* 227 (2003) 113-121.
- Kitis, M.; Adams, C.D.; Daigger, G.T. The effects of Fenton's reagent pretreatment on the biodegradability of nonionic surfactants, *Water Res.* 33 (1999) 2561-2568.
- Klavarioti, M.; Mantzavinos, D.; Kassinos, D. Removal of residual pharmaceuticals from aqueous systems by advanced oxidation processes, *Environ. Int.* 35 (2009) 402-417.
- Kong, L. and Lemley, A.T. Effect of nonionic surfactants on the oxidation of carbaryl by anodic Fenton treatment, *Water Res.* 41 (2007) 2794-2802.
- Kwon, B.G.; Lee, D.S.; Kang, N.; Yoon, J. Characteristics of p-chlorophenol oxidation by Fenton's reagent, *Water Res.* 33 (1999) 2110-2118.
- Labbez, C.; Fievet, P.; Szymczyk, A.; Thomas, F.; Simon, C.; Vidonne, A.; Pagetti, J.; Foissy, A. A comparison of membrane charge of a low nanofiltration ceramic membrane determined from ionic retention and tangential streaming potential measurements, *Desalination* 147 (2002) 223-229.
- Laine, D.F.; Blumenfeld, A.; Cheng, I.F. Mechanistic study of the ZEA organic pollutant degradation system: Evidence for H₂O₂, HO·, and the homogeneous activation of O₂ by Fe^{II}EDTA, *Ind. Eng. Chem. Res.* 47 (2008) 6502-6508.
- Larisch, B.C. and Duff, S.J.B. Effect of H₂O₂ on the characteristics and biological treatment of TCF bleached pulp mill effluent, *Water Res.* 31 (1996) 1694-1700.
- László, Z.; Hodúr, C. Purification of thermal wastewater by membrane separation and ozonation, *Desalination* 206 (2007) 333-340.
- Le-Clech, P.; Chen, V.; Fane, A.G. Fouling in membrane bioreactors used in wastewater treatment, *J. Membr. Sci.* 284 (2006) 17-53.
- Legrini, O.; Oliveros, E.; Braun, M. Photochemical processes for water treatment, *Chem. Rev.* 93 (1993) 671-698.
- Li, C.; Gao, J.; Jiang, Z.; Wang, S.; Lu, H.; Yang, Y.; Jing, F. Selective oxidations on recoverable catalysts assembled in emulsions, *Top. Catal.* 35 (2005) 169-175.
- Li, J.-H.; Zhou, B.-X.; Cai, W.-M. The solubility behaviour of Bisphenol A in the presence of surfactants, *J. Chem. Eng. Data* 52 (2007) 2511-2513.

- Liikanen, R.; Yli-Kuivila, J.; Laukkanen, R. Efficiency of various chemical cleanings for nanofiltration membrane fouled by conventionally-treated surface water, *J. Membr. Sci.* 195 (2002) 265-276.
- Lin, S.H.; Lin, C.M.; Leu, H.G. Operating characteristics and kinetic studies of surfactant wastewater treatment by Fenton oxidation, *Water Res.* 33 (1999) 1735-1741.
- Liotta, L.F.; Gruttadauria, M.; Di Carlo, G.; Perrini, G.; Librando, V. Heterogeneous catalytic degradation of phenolic substrates: Catalysts activity, *J. Hazard. Mater.* 162 (2009) 588-606.
- Liou, R.M.; Chen, S.H.; Hung, M.Y.; Hsu, C.S.; Lay, J.Y. Fe(III) supported on resin as a effective catalyst for the heterogeneous oxidation of phenol in aqueous solution, *Chemosphere* 59 (2005) 117-125.
- Liu, W.; Andrews, S.A.; Stefan, M.I.; Bolton, J.R. Optimal methods for quenching H₂O₂ residuals prior to UFC testing, *Water Res.* 37 (2003) 3697-3703.
- Lobo, A.; Cambiella, A.; Benito, J.M.; Pazos, C.; Coca, J. Ultrafiltration of oil-in-water emulsions with ceramic membranes: Influence of pH and crossflow velocity, *J. Membr. Sci.* 278 (2006) 328-334.
- López-Muñoz, M.J.; Sotto, A.; Arsuaga, J.M.; Van der Bruggen, B. Influence of membrane, solute and solution properties on the retention of phenolic compounds in aqueous solution by nanofiltration membranes, *Sep. Purif. Technol.* 66 (2009) 194-201.
- Ma, Y.-S.; Huang, S.-T.; Lin, J.-G. Degradation of p-nitrophenol using the Fenton process, *Water Sci. Technol.* 42 (2000) 155-160.
- Majewska-Nowak, K.; Kabsch-Korbutowicz, M.; Winnicki, T. Concentration of organic contaminants by ultrafiltration, *Desalination* 221 (2008) 358-369.
- Makhotkina, O.A.; Kuznetsova, E.V.; Preis, S.V. Catalytic detoxification of 1,1-dimethylhydrazine aqueous solutions in heterogeneous Fenton system, *Appl. Catal. B* 68 (2006) 85-91.
- Malato, S.; Fernández-Ibáñez, P.; Maldonado, M.I.; Blanco, J.; Gernjak, W. Decontamination and disinfection of water by solar photocatalysis: Recent overview and trends, *Catal. Today* 147 (2009) 1-59.
- Mänttari, M.; Pekuri, T.; Nyström, M. NF270, a new membrane having promising characteristics and being suitable for treatment of dilute effluents from the paper industry, *J. Membr. Sci.* 242 (2004) 107-116.
- Mänttari, M.; Kuosa, M.; Kallas, J.; Nyström, M. Membrane filtration and ozone treatment of biologically treated effluents from the pulp and paper industry, *J. Membr. Sci.* 309 (2008) 112-119.
- Mantzavinos, D.; Sahinzada, M.; Livingston, A.G.; Metcalfe, I.S.; Hellgardt, K. Wastewater treatment: wet air oxidation as a precursor to a biological treatment, *Catal. Today* 53 (1999) 93-106.
- Marrot, B.; Barrios-Martinez, A.; Moulin, P.; Roche, N. Industrial wastewater treatment in a membrane bioreactor: a review, *Environ. Prog.* 23 (2004) 59-68.
- Marrubini, G.; Coccini, T.; Manzo, L. Direct analysis of urinary trans,trans-muconic acid by coupled column liquid chromatography and spectrophotometric ultraviolet detection: method applicability to human urine, *J. Chromatogr. B* 758 (2001) 295-303.

- Martín, A.; Martínez, F.; Malfeito, J.; Palacio, L.; Prádanos, P.; Hernández, A. Zeta potential of membranes as a function of pH. Optimization of isoelectric point evaluation, *J. Membr. Sci.* 213 (2003) 225-230.
- Martínez, F.; Calleja, G.; Melero, J.A.; Molina, R. Iron species incorporated over different silica supports for the heterogeneous photo-Fenton oxidation of phenol, *Appl. Catal., B* 70 (2007) 452-460.
- Masuyama, A.; Endo, C.; Takeda, S.; Nojima, M.; Ono, D.; Takeda, T. Ozone-cleavage gemini-surfactants. Their surface-active properties, ozonolysis and biodegradability, *Langmuir* 16 (2000) 368-373.
- Mei, L.; Decker, E.A.; McClements, D.J. Evidence of iron association with emulsion droplets and its impact on lipid oxidation, *J. Agric. Food Chem.* 46 (1998) 5072-5077.
- Melero, J.A.; Calleja, G.; Martínez, F.; Molina, R.; Pariente, I. Nanocomposite Fe₂O₃/SBA-15: An efficient and stable catalyst for the catalytic wet peroxidation of phenolic aqueous solutions, *Chem. Eng. J.* 131 (2007) 245-256.
- Méndez-Díaz, J.D.; Sánchez-Polo, M.; Rivera-Utrilla, J.; Bautista-Toledo, M.I. Effectiveness of different oxidizing agents for removing sodium dodecylbenzenesulphonate in aqueous systems, *Water Res.* 43 (2009) 1621-1629.
- Merten, U. Desalination by reverse osmosis, MIT Press, Massachusetts, 1966.
- Miachon, S.; Perez, V.; Crehan, G.; Torp, E.; Raeder, H.; Bredesen, R.; Dalmon, J.-A. Comparison of a contactor catalytic membrane reactor with a conventional reactor: example of wet air oxidation, *Catal. Today* 82 (2003) 75-81.
- Mijangos, F.; Varona, F.; Villota, N. Changes in solution color during phenol oxidation by the Fenton reagent, *Environ. Sci. Technol.* 40 (2006) 5538-5543.
- Molinari, R.; Mungari, M.; Drioli, E.; Di Paola, A.; Loddo, V.; Palmisano, L.; Schiavello, M. Study on a photocatalytic membrane reactor for water purification, *Catal. Today* 55 (2000) 71-78.
- Molinari, R.; Grande, C.; Drioli, E.; Palmisano, L.; Schiavello, M. Photocatalytic membrane reactors for degradation of organic pollutants in water, *Catal. Today* 67 (2001) 273-279.
- Molinari, R.; Borgese, M.; Drioli, E.; Palmisano, L.; Schiavello, M. Hybrid processes coupling photocatalysis and membranes for degradation of organic pollutants in water, *Catal. Today* 75 (2002a) 77-85.
- Molinari, R.; Palmisano, L.; Drioli, E.; Schiavello, M. Studies on various reactor configurations for coupling photocatalysis and membrane processes in water purification, *J. Membr. Sci.* 206 (2002b) 399-415.
- Molinari, R.; Gallo, S.; Argurio, P. Metal ions removal from wastewater or washing water from contaminated soil by ultrafiltration-complexation, *Water Res.* 38 (2004a) 593-600.
- Molinari, R.; Pirillo, F.; Falco, M.; Loddo, V.; Palmisano, L. Photocatalytic degradation of dyes by using a membrane reactor, *Chem. Eng. Process.* 43 (2004b) 1103-1114.
- Molinari, R.; Pirillo, F.; Loddo, V.; Palmisano, L. Heterogeneous photocatalytic degradation of pharmaceuticals in water by using polycrystalline TiO₂ and a nanofiltration membrane reactor, *Catal. Today* 118 (2006) 205-213.

- Monteagudo, J.M.; Durán, A.; San Martín, I.; Aguirre, M. Effect of continuous addition of H₂O₂ and air injection on ferrioxalate-assisted photo-Fenton degradation of Orange II, *Appl. Catal., B* 89 (2009) 510-518.
- Moritz, T.; Benfer, S.; Arki, P.; Tomandl, G. Investigation of ceramic membrane materials by streaming potential measurements, *Colloids Surf., A* 47 (2001a) 25-33.
- Moritz, T.; Benfer, S.; Áрки, P.; Tomandl, G. Influence of the surface charge on the permeate flux in the dead-end filtration with ceramic membranes, *Sep. Purif. Technol.* 25 (2001b) 501-508.
- Mozaia, S.; Tomaszewska, M.; Morawski, A.W. A new photocatalytic membrane reactor (PMR) for removal of azo dye Acid Red 18 from water, *Catal. Today* 59 (2005) 131-137.
- Mukerjee, P. and Mysels, K.J. Critical Micelles Concentrations of Aqueous Surfactant Systems, Nat. Bur. Standards, Washington DC, 1999.
- Mulder, M. Basic Principles of Membrane Technology, 2nd edition, Kluwer Academic Publishers, The Netherlands, 1997.
- Munter, R. Advanced Oxidation Processes – Current status and prospects, *Proc. Est. Acad. Sci., Chem.* 50, 2 (2001) 59-80.
- Narong, P. and James, A.E. Sodium chloride rejection by a UF ceramic membrane in relation to its surface electrical properties, *Sep. Purif. Technol.* 49 (2006) 122-129.
- NHP 2001, National Hydrological Plan 2001. Spanish Water Act 10/2001 of 5th July 2001.
- Neyens, E. and Baeyens, J. A review of classic Fenton's peroxidation as an advanced oxidation technique, *J. Hazard. Mater.* 98 (2003) 33-50.
- Nghiem, L.D.; Schäfer, A.I.; Elimelech, M. Removal of natural hormones by nanofiltration membranes: Measurement, modeling and mechanisms, *Environ. Sci. Technol.* 38 (2004) 1888-1896.
- Nghiem, L.D.; Schäfer, A.I.; Elimelech, M. Pharmaceutical retention mechanisms by nanofiltration membranes, *Environ. Sci. Technol.* 39 (2005) 7698-7705.
- Nollet, L.M.L. (Ed.) Handbook of water analysis, 2nd edition, CRC Press - Taylor&Francis, New York, 2007.
- Nyström, M.; Lindström, M.; Matthiasson, E. Streaming potential as a tool in the characterization of ultrafiltration membranes, *Colloids Surf., A* 36 (1989) 297-312.
- Nyström, M.; Pihlajamäki, A.; Ehsani, N. Characterisation of ultrafiltration membranes by simultaneous streaming potential and flux measurements, *J. Membr. Sci.* 87 (1994) 245-256.
- Ourpold, K.; Masirin, A.; Tenno, R. Estimation of biodegradation parameters of phenolic compounds on activated sludge by respirometry, *Chemosphere* 44 (2001) 1273-1280.
- Pan, Y.; Wang, W.; Wang, T.; Yao, P. Fabrication of carbon membrane and microfiltration of oil-in-water emulsion: An investigation on fouling mechanisms, *Sep. Purif. Technol.* 57 (2007) 388-393.
- Parameshwaran, K.; Fane, A.G.; Cho, B.D.; Kim, K.J. Analysis of microfiltration performance with constant flux processing of secondary effluent, *Water Res.* 35 (2001) 4349-4358.

- Pariante, M.I.; Martínez, F.; Melero, J.A.; Botas, J.A.; Velegraki, T.; Xekoukoulotakis, N.P.; Mantzavinos, D. Heterogeneous photo-Fenton oxidation of benzoic acid in water: Effect of operating conditions, reaction by-products and coupling with biological treatment, *Appl. Catal., B* 85 (2008) 24-32.
- Parra, S.; Henao, L.; Mielczarski, E.; Mielczarski, J.; Albers, P.; Suvorova, E.; Guindet, J.; Kiwi, J. Synthesis, testing and characterization of a novel Nafion membrane with superior performance in photoassisted immobilized Fenton catalysis, *Langmuir* 20 (2004) 5621-5629.
- Parsons, J. (Ed.). *Advanced Oxidation Processes for Water and Wastewater Treatment*, IWA Publishing, London, 2004.
- Pera-Titus, M.; García-Molina, V.; Baños, M.A.; Giménez, J.; Esplugas, S. Degradation of chlorophenols by means of advanced oxidation processes: a general review, *Appl. Catal., B* 47 (2004) 219-256.
- Perry, R.H.; Green, D.W.; Maloney, J.O. *Perry's Chemical Engineers Handbook*, 7th edition, McGraw-Hill, 1999.
- PhysProp Database Demo, Syracuse Research Corporation, 2008. In <http://www.syrres.com/esc/physdemo.htm>. Last time accessed March 2009.
- Piera, E.; Tejedor-Tejedor, M.I.; Zorn, M.E.; Anderson, M.A. Relationship concerning the nature and concentration of Fe(III) species on the surface of TiO₂ particles and photocatalytic activity of the catalyst, *Appl. Catal., B* 46 (2003) 671-685.
- Pignatello, J.J.; Oliveros, E.; MacKay, A. Advanced Oxidation Processes for organic contaminant destruction based on the Fenton reaction and related chemistry, *Crit. Rev. Environ. Sci. Technol.* 36 (2006) 1-84.
- Plakas, K.V.; Karabelas, A.J.; Wintgens, T.; Melin, T. A study of selected herbicides retention by nanofiltration membranes – The role of organic fouling, *J. Membr. Sci.* 284 (2006) 291-300.
- Plakas, K.V. and Karabelas, A.J. Triazine retention by nanofiltration in the presence of organic matter: The role of humic substance characteristics, *J. Membr. Sci.* 336 (2009) 86-100.
- Potential impacts of desalination development on energy consumption, IEEP, Ecologic and ACTeón, 2008.
- Puigdomenech, I. Medusa Software, 2004. In <http://www.kemi.kth.se/medusa>. Last time accessed September 2007.
- Qin, J.-J.; Oo, M.H.; Wong, F.-S. Pilot study on the treatment of spent solvent cleaning rinse in metal plating, *Desalination* 191 (2006) 359-364.
- Radjenović, J.; Petrović, M.; Ventura, F.; Barceló, D. Rejection of pharmaceuticals in nanofiltration and reverse osmosis membrane drinking water treatment, *Water Res.* 42 (2008) 3601-3610.
- Raeder, H.; Bredesen, R.; Crehan, G.; Miachon, S.; Dalmon, J.-A.; Pintar, A.; Levec, J.; Torp, E.G. A wet air oxidation process using a catalytic membrane contactor, *Sep. Purif. Technol.* 32 (2003) 349-355.
- Raskin, P.; Gleick, P.H.; Kirshen, P.; Pontius, R.G.; Strzepek, K. *Comprehensive assessment of the freshwater resources of the world*, Stockholm Environmental Institute, Sweden, 1997.
- Rastogi, A.; Al-Abed, S.R.; Dionysiou, D.D. Effect of inorganic, synthetic and naturally occurring chelating agents on Fe(II) mediated advanced oxidation of chlorophenols, *Water Res.* 43 (2009) 684-694.

- Reiller, P.; Lemordant, D.; Hafiane, A.; Moulin, C.; Beaucaire, C. Extraction and release of metal ions by micellar-enhanced ultrafiltration: influence of complexation and pH, *J. Colloid Interface Sci.* 177 (1996) 519-527.
- Ren, S. Assessing wastewater toxicity to activated sludge: recent research and developments, *Environ. Int.* 33 (2004) 1151-1164.
- Ricco, G.; Tomei, M.C.; Ramadori, R.; Laer, G.; Toxicity assessment of common xenobiotic compounds on municipal activated sludge: comparison between respirometry and Microtox®, *Water Res.* 38 (2004) 2103-2110.
- Rigg, T.; Taylor, W.; Weiss, J. The rate constant of the reaction between hydrogen peroxide and ferrous ions, *J. Chem. Phys.* 22 (1954) 575-577.
- Ríos, G.; Pazos, C.; Coca, J. Destabilization of cutting oil emulsions using inorganic salts as coagulants, *Colloids Surf., A* 138 (1998) 383-389.
- Rivas, F.J.; Beltran, F.J.; Frades, J.; Buxeda, P. Oxidation of p-hydroxybenzoic acid by Fenton's reagent, *Water Res.* 35 (2001) 387-396.
- Roberts, J.D. and Caserio, M.C. Basic Principles of Organic Chemistry, 2nd edition, W.A. Benjamin Inc., New York, 1977.
- Rodríguez, A.; Letón, P.; Rosal, R.; Dorado, M.; Villar, S.; Sanz, J.M. Tratamientos avanzados de aguas residuales industriales. Informe de Vigilancia Tecnológica, CEIM and Dirección General de Universidades e Investigación, Madrid, 2006.
- Rubalcaba, A.; Suárez-Ojeda, M.E.; Carrera, J.; Font, J.; Stüber, F.; Bengoa, C.; Fortuny, A.; Fabregat, A. Biodegradability enhancement of phenolic compounds by Hydrogen Peroxide Promoted Catalytic Wet Air Oxidation, *Catal. Today* 124 (2007a) 191-197.
- Rubalcaba, A.; Suárez-Ojeda, M.E.; Stüber, F.; Fortuny, A.; Bengoa, C.; Metcalfe, I.; Font, J.; Carrera, J.; Fabregat, A. Phenol wastewater remediation: advanced oxidation processes coupled to a biological treatment, *Water Sci. Technol.* 55 (2007b) 221-227.
- Ruiz, B.; Prats, R.; Zoffmann, C. Modelo real de flujo de una planta depuradora de aguas residuales, *Ingeniería Química* 279 (1992) 53-56.
- Sabaté, J.; Pujolà, M.; Llorens, J. Comparison of polysulfone and ceramic membranes for the separation of phenol in micellar-enhanced ultrafiltration, *J. Colloid Interface Sci.* 246 (2002) 157-163.
- Sanchez, I.; Stüber, F.; Font, J.; Fortuny, A.; Fabregat, A.; Bengoa, C. Elimination of phenol and aromatic compounds by zero valent iron and EDTA at low temperature and atmospheric pressure, *Chemosphere* 68 (2007) 338-344.
- Santos, A.; Yustos, P.; Quintanilla, A.; García-Ochoa, F.; Casas, J.A.; Rodríguez, J.J. Evolution of toxicity upon wet catalytic oxidation of phenol, *Environ. Sci. Technol.* 38 (2004a) 133-138.
- Santos, A.; Yustos, P.; Quintanilla, A.; García-Ochoa, F.; Casas, J.A.; Rodríguez, J.J. Lower toxicity route in catalytic wet oxidation of phenol at basic pH by using bicarbonate media, *Appl. Catal., B* 53 (2004b) 181-194.
- Sbaï, M.; Fievet, P.; Szymczyk, A.; Aoubiza, B.; Vidonne, A.; Foissy, A. Streaming potential, electroviscous effect, pore conductivity and membrane potential for the determination of the surface potential of ceramic ultrafiltration membrane, *J. Membr. Sci.* 215 (2003) 1-9.
- Schäfer, A.I.; Fane, A.G.; Waite, T.D. Nanofiltration: Principles and Applications, Elsevier Advanced Technology, Oxford, 2005.

- Shchukin, D.G.; Sviridov, D.V. Photocatalytic processes in spatially confined micro- and nanoreactors, *J. Photochem. Photobiol., C 7* (2006) 23-39.
- Skoog, D.A.; West, D.M.; Holler, F.J. Fundamentals of analytical chemistry, 7th edition, Saunders College Publishing, 1996.
- Song, W.; Ravindran, V.; Koel, B.E.; Pirbazari, M. Nanofiltration of natural organic matter with H₂O₂/UV pretreatment: fouling mitigation and membrane surface characterization, *J. Membr. Sci.* 241 (2004) 143-160.
- Spanish Water Act 11/2005 of 22nd July 2005.
- Spanish Water Act 1620/2007 of 7th December 2007.
- Spanjers, H.; Vanrolleghem, O.; Olsson, G.; Dold, O.L. Respirometry in Control of the Activated Sludge Process: Principles, International Association on Water Quality, London, 1998.
- Stillwell, M.T.; Holdich, R.G.; Kosvintev, S.R.; Gasparini, G.; Cumming, I.W. Stirred cell membrane emulsification and factors influencing dispersion drop size and uniformity, *Ind. Eng. Chem. Res.* 46 (2007) 965-972.
- Stirling, D.A. Persistent Organic Pollutants. An Overview of Historical Manufacturing and Use, 2001. In <http://preprint.chemweb.com/envchem/0007001>. Last time accessed May 2008.
- Stratmann, H.; Giorno, L.; Drioli, E. An introduction to Membrane Science and Technology. Consiglio Nazionale delle Ricerche, Roma, 2006.
- Strotmann, U.J.; Geldern, A.; Kuhn, A.; Gending, C.; Klein, S. Evaluation of respirometric test method to determine the heterotrophic coefficient of activated sludge bacteria, *Chemosphere* 38 (1999) 3555-3570.
- Suárez-Ojeda, M.E.; Stüber, F.; Fortuny, A.; Fabregat, A.; Carrera, J.; Font, J. Catalytic wet air oxidation of substituted phenols using activated carbon as catalyst, *Appl. Catal. B* 58 (2005) 105-114.
- Suárez-Ojeda, M.E.; Guisasola, A.; Baeza, J.A.; Fabregat, A.; Stüber, F.; Fortuny, A.; Font, J.; Carrera, J. Integrated catalytic wet air oxidation and aerobic biological treatment in a municipal WWTP of a high-strength o-cresol wastewater, *Chemosphere* 66 (2007a) 2096-2105.
- Suárez-Ojeda, M.E.; Kim, J.; Carrera, J.; Metcalfe, I.S.; Font, J. Catalytic and non-catalytic wet air oxidation of sodium dodecylbenzene sulfonate: kinetics and biodegradability enhancement, *J. Hazard. Mater.* 144 (2007b) 655-662.
- Suárez-Ojeda, M.E.; Fabregat, A.; Stüber, F.; Fortuny, A.; Carrera, J.; Font, J. Catalytic wet air oxidation of substituted phenols: Temperature and pressure effect on the pollutant removal, the catalyst preservation and the biodegradability enhancement, *Chem. Eng. J.* 132 (2007c) 105-115.
- Suárez-Ojeda, M.E.; Carrera, J.; Metcalfe, I.S.; Font, J. Wet air oxidation (WAO) as a precursor to biological treatment of substituted phenols: refractory nature of the WAO intermediates, *Chem. Eng. J.* 144 (2008) 205-212.
- Suratkar, V. and Mahapatra, S. Solubilization site of organic perfume molecules in sodium dodecyl sulfate micelles: new insights from proton NMR studies, *J. Colloid Interface Sci.* 225 (2000) 32-38.
- Syamal, M.; De, S.; Bhattacharya, P.K. Phenol solubilization by cetyl pyridinium chloride micelles in micellar enhanced ultrafiltration, *J. Membr. Sci.* 137 (1997) 99-107.

- Sychev, A.Y. and Isaak, V.G. Iron compounds and the mechanism of the homogeneous catalysis of the activation of O₂ and H₂O₂ and of the oxidation of organic substrates, *Russ. Chem. Rev.* 64 (1995) 1105-1129.
- Szpyrkowicz, L.; Juzzolino, C.; Kaul, S.N. A comparative study on oxidation of dispersive dyes by electrochemical process, ozone, hypochlorite and Fenton reagent, *Water Res.* 35 (2001) 2129-2136.
- Tabor, C.F. and Barber, L.B. Occurrence and concentrations of aromatic surfactants and their degradation products in river waters of Taiwan, *Environ. Sci. and Technol.* 30 (1996) 161-171.
- Talens-Alesson, F.I.; Urbanski, R.; Szymanowski, J. Evolution of resistance to permeation during micellar enhanced ultrafiltration of phenol and 4-nitrophenol, *Colloids Surf., A* 178 (2001) 71-77.
- Talinli, I. and Anderson, G.K. Interference of hydrogen peroxide on the standard COD test, *Water Res.* 26 (1992) 107-110.
- Tanninen, J.; Mänttari, M.; Nyström, M. Effect of salt mixture concentration on fractionation with NF membranes, *J. Membr. Sci.* 283 (2006) 57-64.
- The United Nations World Water Development Report 3: Water in a Changing World, UNESCO Paris and Earthscan: London, 2009.
- Tung, C.-C.; Yang, Y.-M.; Chang, C.-H.; Maa, J.-R. Removal of copper ions and dissolved phenol from water using micellar-enhanced ultrafiltration with mixed surfactants, *Waste Manage.* 22 (2002) 695-701.
- Ubay Çokgör, E.; Sözen, S.; Orhon, D.; Henze, M. Respirometric analysis of activated sludge behaviour – I. Assessment of the readily biodegradable substrate, *Water Res.* 32 (1998) 461-475.
- Van der Bruggen, B.; Schaep, J.; Wilms, D.; Vandecasteele, C. Influence of molecular size, polarity and charge on the retention of organic molecules by nanofiltration, *J. Membr. Sci.* 156 (1999) 29-41.
- Van der Bruggen, B. and Vandecasteele, C. Removal of pollutants from surface water and groundwater by nanofiltration: overview of possible applications in the drinking water industry, *Environ. Pollut.* 122 (2003) 435-445.
- Verliefde, A.R.D.; Cornelissen, E.R.; Heijman, S.G.J.; Verberk, J.Q.J.C.; Amy, G.L.; Van der Bruggen, B.; van Dijk, J.C. The role of electrostatic interactions on the rejection of organic solutes in aqueous solutions with nanofiltration, *J. Membr. Sci.* 322 (2008) 52-66.
- Verliefde, A.R.D. PhD Thesis - Technische Universiteit Delft. Rejection of organic micropollutants by high pressure membranes (NF/RO), Water Management Academic Press, Delft, 2008.
- Vospernik, M.; Pintar, A.; Levec, J. Application of a catalytic membrane reactor to catalytic wet air oxidation of formic acid, *Chem. Eng. Process.* 45 (2006) 404-414.
- Wang, J.; Guan, J.; Santiwong, S.R.; Waite, T.D. Characterization of floc size and structure under different monomer and polymer coagulants on microfiltration membrane fouling, *J. Membr. Sci.* 321 (2008) 132-138.
- Water Resources across Europe – confronting water scarcity and drought, EEA Report No 2/2009, European Environment Agency, Copenhagen, 2009.
- Water supply and wastewater treatment in Spain, Instituto Nacional de Estadística (INE), 2006.

- Weast, R.C. (Ed.). Handbook of Chemistry and Physics, 58th edition, CRC Press, Ohio, 1977.
- Weis, A.; Bird, M.R.; Nyström, M. The chemical cleaning of polymeric UF membranes fouled with spent sulphite liquor over multiple operational cycles, *J. Membr. Sci.* 216 (2003) 67-79.
- Winkler, J. and Marmé, S. Titania as a sorbent in normal-phase liquid chromatography, *J. Chromatogr. A* 888 (2000) 51-62.
- Witek, A.; Kołtuniewicz, A.; Kurczewski, B.; Radziejowska, M.; Hatałski, M. Simultaneous removal of phenols and Cr³⁺ using micellar-enhanced ultrafiltration process, *Desalination* 191 (2006) 111-116.
- Xi, W. and Geissen, S.-U. Separation of titanium dioxide from photocatalytically treated water by cross-flow microfiltration, *Water Res.* 35 (2001) 1256-1262.
- Ying, G.-G. Fate, behaviour and effects of surfactants and their degradation products in the environment, *Environ. Int.* 32 (2006) 417-431.
- Zazo, J.A.; Casas, J.A.; Mohedano, A.F.; Gilarranz, M.A.; Rodríguez, J.J. Chemical pathway and kinetics of phenol oxidation by Fenton's reagent, *Environ. Sci. Technol.* 39 (2005) 9295-9302.
- Zazo, J.A.; Casas, J.A.; Molina, C.B.; Quintanilla, A.; Rodríguez, J.J. Evolution of Ecotoxicity upon Fenton's oxidation of phenol in water, *Environ. Sci. Technol.* 41 (2007) 7164-7170.
- Zazo, J.A.; Casas, J.A.; Mohedano, A.F.; Rodríguez, J.J. Semicontinuous Fenton oxidation of phenol in aqueous solution. A kinetic study. *Water Res.* 43 (2009) 4063-4069.
- Zeng, G.-M.; Xu, K.; Huang, J.-H.; Li, X.; Fang, Y.-Y.; Qu, Y.-H. Micellar enhanced ultrafiltration of phenol in synthetic wastewater using polysulfone spiral membrane, *J. Membr. Sci.* 310 (2008) 149-160.

UNIVERSITAT ROVIRA I VIRGILI

TREATMENT OF BIOREFRACTORY WASTEWATER THROUGH MEMBRANE-ASSISTED OXIDATION PROCESSES

Xavier Bernat Camí

ISBN:978-84-693-1529-3/DL:T-652-2010

UNIVERSITAT ROVIRA I VIRGILI

TREATMENT OF BIOREFRACTORY WASTEWATER THROUGH MEMBRANE-ASSISTED OXIDATION PROCESSES

Xavier Bernat Camí

ISBN:978-84-693-1529-3/DL:T-652-2010

UNIVERSITAT ROVIRA I VIRGILI

TREATMENT OF BIOREFRACTORY WASTEWATER THROUGH MEMBRANE-ASSISTED OXIDATION PROCESSES

Xavier Bernat Camí

ISBN:978-84-693-1529-3/DL:T-652-2010

UNIVERSITAT ROVIRA I VIRGILI

TREATMENT OF BIOREFRACTORY WASTEWATER THROUGH MEMBRANE-ASSISTED OXIDATION PROCESSES

Xavier Bernat Camí

ISBN:978-84-693-1529-3/DL:T-652-2010

